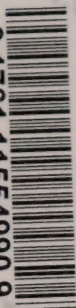



3 1761 11554990 9



CA1
EP 321
-73R06-08

GOVT



Digitized by the Internet Archive
in 2022 with funding from
University of Toronto

<https://archive.org/details/31761115549909>

CAI EP 321

-73R06 (3)

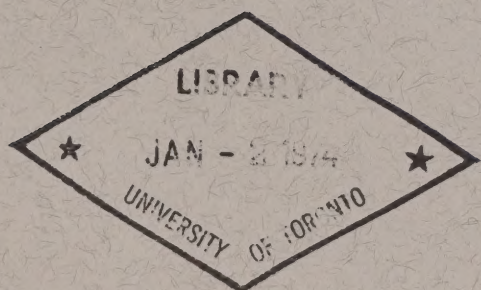
Pacific Marine Science Report 73-6

Government
Publications

THE DISTRIBUTION AND VARIABILITY OF PHYSICAL OCEANOGRAPHIC PROPERTIES ALONG LINE P

May 8-18, 1972

Richard E. Thomson



ENVIRONMENT CANADA
Fisheries and Marine Service
Marine Sciences Directorate
Pacific Region
1230 Government St.
Victoria, B.C.

MARINE SCIENCES DIRECTORATE, PACIFIC REGION

PACIFIC MARINE SCIENCE REPORT 73-6

THE DISTRIBUTION AND VARIABILITY OF
PHYSICAL OCEANOGRAPHIC PROPERTIES ALONG LINE P,

MAY 8-18, 1972

Richard E. Thomson

Victoria, B.C.
Marine Sciences Directorate, Pacific Region
Environment Canada
July, 1973

Thomson, Richard E.

The distribution and variability of physical oceanographic properties along line P, May 8-18, 1972. Pacific Marine Science Report 73-6.

ERRATA

Section 2.6

All temperature variances quoted in this section should read ($^{\circ}\text{C}^2 \times 10^3$).

Section 3.3

Pressures plotted in figures 25a - 25q are in millibars (mb).

PREFACE

The object of this report is to communicate certain aspects of the oceanographic observations taken along, and in the vicinity of, Line P during May 1972. For this reason, some effort has gone into reducing and interpreting the data obtained. It is hoped that the results presented will facilitate a better understanding of the physical oceanography in the oceanic region adjacent to the coast of British Columbia and also aid in the planning of similar surveys in the future.

As with any work of this type, there has been a large amount of input from other individuals. For assistance in collecting the data, I would like to thank the officers and crews of the weatherships CCGS VANCOUVER and QUADRA with special thanks to Captain A.A.R. Dykes of the QUADRA for his cooperation in allowing a replacement sensor to be transferred aboard his ship while at sea and for occupying all inbound Line P stations. In this connection also, the effort of Mr. W. Hansen in his role as the sea-going technician on the QUADRA is gratefully acknowledged.

The amiable and generous assistance of Captain M. Dyer, his officers and crew of the CFAV LAYMORE made for both a useful and pleasurable cruise. My co-worker, Mr. C. de Jong is especially thanked. Without his expertise and hard work much less would have been accomplished.

With regards the onshore reduction of the data, I would like to thank Mr. B. Minkley, Ms. M. Dyer and Ms. R. Thomas. Mssrs. D. Smith, E. Luscombe, B. Johns and A. Douglas and Ms. L. Kuwahara are especially acknowledged for their excellent work in the computational portion of the data analysis. Moreover, the assistance of Ms. Kuwahara, Ms. S. Greckol

and Mr. P. Huggett in plotting the results has been very much appreciated, as has that of the photographic section of the Hydrographic Service (Victoria). Finally my thanks to Drs. J. Garrett and S. Tabata for reviewing the manuscript and for making useful suggestions.

TABLE OF CONTENTS

	<u>Page</u>
Preface.....	i
Table of Contents.....	iii
List of Tables.....	v
List of Figures.....	vi
 Section.	
1. Introduction.....	1
2. Results of the C.F.A.V. "LAYMORE" Cruise, May 8-18, 1972.....	7
2.1 General Discussion.....	7
LAYMORE Outbound.....	7
LAYMORE Inbound.....	7
Corrections to S.T.D. Readings.....	9
2.2 The Spatial Distribution of Physical Properties.....	15
Temperature Sections (S.T.D.).....	17
Temperature Sections (X.B.T.).....	17
Salinity Sections.....	19
Density Sections.....	19
Potential Energy Anomaly Sections.....	20
2.3 A Surface Temperature Comparison.....	57
2.4 A Surface Salinity Comparison.....	64
2.5 Tidal/Inertial Motions in the Vicinity of Line P....	67
2.6 Temperature Microstructure in the vicinity of Line "P": Evidence of the Mixing of Two Water Masses...	75
Discussion.....	75
Upper and Lower Layer Blocks.....	81
Division into Nine Blocks.....	85
3. The Variability of Water Properties Along Line "P".....	103
3.1 General Discussion.....	103
3.2 A Comparison of Surface Salinities and Temperatures.	104
3.3 Depth of the Surface Mixed Layer.....	107

	<u>Page</u>
3.4 Depths of the 33.0 ⁰ /oo and 33.5 ⁰ /oo Salinity Surfaces..	128
3.5 Depth of the Dichothermal Layer	132
3.6 Geostrophic Mass Transport Across Line "P"	137
3.7 Comparison of Temperature Variances Along Line "P"	139
4. Summary.....	146
REFERENCES	154
APPENDIX	155

LIST OF TABLES

	Page
Table I. Temperatures at several standard depths at six Line P stations (LAYMORE STD observations).	16
Table II. Magnitudes of the Fourier Tidal Constituents from the depths (h) of the 33.00/oo and 33.50/oo isohaline surfaces versus time t.	73

LIST OF FIGURES

	Page
Figure 1. Location of Line P stations	2
2. Positions of the QUADRA, VANCOUVER, and LAYMORE versus time for the period May 8-18, 1972.	4
3. Location of the STD and XBT stations for the LAYMORE cruise	8
4a. Nansen bottle salinities minus STD salinities versus depth; QUADRA cruise 72-05	11
4b. Nansen bottle temperatures minus STD temperatures versus depth; QUADRA cruise 72-05	12
5a. Temperature corrections with depth for the LAYMORE STD observations	13
5b. Salinity corrections with depth for the LAYMORE STD observations	14
6a - 6i. Temperature sections (STD) at 0, 50, 100, 200, 300, 500, 1000, 1200, and 1500 m ($^{\circ}\text{C}$) LAYMORE cruise	23 - 31
7a - 7e. Temperature sections (XBT) at 0, 50, 100, 200 and 500 m ($^{\circ}\text{C}$). LAYMORE cruise	32 - 36
8a - 8e. Salinity sections at 0, 50, 100, 200, and 500 m ($^{\circ}/\text{oo}$) LAYMORE cruise	37 - 41
9a - 9h. Density (σ_t) sections at 0, 50, 100, 200, 300, 500, 1000 and 1200 m. LAYMORE cruise	42 - 49
10a -10g. Potential energy anomaly sections at 50, 100, 200, 300, 500, 1000 and 1200 m ($10^8\text{ergs}/\text{cm}^2$). LAYMORE cruise	50 - 56
11. Sea surface temperature obtained from the LAYMORE STD observations versus time	58
12a. Surface bucket temperature minus the surface STD temperature (.) and bucket temperature minus the surface XBT temperature (x) versus time. LAYMORE cruise..	59
12b. The air temperature at a height of 10 m at the time of the LAYMORE STD observations	61

	Page
13a. The surface bucket temperature minus the air temperature at 10 m at the time of the LAYMORE STD observations	62
13b. The wind at 10 m at the time of the LAYMORE STD observations	62
13c. The relative humidity at a height of 10 m at the time of the LAYMORE STD observations	62
14a. The sea surface salinity from the STD and bucket sample versus time. LAYMORE cruise	65
14b. The bucket salinity minus the STD salinity at the sea surface versus time. LAYMORE cruise	66
15a. Depths of the 33.0 ⁰ /oo and 33.5 ⁰ /oo isohaline surfaces versus time (original data). LAYMORE, QUADRA and VANCOUVER cruises	68
15b. Depth of the 33.0 ⁰ /oo isohaline surface versus time (smoothed data, hourly values). LAYMORE cruise ...	70
15c. Depth of the 33.5 ⁰ /oo isohaline surface versus time (Smoothed data, hourly values). LAYMORE cruise ...	71
15d. Spectra of depths of the 33.0 ⁰ /oo and 33.5 ⁰ /oo isohaline surface	72
16. STD temperature profiles for the 300-1500 m range from consecutive stations 5 and 11. LAYMORE cruise	76
17a - 17b. Temperature versus depth at consecutive station 5 for the two ranges 0-300 and 300-500 m: T original data, \bar{T} after low pass filtering; T' fluctuation. LAYMORE cruise	77 - 78
17c - 17d. Temperature versus depth at consecutive station 17 for the two ranges 0-300 and 300-1500 m. LAYMORE cruise	79 - 80
18a. Spatial distribution of the temperature variance for the depth interval 0-300 m. LAYMORE cruise	82
18b. Spatial distribution of the temperature variance for the depth interval 300-1500 m. LAYMORE cruise	84
19. Temperature-Salinity (T-S) plots for consecutive LAYMORE stations 4, 5, 8, 11, 31 and 36.....	86

	Page
20a - 20i. Horizontal of the temperature variance for the 9 depth intervals: 0-50; 50-150; 150-300; 300-500; 500-700; 700-900; 900-1100; 1100-1300; 1300-1500 m. LAYMORE cruise	90 - 98
21a - 21c. Vertical distribution below 150 m of the temperature variance at a selected number of LAYMORE stations	99 -101
22. East-west profile of Cobb Seamount (46°40'N, 130°40'W)	102
23a. Surface salinities versus longitude along Line P, the LAYMORE (outbound), QUADRA and VANCOUVER cruises, May 1972	105
23b. Surface temperatures versus longitude along Line P, the LAYMORE (outbound), QUADRA and VANCOUVER cruises, May 1972	106
24. Depth of the surface mixed layer versus longitude along Line P, for the LAYMORE (outbound), QUADRA and VANCOUVER cruises, May 1972.....	108
25a.- 25q. Sea-surface pressure, winds, cloud cover, and frontal positions at 00 hrs GMT over the northeast Pacific from May 2 to May 18, 1972	111-127
26a. Depth of the 33.0°/oo isohaline surface versus longitude along Line P for the LAYMORE (outbound), QUADRA and VANCOUVER cruises, May 1972	129
26b. Depth of the 33.5°/oo isohaline surface versus longitude along Line P	130
26c. Depth difference of 33.5°/oo isohaline versus time difference: LAYMORE minus QUADRA (.); LAYMORE minus VANCOUVER (o); QUADRA minus VANCOUVER (x)	131
27. Typical temperature profile for the subarctic Pacific region in summer (after Uda, 1963)	133
28. Depth of the dicothermal layer versus longitude along Line P for the LAYMORE (outbound), QUADRA and VANCOUVER cruises, May 1972	134
29. Temperature gradient across the dicothermal layer versus longitude along Line P. All three cruises	136

30. Potential energy anomaly, referred to 1200 m, versus longitude along Line . All three cruises	138
31a. Temperature variance versus longitude along Line P for the depth interval 0-300 m. All three cruises	141
31b. Temperature variance versus longitude along Line P for the depth interval 300-1500 m. All three cruises	142
31c - 31g. Temperature variance versus longitude along Line P for the 5 depth intervals: 300-500; 500-700; 700-900; 900-1100; 1100-1300 m. All three cruises	143-145

1. INTRODUCTION

Canadian operation of Ocean Weather Station P (latitude $50^{\circ}00'$ N, longitude $145^{\circ}00'$ W) commenced in December 1950 with the naval frigate class ships CCGS St. CATHARINES and CCGS STONETOWN alternatively occupying the station for periods of six weeks at a time. A program of twice-daily bathythermograph (BT) observations was added to the ships' routines in July 1952. In August 1956, St. CATHARINES further augmented its oceanographic observations with a more extensive BT program which by April 1959 had been extended to include a series of "Line P" stations en route to and from Station P.

The present weatherships, CCGS VANCOUVER and CCGS QUADRA, which replaced the frigates in April 1967 and October 1967, respectively, now occupy twelve positions along the Line (see figure 1). In addition, these ships have since augmented the BT observations with a program of Expendable BT (XBT) and Salinity-Temperature-Depth (STD) observations. The latter program, which is still in operation, began in May 1968 onboard the VANCOUVER and in February 1969 onboard the QUADRA, using Bissett-Berman model 9006 or 9040 STD's.

The results of this report stemmed from a desire to make use of the weathership observations along Line P to gain some understanding of the spatial distribution of the physical oceanographic properties off the coast of B.C. and their temporal variability over periods of days. As a consequence of the ships' routines and speeds, however, weathership observational data alone is not sufficient to give the required information. The difficulty is that of the six weeks spent at sea by each ship, only about two and one-half days are required to complete all Line P stations during the outbound or inbound leg of a particular cruise. This, together with the requirement of keeping P continuously occupied leads to a difference of only a few hours

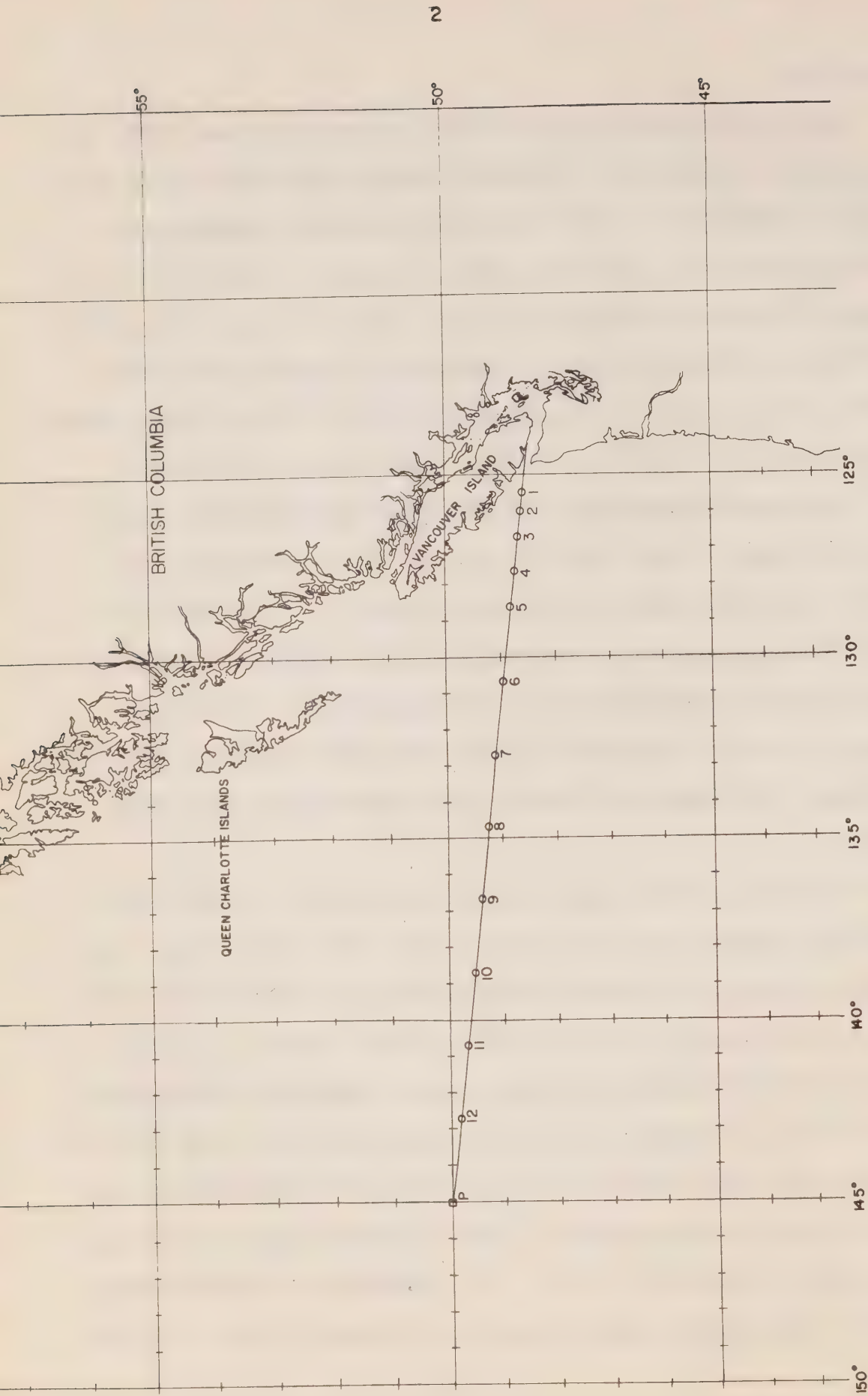


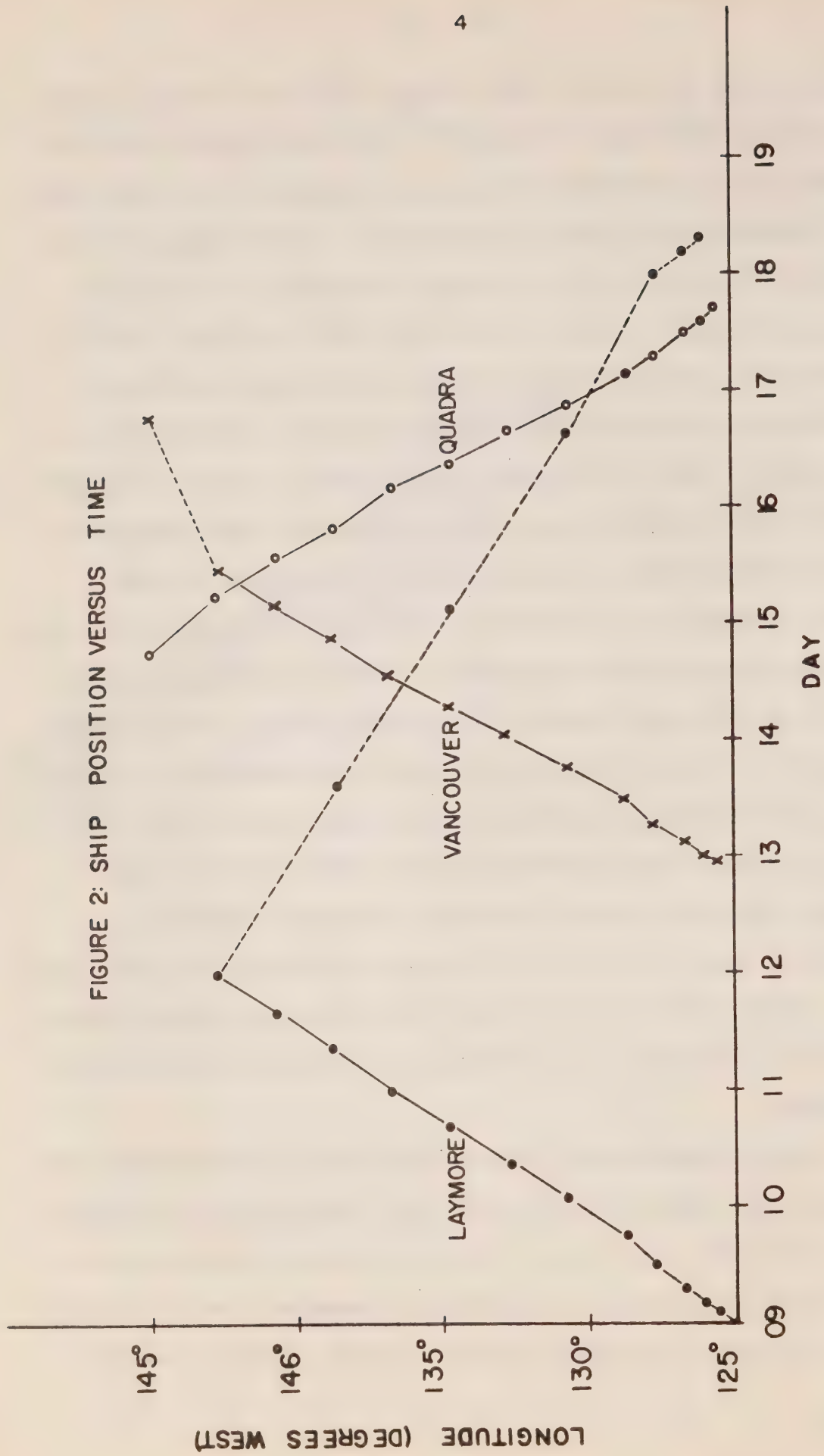
FIGURE 1: LINE "P" STATIONS

between observations at the most oceanic station (12) but five days between observations at the most coastal station (1). To obtain temporal variations based on more evenly distributed time lags at all stations, it was therefore necessary to employ the services of a third vessel. By arranging the departure time of this vessel to P to be a few days in advance of the outbound weathership, and its arrival time in port to be nearly coincident with the inbound weathership, the desired lags (days) were achieved (see figure 2).

Although it would have been preferable to have a ship capable of a speed comparable to that of the weatherships (16 knots), only the relatively slow (11 knots) CFAV LAYMORE was available. Nonetheless, the disadvantage in speed was somewhat compensated by the LAYMORE's maneuverability and working area arrangement which permitted stations to be done rather efficiently. The month of May was chosen for two reasons. The first and most important consideration was the weather which at that time of year is usually pleasant enough to permit all Line P stations to be done by the weatherships; in high winds their large amount of superstructure makes observing very difficult. Second, May is a time midway between the minimal stability in the upper oceanic layers that occurs in early March and the maximal stability in these waters that occurs in late July. The depth of the surface mixed layer is for example, shallow enough to be distinguishable from more permanent thermocline(s) but deep enough not to be affected by the local short period (hours) surface heating.

As with the weatherships, observations from the LAYMORE during the May 8-18 cruise were taken using XBT's (Sippican Corporation) and a Bissett-Berman STD (model 9006 in this case). The latter measures temperature via a thermistor, conductivity through a temperature compensated conductivity cell and depth via a frequency modulated transducer signal. Output is recorded

FIGURE 2: SHIP POSITION VERSUS TIME



as an analog trace of temperature and salinity versus depth on lined chart paper. These are then digitized ashore using a digitizing table. As the accuracy of the STD's is $\pm 0.03^{\circ}\text{C}$ for temperature, $\pm 0.05^{\circ}/\text{oo}$ for salinity and $\pm 1\%$ for depth, there should in theory be no loss of accuracy during digitizing since the charts can be read to higher precision than this. In practice, however, the fact that the salinity traces 'spike' each time there is a sharp temperature gradient leads to a significant information loss in the case of salinity. This feature of the Bissett-Berman's, arising through the difference in the time constants between the temperature sensor and the compensated conductivity sensor, necessitates a hand smoothing of the salinity traces and therefore to a loss of detail. There is also a tendency for all B.B. sensors to drift with time. For each cast, then, a correction factor should be determined through a simultaneous Nansen bottle cast. As this is extremely time consuming, a few Nansen casts only are usually taken to give an indication of the mean correction factors to be applied. On the LAYMORE cruise, surface bucket samples were also taken at the time of STD stations. These had the advantage that they gave a truer indication of the temperature and salinity of the top layer of water than possible with the STD. The reason for this, of course, is that the STD being subject to the roll of the ship had to be commenced with the instrument a meter or so below the surface. In the data, there has been no attempt to correct for this since it is virtually impossible to visually ascertain the actual depth of the STD once it is in the water.

For the purposes of this report, the results of the data reduction are presented in two sections. The first deals basically with the spatial distribution of physical properties in the vicinity of Line P although there is also some discussion of time variability. In the second section, results

from all three ships are compared to give some indication of the temporal changes that occurred. In both cases, explanations are presented where warranted, and possible. Digitized plots of the original data are given in the Appendix.

2. RESULTS from the CFAV LAYMORE cruise: May 8-18, 1972

2.1. General Discussion

LAYMORE outbound

The LAYMORE departed Esquimalt, B.C. at about 1800 GMT on May 8 bound for Ocean Weather Station P. Station 1 was occupied at about 0200 GMT the next day. Except for the continental-margin stations 1, 2 and 3 which were taken to 100, 100 and 1000 m, respectively, all STD casts went to 1500 m with station 4 further extended to 2400 m using Nansen bottles (at 1200, 1400, 1600, 1800, 2000 and 2400 m). At each STD station a surface bucket sample was obtained, the temperature read using a thermometer and a sample bottled for salinity determination ashore. In addition, Expendable Bathythermographs (XTB's) were taken at each Line P outbound station as well as at intermediate positions (figure 3). An attempt to extend station 9 to 2400 m using Nansen bottles had to be abandoned because of bad weather. The outbound leg of the cruise was completed with a rendez-vous with the QUADRA at the edge of the Station P grid at about 0500 GMT on the 12th. A replacement STD sensor for the malfunctioning unit on the weathership was then successfully transferred from the LAYMORE and installed.

LAYMORE inbound

The inbound portion of the LAYMORE cruise was altered somewhat from the outbound track so that some information on the water properties north and south of the Line could be obtained (figure 3). North-south legs of this course which intersected Line P so as to extend $1\frac{1}{2}^{\circ}$ of latitude on either side of it, were joined by legs parallel to the Line. The longitudinal positioning of stations in this case were determined by the longitude of the Line P stations and the latitudinal positions by the requirement of a spacing similar to those along the Line.

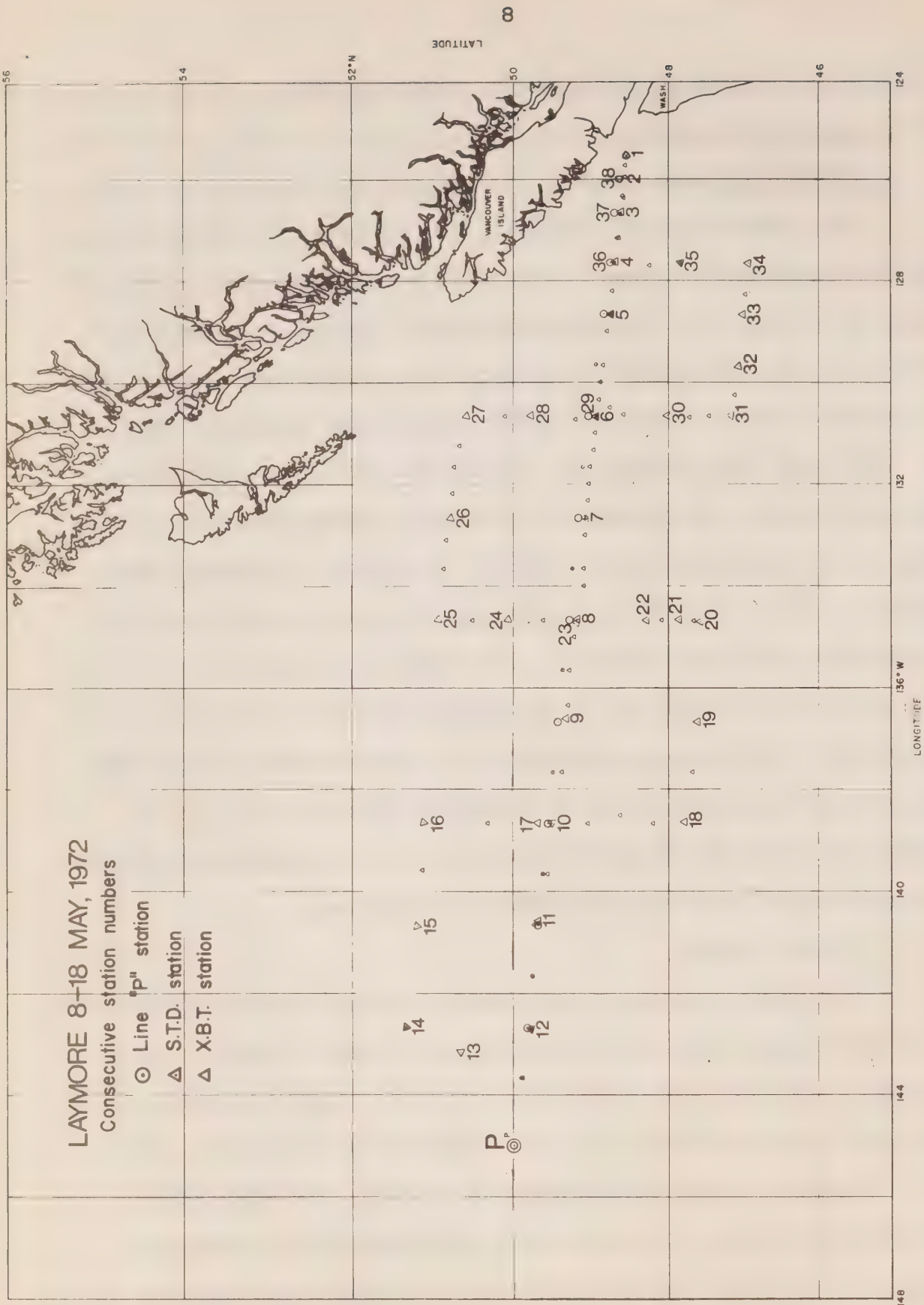


FIGURE 3

As with the outbound part of the cruise, a bucket sample was taken at each STD station. XBT's, however, were only taken between stations because of the limited supply of probes resulting from the fairly high rate of failure ($\sim 20\%$). Also, an attempt to extend station 18 with a Nansen cast had to be abandoned at 300 m due to the large amount of wind drift and subsequent large wire angle ($\sim 70^\circ$). Moreover, station 1 inbound was cancelled because of high seas.

Corrections to STD readings

Despite the fact that data for only one shallow and one deep Nansen cast are available from the LAYMORE survey, it has been possible to determine mean corrections to the STD readings using these and the greater number of comparisons performed with the same instrument during the June 23-August 10 patrol (72-005) of the QUADRA. The latter are plotted in figures 4a, b as Nansen readings minus STD readings versus depth. The heavy solid line on each curve is the mean correction to be applied for that particular cruise. Since the points from the 0-300 m Nansen cast of the LAYMORE fall within the range of those from the QUADRA, the same surface error is assumed for both cruises. The slight deviation with depth between the corrections applied to the LAYMORE observations and those applied to the QUADRA observations (figures 5a, b) are a result of assuming that near 1400 m the points from the former are more correct than those from the latter. Strictly speaking, the difference at this depth is rather insignificant when compared to the cast-to-cast variations shown by figure 4. Thus the QUADRA corrections could just as readily be used. Moreover, comparison with an even later cruise (QUADRA, 15 September-2 November), in which the same instrument was used, shows only a slight deviation between mean curves, although again the cast-to-cast variations are large. Finally, in accordance with the present

procedure followed by the Weathership Group, spikes in the salinity traces have been removed by hand before digitizing. A salinity value has been considered to be a spike when it is associated with a sharp, localized temperature gradient provided the initial change in salinity is in the same sense as the initial temperature change and is then followed by a salinity change in the opposite sense.

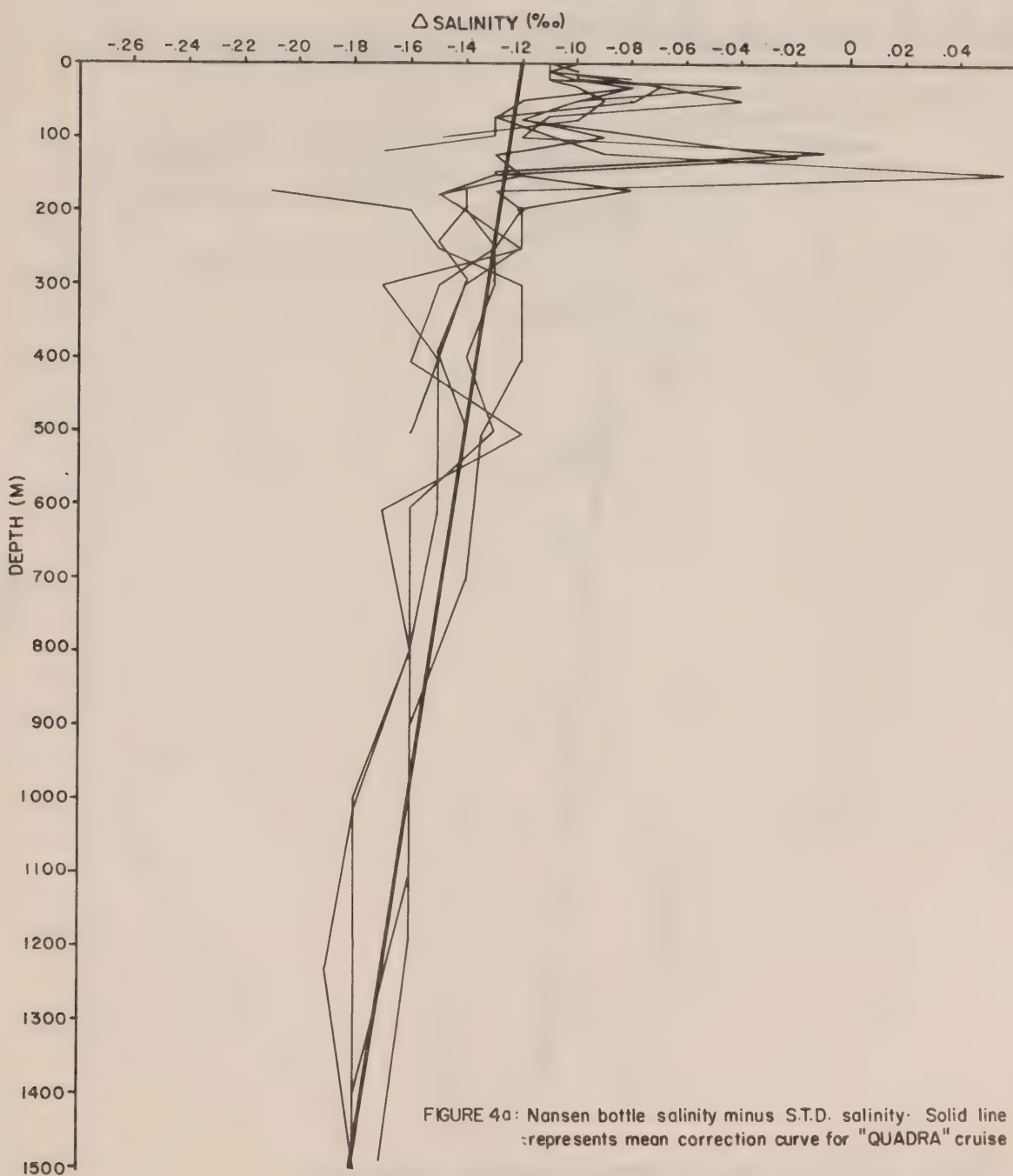


FIGURE 4a: Nansen bottle salinity minus S.T.D. salinity. Solid line (—) represents mean correction curve for "QUADRA" cruise 72-05

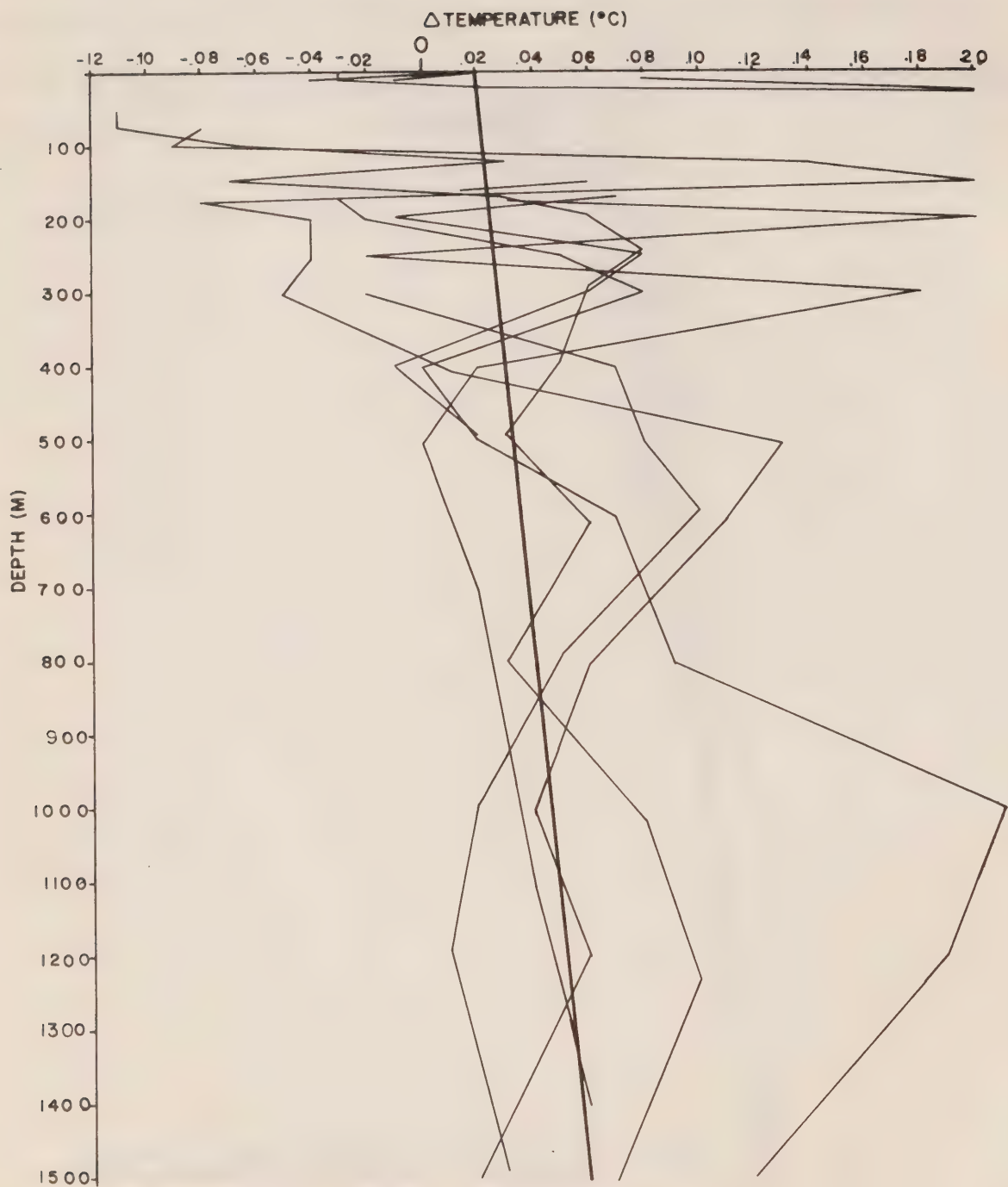


FIGURE 4b: Nansen bottle temperature minus S.T.D. temperature. Solid line (—) represents mean correction curve for QUADRA cruise 72 - 05.

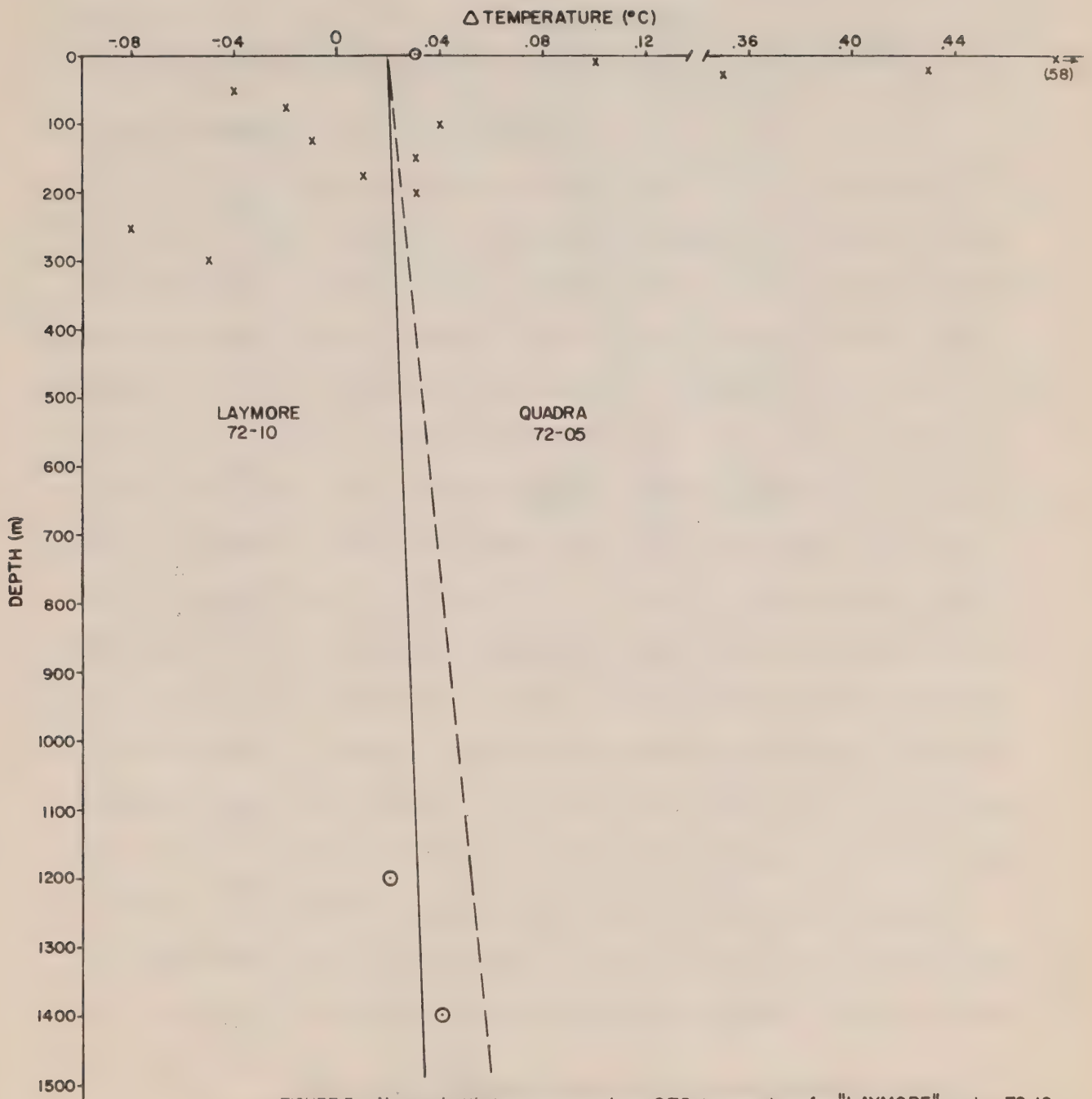


FIGURE 5a: Nansen bottle temperature minus S.T.D. temperature for "LAYMORE" cruise 72-10. x surface waters, o deep waters. Correction curves.

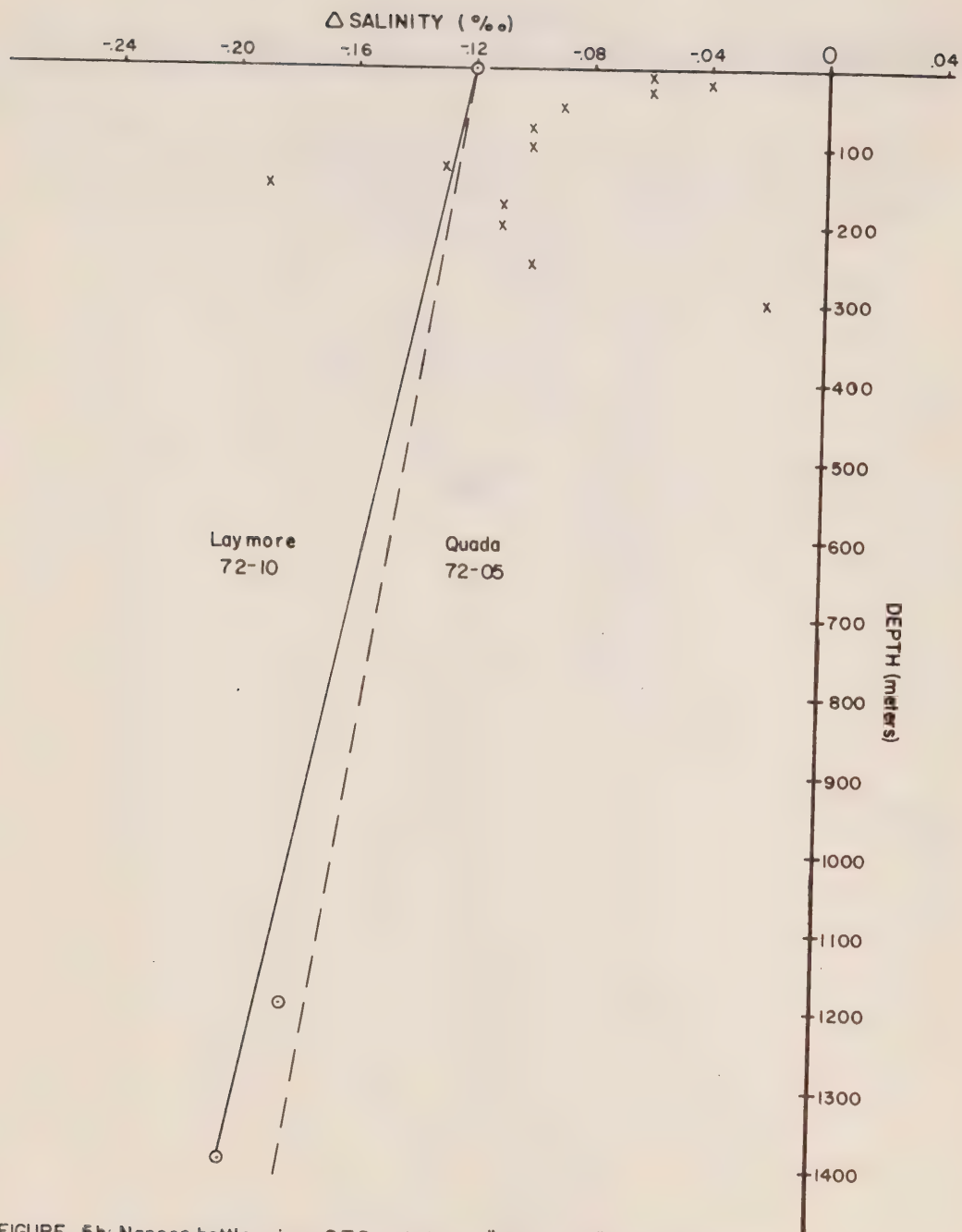


FIGURE 5b: Nansen bottle minus STD salinity for "LAYMORE" cruise 72-10;
 x surface water, o deep water; correction curves.

2.2. The Spatial Distribution of Physical Properties

Use of the STD and XBT data makes it possible to obtain the mean horizontal distribution of water properties in the vicinity of Line P during early May 1972. For consistency, outbound values have been used where there are two values for a given station. Plots presented are for a number of standard depths over the 0-1500 m range.

As with any presentation of this kind, only an estimate of the mean horizontal distribution of a particular property is obtainable since variations due to internal tides, internal waves, inertial waves, horizontal advection, etc. cannot be removed. The effects of vertical motions are especially strong in regions of large vertical gradients such as occur in the upper 100-200 m of the subarctic Pacific. An example of this is figure 4 which shows the large differences between STD and Nansen observations taken in the highly structured upper layer at slightly different times at the same location (Station P). In addition, near-coastal water properties can be significantly changed by tidal mixing and river discharge. Only below the main pycnocline, (> 200 m) where temporal variations should be relatively small, would a single cast be expected to closely reproduce the mean values. Even then one is limited by the accuracy of the instrument since with increasing depth below the pycnocline observational errors begin to become more comparable to changes that can be produced by advection. These remarks are partly demonstrated in Table 1 which, as an example, gives the differences in temperature at selected depths between the two different samplings of six Line P stations.

In summary, then, any plot of the horizontal distribution of a water property over an extensive oceanic region will contain the integrated effect of temporal variations over the observational period. Confidence can,

STATION	DATE	DEPTH						
		0	50	100	200	300	500	1000
2	0435/09	9.61	7.36	6.92				
	0700/18	10.12	7.48	6.74				
3	0730/09	9.35	7.51	7.71	6.66	5.83	4.78	
	0425/18	9.49	7.47	7.44	6.57	5.82	4.81	
4	1200/09	8.65	7.44	8.08	6.70	5.81	4.89	3.39
	0030/18	9.92	7.77	7.79	6.77	6.01	4.84	3.49
6	0100/10	7.56	6.47	6.07	5.74	4.54	3.84	3.11
	1450/16	7.66	6.36	6.03	5.49	4.70	4.05	2.74
8	1630/10	6.52	5.85	5.52	5.18	4.33	3.73	2.95
	0250/15	7.52	6.11	5.66	4.99	4.30	3.75	2.95
10	0830/11	6.25	5.19	4.95	4.25	4.07	3.57	2.84
	1415/13	6.87	5.36	4.98	4.66	4.01	3.57	2.86
								3.05
								3.11
								2.74
								2.82
								2.67
								2.67
								2.60
								2.61

TABLE 1 : Temperature (°C) at various depths at six Line P stations.

therefore, only be given to the gross features of the observed distributions.

Temperature Sections (STD)

The horizontal distribution of temperature at depths obtained from the STD observations is presented in figures 6a-i. Except at 1500 m, where there is little structure, the isotherms over most of the region show a northward decrease in temperature with the nearly zonal orientation in the interior tending more north-south as the coast is approached. The main deviation from this trend occurs in the vicinity of consecutive station 26 ($50^{\circ}47'$ N, $132^{\circ}40'$ W) and appears to extend from about 100 to 500 m.

When the isotherm pattern at "0" m is compared with that at other depths, the time integrated effect of surface heating over the observation period becomes apparent. In particular, the change in orientation of the 0 m isotherms that occurs along Line P between 128° W and 136° W has probably been exaggerated as a result of the time delay between Line P outbound observations and those to the north and south. At subsurface depths, where the heating trend in May has not been felt, the change in isotherm orientation is more gradual and undoubtedly gives a more accurate picture of the gross distribution.

Temperature Sections (XBT)

Horizontal sections of temperature at five selected depths from the XBT observations are plotted in figures 7a-e. Comparison of these to the previous plots demonstrates an obvious difference in detail between the results of the two surveys. In addition, the XBT temperature distributions appear to also give generally higher temperatures at a given location.

Part of the reason for the greater detail in the XBT survey is obviously related to the increased number of observations, from 40 for the STD survey to 80. This increase greatly complicates interpolation during

plotting since one has too many points to obtain a simple mean distribution~ but not enough to obtain a truly detailed distribution. Moreover, there is the limited accuracy of the XBT ($\pm .2^{\circ}\text{C}$ and $\pm 1\%$ of depth) and the digitizing errors ($\pm .1^{\circ}\text{C}$ and $\pm 1\text{ m}$) that accompany reading of the chart output. The net result is a number of closed contours which may or may not accurately represent the real oceanic situation. Although the latter case is most likely, the fact that the isolated contours exist mostly in the region where the eastward moving current divides (and is joined by the northward flow from the south along the coast -§ 2.6) does not completely rule out the existence of such closed isotherms at fixed levels. The comparatively large values of the XBT survey may also be related to its low accuracy. Other reasons that could account for the difference with the STD survey are: the difference of about 1 m between what is considered the 'surface' for XBT and what is considered the 'surface' for the STD; the tendency for the XBT thermistor to crack or be otherwise damaged and still produce what appears to be a reasonable trace. This 'recovery' of the XBT has the drawback that although the shape of the profile is real, an offset takes place whereby the absolute reading cannot be accurately determined. In this regard also, it should be mentioned that the known failure rate was about 20% with some XBT's showing malfunction immediately upon entering the water and others not until a few hundred meters. In the latter case, the temperatures to that depth were usually considered to be correct.

It therefore seems reasonable to remark that an XBT survey is much more inaccurate than a corresponding STD survey in the sense of giving an 'instantaneous' view of the spatial temperature distribution. There are just too many sources of error in this instrument to expect it to give a detailed ($< 0.2^{\circ}\text{C}$) knowledge of the temperature structure, notwithstanding

effects due to internal motions.

Salinity Sections

The low surface salinities appearing off the coast in figure 8a are indicative of the large amount of river runoff in this region that is occurring at this time of year. Included in this, of course, is that from the inland areas (via the Fraser River, for example) which is being advected seaward through Juan de Fuca Strait. At 50 m, the salinity still decreased shoreward but with a much reduced gradient. By 100 m, the pattern had changed, with maximum salinities now appearing near the coast and Station P, and minimum values near 136°W longitude. At this depth, of course, the horizontal distribution is complicated the most by internal motions associated with the halocline (~100-200 m) and undoubtedly accounts for the irregularity of the pattern. Below 100 m, salinity becomes increasingly uniform throughout the region although at 200 m more coastal values are slightly larger than those in the interior (figure 8d). In addition, there appears to be a difference in the salinity distribution between the region west of 128°W and that to the east, at least in the upper 100 m. Line P station 5 (48°50'N, 128°40'W), therefore, seems to mark a transition from the coastal to the oceanic domain (see e.g. Dodimead, Favorite & Hirando, 1963).

Density Sections

Figures 9a-h show the horizontal distribution of sigma-t (σ_t) which is related to the density ρ at salinity = s, temperature = t and pressure = 0 db via the relation

$$\sigma_t = (\rho_{s,t,0} - 1) \times 10^3 .$$

As with the temperature and salinity from which it is derived, the σ_t distribution has more or less a zonal orientation in the oceanic interior which gives way to coastally orientated contours in the near-shore region.

In all cases, there is a shoreward decrease in density, with maximum spatial gradients occurring essentially near the coast.

This shoreward decrease in density clearly indicates that upwelling was not at yet taking place in the particular coastal region observed.

At 100 m, the increased complexity of the spatial pattern is most certainly the result of the irregular salinity distribution described in the previous subsection. The strong dependence of density on salinity, therefore, also makes it impossible at this depth to obtain a consistent picture of the mean density field from only one set of observations. This dependence also accounts for Line P station 5 again marking the transition from the coastal to the oceanic domain.

Potential Energy Anomaly Sections

In order to obtain a measure of the mean direction and magnitude of the baroclinic flow associated with the density structure, it is necessary to calculate certain properties which average over depth and include the influence of the earth's rotation. One of these is the 'dynamic height' ΔD defined at some pressure P by

$$\Delta D(P) = \int_0^P \delta \, dP,$$

where δ is the anomaly of specific volume (density⁻¹). The spatial gradient of this quantity divided by the local value of the Coriolis parameter, f , then gives the magnitude of the surface geostrophic currents relative to the pressure surface P ; the current direction is parallel to ΔD contours.

In a similar manner, the potential energy anomaly χ is defined by

$$\chi(P) = g^{-1} \int_0^P \delta \, dP, \quad (1)$$

where g is the acceleration of gravity. Since

$$\chi(P) \propto \Delta D \cdot P/g,$$

the spatial gradient of χ divided by f gives the magnitude of total mass transport per unit horizontal width from the surface to the depth (z) at P . That is, relative to z , the vertically integrated geostrophic transport component U parallel to the χ -contours is given by

$$fU = |\partial\chi/\partial s|$$

where s is normal to the contours.

Figures 10a-g are plots of χ • width of 1 cm. for some selected levels. Moreover, in the calculations of (1), the pressure has been replaced with

$$P = \rho g z$$

by means of the hydrostatic equation since the error in going from P to z is only about 1% at 1500 m. If we now assume that baroclinic motions at 1200 m are very small, figure 10e can be used to determine the mean mass transport within the top 1200 m in the vicinity of Line P. Basically this transport approaches the coast from the west as a zonal flow with the more southerly portion eventually turning southward and the more northerly portion moving northward, in agreement with previous findings in this region (c.f. Dodimead, Favorite & Hiram, 1963). East of 130°W longitude, the transport apparently moves northward, parallel to the coast and with a much greater magnitude than in the more interior regions. The closed contours, if real, could be a consequence of the large amount of variability associated with the north-south splitting of the currents (Thomson, 1971).

The magnitude of the transport between any two contours is readily obtainable since it is simply the difference divided by the mean of the Coriolis parameter over the line of separation. At 50°N, for example, contours whose difference is 0.5×10^8 ergs/cm² have between them a net transport of 0.5×10^{12} gm/s or 0.5 sverdrups, referred to the appropriate

depth. The average speed of the surface current in cm/s relative to the depth of the potential energy surfaces can then be found by dividing the transport magnitude by the depth and spatial separation of the contours (in cm). For contours separated by 25 km at 1200 m, mean surface speeds are about 2 cm/s, while near Vancouver Island where the distance between contours is less, speeds increase to the order of 4 cm/s.

Except for a slight decrease in magnitude, the mean transport relative to 1000 m is similar to that relative to 1200 m. At a reference level of 500 m there remains a good similarity with the deeper patterns although the magnitudes are much reduced. Finally, even referred to 100 m the transport retains the general pattern for deeper waters although it is relatively very small.



FIGURE 60



FIGURE 6b

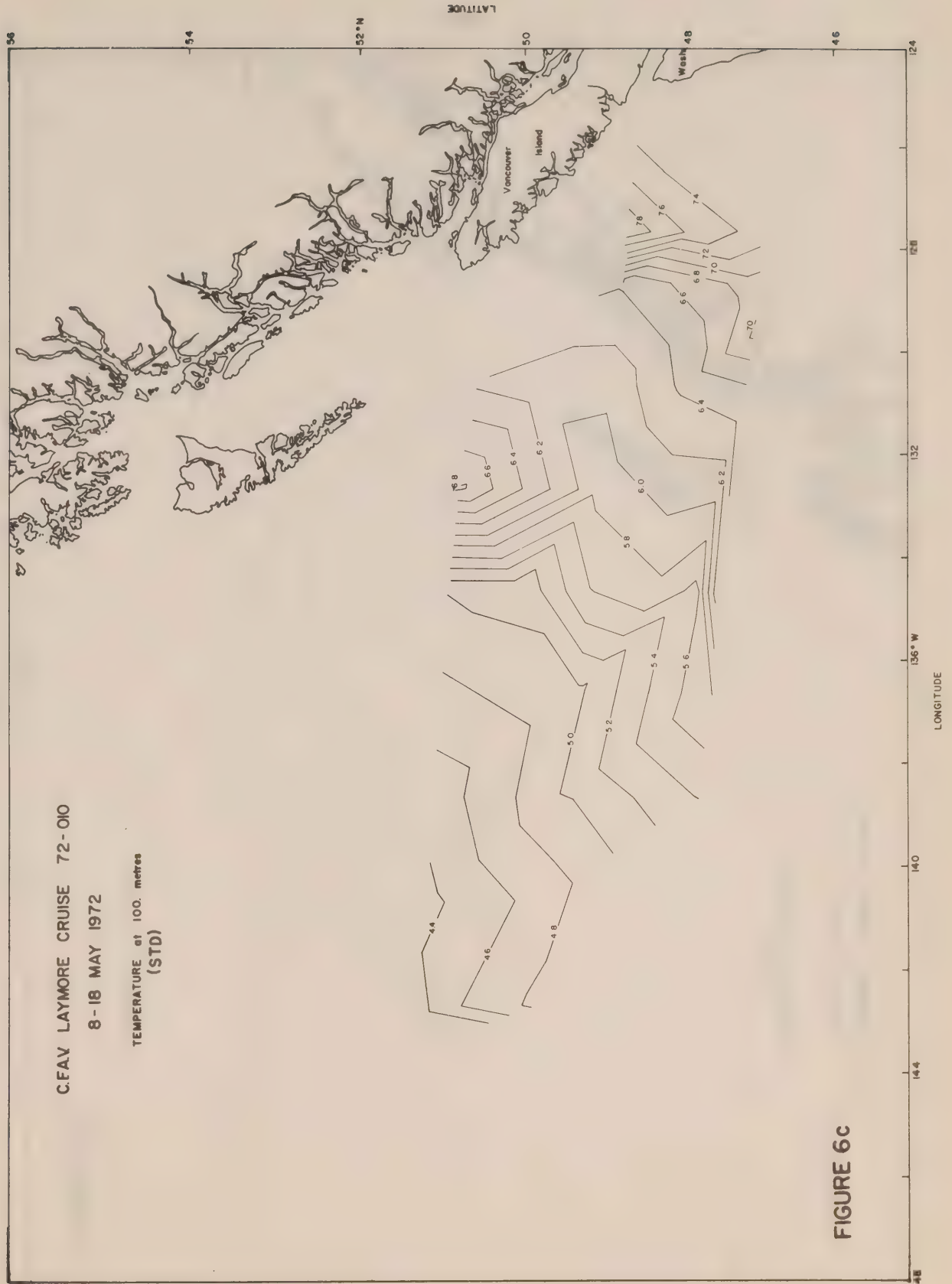


FIGURE 6c

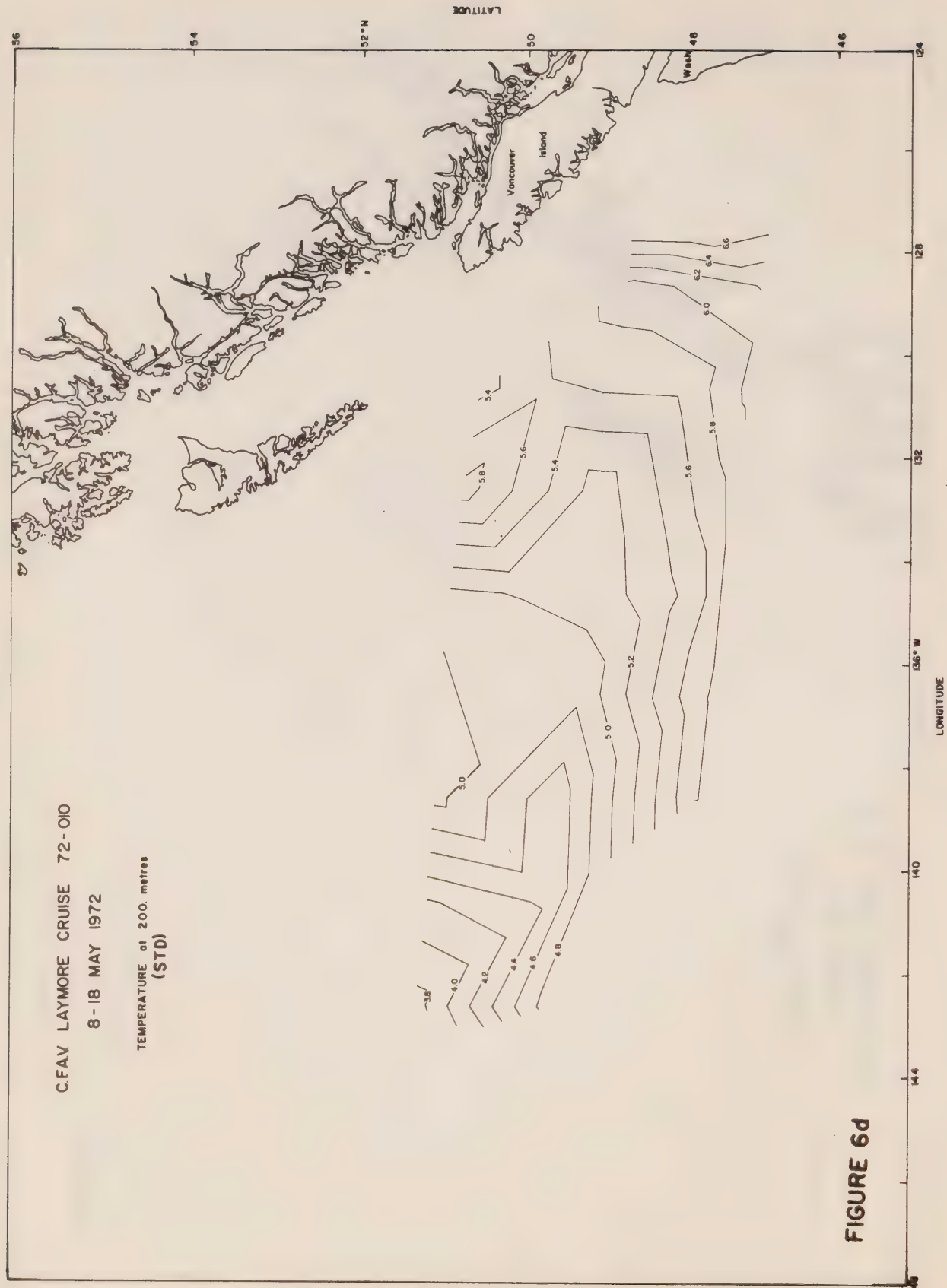


FIGURE 6d

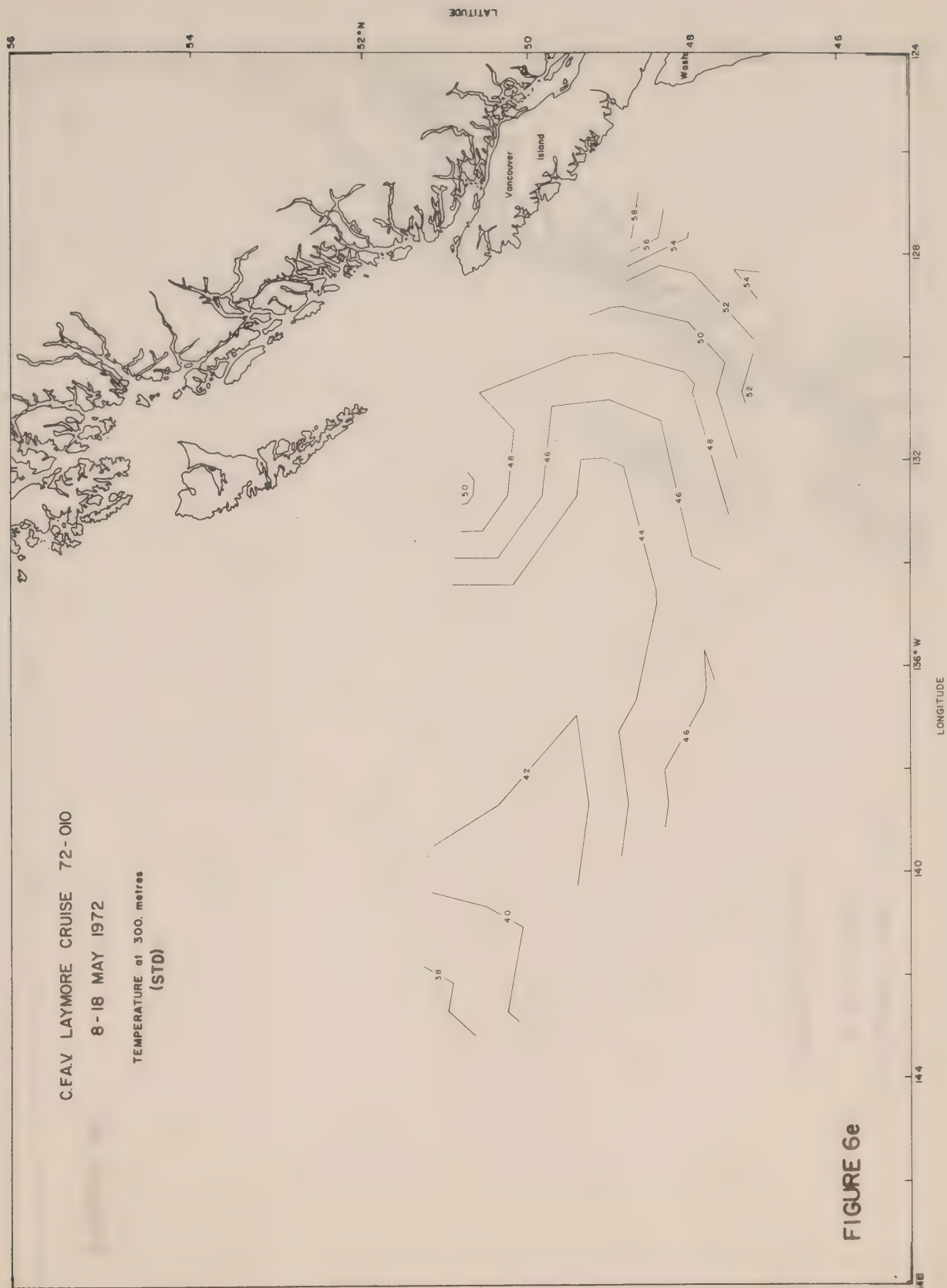


FIGURE 6e

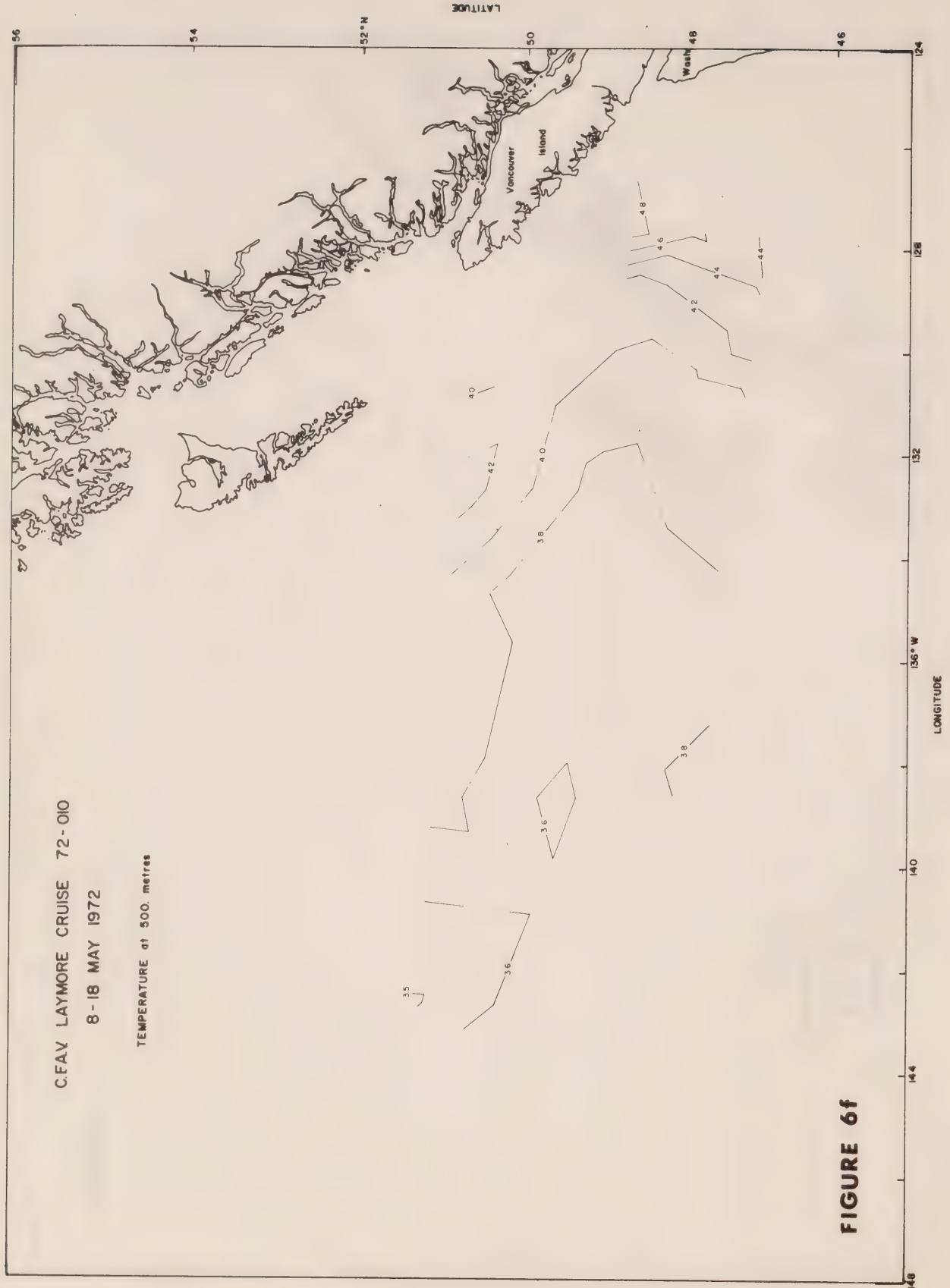


FIGURE 6f

C.FAV LAYMORE CRUISE 72-010
8-18 MAY 1972

TEMPERATURE at 1000. metres
(STD)

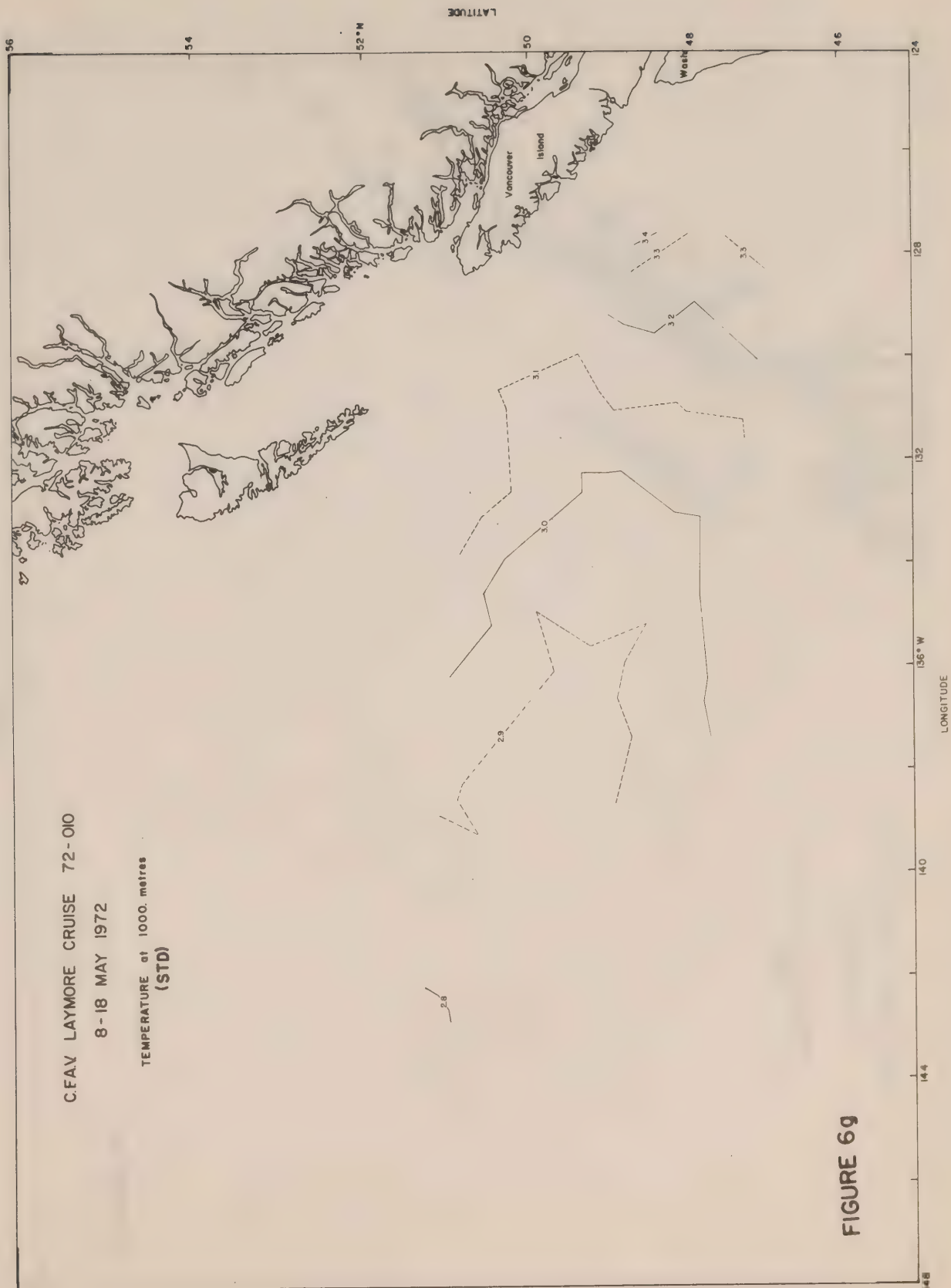


FIGURE 69

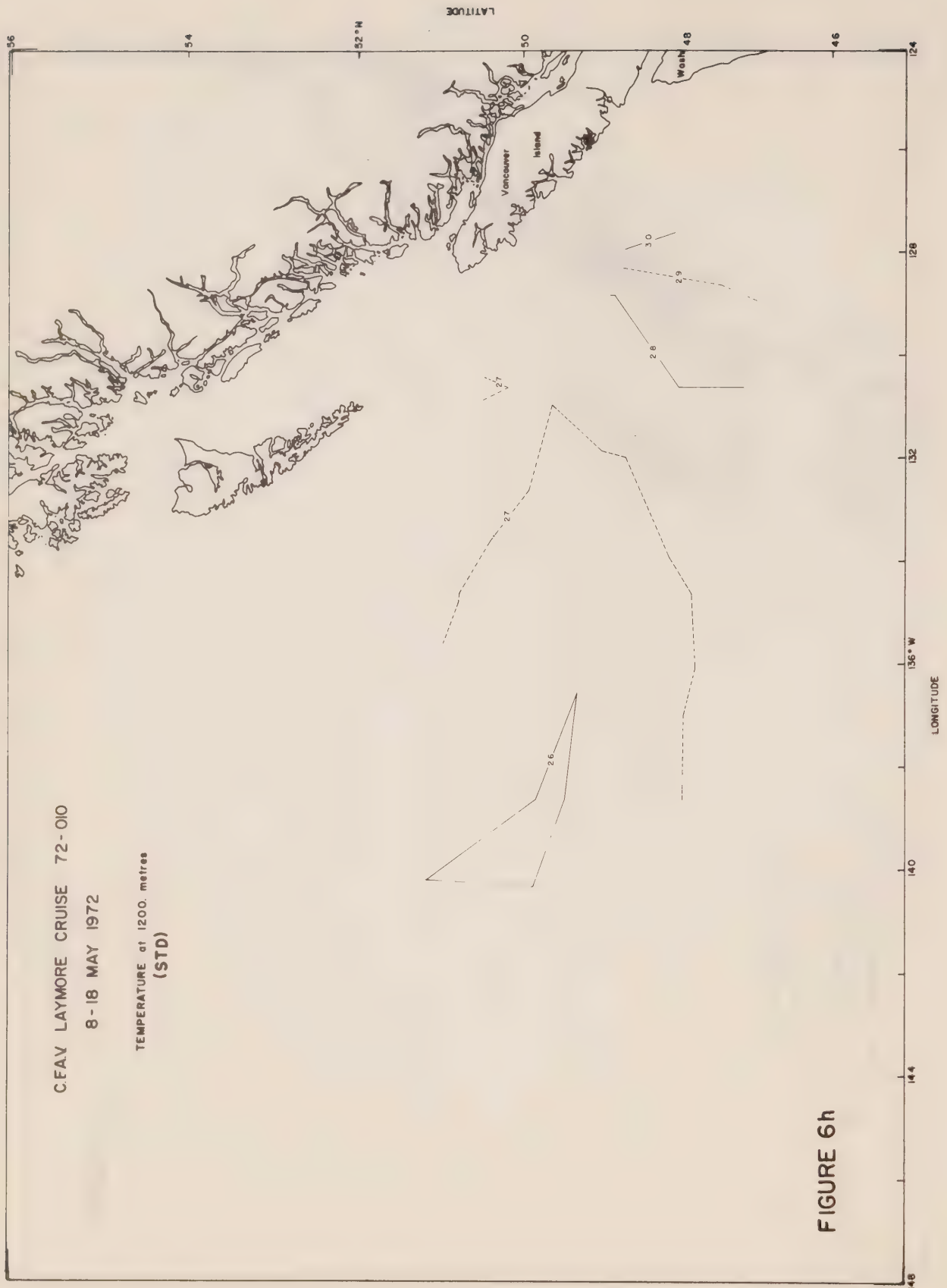


FIGURE 6h

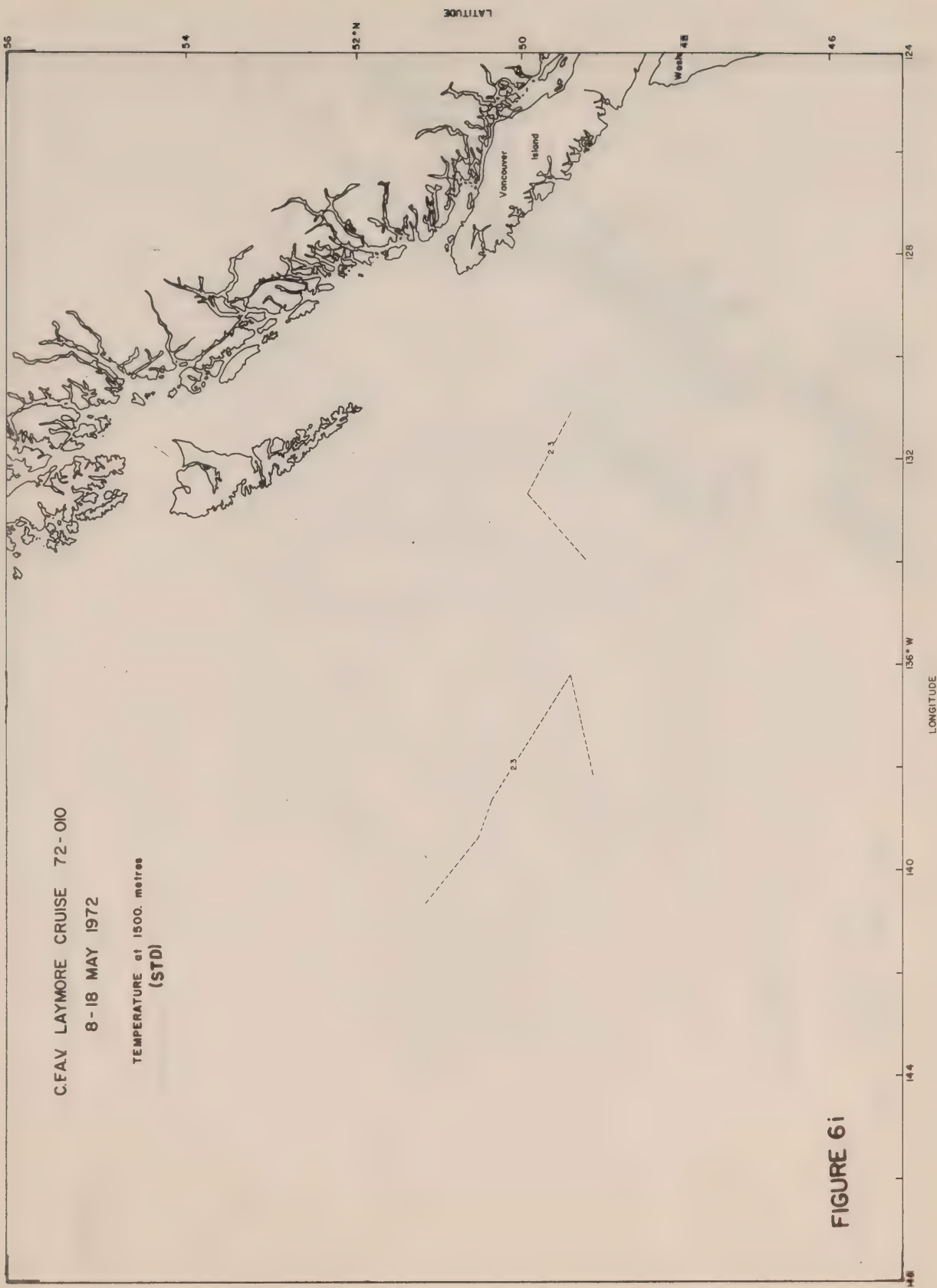


FIGURE 6i

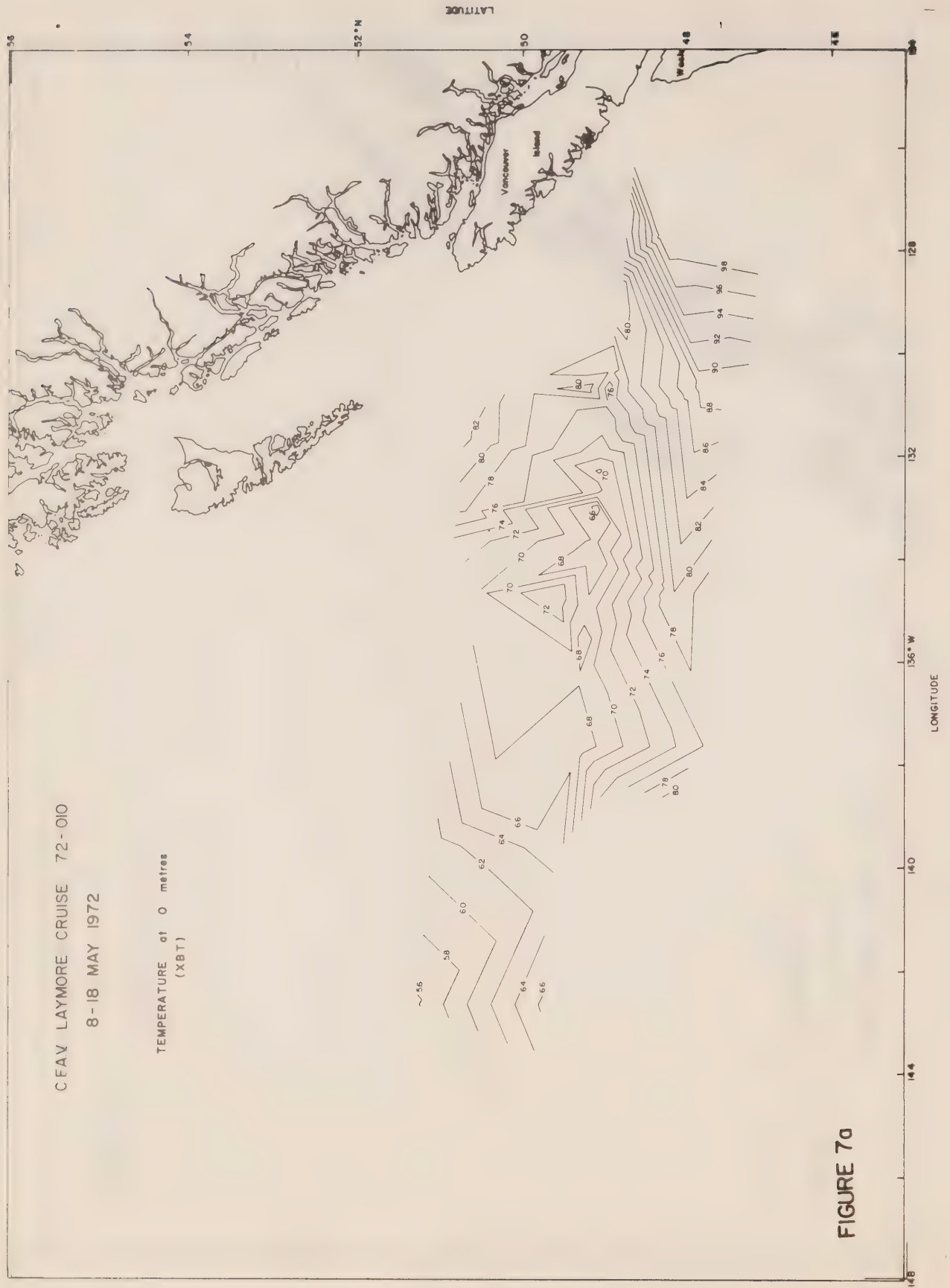


FIGURE 7a

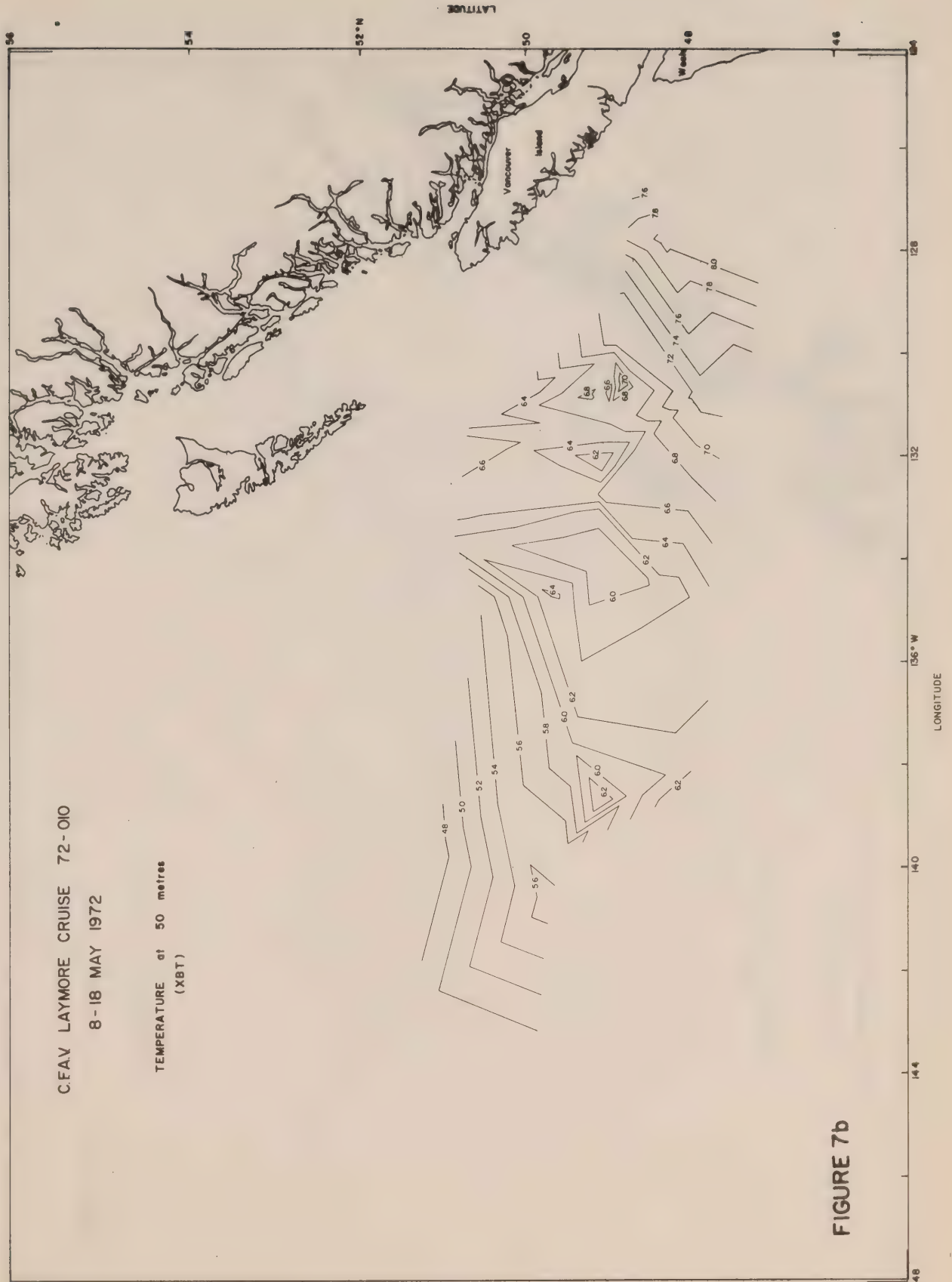


FIGURE 7b

CEAV LAYMORE CRUISE 72-010
8-18 MAY 1972

TEMPERATURE at 100 metres
(XBT)

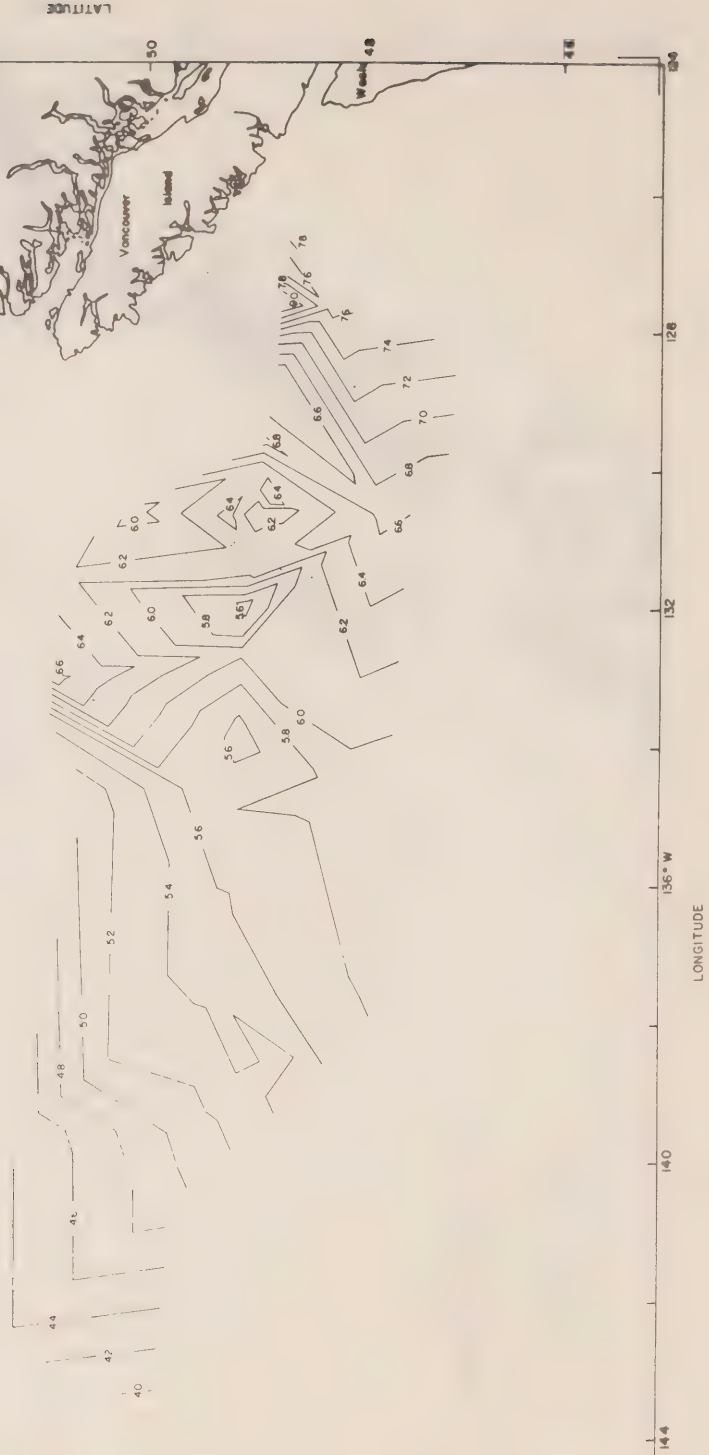
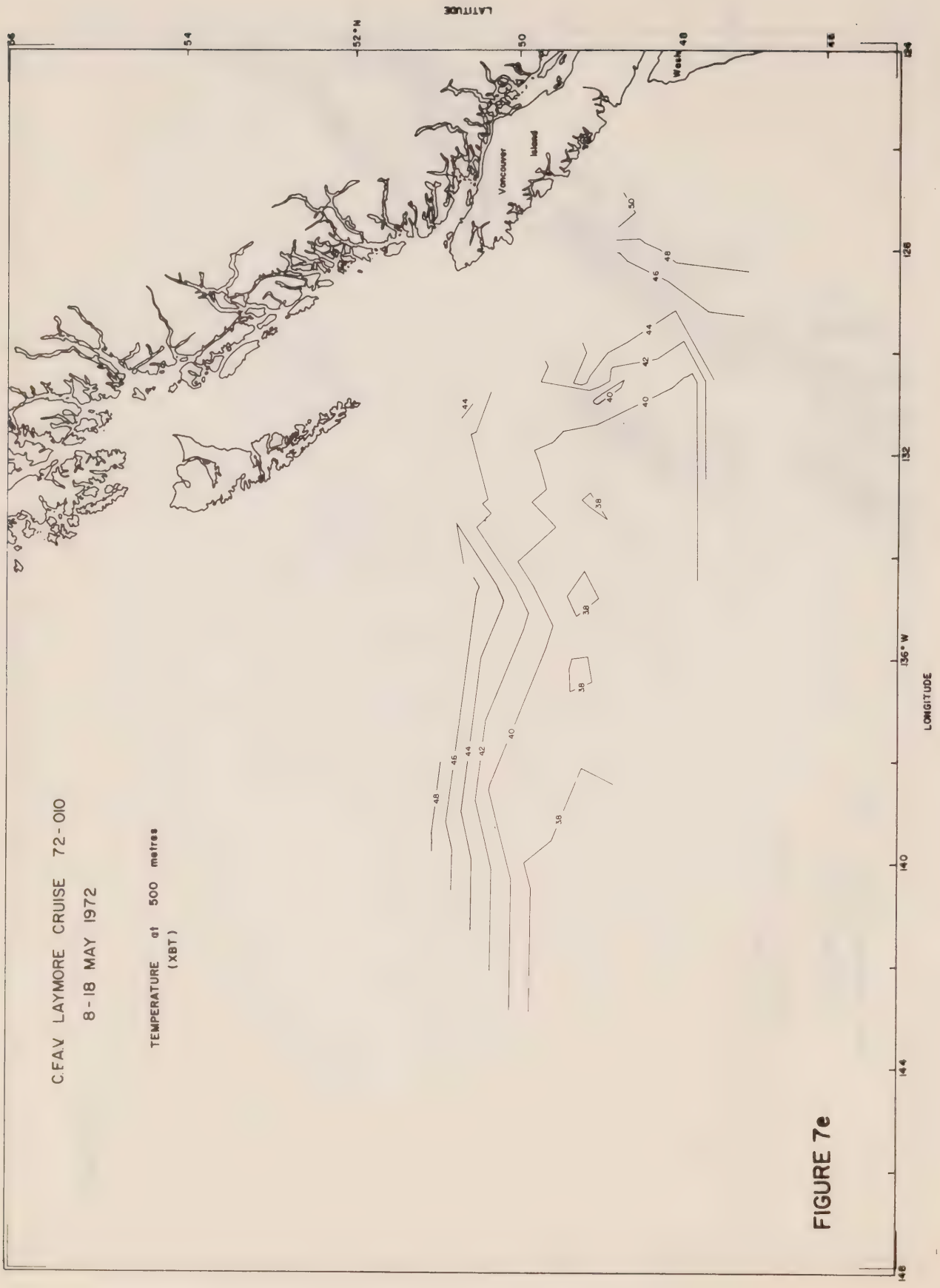


FIGURE 7c



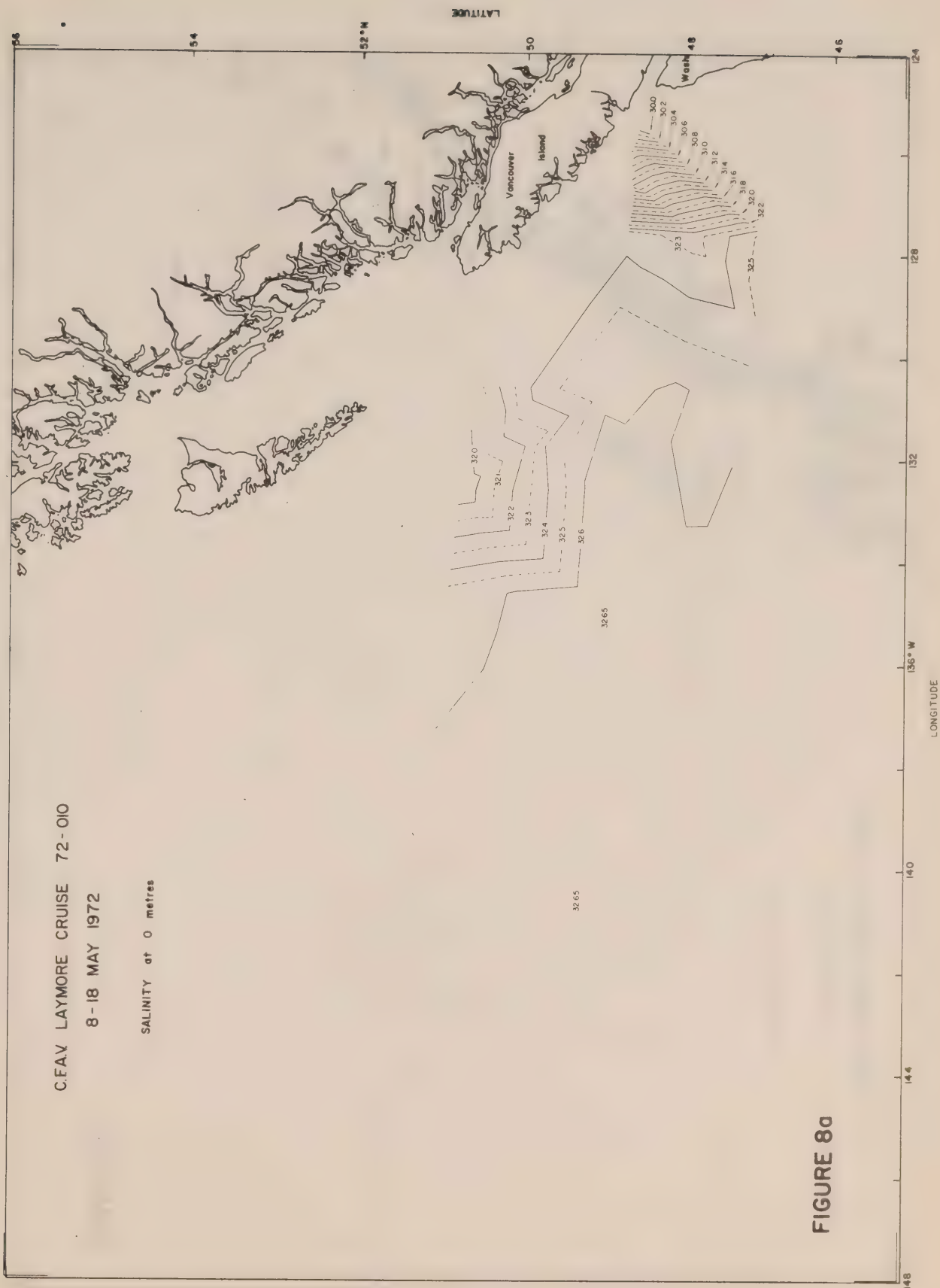
FIGURE 7d



CFAY LAYMORE CRUISE 72-010
8-18 MAY 1972

TEMPERATURE at 500 metres
(XBT)

FIGURE 7e



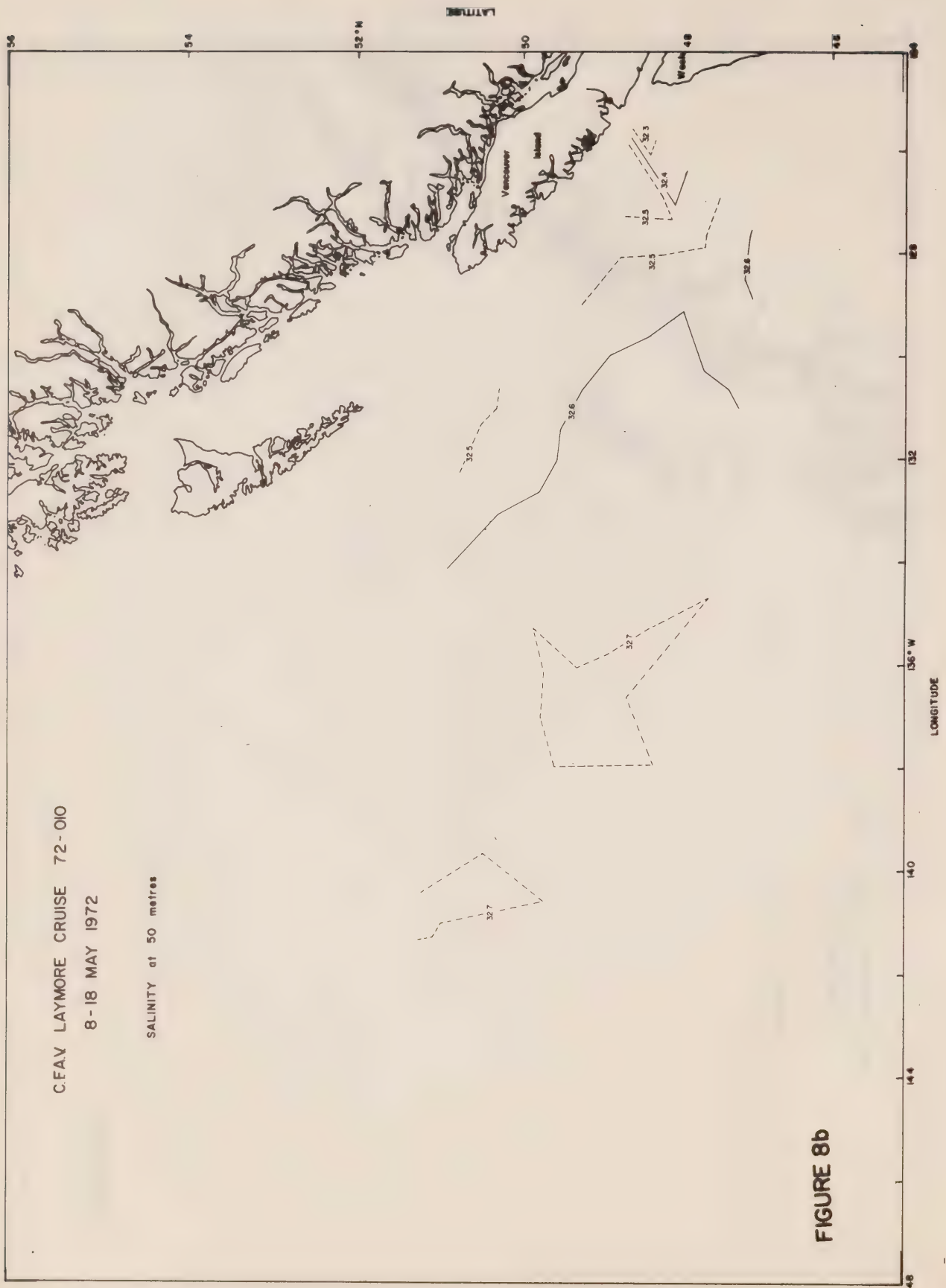


FIGURE 8b

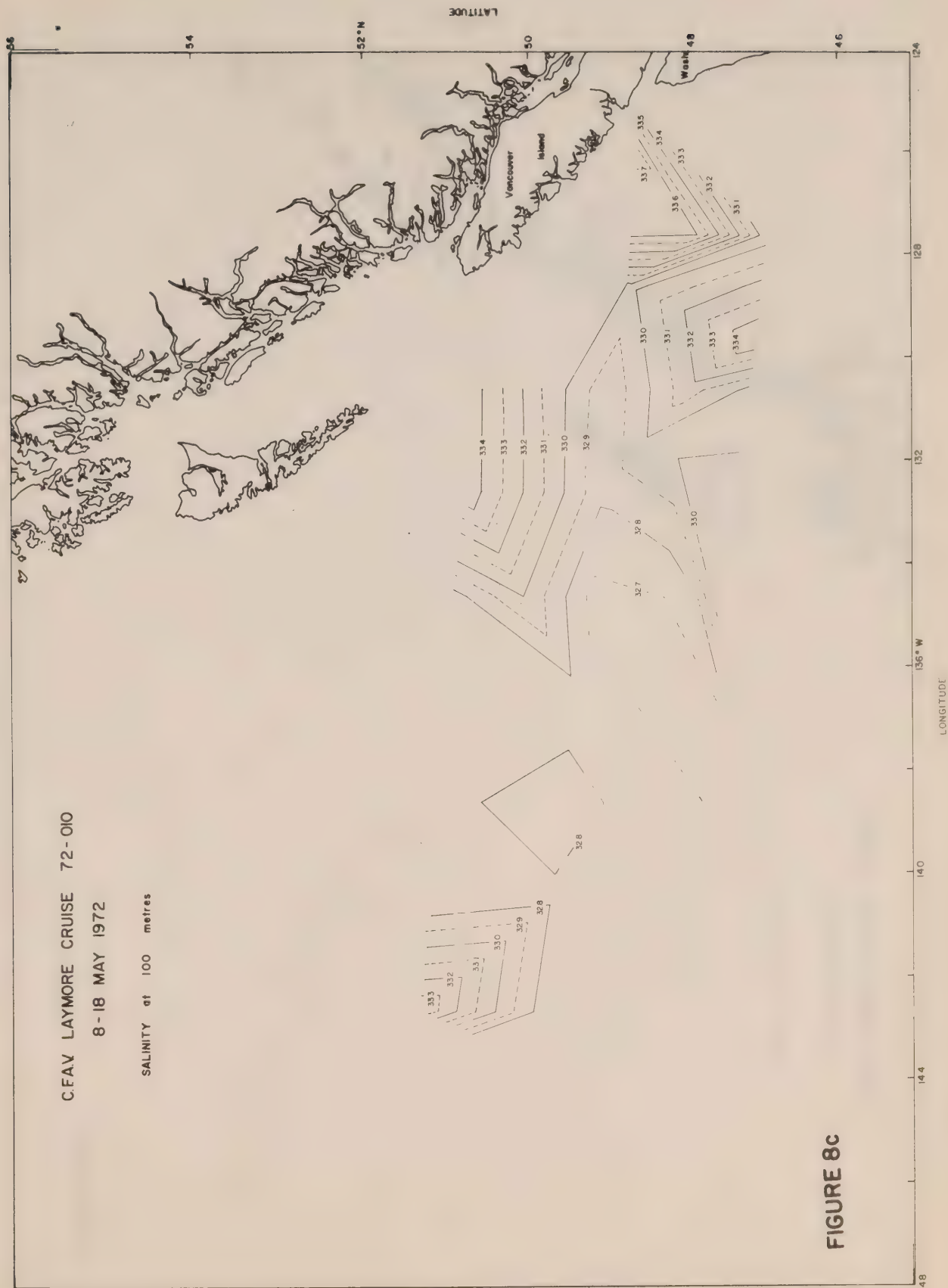


FIGURE 8c

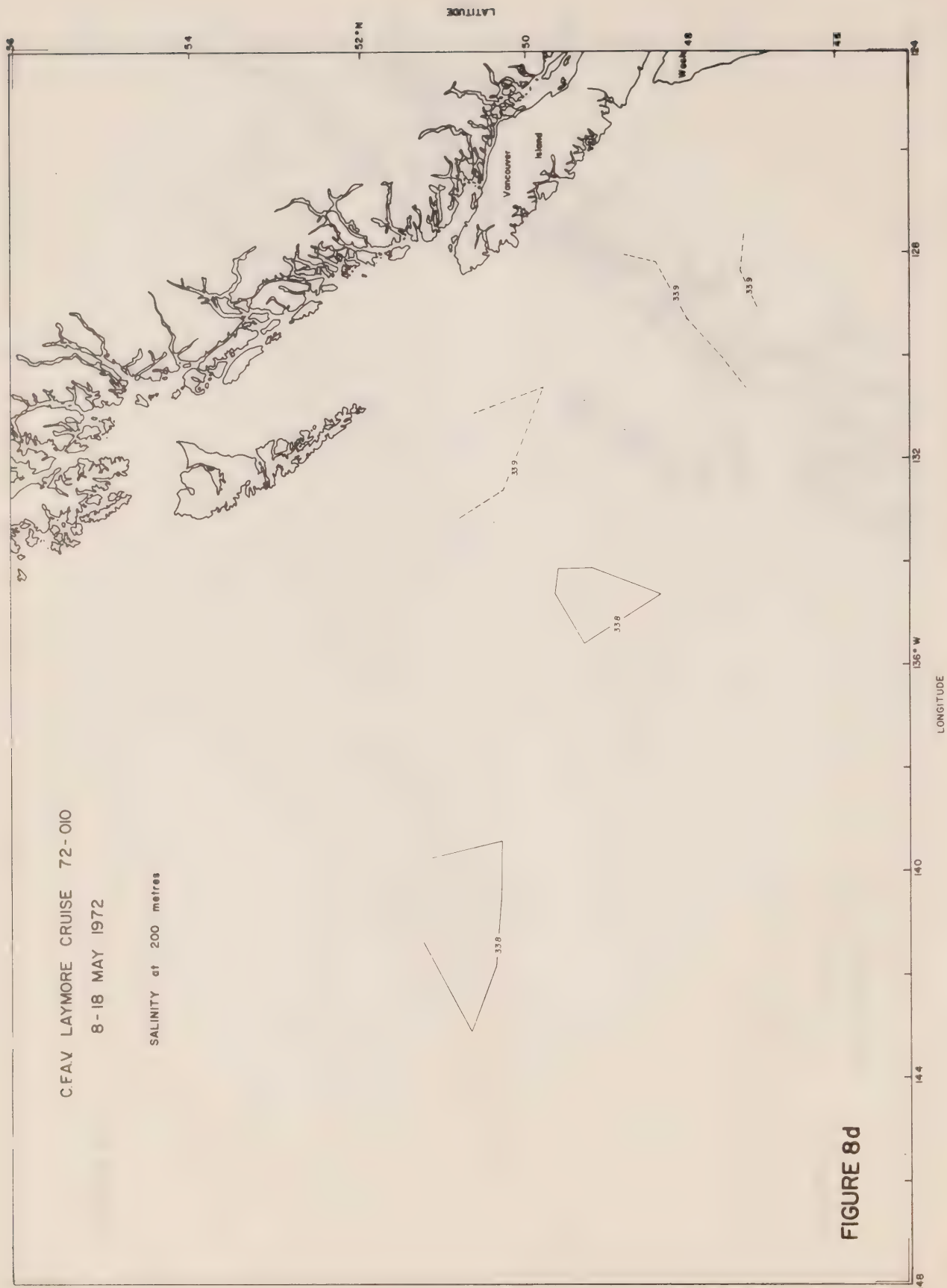


FIGURE 8d

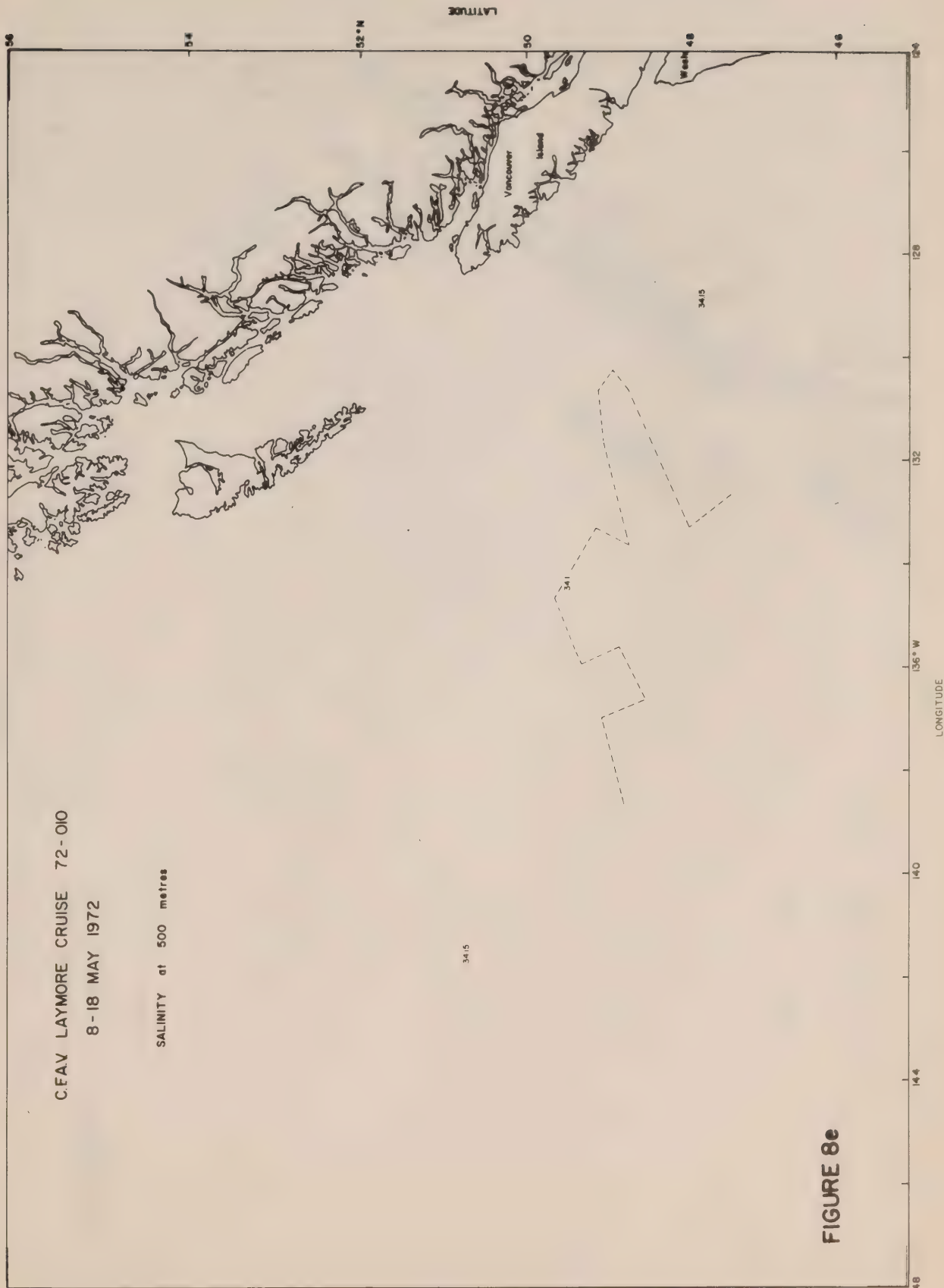
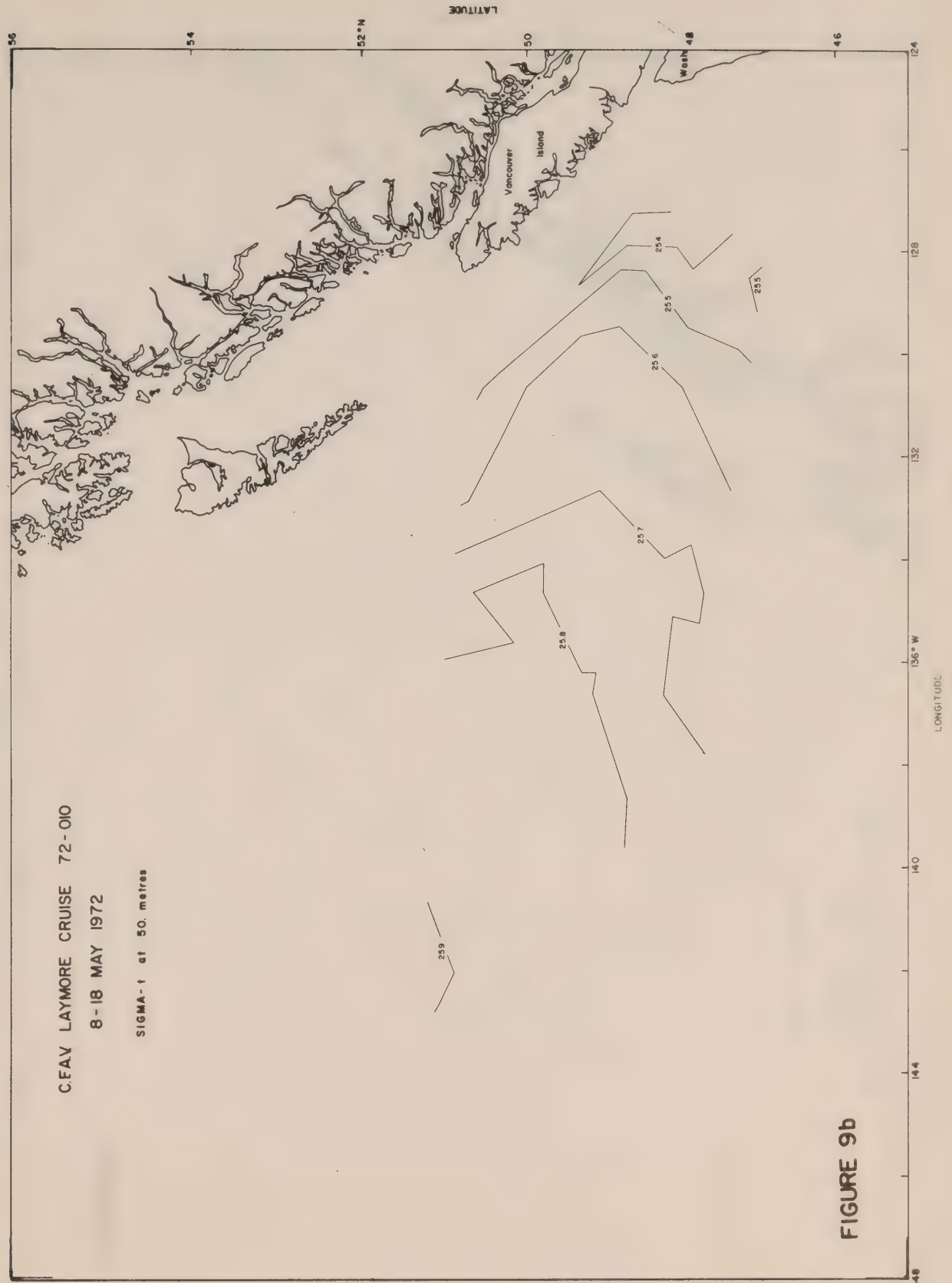


FIGURE 8c





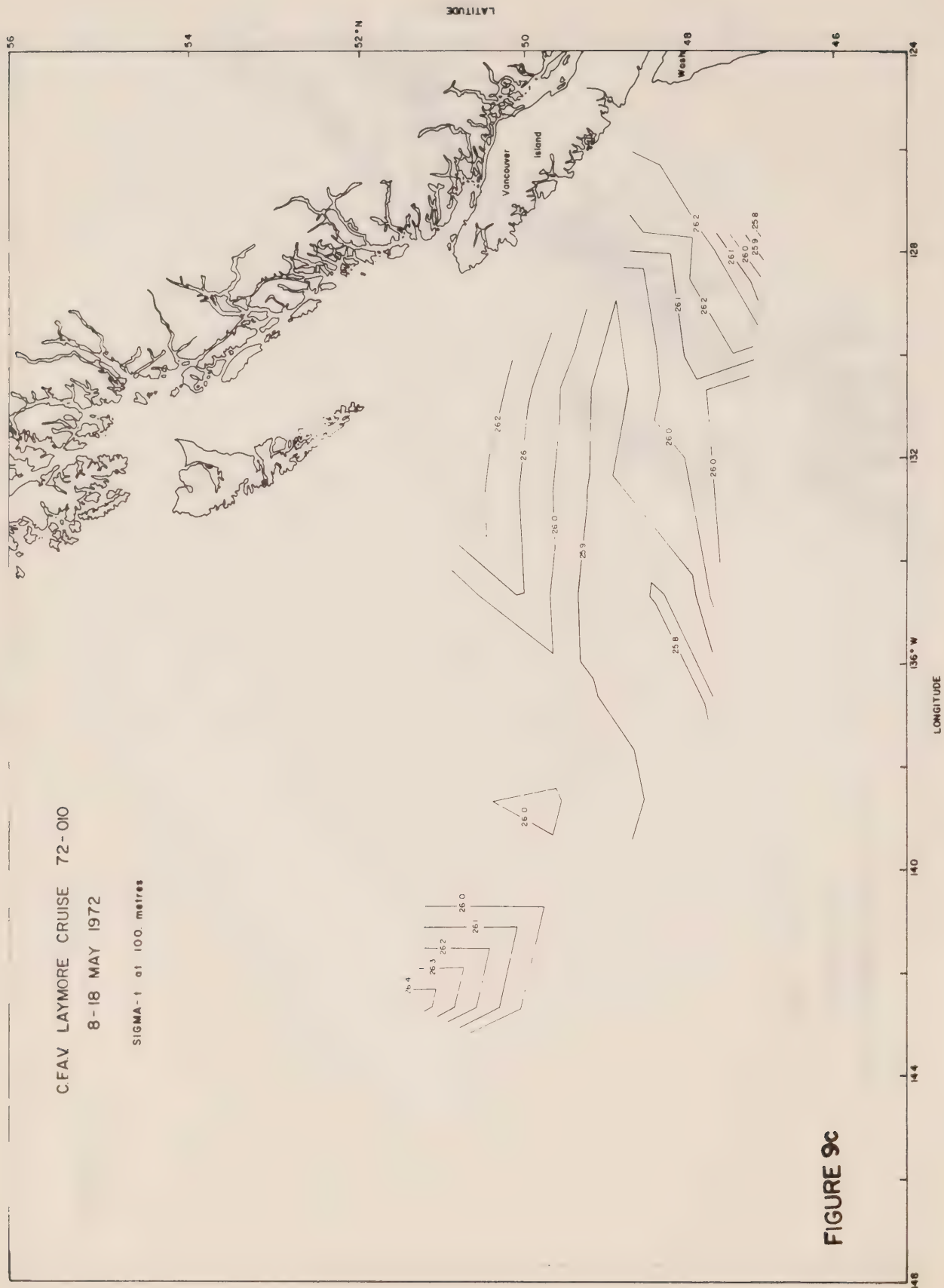




FIGURE 9d

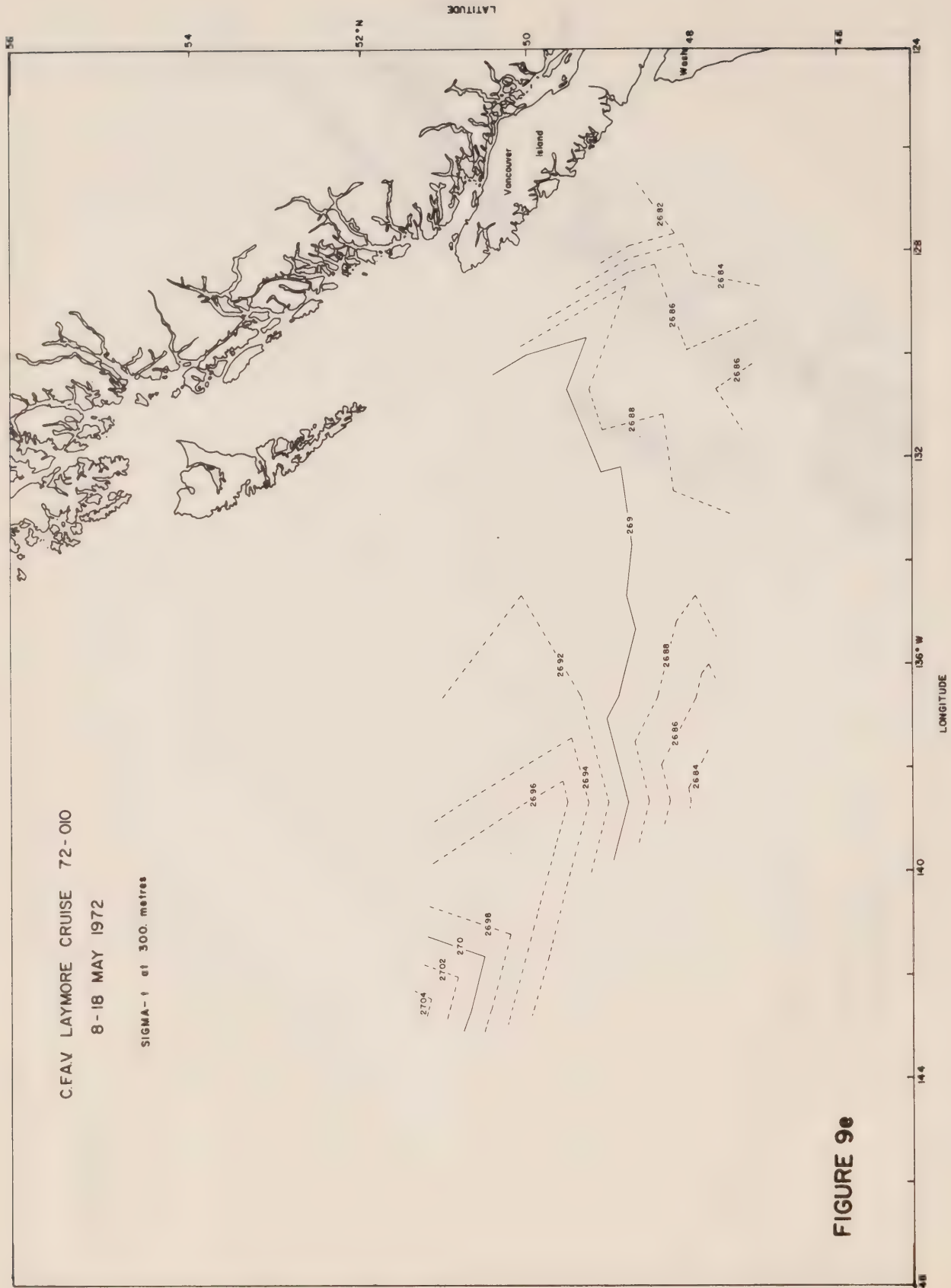


FIGURE 90



FIGURE 9f



FIGURE 9g



FIGURE 9h

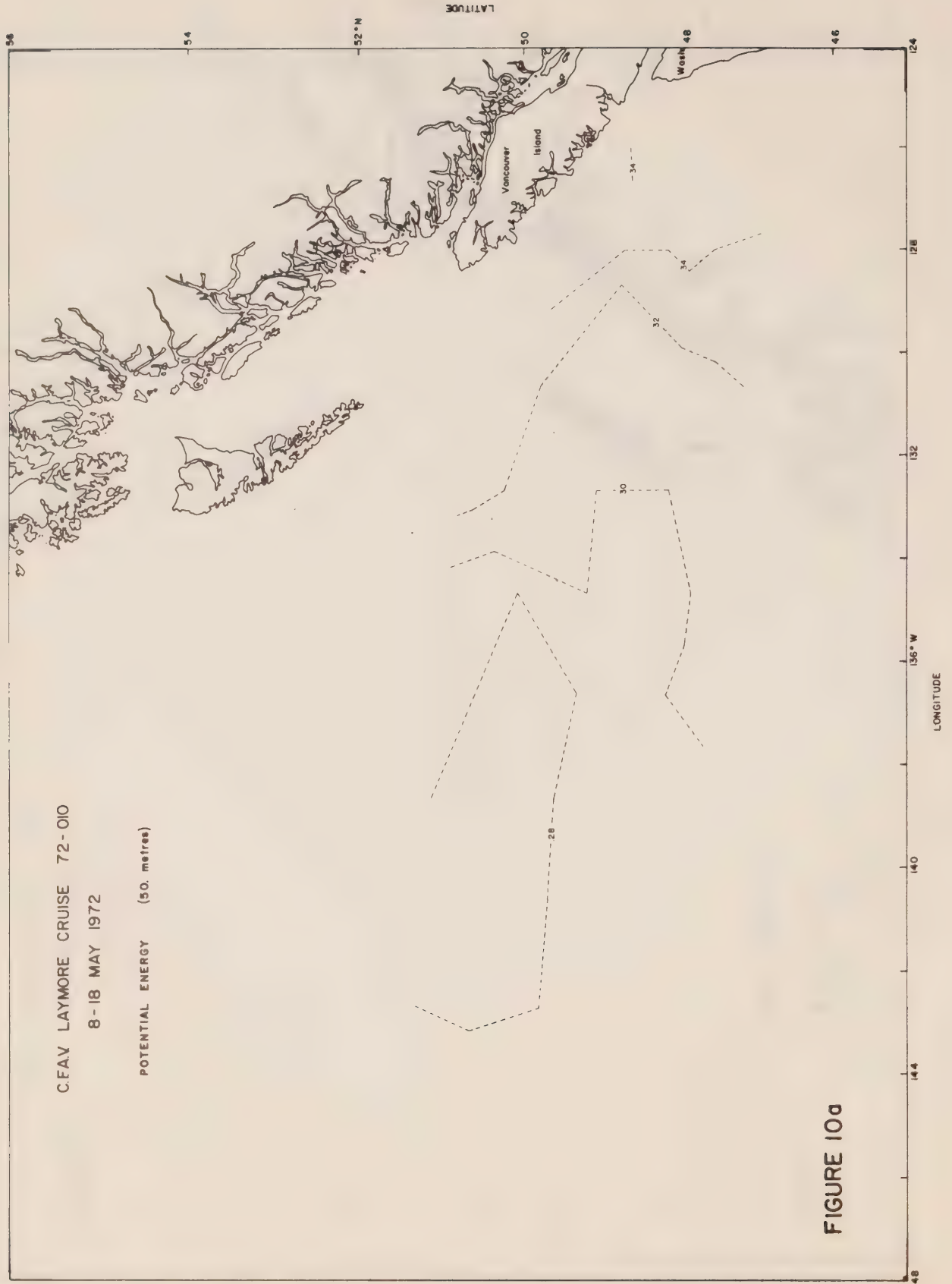


FIGURE 10a

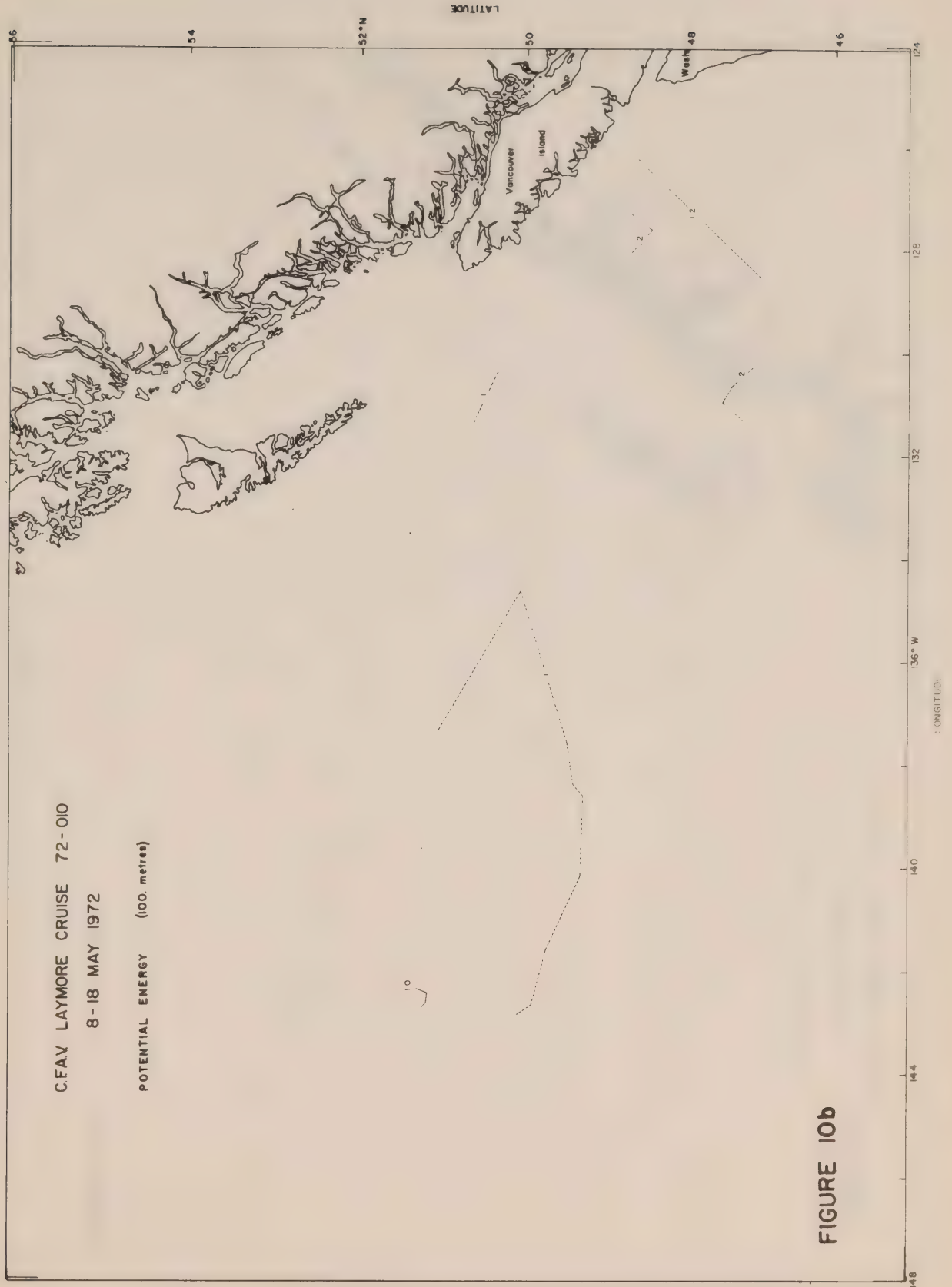


FIGURE 10b



FIGURE 10c





FIGURE 10e

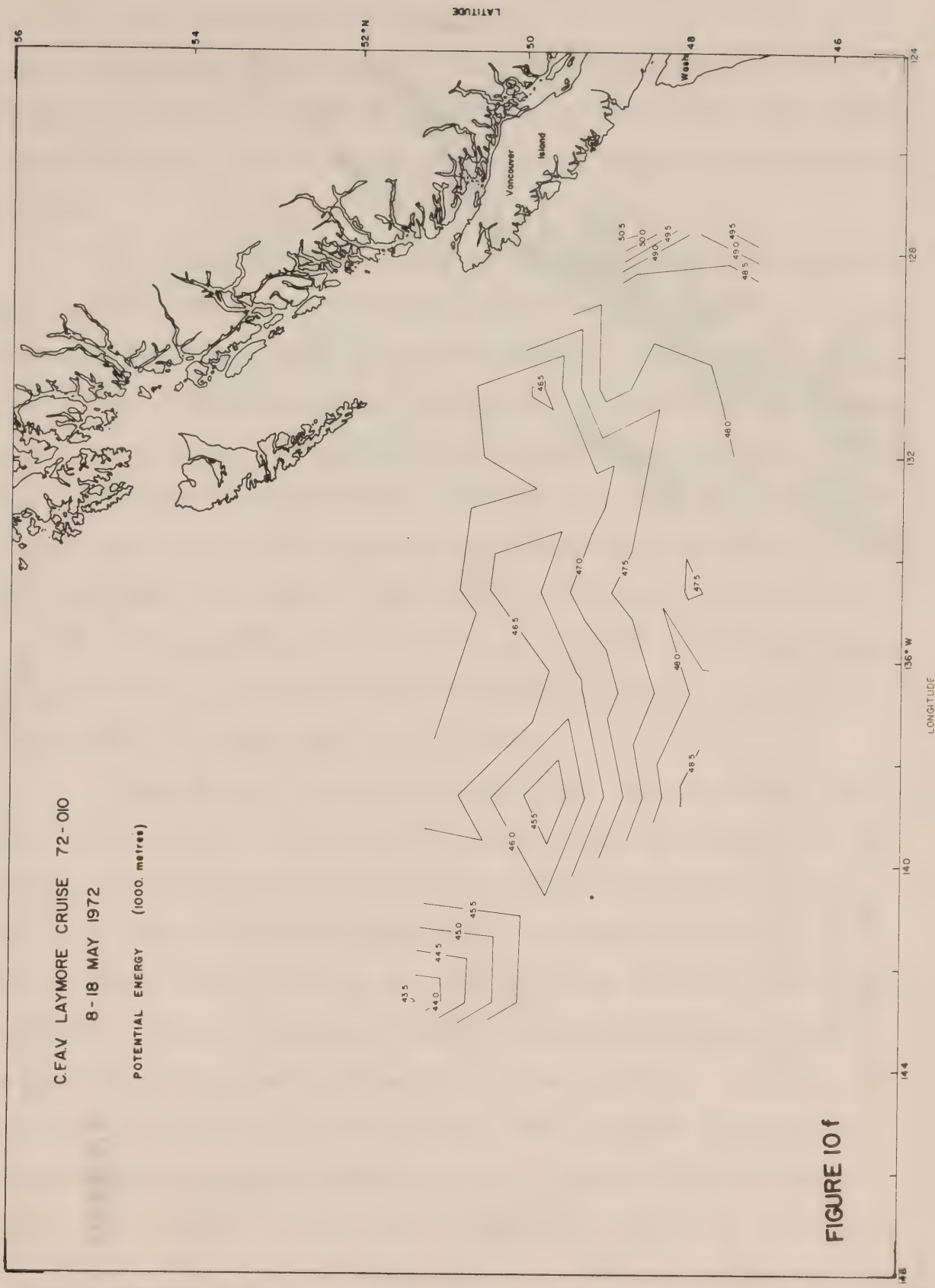
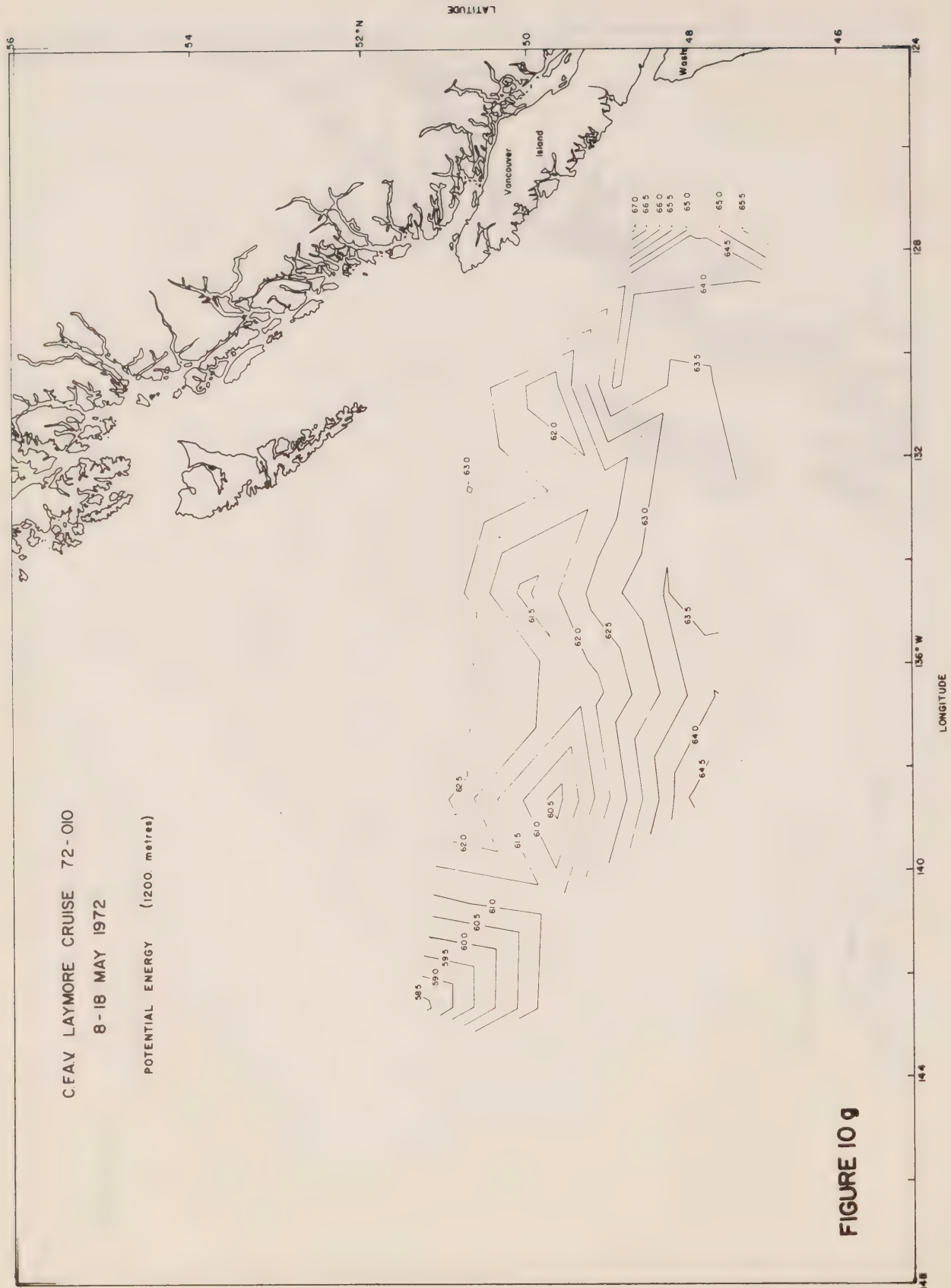


FIGURE 10 f



2.3. A surface temperature comparison

The solid line in figure 11 is a plot of the surface (0 m) temperature obtained from the STD versus time of observation. Corresponding temperature values from XBT traces (x) and bucket samples (o) have also been included.

Up to and including consecutive station 14, which marked commencement of the shore-bound portion of the cruise, the STD values are consistently lower than those obtained by the other two methods. During the inbound legs, however, the difference between the STD and bucket values appeared to fluctuate in sign as well as magnitude (no on-station XBT's were taken). These remarks are clearly demonstrated by figure 12a which gives the bucket temperature minus the STD temperature and the bucket temperature minus the XBT temperature versus time of observation. Furthermore, the curves show that the difference between the bucket temperature and the XBT temperature is consistently less than that between the STD and the bucket but that the fluctuations in the two cases remain in phase.

Since May is a period of net solar flux into the upper layers of the subarctic Pacific, the above differences are for the most part related to the existence of temperature gradients in the upper 1 meter of water. Thus, the STD, which must be lowered at least a meter into the water to avoid spiking of the signal due to surfacing during ship roll, will measure a slightly different temperature than that from the bucket sample which essentially gives an average temperature in the top 30 cm. In the case of the XBT, its thermistor requires a finite time to respond to the ambient temperature and so can be expected to give a slightly different reading than either the STD or bucket sample. Nonetheless, figure 12a indicates that this response time is at least rapid enough to attain ambient temperatures

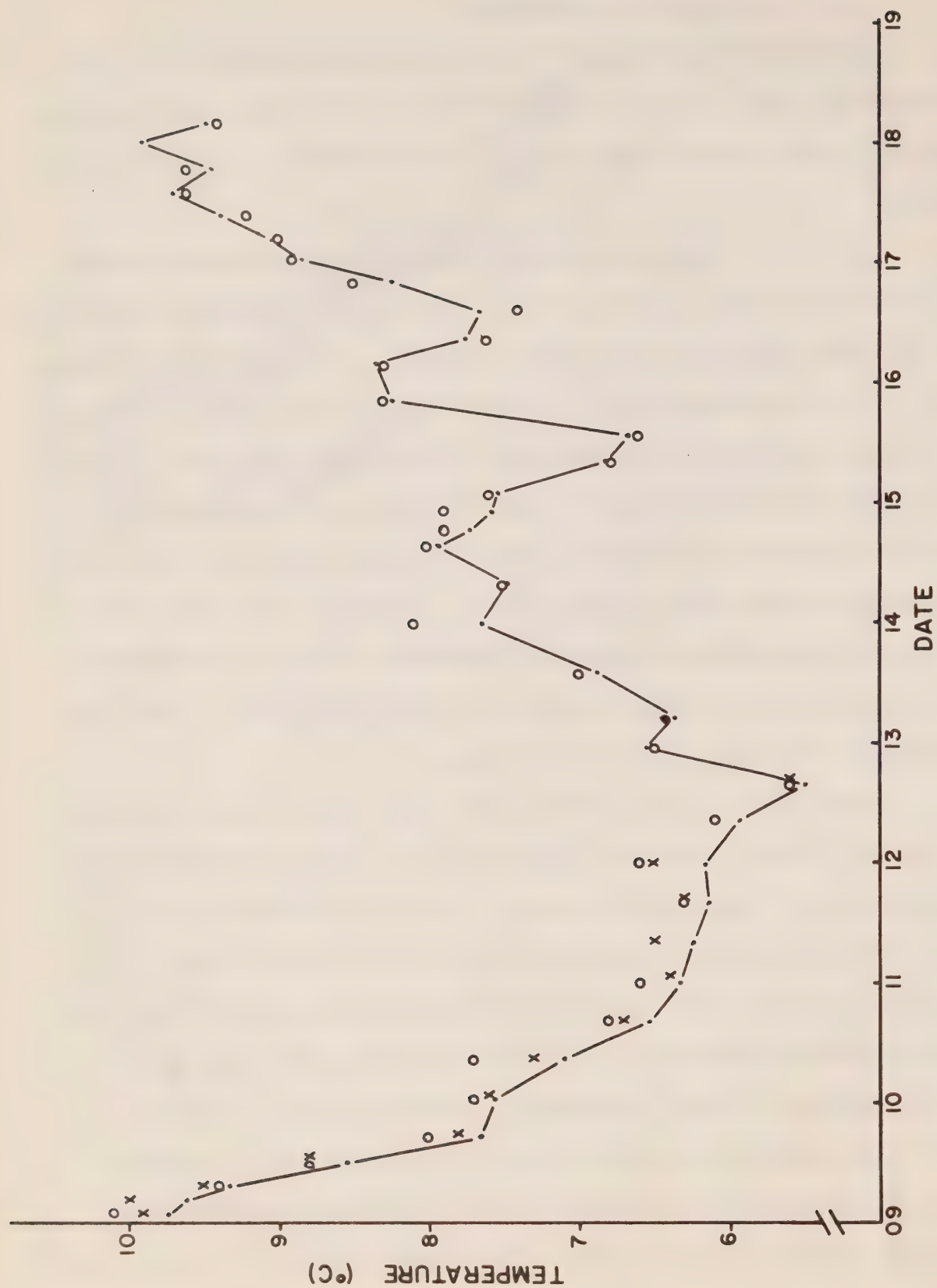


FIGURE 11: Sea surface temperatures versus time, • S.T.D.; • Bucket; x X.B.T.

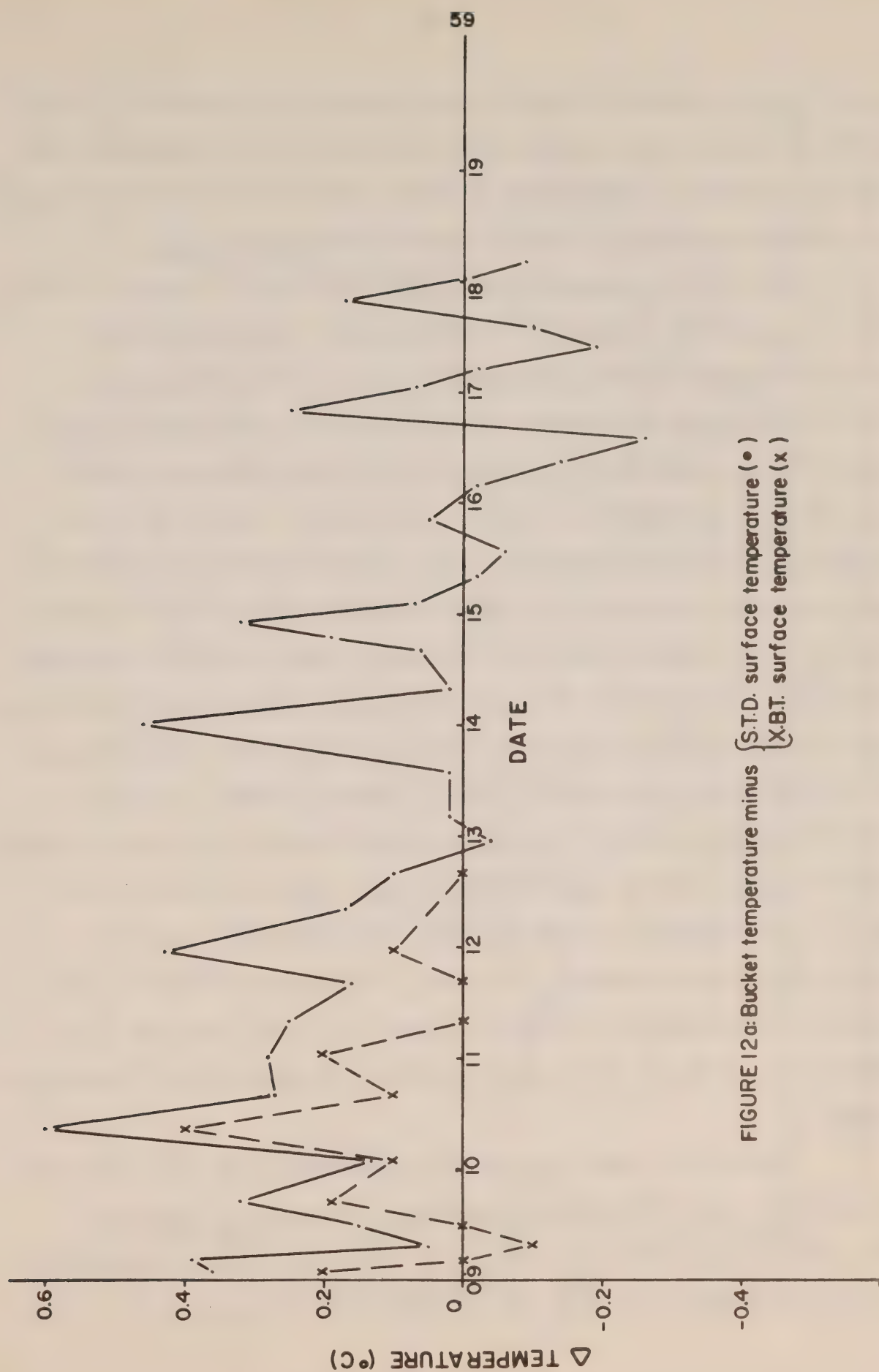


FIGURE 12a: Bucket temperature minus { S.T.D. surface temperature (•)
X.B.T. surface temperature (x) }

before a depth comparable to that of the 'surface' STD is reached. In fact, in five of the thirteen available cases the bucket and XBT temperatures were identical to within $\pm 0.05^{\circ}\text{C}$ which is rather surprising when one considers that the individual accuracies of these instruments is at best $\pm 0.1^{\circ}\text{C}$.

On first considerations, the diurnal variation in the solar heating would be expected to account for a large portion of the difference in temperature measured by the three methods. Based on this effect alone, greatest differences should occur sometime in the afternoon when the surface layer is being heated the most. Contrarily, smallest differences should occur at night when radiative cooling is at a maximum. According to the LAYMORE data, this would appear to be the situation particularly from May 14 onward where positive peaks occur regularly between noon and 1700 hrs PDST ($= \text{GMT} - 7 \text{ hrs}$). Similar peaks are also seen to occur in the air temperature at about 10 m (figure 12b). Moreover, the negative values suggest significant cooling of the top thin layer usually takes place at night. The difficulty in relating cooling to a radiative effect, however, is that it is much too large in relation to the air-sea temperature difference -- the latter difference being either small or negative (figure 13a). Also, at times prior to May 14, the succession of maxima and minima in figure 12a is far less regular than would be expected. The large air temperature of May 13, for example, is associated with a negative bucket - STD value while the large positive peak on May 10 is not associated with a corresponding air temperature maxima.

Some of the latter features may be explained if we now include the effect of the wind. The negative temperature differences in figure 12a which existed after May 15 are probably the result of the night-time surface cooling and mixing of the winds that had attained speeds greater than 10 knots

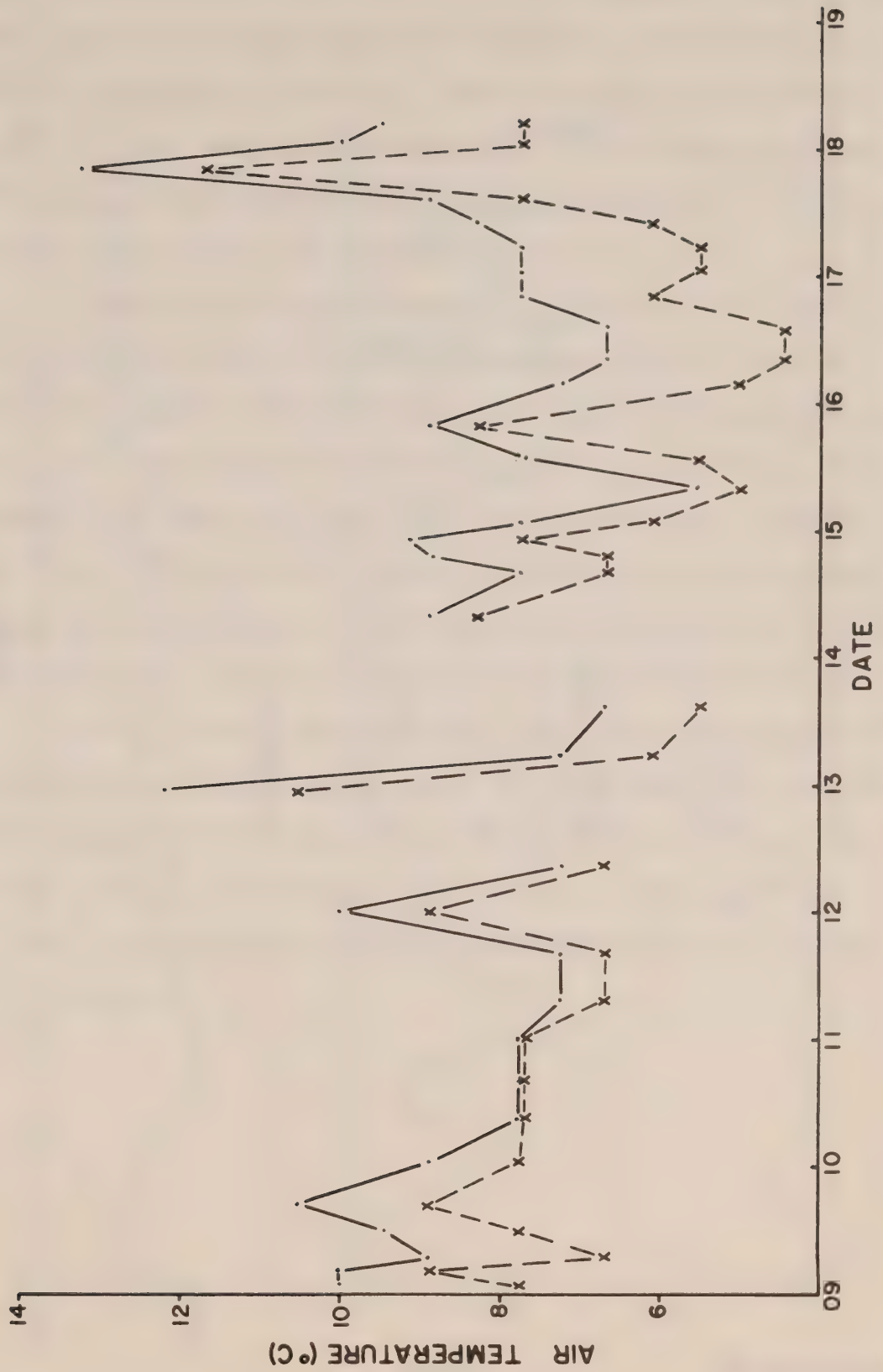


FIGURE 12b: Air temperature at 10 meters at time of LAYMORE S.T.D. casts: • dry bulb; x wet bulb

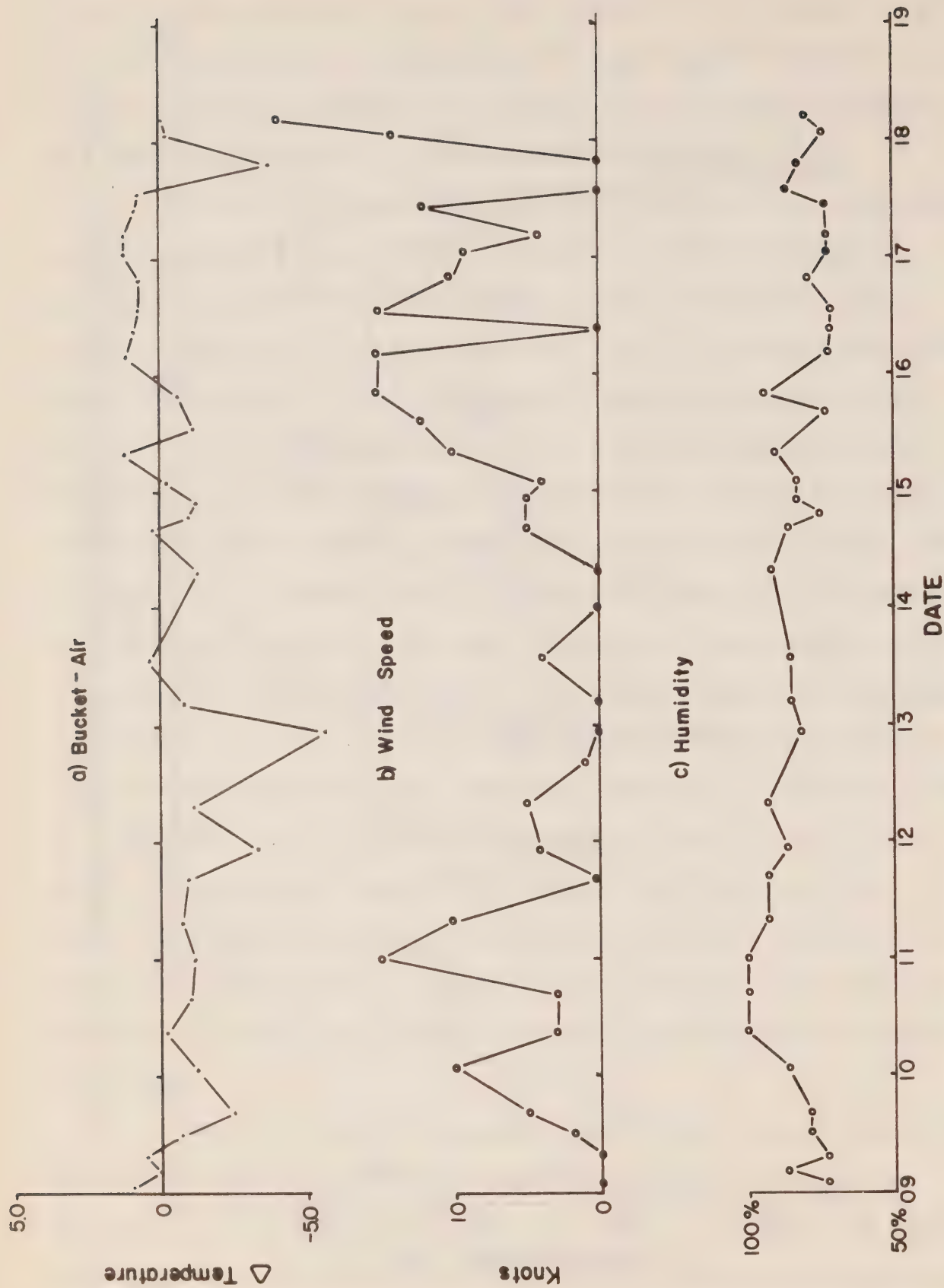


FIGURE 13: a) Bucket temperature minus air temperature (10 m)

b) Wind speed at 10m

c) Relative humidity (10m)

on these occasions (figure 13b). The relatively low daytime values during the 10th, 11th and 15th appear also to be related to wind strength maxima. The minimal temperature differences at 0700 GMT on May 9 and 2300 GMT on May 13, on the other hand, are not relatable to wind-strength but to the fact that the sky was completely overcast and a slight drizzle was falling -- the only two days on which the situation occurred.

In connection with the wind-effect, it should be noted that increased winds also result in increased ship drift. Since all sampling was done on the weather side (starboard), there was, therefore, an increased amount of turbulent wake activity and hence mixing at the surface. This, together with the breaking of waves on the hull, would lead to measured surface values indistinguishable from those produced by the winds in the absence of ship interference. It should also be appreciated that instrument and digitizing errors could account for some of the observed differences.

Finally, a comparison of humidity (figure 13c) obtained from the air temperatures of figure 12b with use of figure 12a, indicates a fairly good correspondence between the bucket - STD temperature difference and water vapor content. In particular, the trends in the two graphs are almost identical as might be expected for phenomena arising as a result of surface heating.

2.4. A Surface Salinity Comparison

A plot of the surface salinity obtained from the STD and bucket samples is illustrated in figure 14a. The low values, including those centered around the 16th of May, are associated with the coastal zone off the B.C. coast and are a result of river discharge together with local advection. The effect of these is further indicated by figure 11 which shows that temperature maxima are coincident with each of the low salinity regions.

For the most part, figure 14b indicates that the bucket salinities are larger than the STD salinities although differences less than $0.05^{\circ}/\text{oo}$ may not be significant because of the limited STD accuracy. Furthermore, in the near-surface layer of water, temperature gradients produce spikes which must be smoothed out. This introduces an additional uncertainty of about $\pm 0.01^{\circ}/\text{oo}$. Nonetheless, it would appear that the surface water sampled by the bucket was slightly more salty than that just below the surface. This, together with the absence of discernable transient haloclines in the top few meters, suggests that prolonged periods of evaporation which would account for such a situation were only beginning to take place. The large peak that occurs on the 17th of May, however, may be an example of persistent localized evaporation since it also corresponds to the occurrence of a positive temperature gradient at the ocean surface (figure 12a).

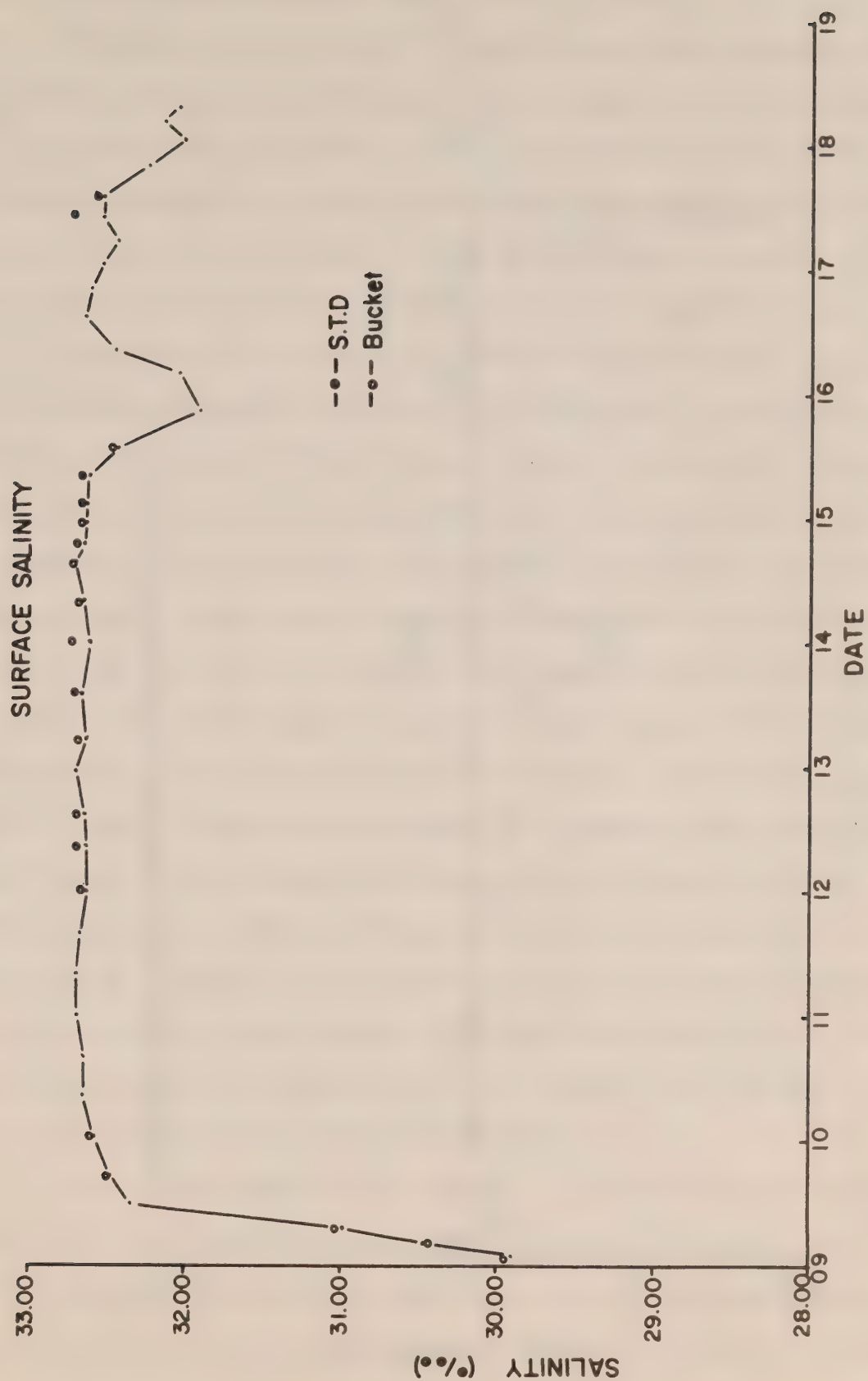


FIGURE 14a: Sea surface salinity versus time, ● S.T.D.; ● Bucket.

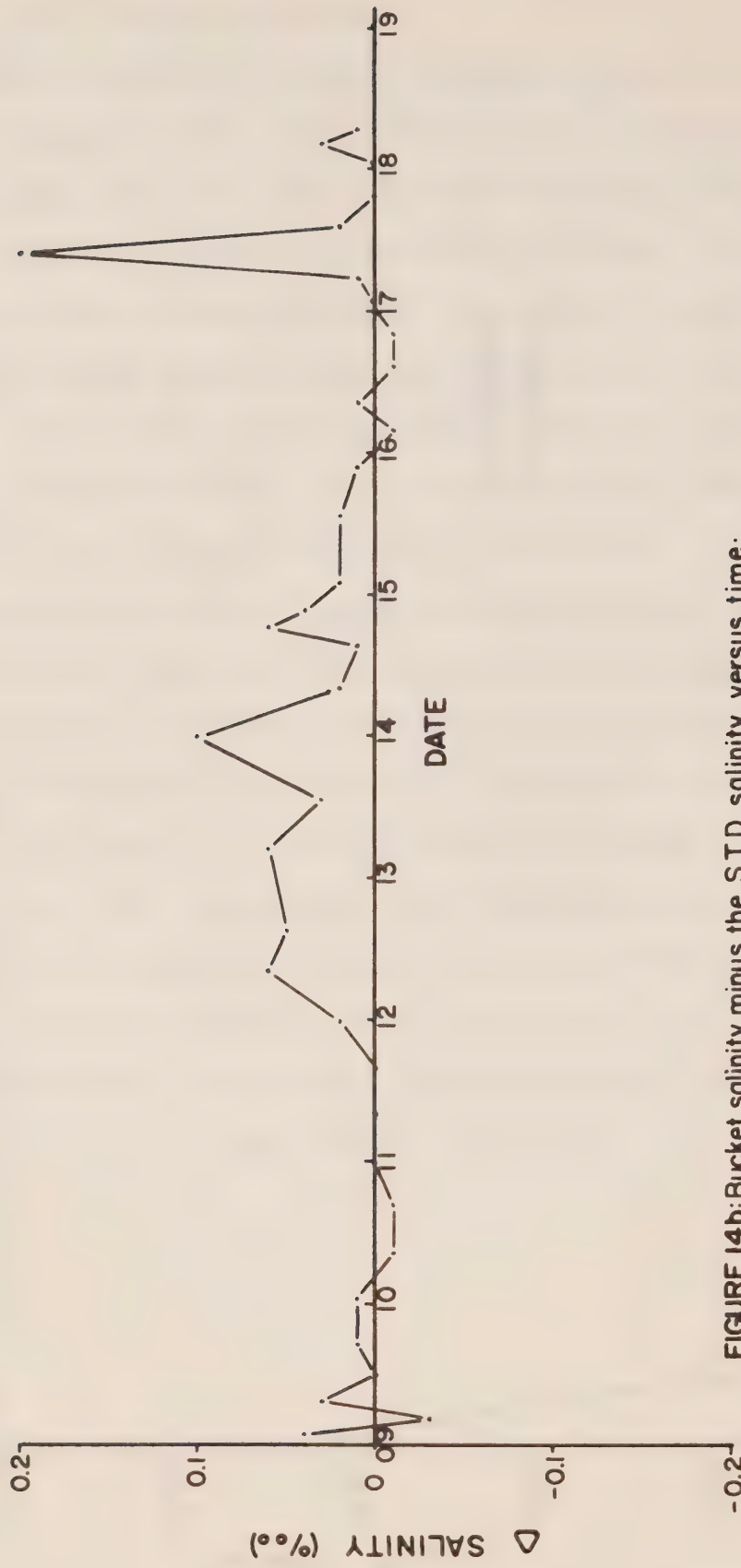


FIGURE 14b: Bucket salinity minus the S.T.D. salinity, versus time.

2.5. Tidal/Inertial Motions in the Vicinity of Line P

The subarctic Pacific water is typified by a large permanent halocline between about 100-200m over which the salinity increases from approximately $32.5^{\circ}/\text{oo}$ to approximately $34.0^{\circ}/\text{oo}$. As a result, the $33.0^{\circ}/\text{oo}$ and $33.5^{\circ}/\text{oo}$ isohalines are located well within the depths of most vertically stable water. The time variations in the depths of these surfaces should, therefore, be indicative of any vertical motions occurring at their respective levels.

Plotted in figure 15a are the depths of the above isohalines versus the observation time for the LAYMORE STD casts (those for the VANCOUVER and QUADRA are also included). Some of the variability is, of course, attributable to the spatial trend in the mean depth that was associated with all oceanographic properties in the region. Their relative shallowness in the coastal region, for example, was clearly contrasted to the deeper levels in the more interior region. In addition, however, there appeared to be a distinctive periodicity to the depth changes at periods one would expect for the tides (~ 12 and 24 hours) and inertial motions (~ 16 hours). Internal waves with periods of minutes to hours and wavelengths of kilometers would necessarily be superimposed on these longer period motions but could not be expected to produce such regular variations between stations which are separated by 2-4 hours and 20-40 kilometers. On the contrary, such spacing would have been sufficient to obtain a nearly regular sampling of any tidal/inertial motions provided their amplitude exceeded those of the internal waves and the spatial trend in the depths of surfaces of constant property.

The relative brevity of the record (~ 10 days) obviously limits the number of tidal constituents that can be identified. Moreover, the fact that the observations were not taken at a fixed location would cause a spatial aliasing of the temporal variations, which in turn would be dependent

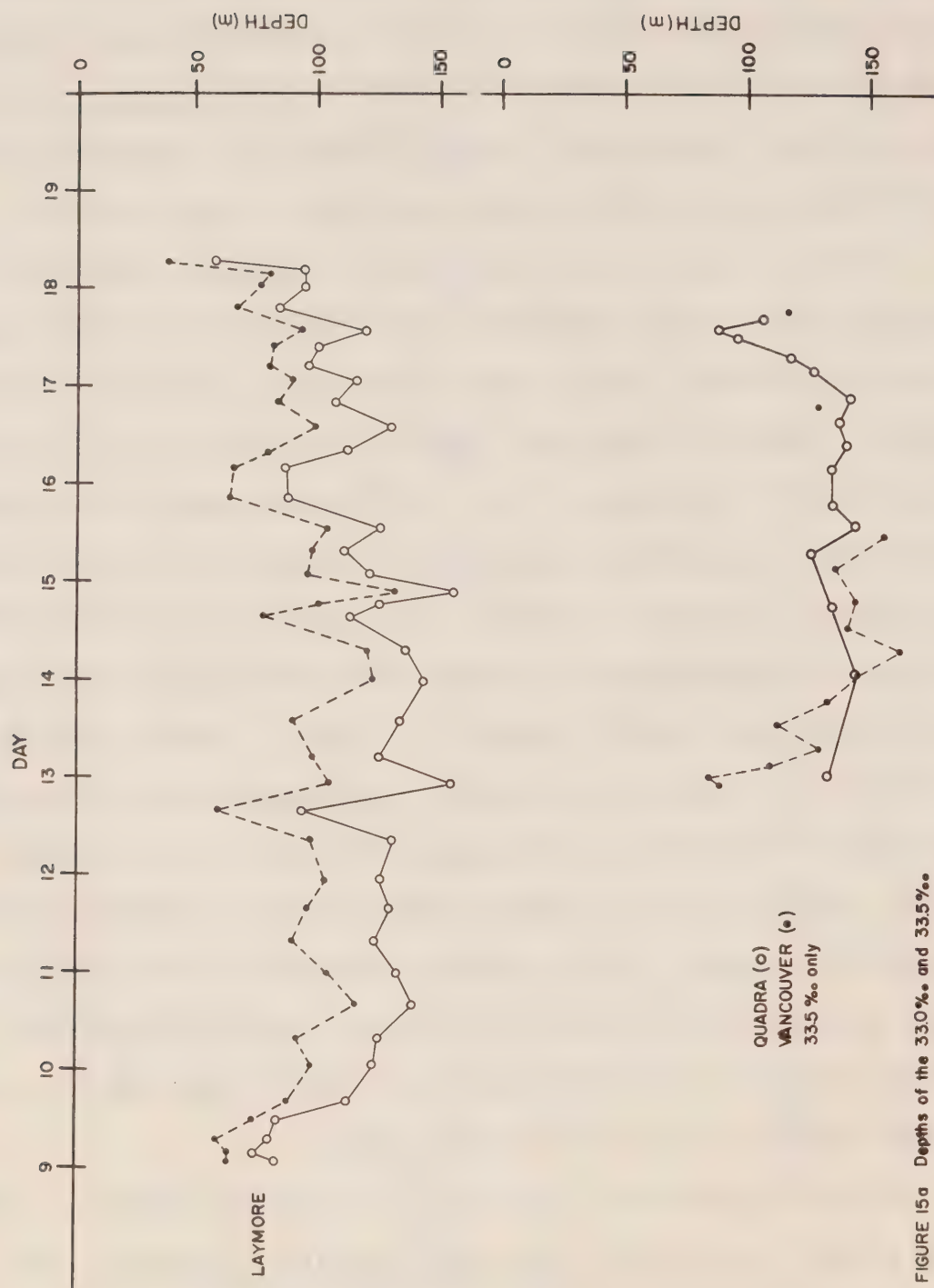


FIGURE 15a Depths of the 33.0‰ and 33.5‰ isohalines versus time; May 1972

on the direction of the ship's course in relation to the direction of tidal/inertial wave propagation. Availability of computer programs to determine the spectrum and the harmonic tidal constituents, however, made analysis worthwhile despite the limitations of the data -- the only step required to meet the input formats being a smoothing of the records to give values every hour (see figures 15b, c).

Figure 15d gives the spectra obtained for the unfiltered time variations in depth of the 33.0⁰/oo and 33.5⁰/oo isohalines (a Fast Fourier Transform method was used to determine the necessary Fourier components). Aside from the large amount of 'energy' associated with spatial trends, there are three main peaks near 4×10^{-2} , 6×10^{-2} and 8×10^{-2} cycles/hour corresponding to the diurnal, inertial and semi-diurnal periods. That the magnitude at the diurnal period appears to be greater than that at the semi-diurnal period may have been due to the separation of hours and tens of kilometers between stations whereby the spectra are determined by the sampling as well as by the actual tidal motions.

The magnitudes of the various tidal constituents for the two isohaline variations is presented in Table II (the inertial period is not included). Analysis has been based on the commonly used relation (Schureman, 1958);

$$h = H_0 + \sum F H \cos(\omega t + V_0 + U)$$

where h = depths of the isohaline surface in meters at time t ,

H_0 = the mean depth over the record length,

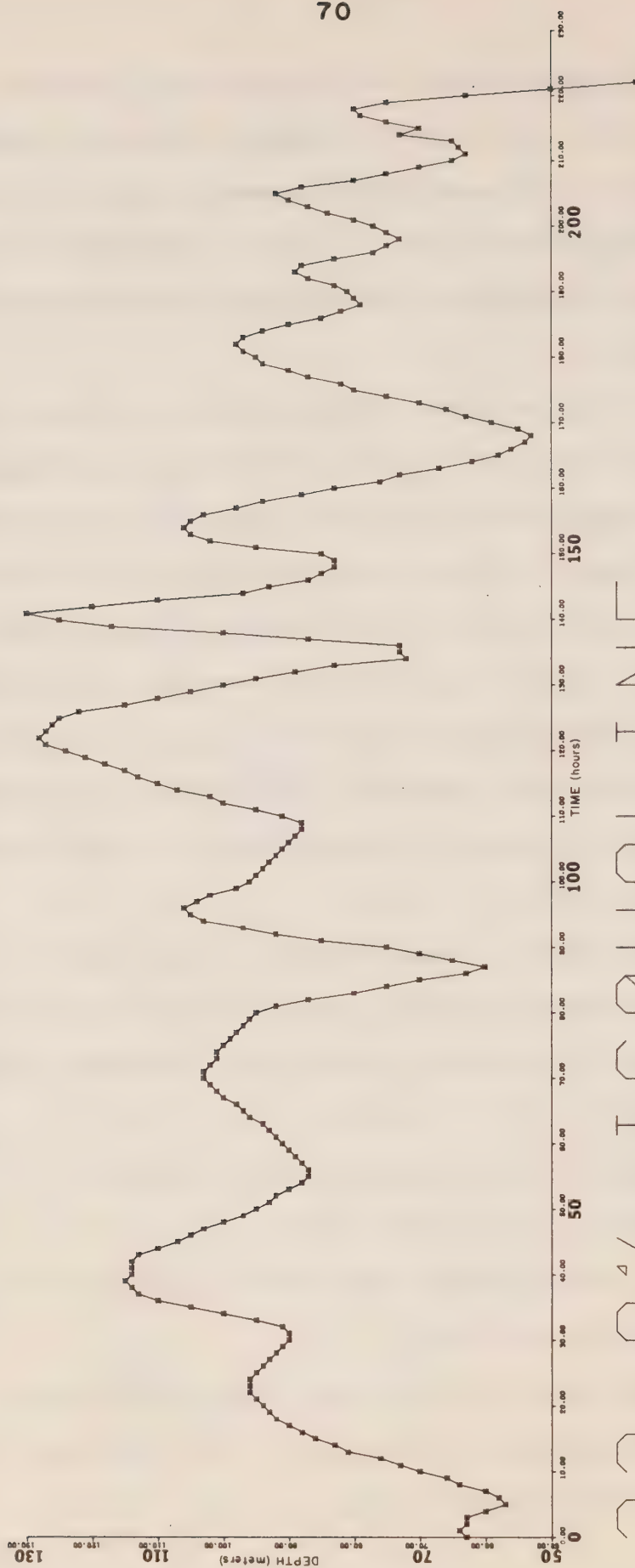
F = factor for reducing the mean amplitude H to the year of calculation,

ω = frequency of the constituent,

t = time reckoned from the initial epoch (midnight 1973), and

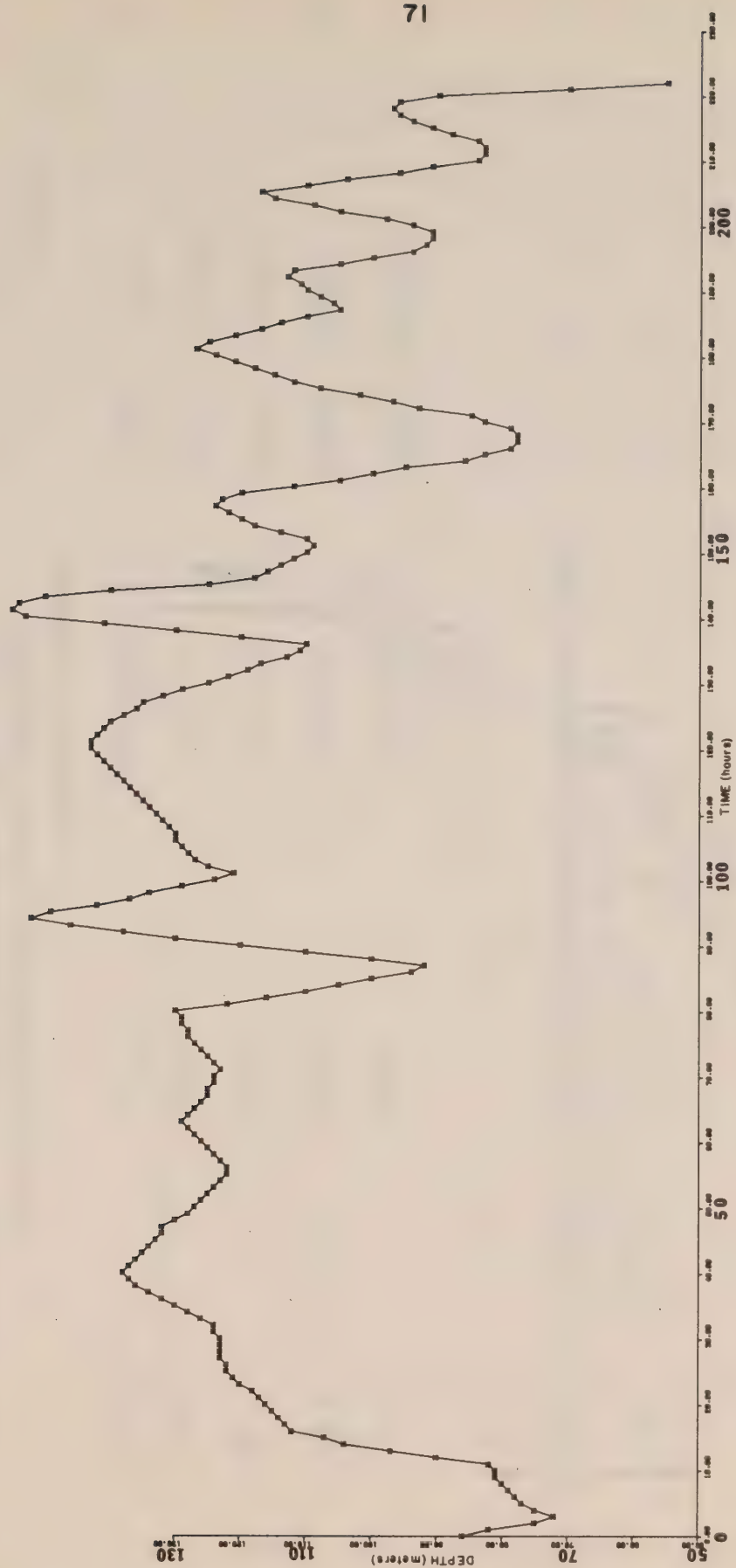
$V_0 + U$ = value of the equilibrium argument of the constituent when

$t = 0$ (longitude dependent).



33.0% ISOHALINE

FIGURE 15b



33.5% ISOHALINE

FIGURE 15c

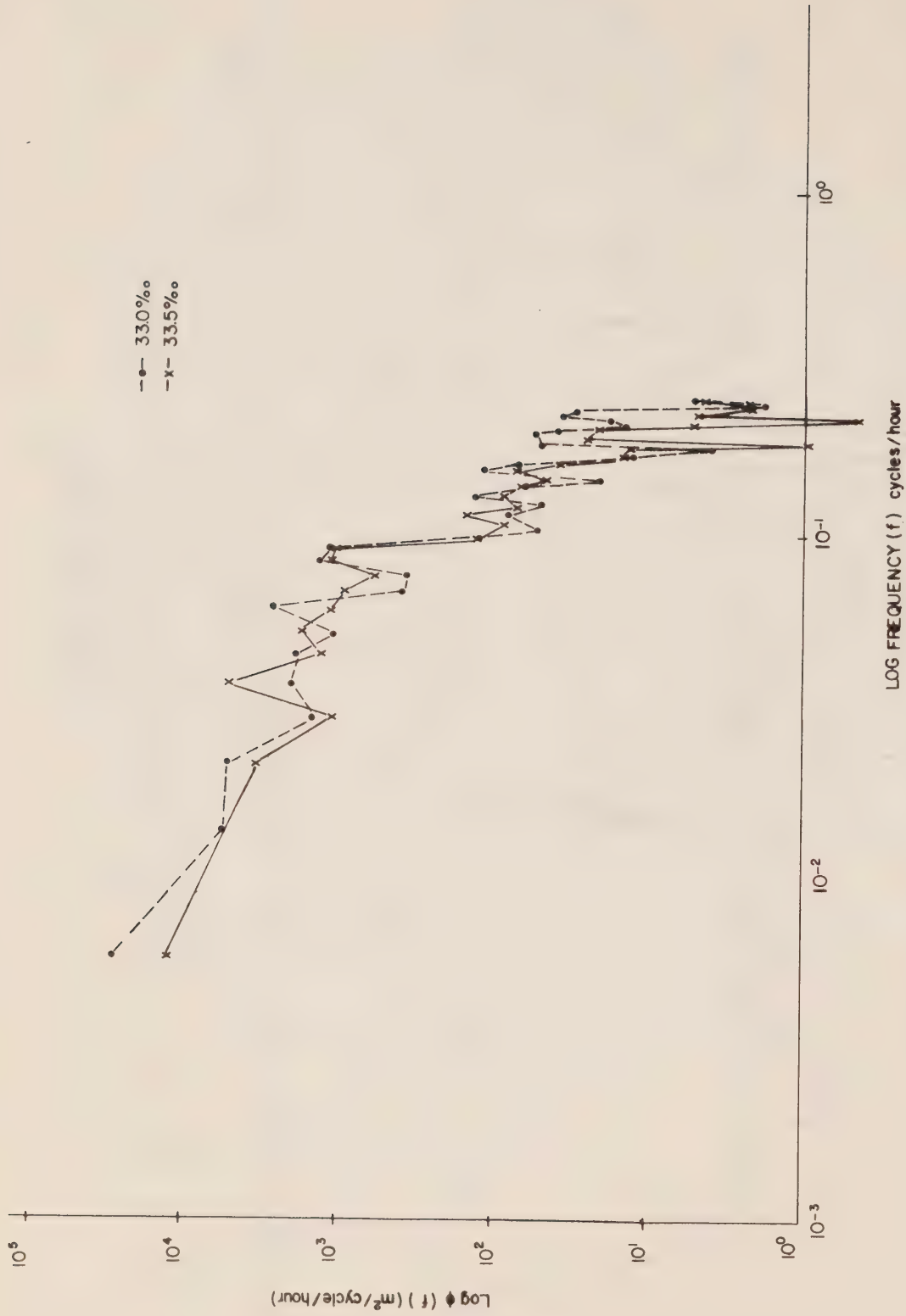


FIGURE 15d: Spectra (Φ) of depths of isohalines versus frequency.
Bandwidth 7.81×10^{-3} cycles/hour.

33.0‰ ISOHALINE / 33.5‰ ISOHALINE

TIDAL COMPONENT	FREQUENCY W (CYC/HR)	MAGNITUDE H (METERS)	F	V ₀ + U (DEGREES)
MEAN (H ₀)	0.0	89.50/116.05	1.000	0.0
K1	0.0418	2.58/4.25	1.066	28.69
M2	0.0805	3.47/4.24	0.984	109.42
M4	0.1610	0.34/0.52	0.968	218.85
M6	0.2415	0.19/0.31	0.952	329.06

TABLE II : Magnitude of Fourier Tidal Constituents from depth (h) of 33.0‰ and 33.5‰ Isohaline Surfaces versus time (t).

$$h = H_0 + \sum F \cos(\omega t + V_0 + U)$$

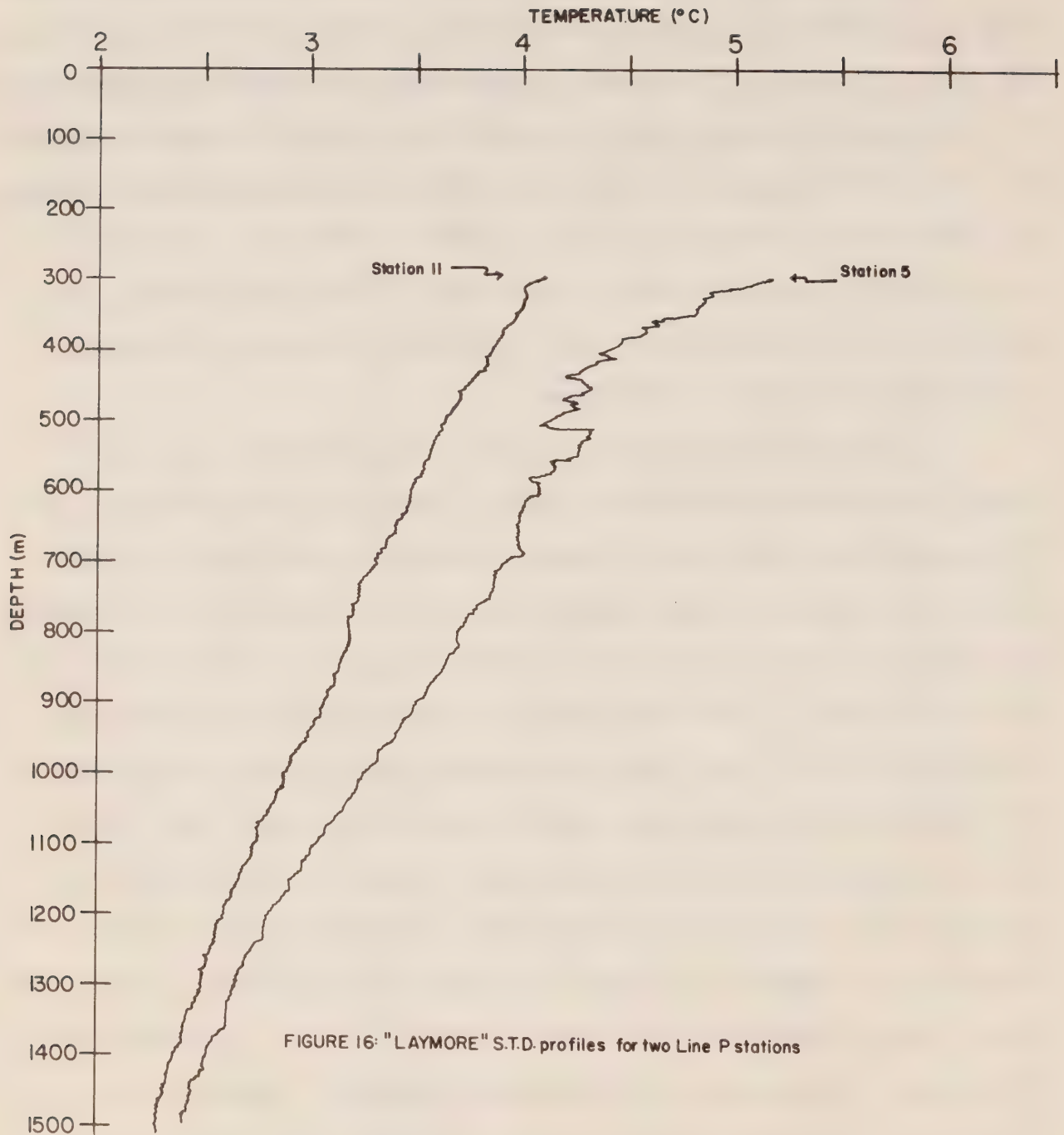
It is clear from this table that the Lunisolar tide K1 (~ 1 cycle/day) and the Lunar tide M2 (~ 2 cycles/day) were the major constituents, with aliasing probably accounting for a large portion of the magnitude at the higher frequencies. The fact that the semi-diurnal component is of equal, or greater, magnitude than the diurnal component in this analysis (the reverse of the spectral analysis case) is most likely a consequence of the inertial variations having a period closer to 12 hours than to 24 hours.

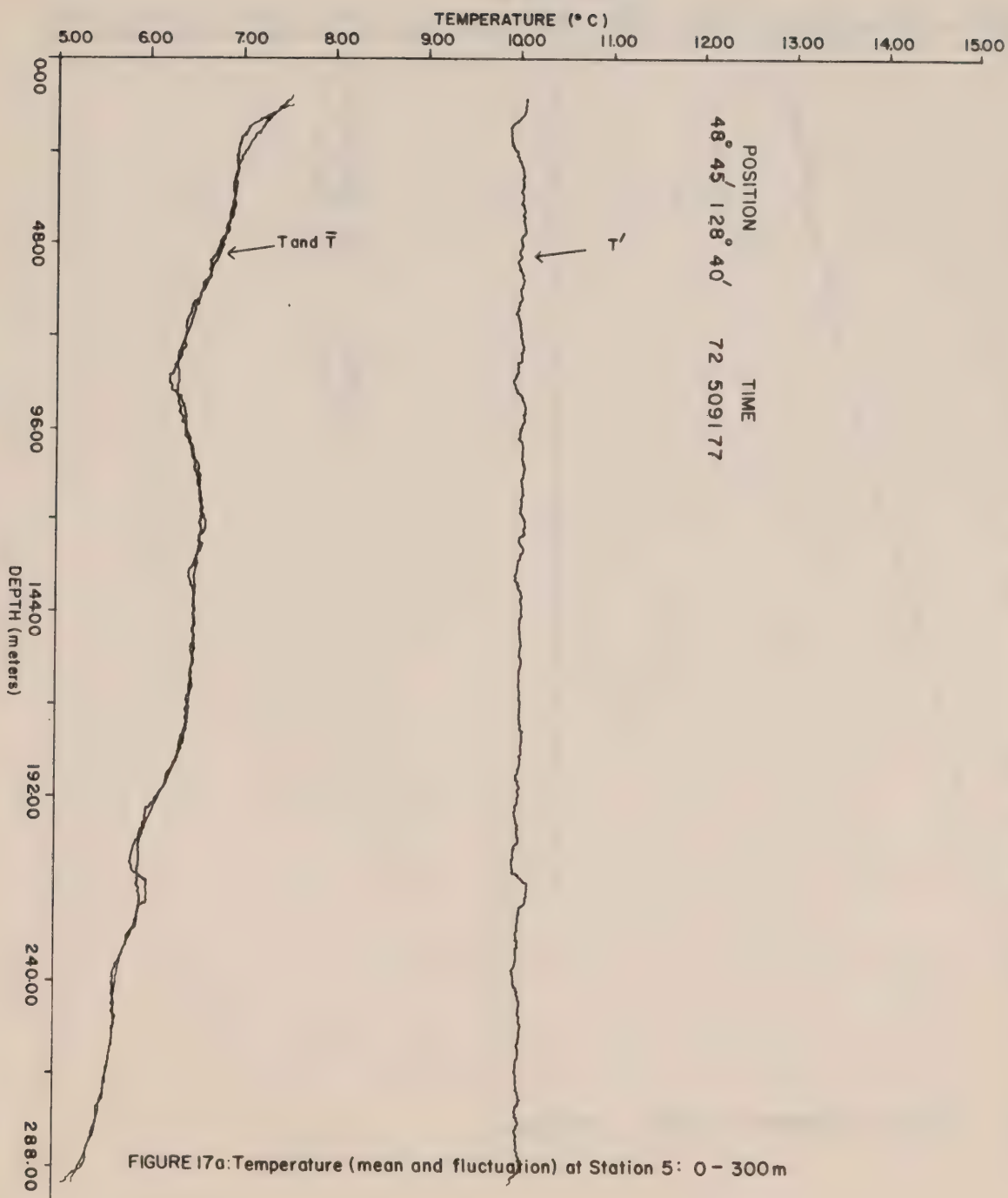
2.6. Temperature Microstructure in the Vicinity of Line P: Evidence of the mixing of two water masses.

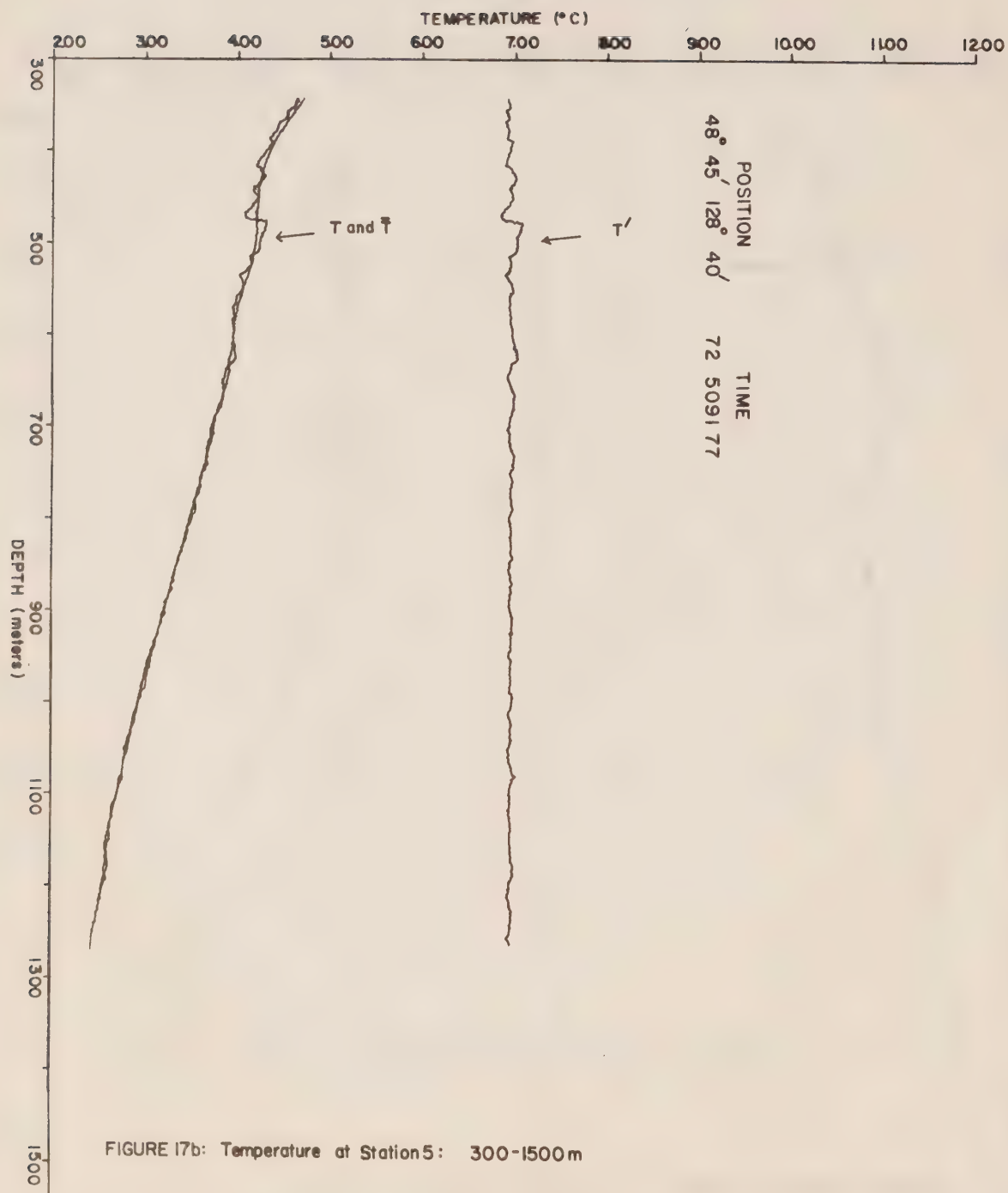
Discussion

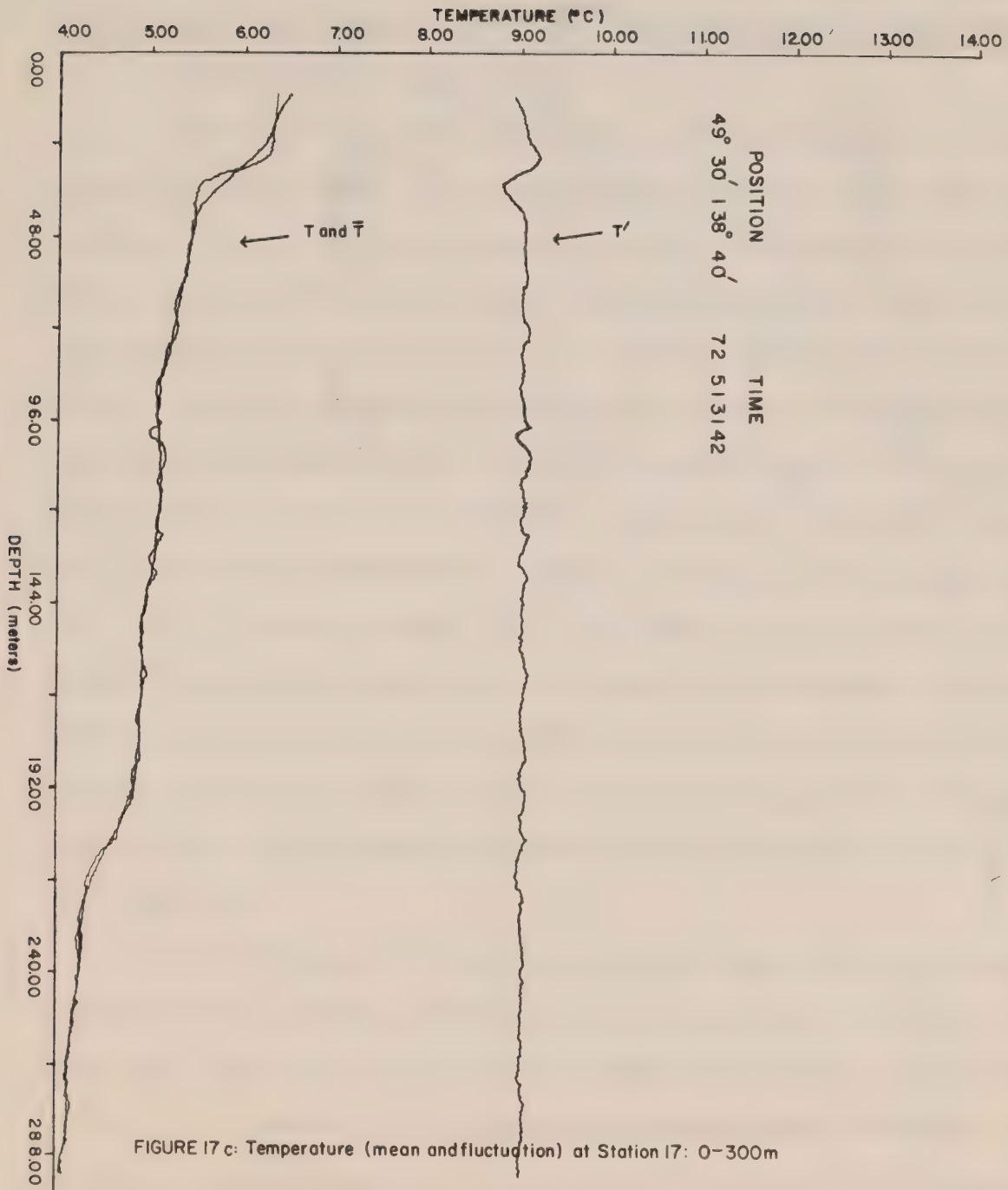
At the time of the LAYMORE cruise, it became increasingly apparent that, for the deep (300-1500 m) section of the STD casts especially, there was a marked decrease in the amount of temperature fine-structure seaward of the near-coastal regions. This is exemplified by figure 16 in which the deep cast at consecutive station 11 (49°41'N, 140°37'W) is plotted together with the deep cast at consecutive station 5 (48°51'N, 128°40'W). The noisiness of the signal at the more coastal station was definitely much greater than that at the more oceanic station, with significant temperature structure still prevalent at 700 m in the former.

The above discussion is of course only qualitative. In order to obtain a consistent measure of the amount of temperature fine-structure, it is necessary to do some sort of numerical analysis on the digitized records. One of the simplest and most straightforward forms of analysis is to determine the variance by first calculating a running mean and then subtracting it from the actual record. To this end, both the shallow (0-300 m) and deep (300-1500 m) parts of the casts have been smoothed using a box-car running mean of 19 m width in the upper layer and 95 m width in the lower layer. Choice of these averaging intervals was made after a number of trials to determine which gave the best visual fit to the actual temperature traces. As it turned out, an interval of 19 points gave the most satisfactory results, and since vertical resolution of the analog traces is 1 m and 5 m in the respective layers, the above averaging depths were obtained. Subtraction of the mean values \bar{T}_j , at each digitized point j , from the actual values T_j then gave the fluctuations T'_j at each point (see e.g. figures 17a, d). The variance σ_k^2 (where σ is the standard deviation) over any block k was then









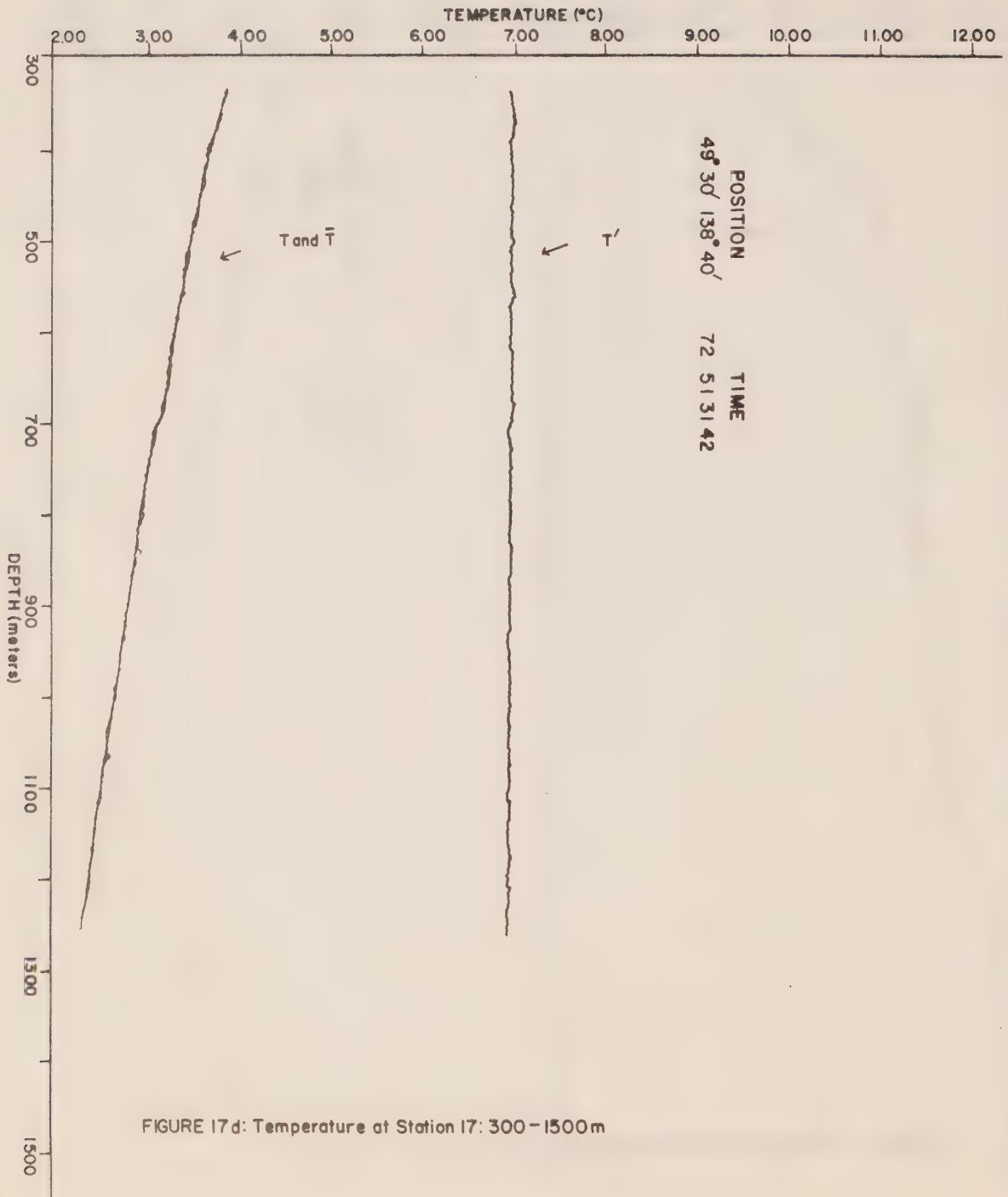


FIGURE 17d: Temperature at Station 17: 300-1500m

determined via the relation,

$$\sigma_k^2 = \frac{1}{N-1} \sum_{j=1}^N (T_j - \bar{T}_j)^2 ,$$

where N is the number of data points within the block. In these calculations, a block consists of values from a specified depth range for each station.

Upper and lower layer blocks

For these cases, the variance has been determined for the two depth intervals 0-300 m and 300-1500 m corresponding to the two ranges used during lowering of the STD. The calculated values in $^{\circ}\text{C}^2$ are plotted in figures 18a, b with the numbers in brackets representing results from the second (later) occupation of a given station. In the top 300 m, there was obviously a sharp increase of the amount of temperature structure in the outbound compared to the inbound observations in the coastal region. Within this region, therefore, inbound values rather than outbound values have been used since in time they correspond more closely with those north and south of the Line. West of station 6 either value is applicable since the contour positions are nearly the same for both. As figure 18a shows, the contours indicate a maximum region extending from about 47°N , 130°W through to 49°N , 128°W with an additional relative maximum occurring 2° south of station 4. Relatively large values also occur west of the northern end of Vancouver Island to about 140°W longitude.

The difficulty with associating these results with temperature 'microstructure', however, is that the smoothing process is incapable of removing all temperature variations with depth which are due to large scale features (10's of meters), such as the surface mixed layer. Therefore what one has is a combined measure of the detailed fine-structure and the magnitude of the large scale temperature gradients. Moreover, the effect of the latter



FIGURE 18a

features can be highly variable over short periods because of internal waves whose motion can increase or decrease the local temperature gradients by compressing or expanding the depth between isotherms. In the latter situation, application of the low pass running mean will give rise to larger apparent fluctuations than in the former situation. Nonetheless, the present plot does give an indication of the overall temperature structure and confirms the notion of greater temperature variability in the coastal areas relative to the deeper oceanic areas. Furthermore, all indications of the amount of microstructure in the top layer are not completely lost since by dividing this layer into two, the large scale temperature features become confined to the upper 150 m only. This will be done shortly.

With regards the temperature variance in the 300-1500 m range, one can be more assured that values obtained are representative of the fine structure alone since the mean profile remains smooth throughout. This is supported by figure 18b which indicates relatively small changes in variance between temporally spaced observations at the same location. For this range, therefore, there is little difference in contour positions if the inbound casts rather than the outbound casts are used for determination of the variance. Comparison of figures 18a and b shows that the spatial distribution in the deeper range is nearly identical to that in the 0-300 m range although the magnitude is reduced by an order of ten or so at all positions. Thus, in this layer we again find maximum variances occurring in a narrow strip near 130°W, with values west of this decreasing monotonically towards Ocean Station P. It should also be noted that the value of 1.01 used for station 5 probably gives an underestimate of the values in this region since it is from the outbound portion of the cruise while all others are from the inbound portion. Judging by the increases that occurred at stations 4 and 6 a value



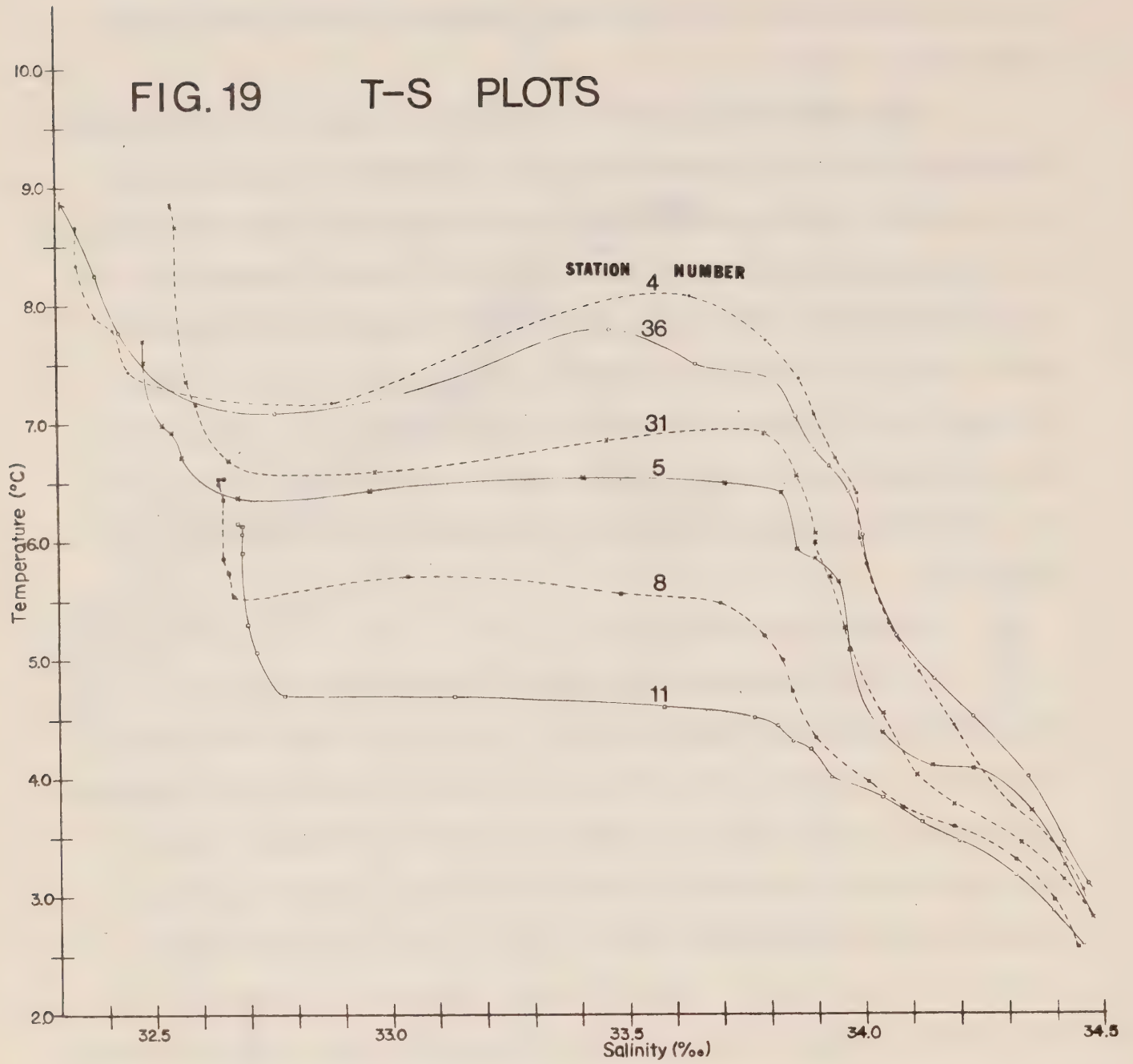
closer to 1.5 might be more realistic. A similar situation arose in connection with the 0-300 m range, but there it was expedient to simply ignore the out-bound value at station 5.

Aside from what occurred in the top 150 m, which will be discussed in the next subsection, the most plausible explanation for the proceeding distributions is that the positions of large variances are associated with areas of horizontal mixing between two water masses of different temperature. The larger variances mark the 'front' where the confluence of the two waters is taking place. According to the potential energy anomaly plots of figures 10a-q and the T-S diagram of figure 19, the mixing is in fact between the relatively cool mass of water moving eastward from the oceanic interior and the relatively warm mass of water moving northward off the coast of B.C. and Washington.

Division into nine blocks

In order to determine the degree of temperature variance with depth, the two previous ranges have been further divided into the following nine layers: 1) 0-50 m, 2) 50-150 m, 3) 150-300 m, 4) 300-500 m, 5) 500-700 m, 6) 700-900 m, 7) 900-1100 m, 8) 1100-1300 m, and 9) 1300-1500 m. Layers 1 and 2 have been so chosen in an attempt to separately confine the effects of averaging through the mixed layer (< 50 m) and the dicothermal layer (50-150 m), respectively. Figure 20a gives a measure of the magnitude of the temperature gradients associated with the surface mixed layer. Obviously, the gradients are much larger in the coastal areas than in the oceanic areas. There is also a greater amount of temporal variability in the temperature structure in the coastal region. For the 50-150 m range, the temperature variance is not so dependent on relative proximity to the coast although, for the available stations, the greatest time variability appears to have

FIG. 19 T-S PLOTS



occurred in the coastal region. Consideration of the original data suggests that the latter result is probably indicative of steepening of the vertical temperature gradients by surface mixing and internal waves at places where there was much temperature structure to begin with.

The temperature variations plotted in figure 20c for the range 150-300 m conform more to those for the deeper ranges than for the more shallow ones. Therefore, for depths exceeding 150 m the values obtained for the variances are mostly independent of contamination from large scale gradients that are not removed by the smoothing technique. What remains is microstructure produced by the confluence of the two water masses. Figures 20d-i then give the following picture for 150-1500 m range.

a) in the range 150-700 m, maximum variation occurs near the coast in a region extending from about 47°N, 131°W to about 49°N, 129°W. Westward of the coast, variances tend to decrease, with minimum values appearing in the vicinity of station 12 (Line P). In addition, the horizontal sections indicate a fairly extensive area of relatively large values near 50°N between Vancouver Island and about 135°W. Vertically, the maximum values for stations east of the longitude of Line P station 7 occur always in range 4, 300-500 m (see figure 21a). West of this (including station 7), however, maximum values with depth alternate between levels 3,4 and 5, with the exception of those at the longitude of Line P station 8 which again have their maximums at level 4 only (figures 21b, c).

b) in the range 700-1300 m, the region of maximum structure has shifted more towards the coast although values to the north of 50° continue to remain relatively large for these depths. In the vertical, the magnitude of the variance is nearly uniform with depth at all stations and is small ($< .5 \times 10^{-3} \text{ } ^\circ\text{C}^2$).

c) averaged from 1300-1500 m, the magnitude of the temperature variance is comparable to that in (b) but with the maximum in the horizontal shifted more away from the coast. The pattern is similar to that in (a).

Because of the continued persistence of the strip of maximum variance near 130°W longitude in all horizontal sections, it would appear that the northward flowing coastal current extends below 1500 m. The fact that the magnitude of the variance generally decreases with depth is simply due to the corresponding decrease in the difference in mean temperature between the two mixing water masses (see figure 19). The most obvious exception to the latter trend is the finding that below 150 m the greatest variances east of 132°W longitude occur between 300-500 m. This suggests that the temperature contrast between the two water masses was greatest at this level and/or that the mixing was particularly vigorous. Further seaward, where the amount of temperature structure with depth is significantly smaller, the level of maximum variance is much more variable. Such a result is to be expected for this oceanic region since its temperature structure is an inherent feature of a particular water type formed on the western side of the subarctic Pacific and not a result of more local mixing between two water masses.

Another feature of the variance distribution is that, compared to other levels, there is in the general range 700-1300 m a greater westward penetration of the northward flow with maximum extent occurring near 48°N latitude. Below 1300 m, however, the pattern outlining the mixing region returns to the form for depths less than 700 m. Associated with this changing spatial distribution with depth is the varying magnitude of the temperature variance at consecutive station 31 ($47^{\circ}10'\text{N}$, $130^{\circ}40'\text{W}$). Excluding level 2, the variances at this station for depths less than 700 m appear

to be much larger than at any neighbouring station and usually represent the maximum value for the survey. It is, therefore, not unlikely that these rather large values are somehow related to the presence of Cobb Seamount ($\sim 46^{\circ}45'N$, $130^{\circ}40'W$) only 35 km to the south. In particular, there may be some sort of turbulent wake associated with this mountainous feature since, by rising to within 35 m of the surface from depths of over 2700 m in a distance of only 20 km (see figure 22), it penetrates abruptly into most levels of the baroclinic flow. In the presence of such a wake, the horizontal mixing of the two different temperature water masses in this region may be enhanced compared to more distant regions. This would be particularly true of the more shallow flow where the baroclinic motions are strongest. A less speculative understanding of the influence of the seamount, however, awaits a more detailed survey.

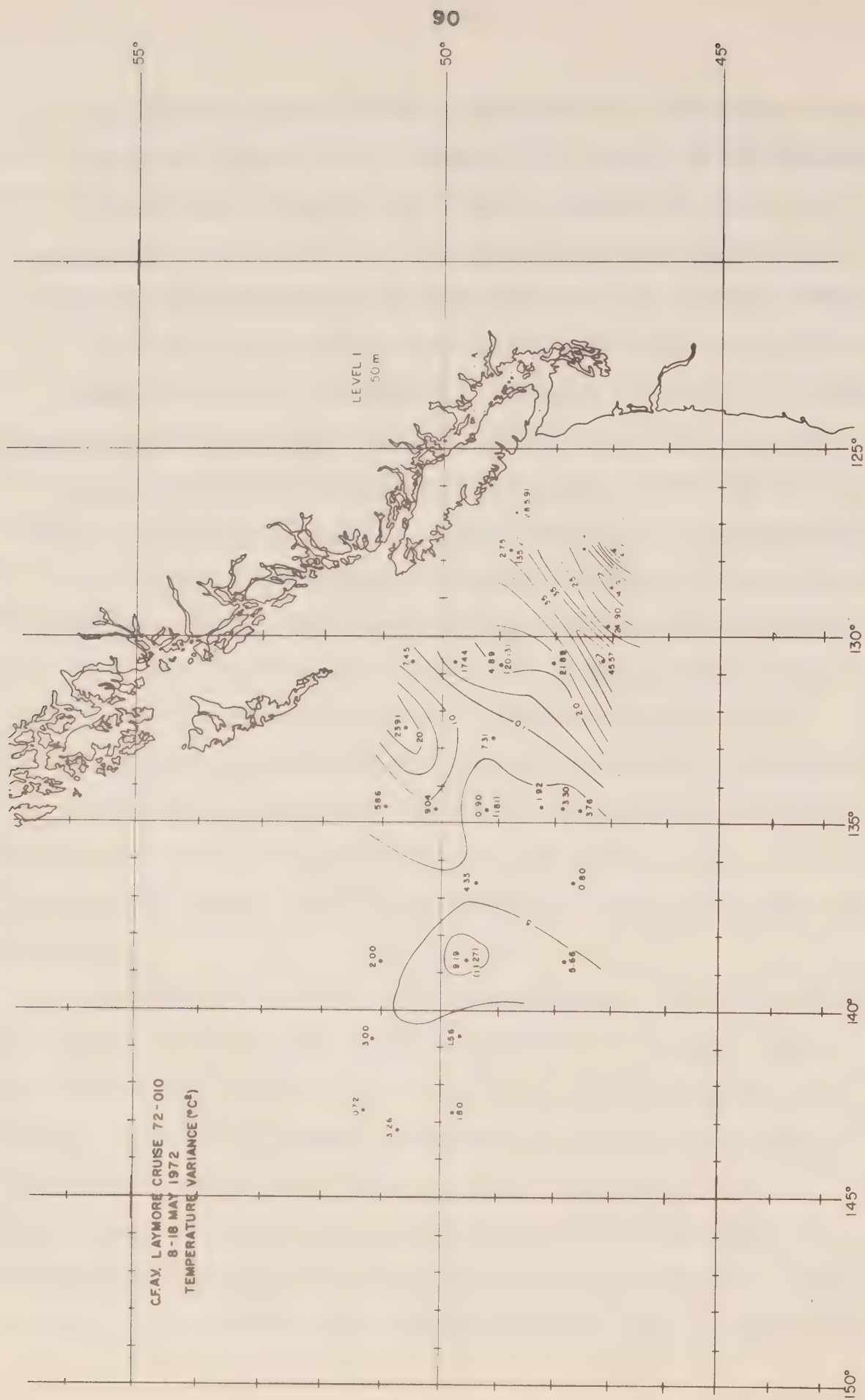


FIGURE 20a

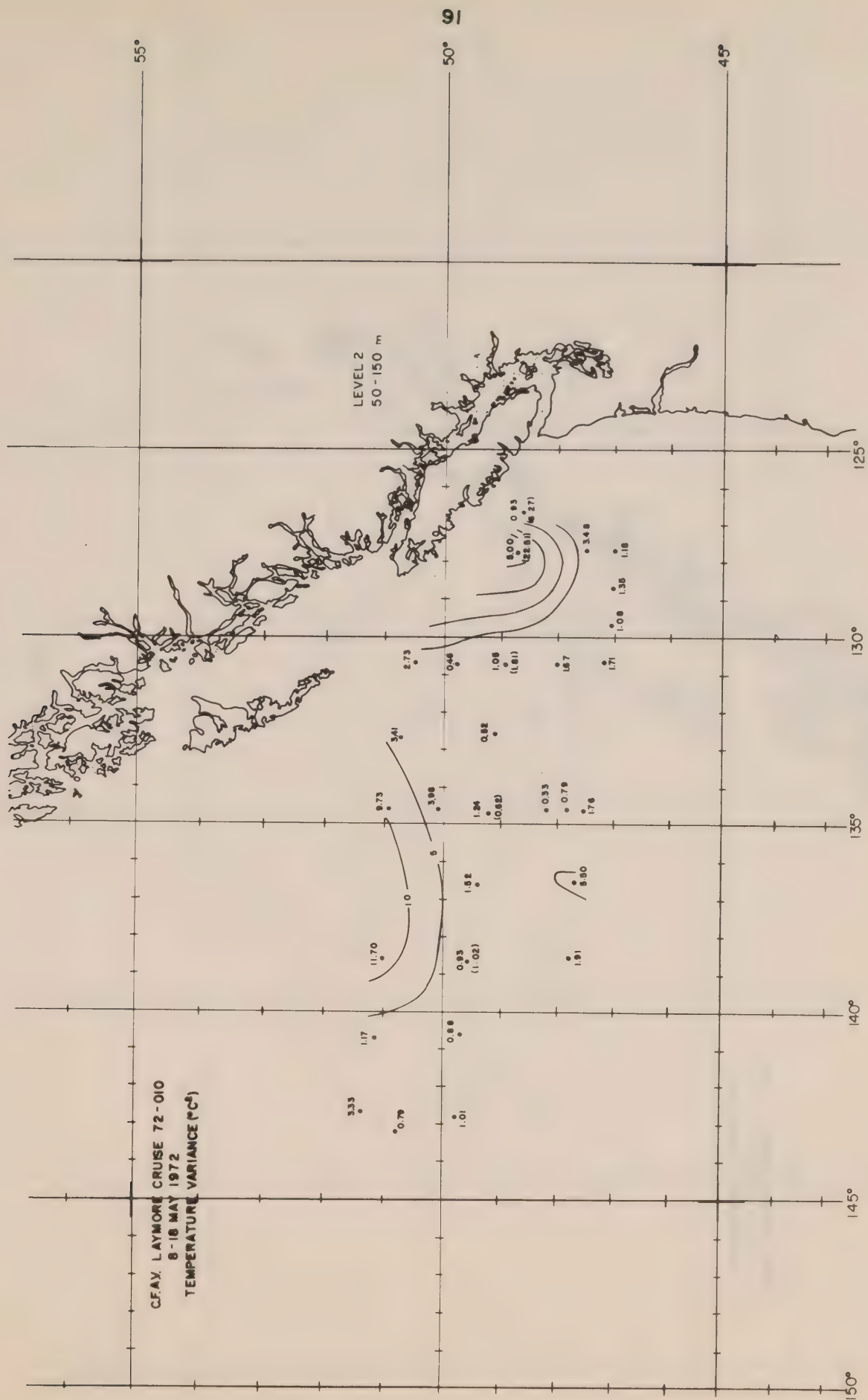


FIGURE 20b



FIGURE 20c

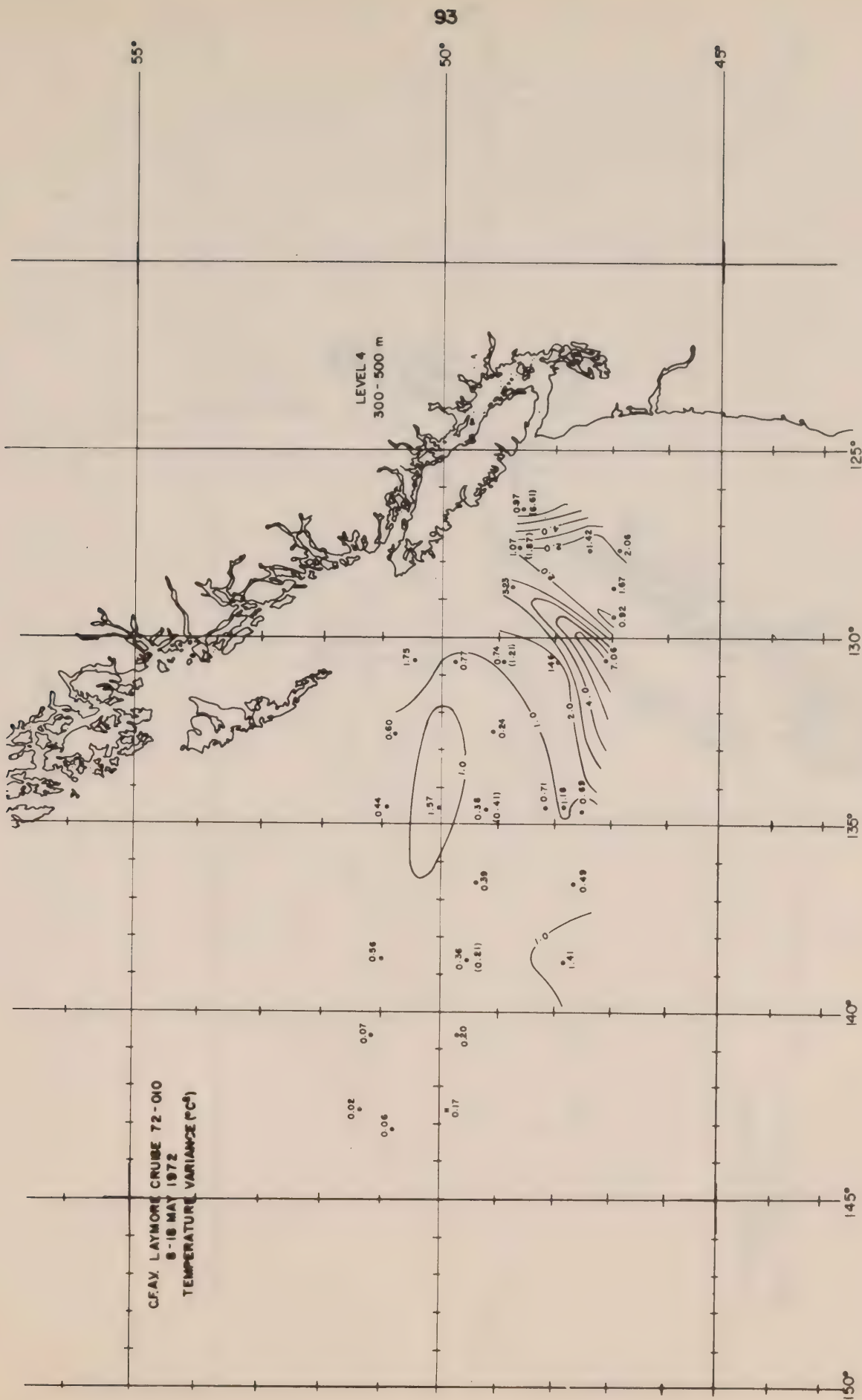


FIGURE 20d



FIGURE 20e



FIGURE 20f

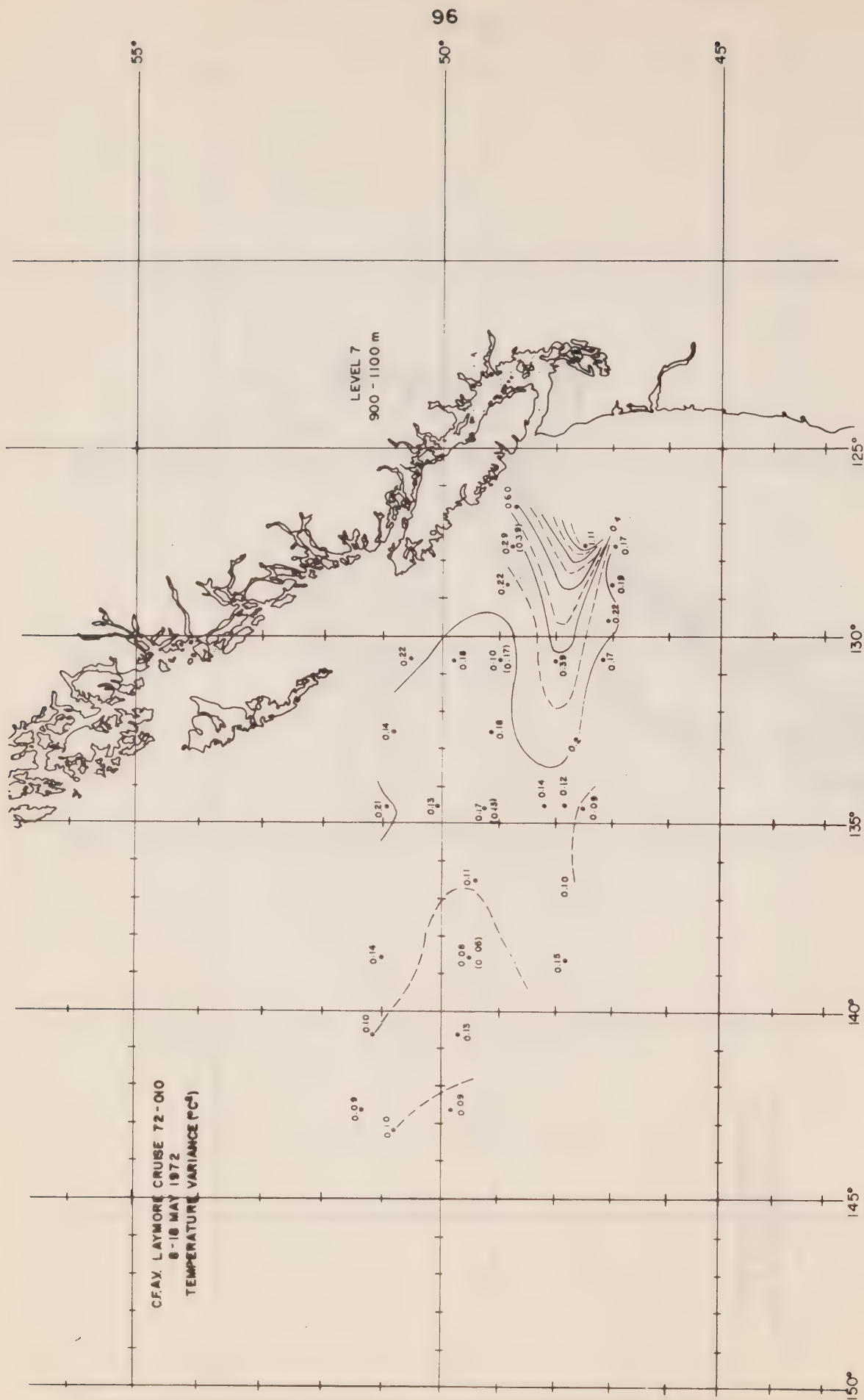


FIGURE 20g



FIGURE 20h

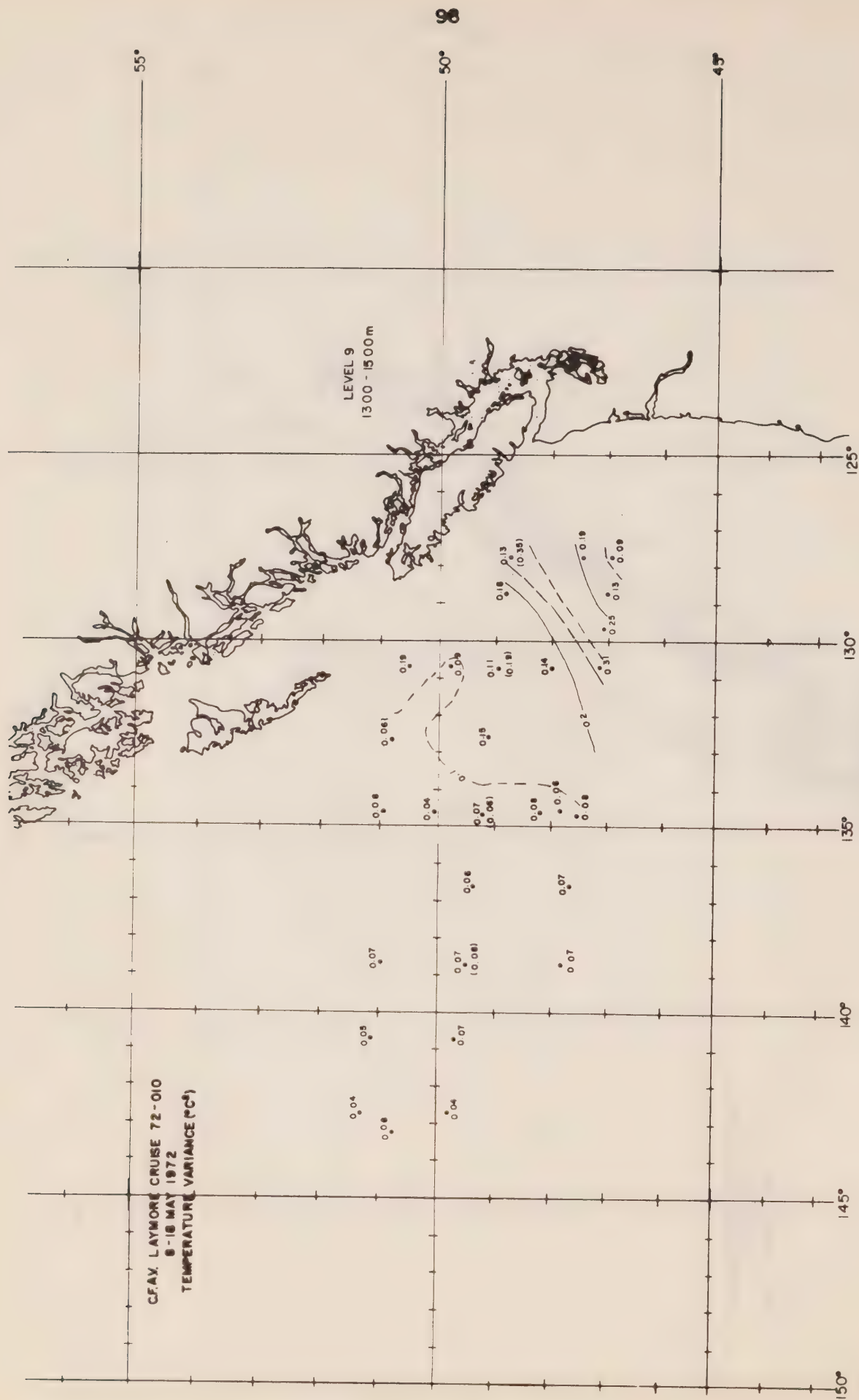
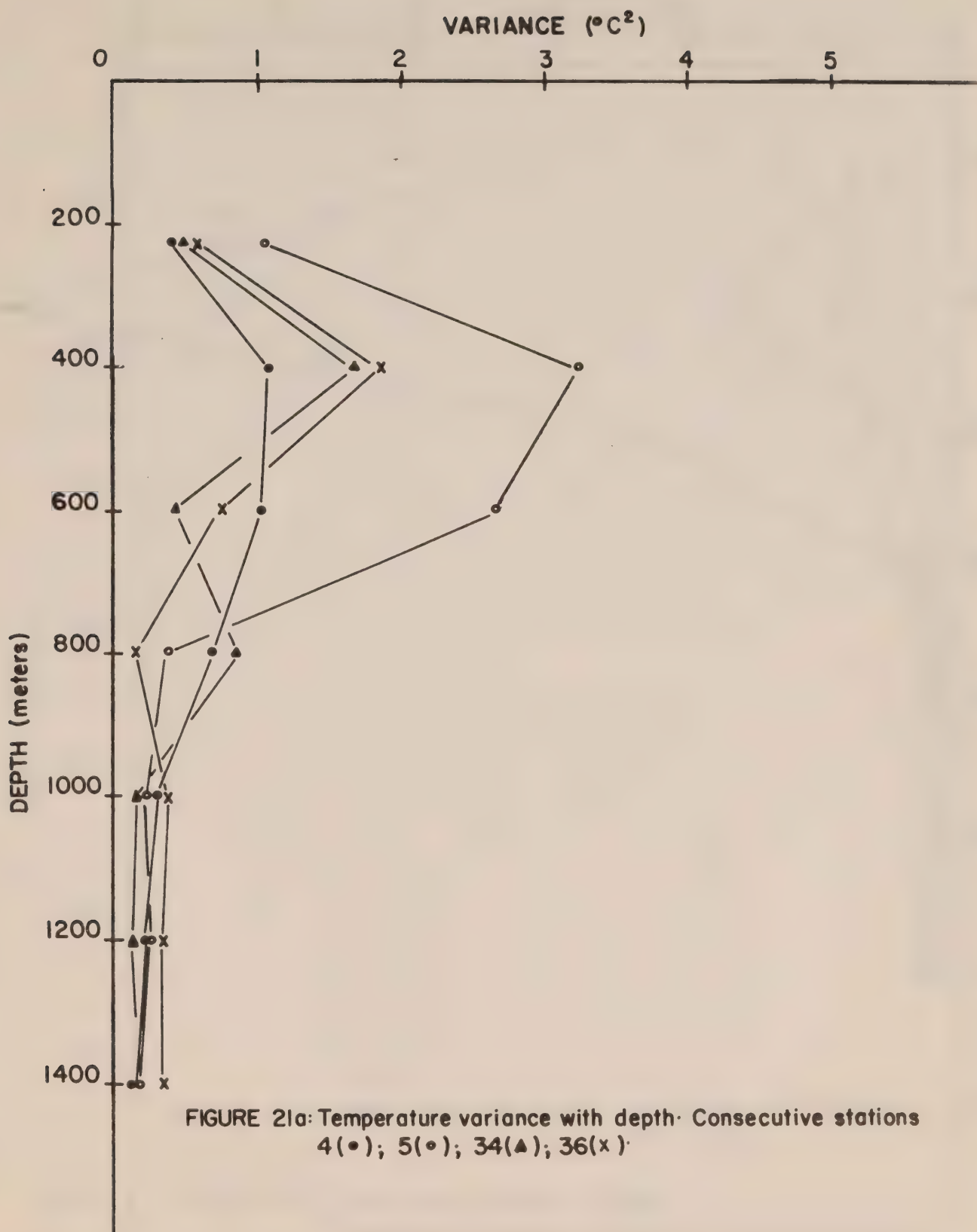


FIGURE 20i



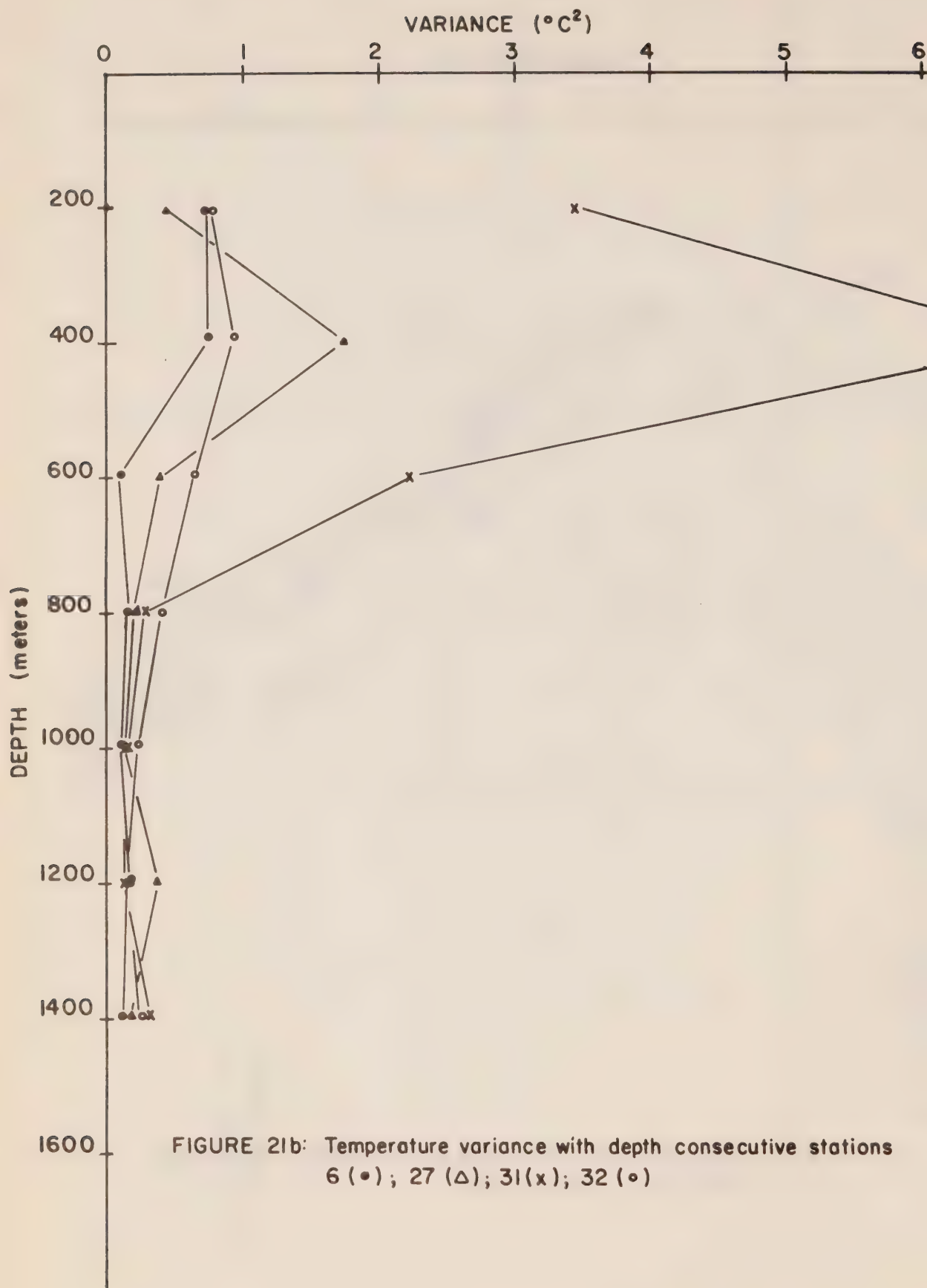
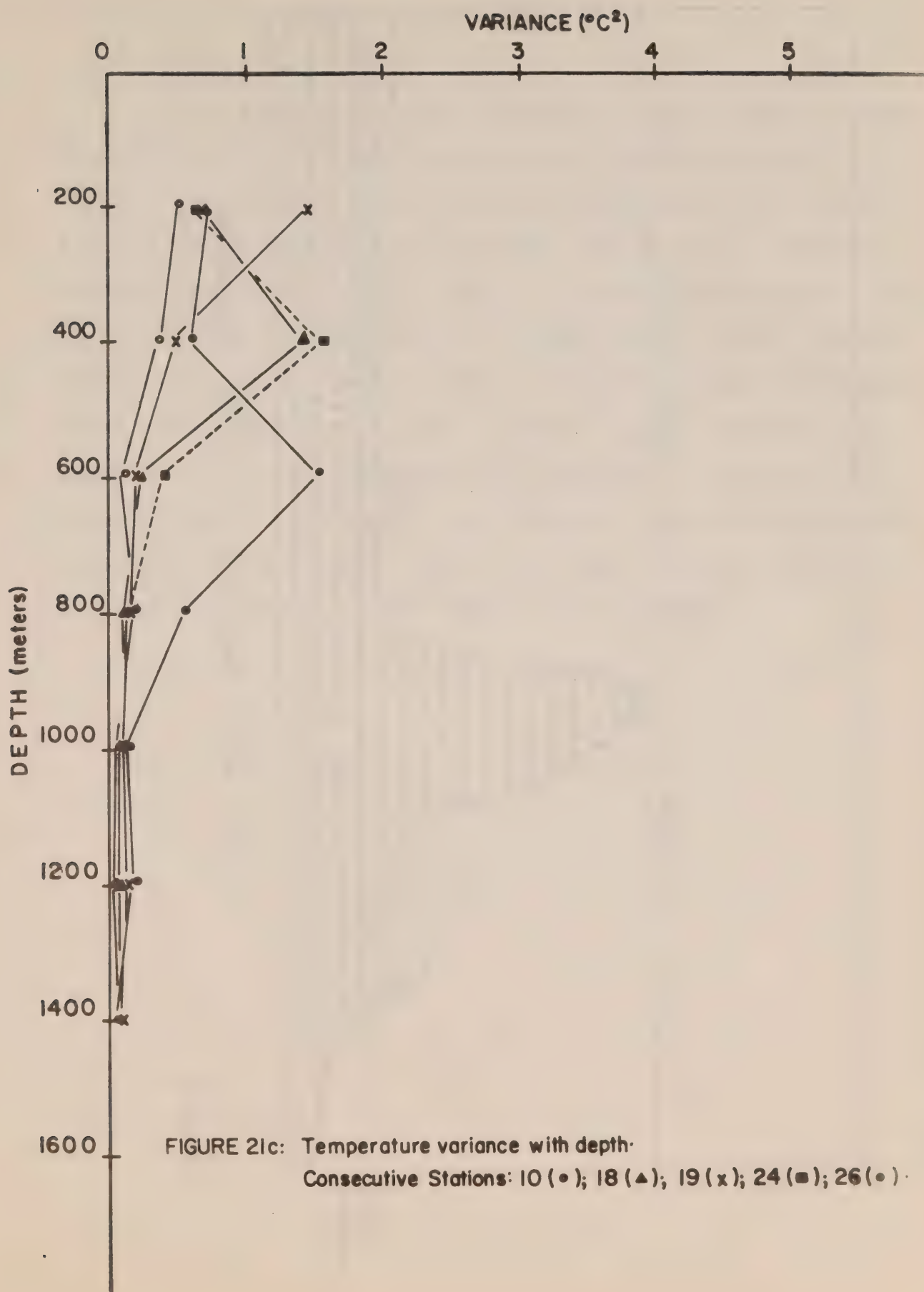
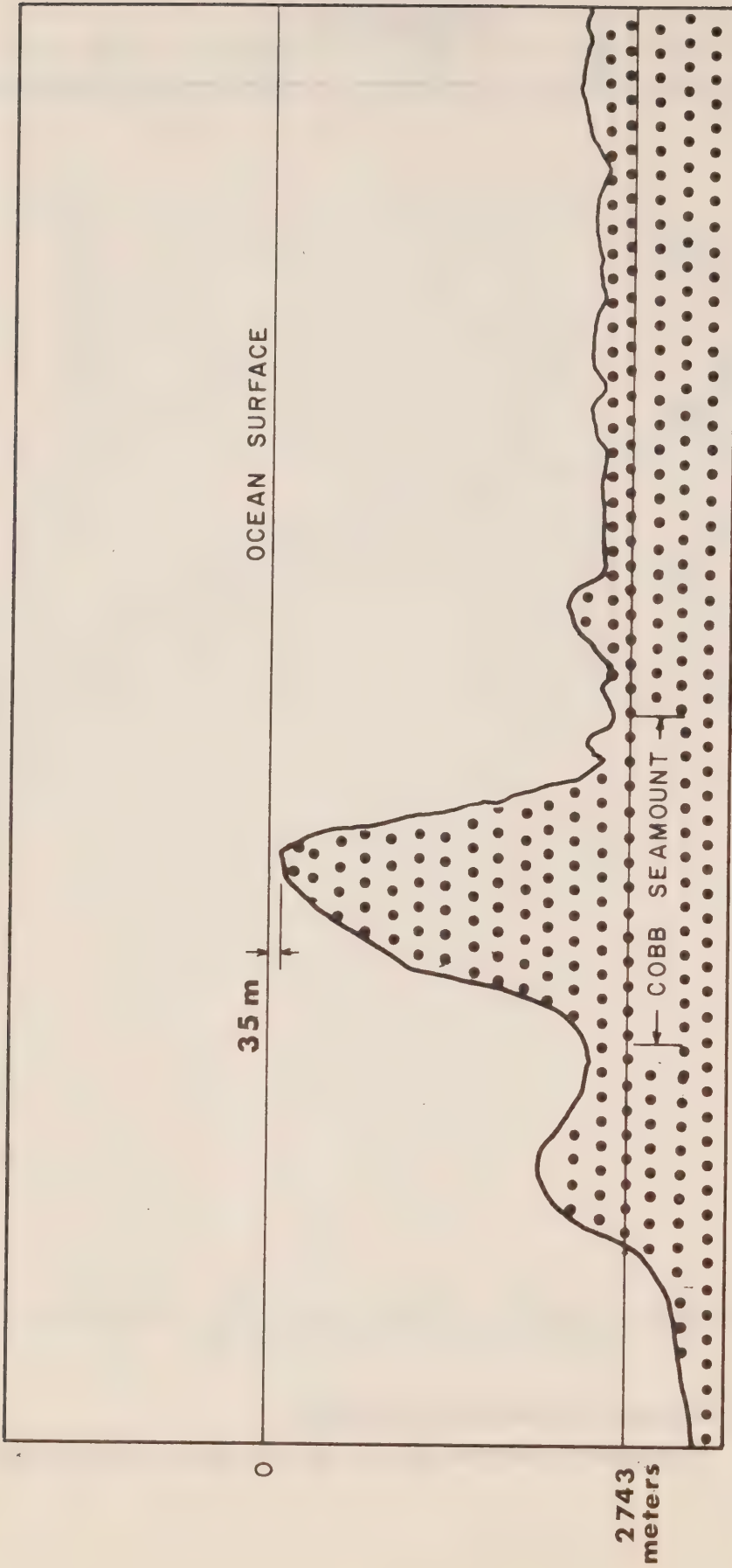


FIGURE 21b: Temperature variance with depth consecutive stations
6 (•); 27 (Δ); 31 (x); 32 (o)





EAST - WEST PROFILE OF COBB SEAMOUNT

FIGURE 22

3. The Variability of Water Properties Along Line P

3.1. General discussion

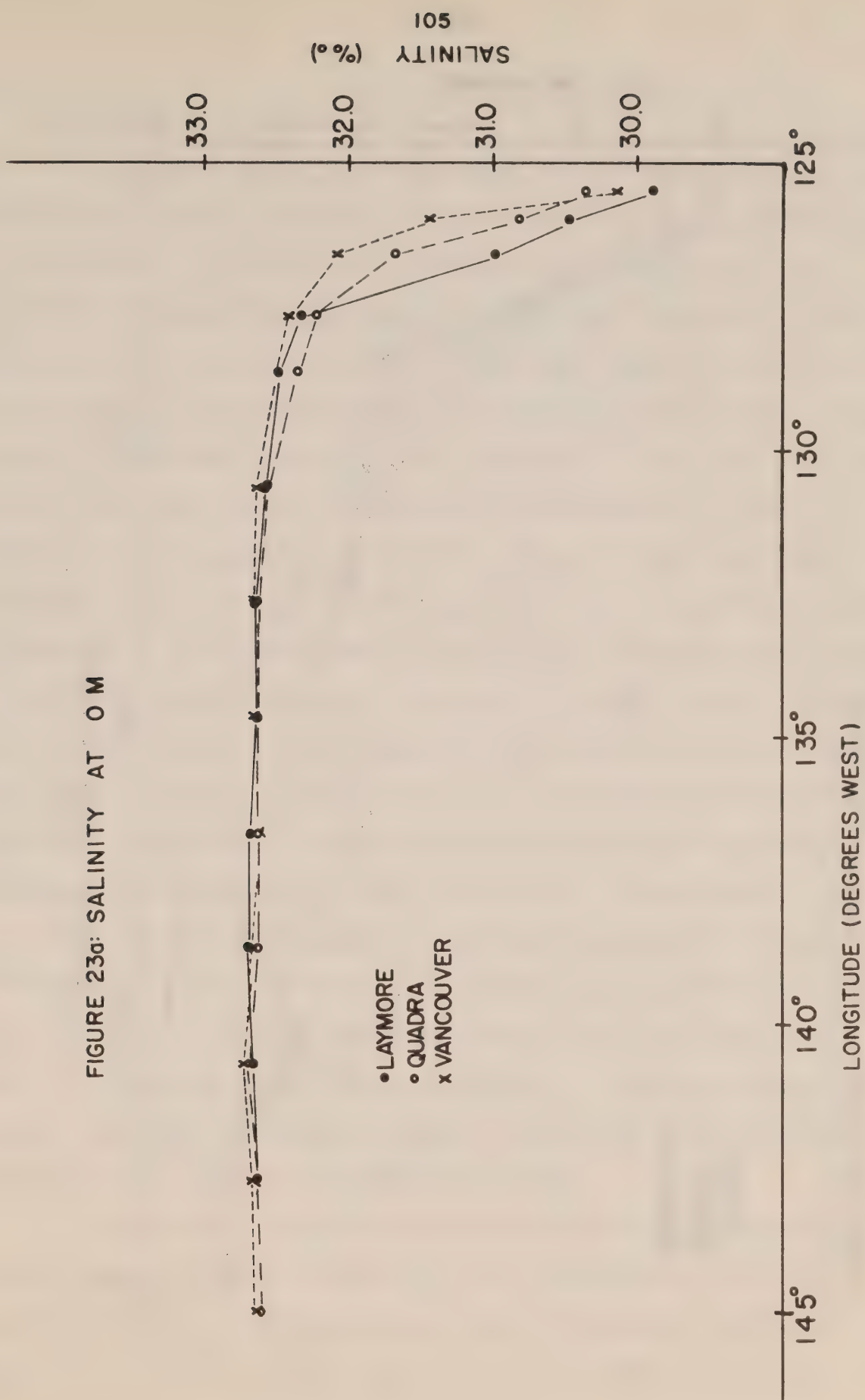
In this section, results of observation from the LAYMORE are used in conjunction with those from the weatherships VANCOUVER and QUADRA to determine the variability of water properties along Line P from 8-18 May. A plot of station number and longitude versus time for each of the three ships was presented previously in figure 2. One interesting feature of this was that the mean outbound speed of the LAYMORE was only slightly less than that of the VANCOUVER. Therefore, the relatively slow between-station speed of the former, which is only 11 knots compared to about 16 knots for the weatherships, was nearly compensated for by the shorter time required to do each station. As indicated in the Introduction, this is not a reflection on the ability of the crew or scientists but rather on the ship designs which make observations from the LAYMORE easier to perform.

3.2. A Comparison of Surface Salinities and Temperatures

The surface salinities and temperatures from the STD observations of the three ships is shown in figures 23a and 23b, respectively. Station 5 is seen to delineate the transition region from the more uniform structure in the oceanic domain to the more rapidly varying structure in the coastal domain. This is mostly true of salinity, where there is a rapid salinity increase seaward of the coast and a nearly uniform and constant salinity in the interior. Because of the small changes in the latter region, it is not possible to distinguish actual variations in space and time from those due to instrument error. East of station 5, however, the variations are probably significant. With the VANCOUVER observations (x) taken consistently between those of the LAYMORE (.) and QUADRA (o), these variations indicated a shifting of the isohalines by horizontal currents and/or by changes in the amount of river runoff.

Aside from instrument errors, the most likely explanation for the generally increased surface temperature over the 2-week period is that the LAYMORE observations were taken during passage of a fairly intense storm front. As a result of cooling and wind mixing at that time, surface temperatures taken by the LAYMORE would be somewhat low compared to those of the QUADRA and VANCOUVER which were taken at more calm periods. This would also account for the greater temperature changes that occurred west of station 7 as compared to more easterly stations since it was there that the maximum effect of the storm was first encountered (see also figures 25a-q). Northward advection of relatively warm water could account for some of the general temperature increase but not all of it since surface flow tends to be zonal and weak.

FIGURE 23a: SALINITY AT 0 M



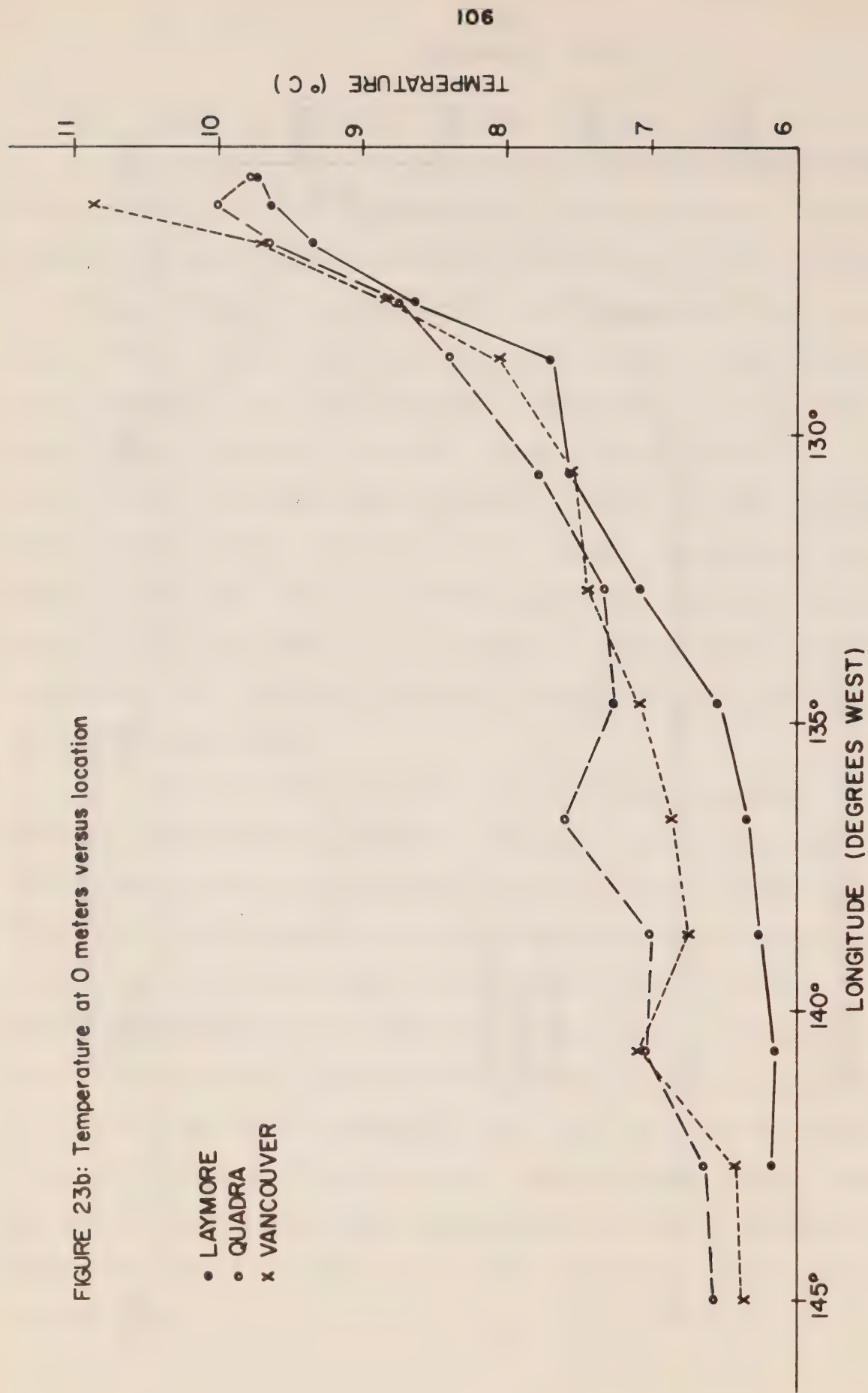


FIGURE 23b: Temperature at 0 meters versus location

3.3. Depth of the Surface Mixed Layer

During the spring, the accumulated effects of surface heating and wind mixing over most of the subarctic Pacific combine to produce a surface layer of water (< 50 m) that has a nearly uniform temperature with depth and which is truncated by a temperature discontinuity. Formation of this layer is part of a cycle that consists of an upper layer of uniform temperature to about 100 m in mid-winter (January), to highly temperature-structured upper waters in summer when surface heating is greatest and wind least. Since in May the mixed layer depth is intermediate between these two extremes, it should be highly susceptible to variations induced by the winds through turbulent mixing. Moreover, as the pycnocline (which is essentially salinity determined) is always deeper than the mixed layer, the effectiveness of the mixing is not dampened by large scale density gradients. Hence, the mechanical energy input by the wind should be rapidly distributed to the base of the layer by turbulent diffusion where it will work against the temperature gradient. As a result, it should be possible to associate large temporal changes in mixed layer depth to the wind strength. Internal waves, tides, inertial waves and Ekman divergence (convergence) generated by the surface wind-stress curl will, of course, also influence the observations although only the latter is actually capable of altering the 'mean' depth in any spatially consistent manner over periods of days. According to Denman (1972), however, who conducted studies at Station P, the latter is probably not significant when compared to the turbulent mixing.

Illustrated in figure 24 is the spatial variation in mixed-layer depth as measured upward from the top of the thermocline for the three samplings of Line P. Between stations 1 and 7, the LAYMORE depths were consistently much more shallow than those from the QUADRA, while those

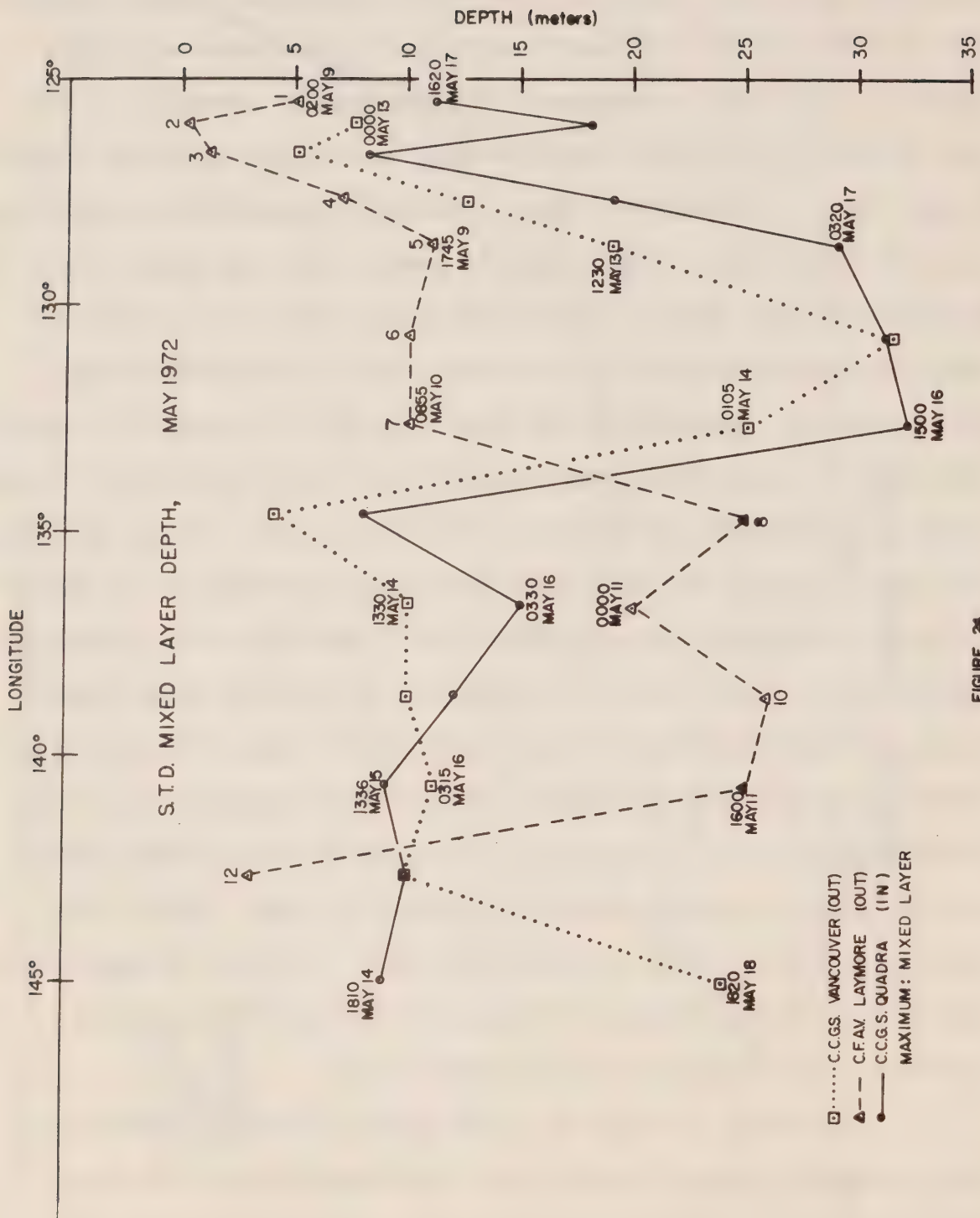


FIGURE 24

from the VANCOUVER were intermediate. West of station 7, LAYMORE values deepened, while the weathership values rapidly shallowed. A thin mixed layer was then recorded by the LAYMORE at station 12 and a deep mixed layer by the VANCOUVER at station P. As the dates on the curves indicate, LAYMORE observations proceeded all others in every case while VANCOUVER observations proceeded those of the QUADRA except at stations 12 and P (see also figure 2).

The surface pressure, winds, cloud cover and frontal positions at midnight (00hrs) GMT for the period May 2 to May 18 are presented in figures 25a-q. On May 2, the cyclone which had started to form in the vicinity of the Aleutian Islands at the end of April, began to move eastward over the northeastern Pacific. East of about 150° longitude, however, winds remained light and skies clear. By May 5, the storm had penetrated only to about 137°W and was much reduced in strength while on the next day, its effect was limited to the vicinity of the cold front marked in figure 25e. By May 7, winds over the region of Line P were again light and skies partly clear. This situation prevailed until May 9 when another eastward moving disturbance had begun to penetrate east of station P.

The fairly extensive period of calm weather that existed over Line P up to May 9 would then account for the shallowness of the mixed layer observed by the LAYMORE for stations 1 to 4. On the other hand, the slight deepening that occurred at stations 5-7 appears to coincide with the time of arrival of the storm's edge at these positions. By the time the LAYMORE had arrived at station 8, the mechanical wind-mixing effect of the storm had had sufficient time to markedly deepen the layer. This would account for the abrupt deepening observed between stations 7 and 8. The shallowness of the mixed layer at station 12 (00GMT May 12) resulted from the low winds (< 10 knots) and clear skies in its vicinity for the day or so prior to observation.

By May 13, the greatest effect of this particular storm was being felt east of 135°W on Line P and would account for the rapid deepening of the mixed layer observed by the outbound VANCOUVER. West of 135°W, there was not a significant increase in the wind until May 18 when the third storm was just beginning to move past Station P. This would explain the relatively shallow values from station 8 westward during the VANCOUVER cruise as well as the large depth observed at P at 1820 on May 18. Finally, the continued deepening of the mixed layer in the more coastal regions as obtained by the QUADRA, are probably a result of the low pressure regions that built up near the coast after May 16.

In general, then, it appears that the depth of the mixed layer over the period of observation is closely related to the availability of mechanical energy from the winds. Moreover, Ekman layer divergence (convergence) generated by a positive (negative) wind-stress curl at the surface is clearly not of importance since it would produce an effect opposite to that observed. For example, cyclonic winds which would generate a divergence of the surface waters and therefore an upward vertical velocity at the base of the main pycnocline should be associated with a decrease in the thickness of the upper layer; anticyclonic winds on the contrary should be associated with an increase in layer thickness. That the reverse situation actually occurs is evidence of the unimportance of the Ekman divergent effect compared to the mechanical mixing of the surface winds in altering the thickness of the surface mixed layer. Below the depth of direct surface influence, however, the vertical velocities induced by the Ekman layer divergences can be of importance as shown in the next subsection.

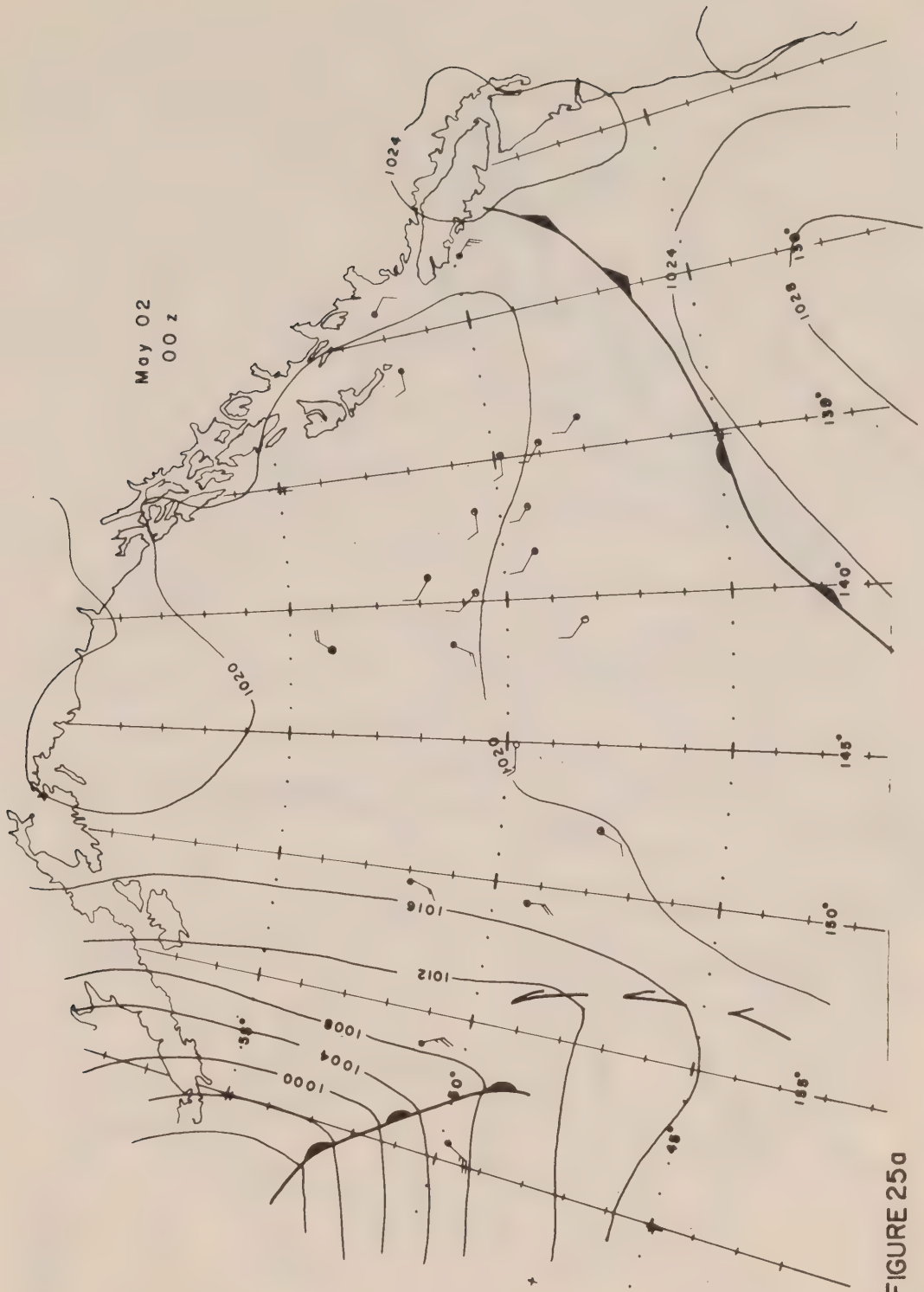
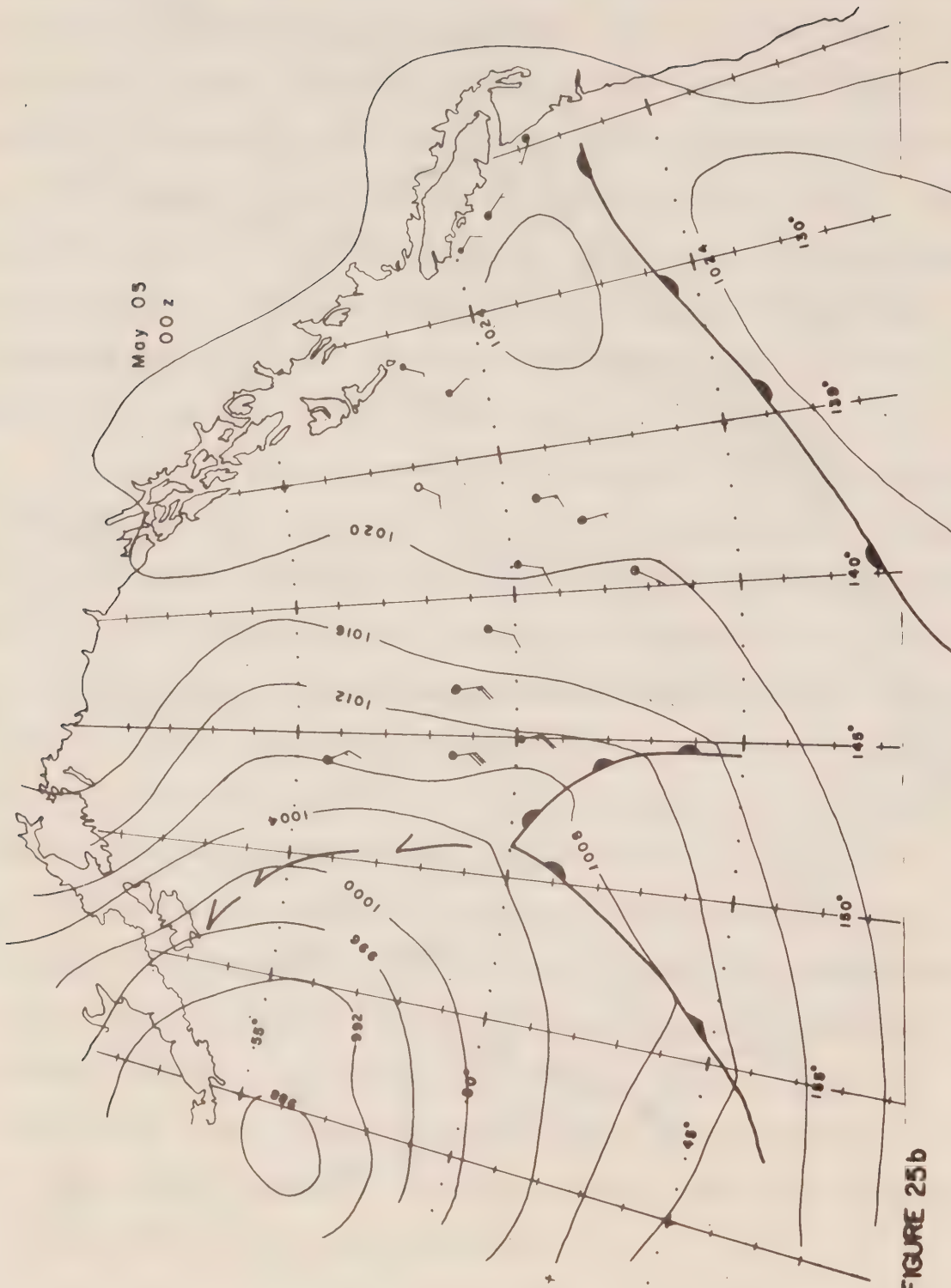


FIGURE 25a



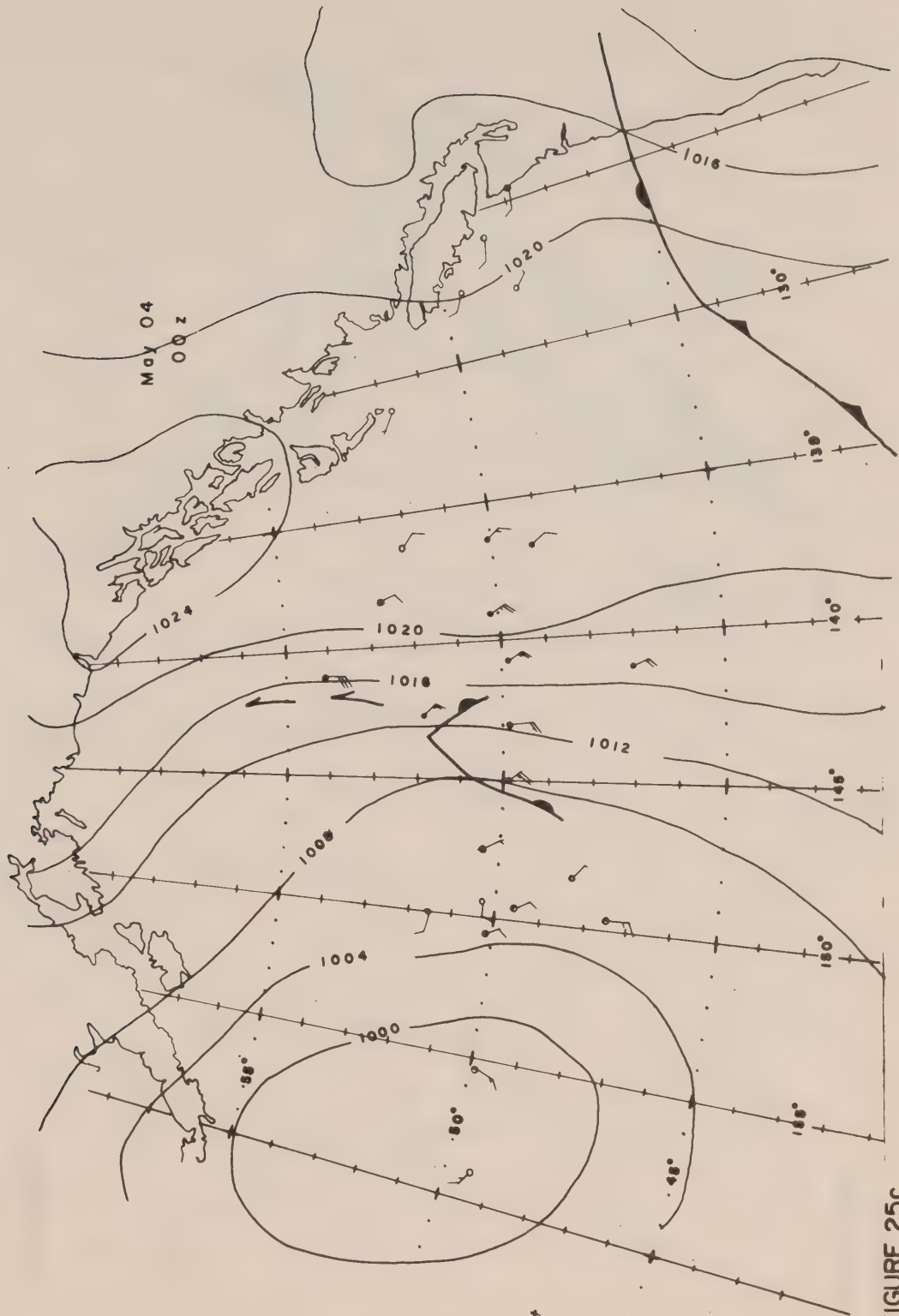


FIGURE 25c

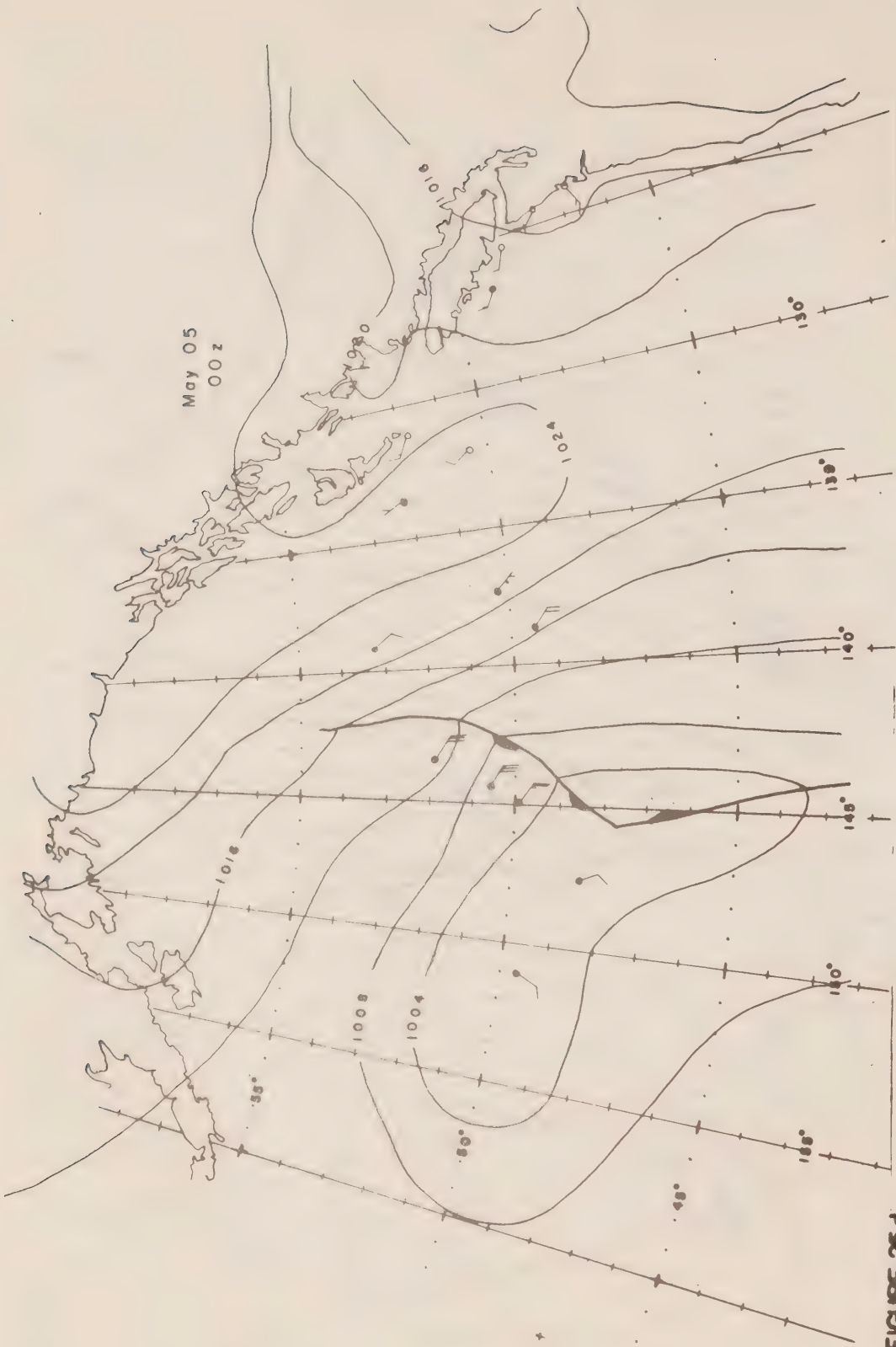


FIGURE 25d

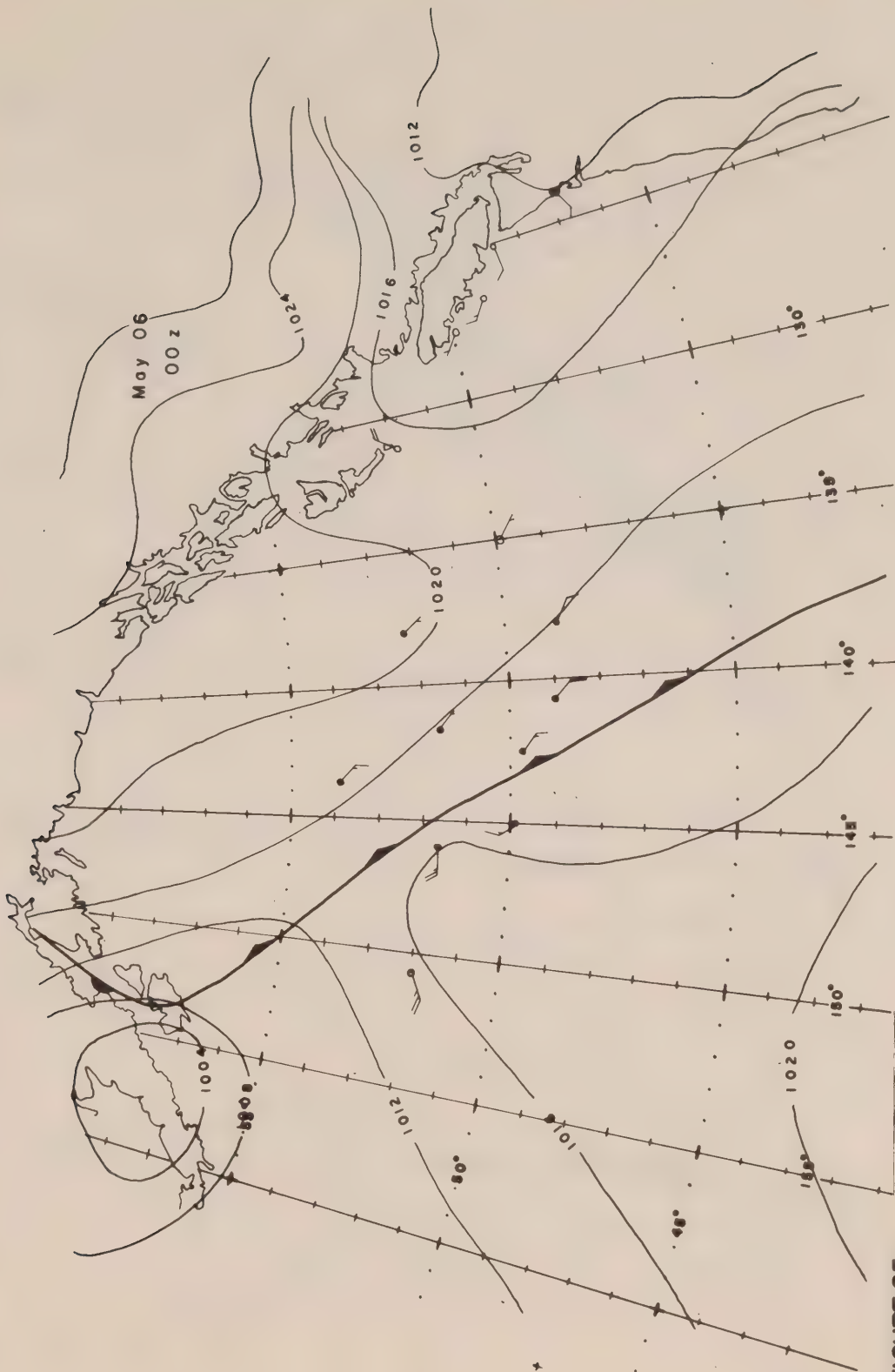


FIGURE 25e

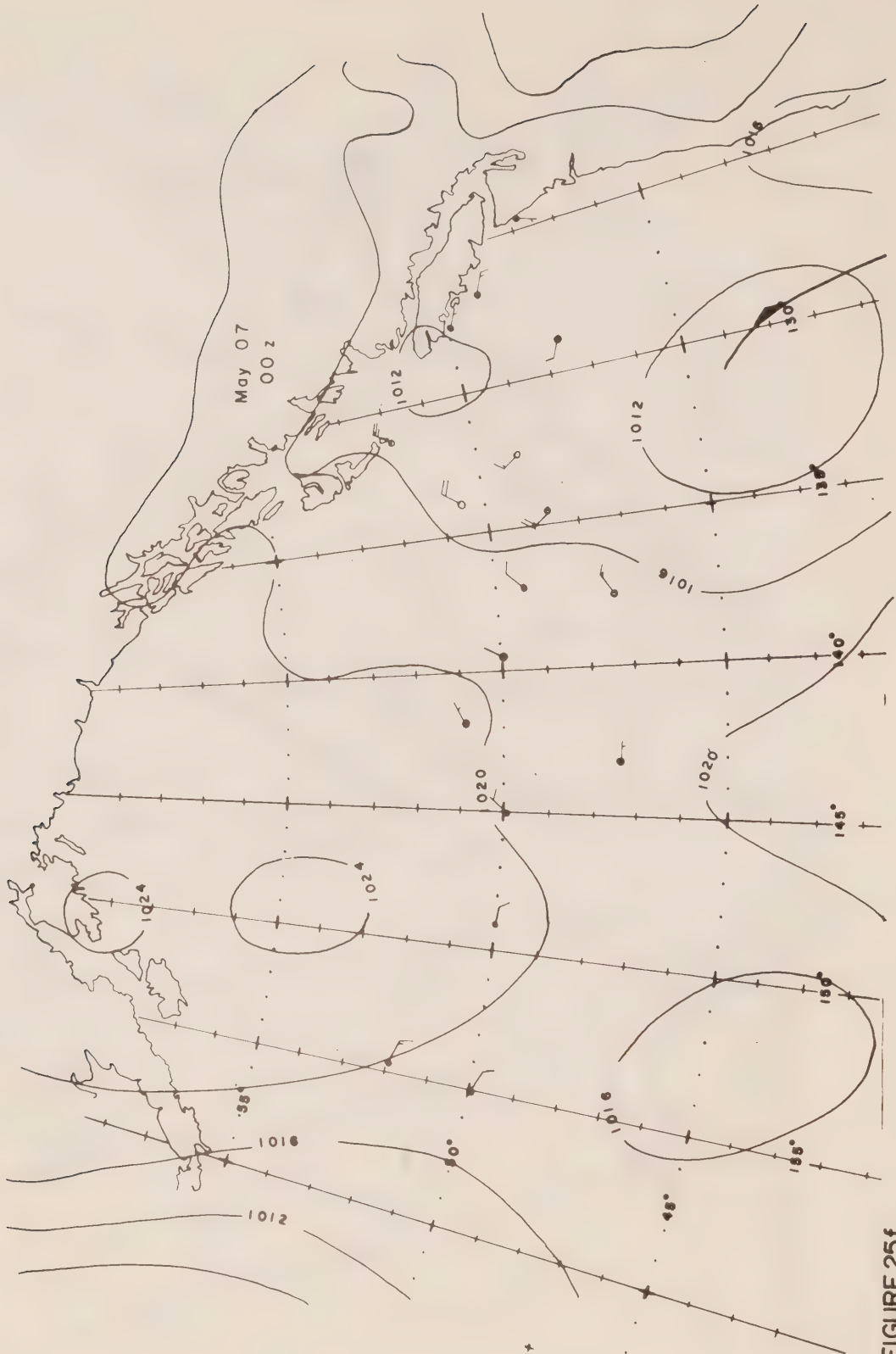


FIGURE 25f

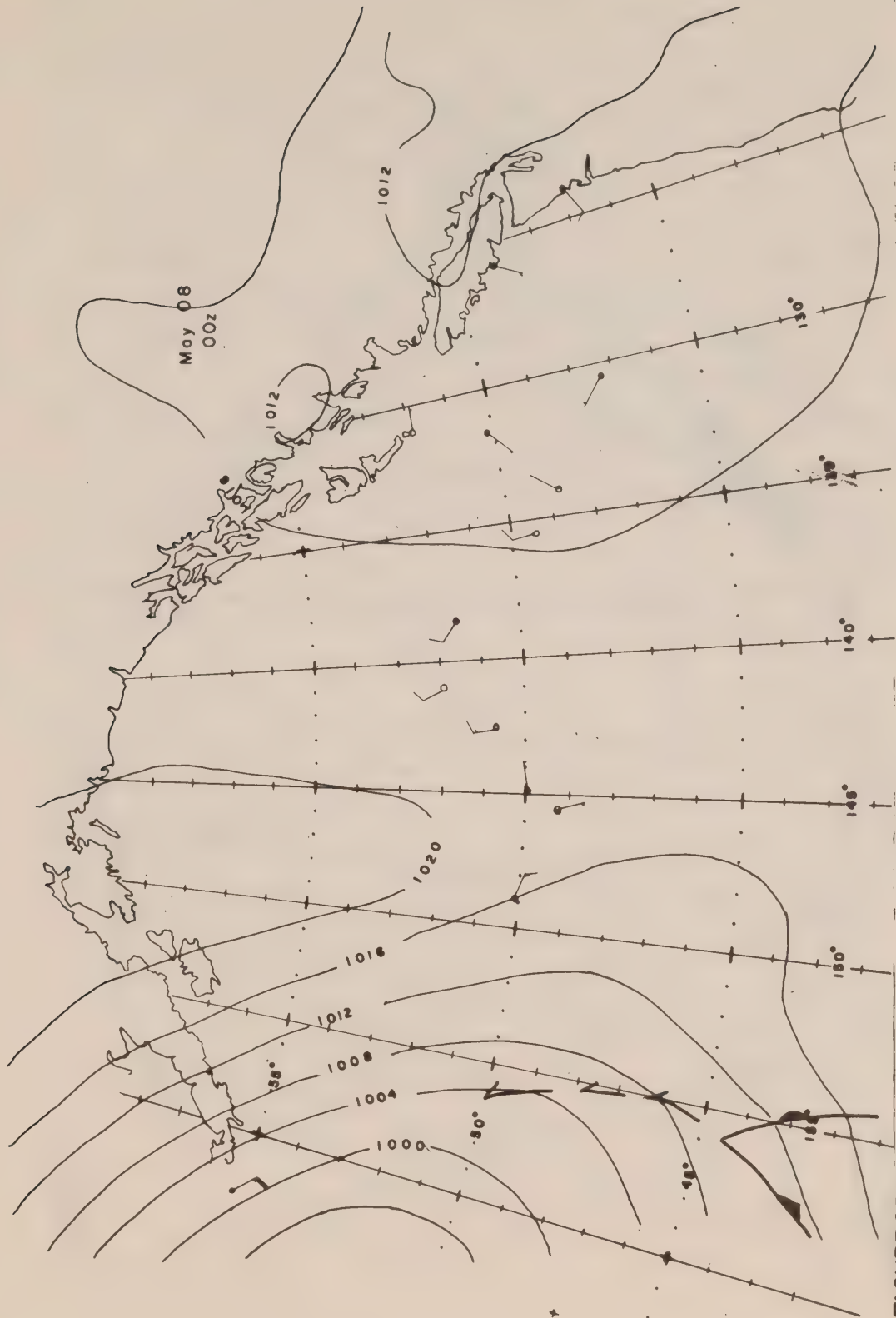
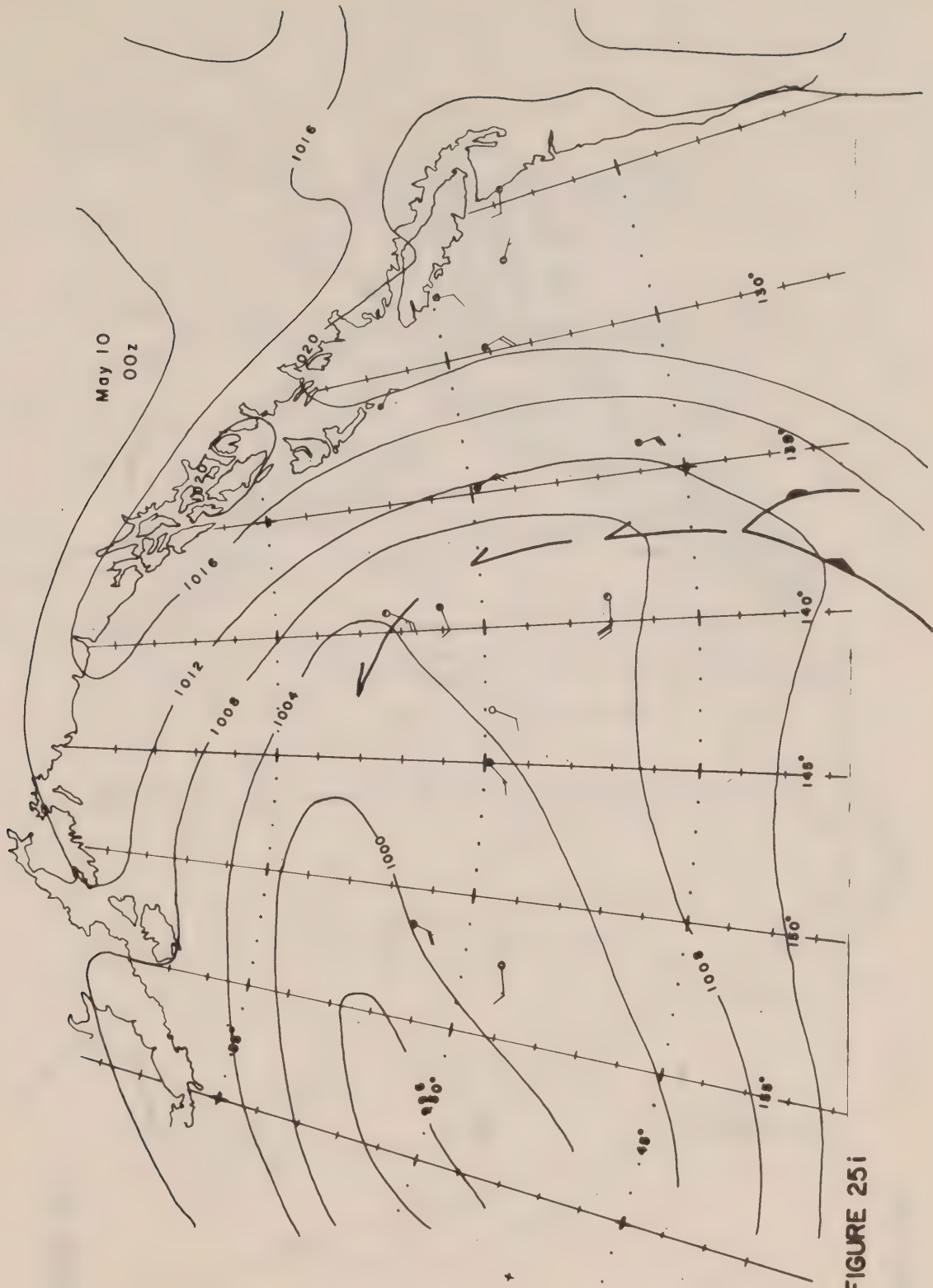
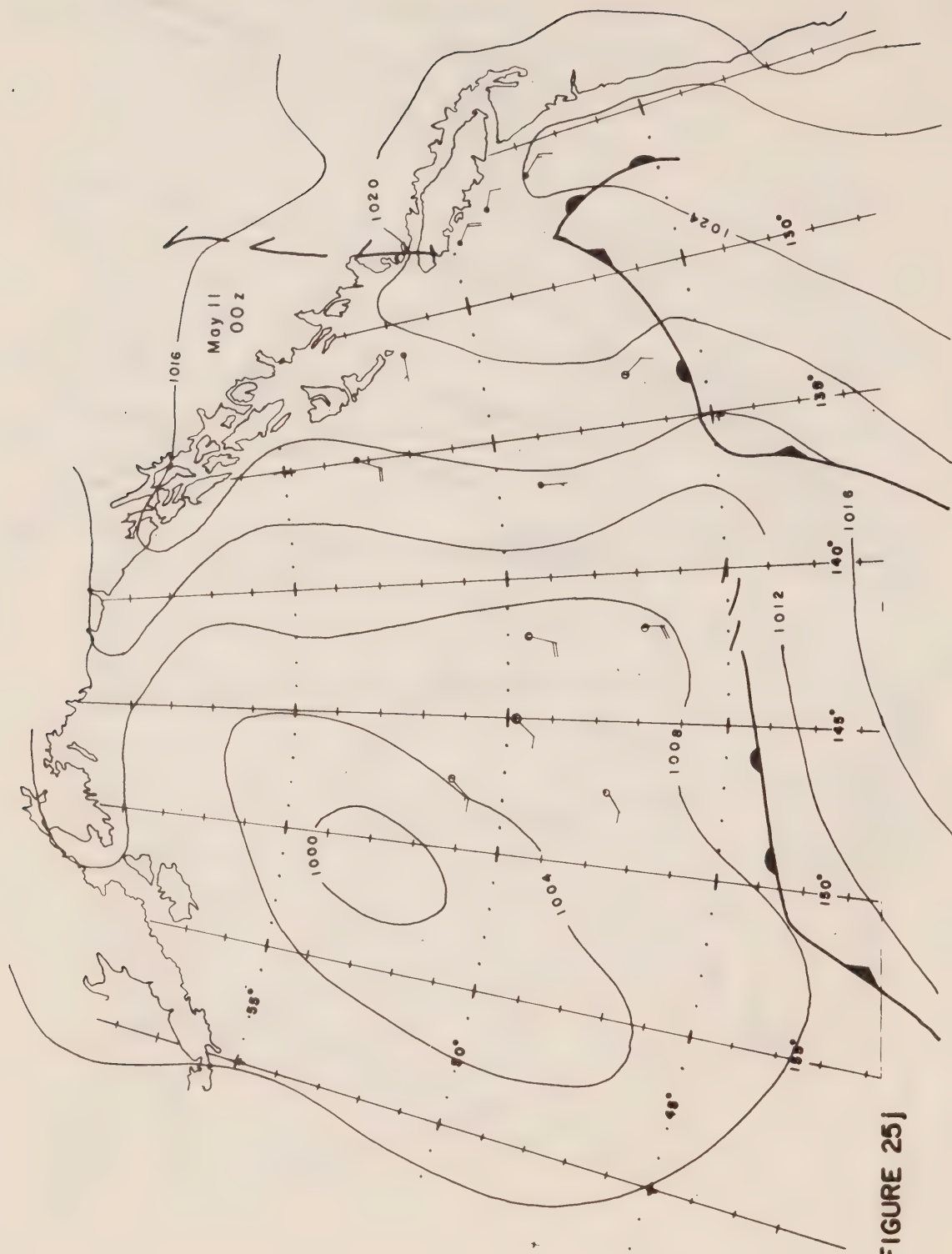


FIGURE 25g







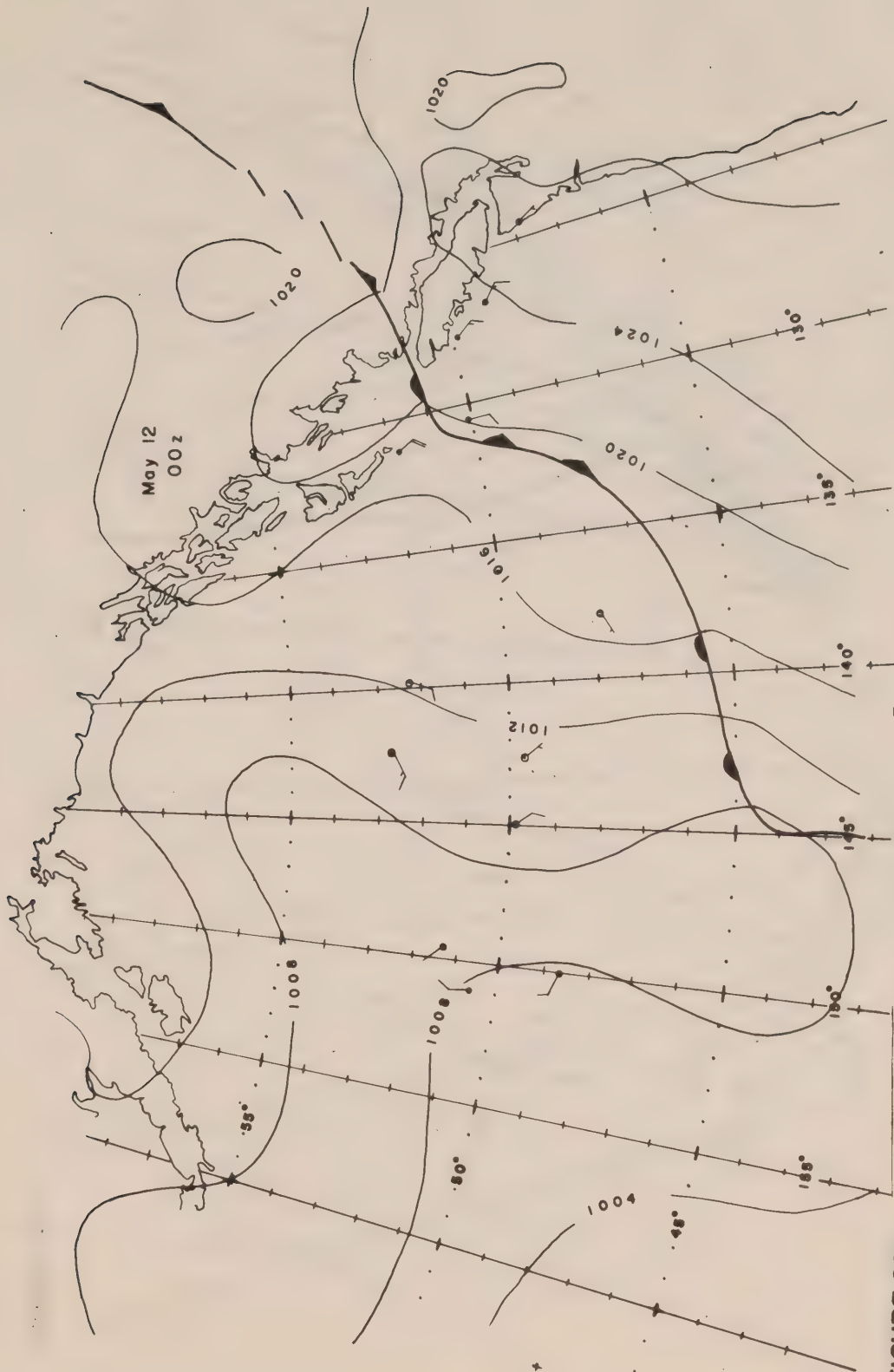


FIGURE 25k

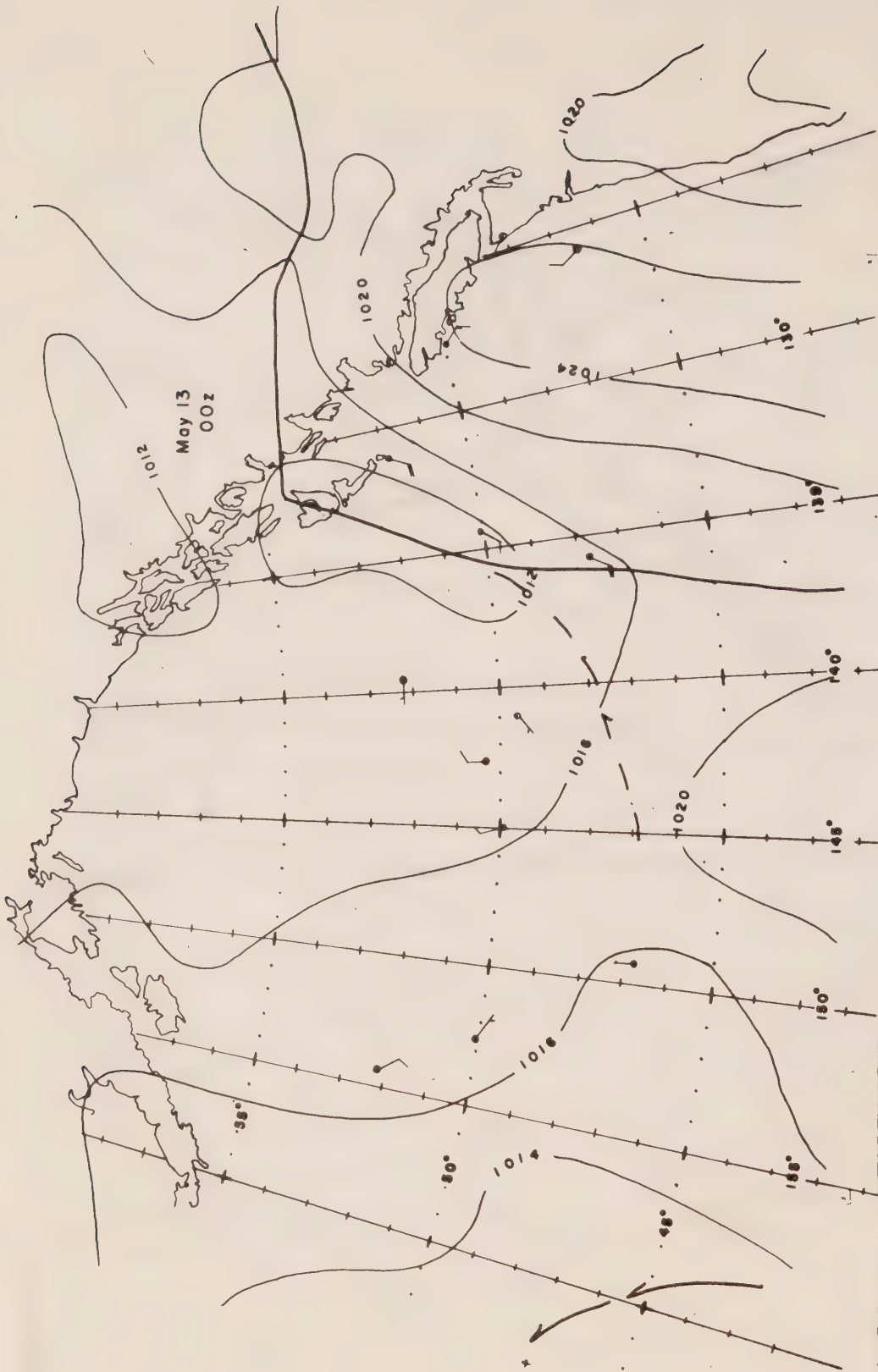


FIGURE 251

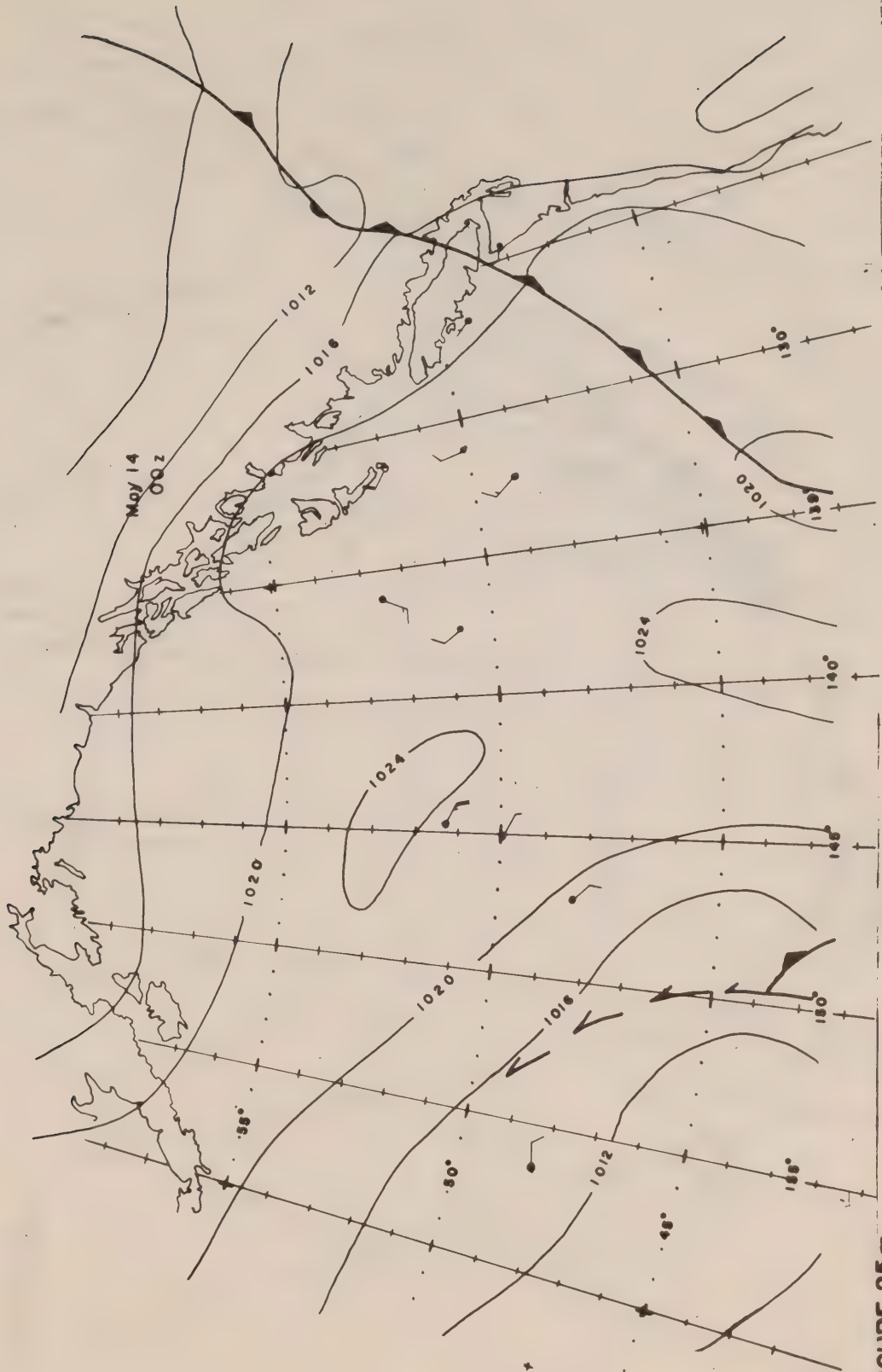
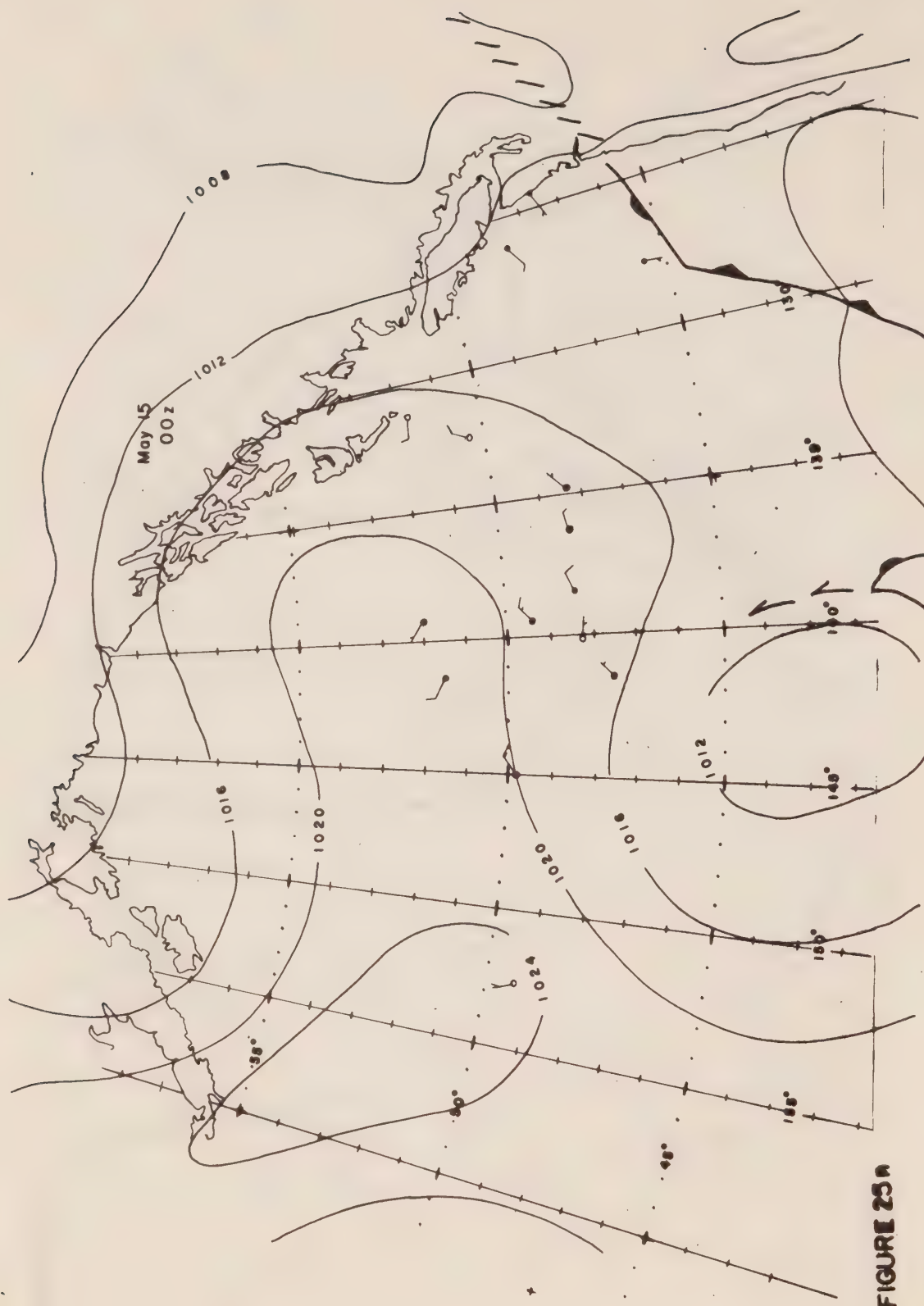


FIGURE 25m



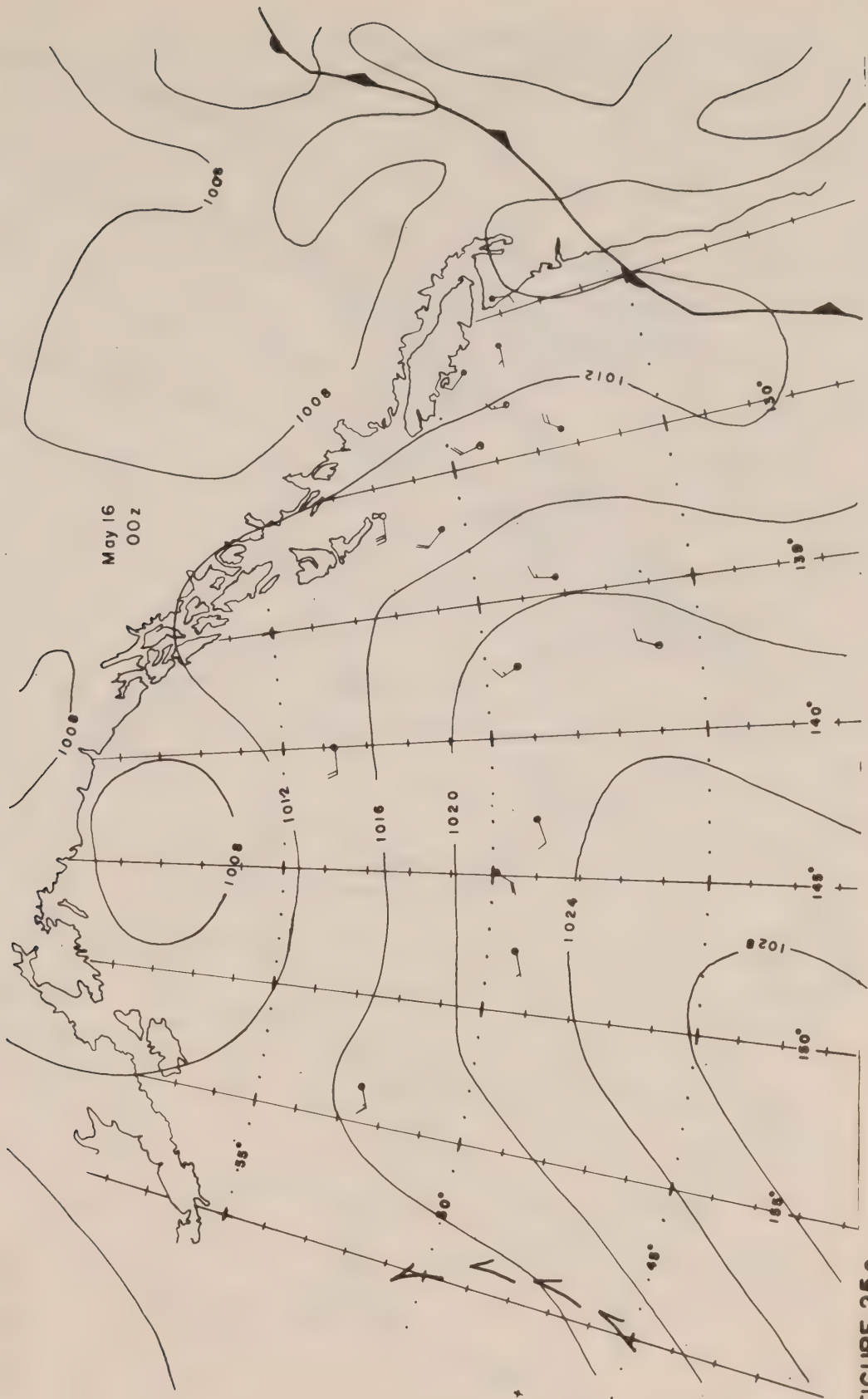


FIGURE 250

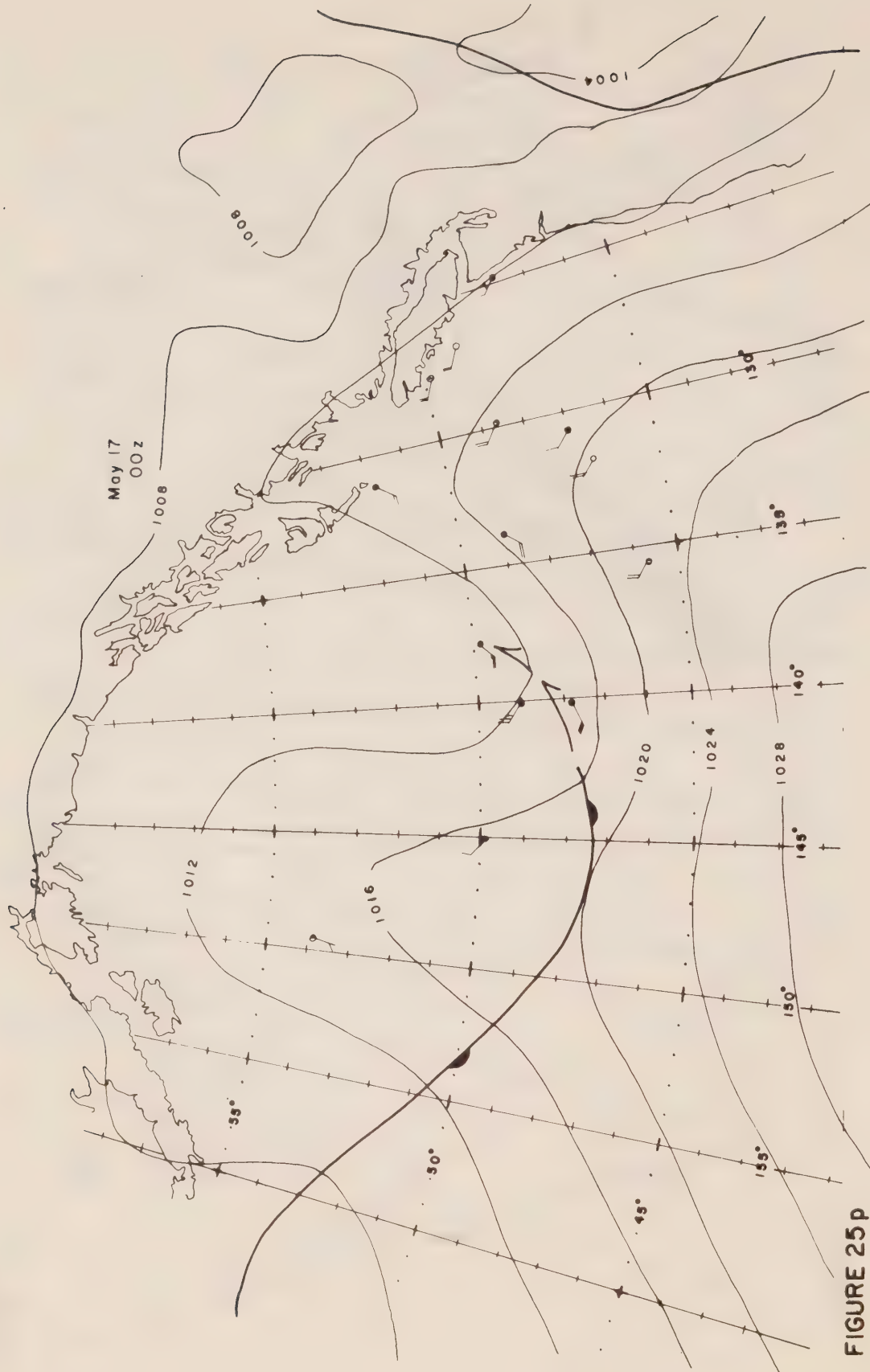
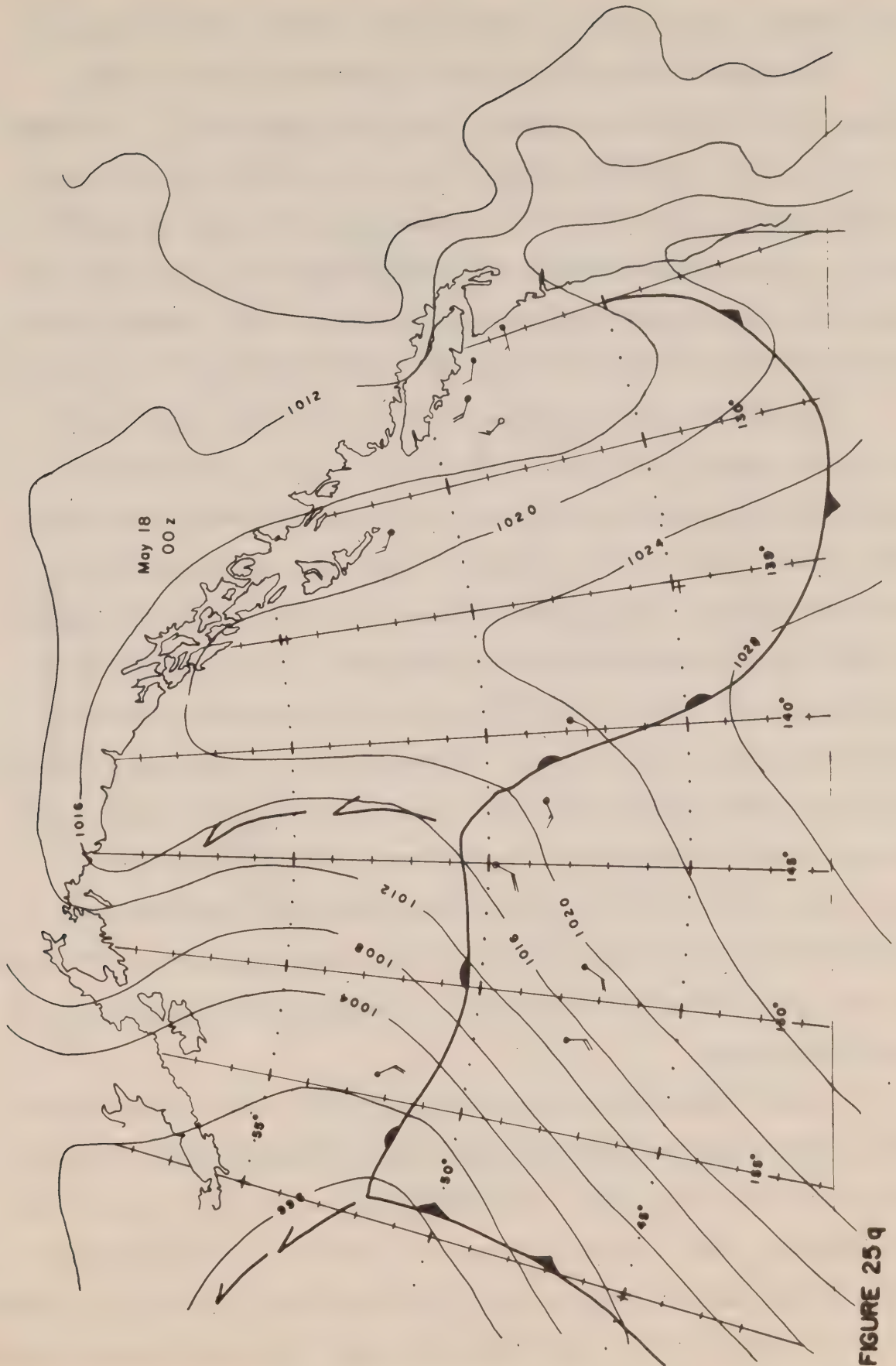


FIGURE 25 p



3.4. Depths of the 33.0% and 33.5% Salinity Surfaces Versus Longitude

The depths of these two surfaces as determined from the three samplings of Line P are plotted versus distance in figures 26a, b. Although much of the station-to-station change within a given cruise is attributable to internal motions (see § 2.5), it is apparent that there was an overall increase in the mean levels between the LAYMORE observations (9-12 May) and the weathership observations that followed. There did not, however, appear to be any consistent change in the mean level between weathership cruises. (Fig. 26c).

The spatial trend of shallow values near the coast tending to deeper values seaward is typical of Line P and is simply a manifestation of the shallowing topography and coastal currents. The temporal increases in depth, however, must be the resultant of large scale processes over this corner of the Pacific. One possible explanation is that between the time of the LAYMORE and the weathership samplings there was a general relaxation in the upward vertical velocities at the base of the halocline as a result of decreased cyclogenesis over the region. Examination of figures 25a-q indicate that this may indeed have been the case since the cyclonic wind patterns that existed over much of the subarctic region from 9-12 May gave way to anti-cyclonic winds from 12-15 May. The resultant "spin-down" associated with the Ekman layer convergence, which occurs within a half-pendulum day (~ 18 hours), would then allow sinking of the surfaces of constant physical properties to a new equilibrium level.

Another feature of the subarctic Pacific which would induce similar results, would be a weakening of the Alaska gyre by the advent of anticyclogenesis over the Gulf of Alaska. Its effect would be contrary to what is observed, however, since it would be expected to produce a relative decrease in the depth of the salinity surfaces along the Line through a decrease in northward advection into the gyre in a region where the depth of salinity surfaces increases southward.

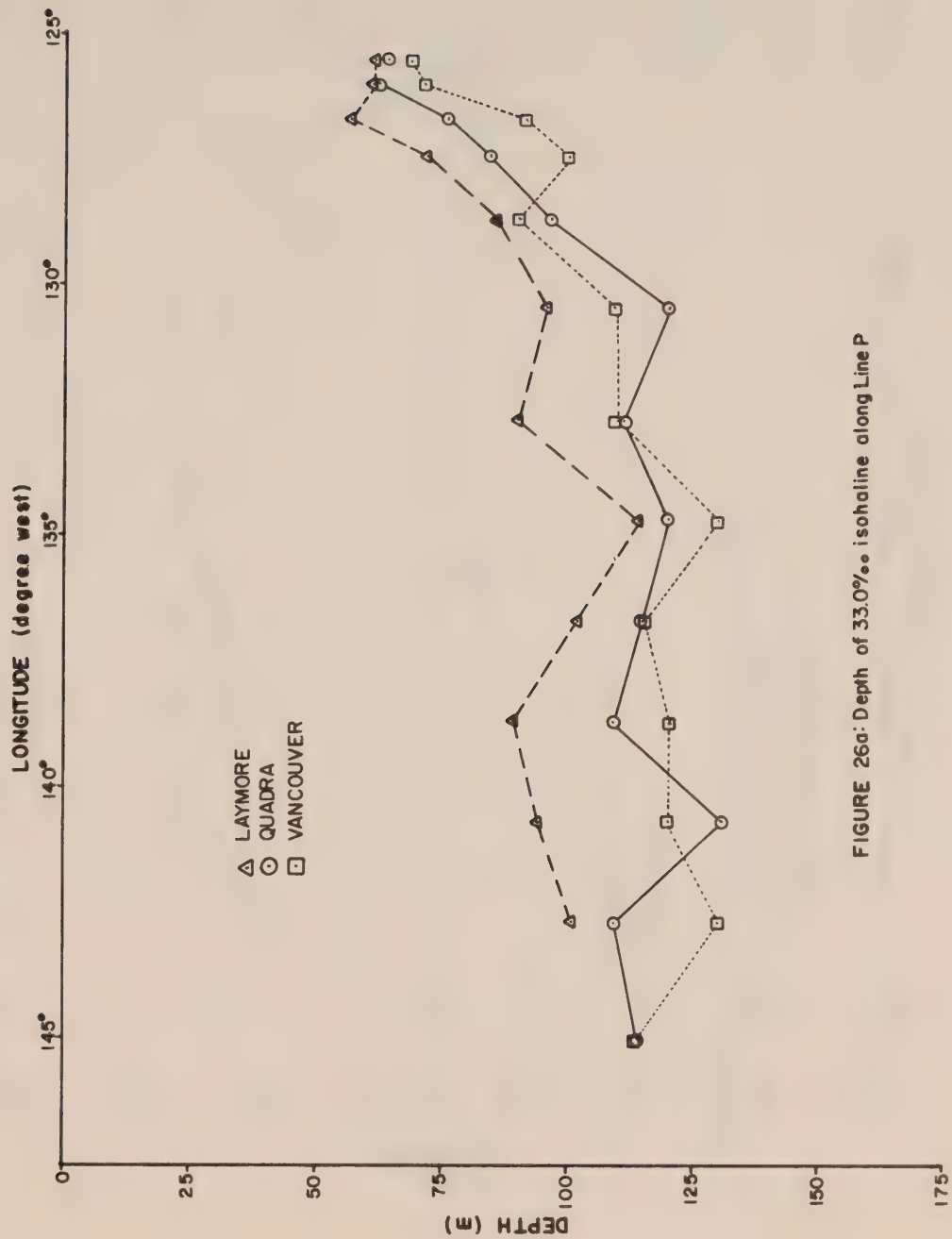


FIGURE 26a: Depth of 33.0‰ isohaline along Line P

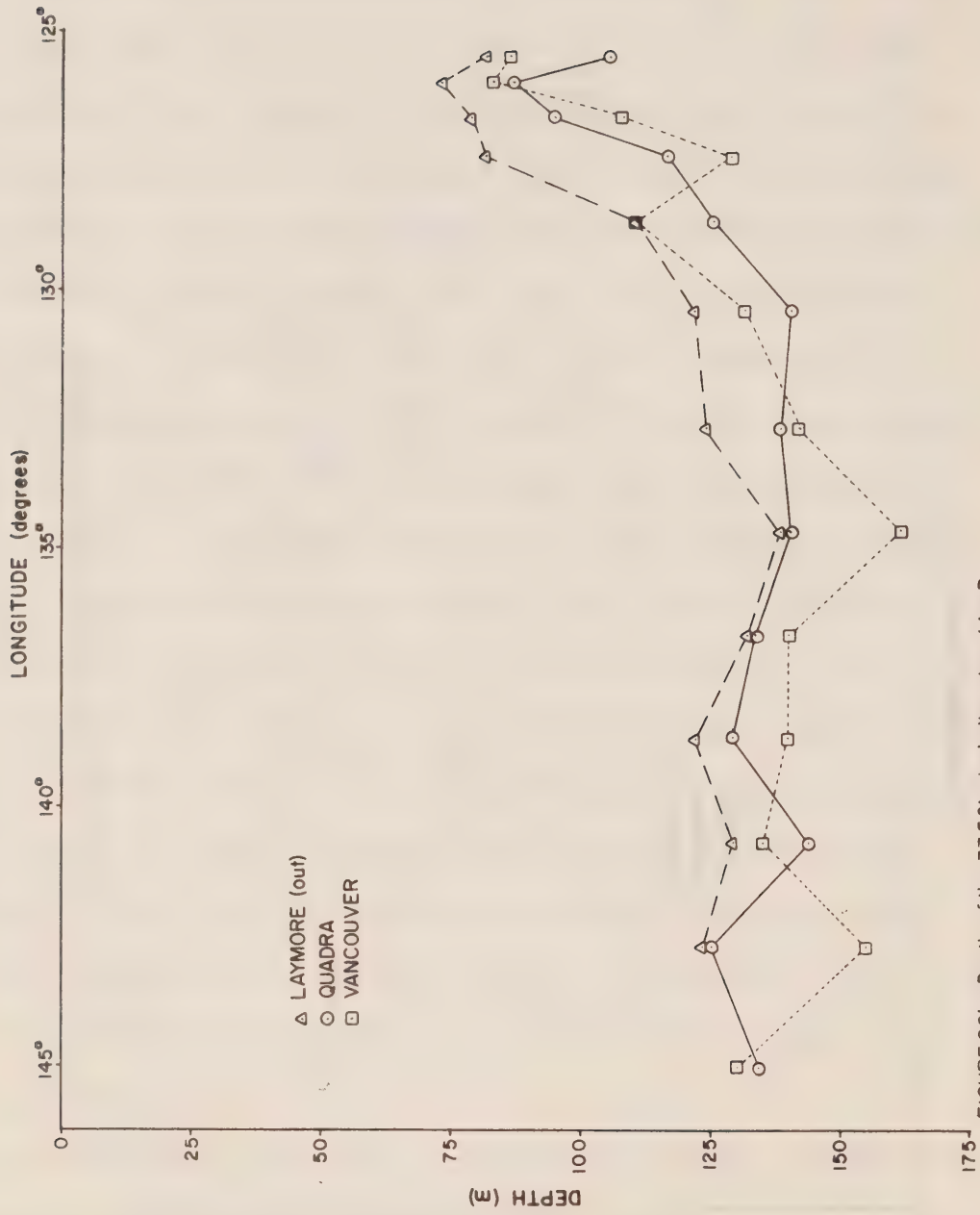


FIGURE 26b: Depth of the 33.5‰ isohaline along Line P

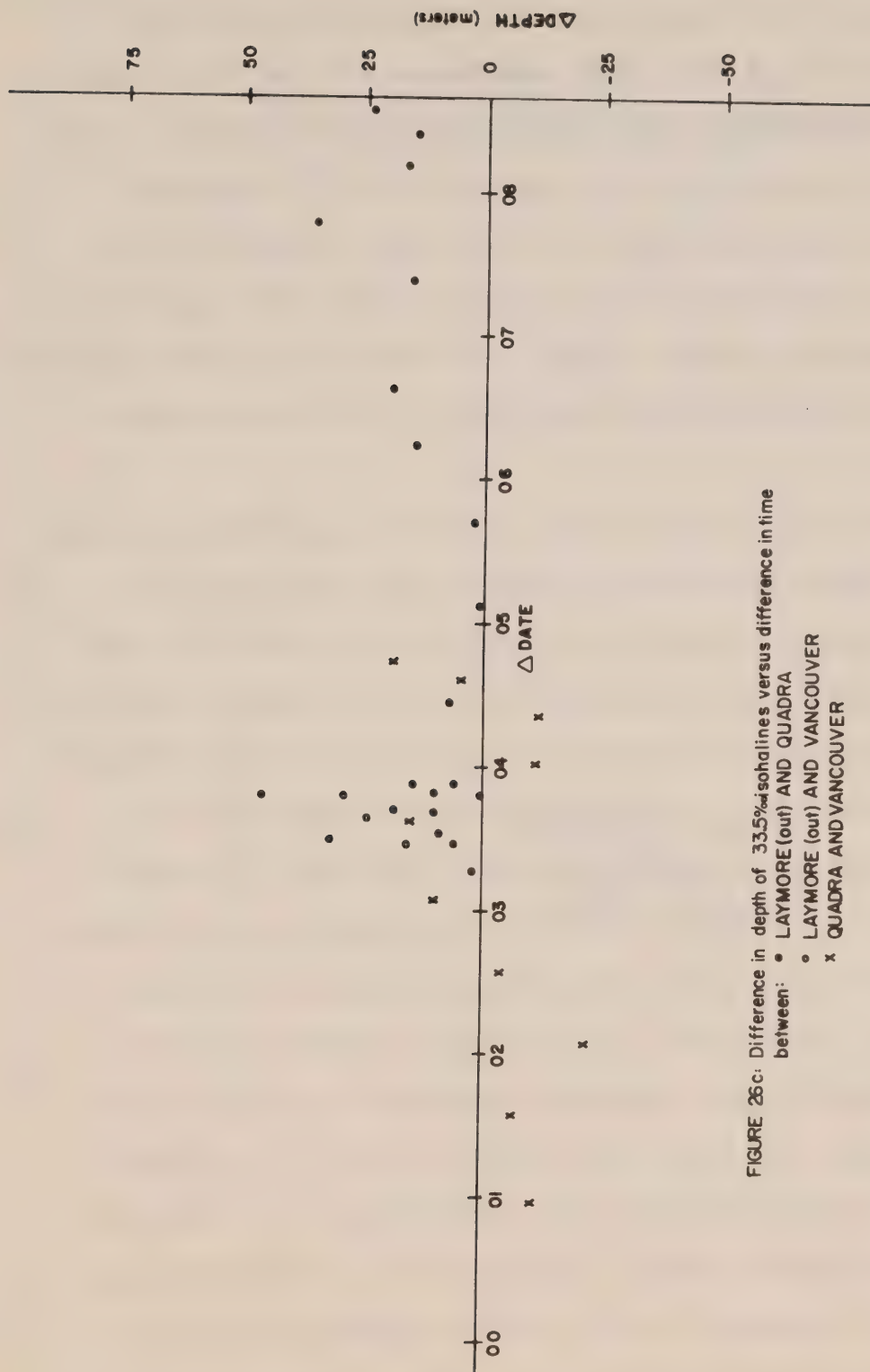


FIGURE 26c: Difference in depth of 33.5‰ isohalines versus difference in time between:
 • LAYMORE(out) AND QUADRA
 ○ LAYMORE (out) AND VANCOUVER
 x QUADRA AND VANCOUVER

3.5. Depth of the Dichothermal Layer

As defined by Uda (1963) the Dichothermal layer is a tongue of relatively cold water which sometimes exists at a depth of around 100 m in the subarctic Pacific Ocean (figure 27). On the eastern side of the ocean, formation of this water begins with intense winter cooling and wind mixing. By late winter this results in a surface layer (~ 100 m) of isothermal water that is colder than that below. With the advent of spring, surface heating occurs and warmer water is mixed downward but not far enough to remove the positive temperature gradient at depth. The feature then usually persists until the next cooling period (fall-winter) when it is either destroyed or enhanced.

The difficulty with determining a depth for the dichothermal layer is that various internal wave modes can greatly distort the temperature profile. This distortion is particularly prohibitive in 0-300 m STD casts because of the expanded scale so where possible 0-1500 m reverse traces have been used. Even then, errors of order ± 10 m (or more) in reading the mean depth are readily possible. Furthermore, what can be interpreted as a dichothermal layer may in fact be associated with the mixing of different water masses and not with the past effects of winter cooling. As discussed in § 2.6, this is particularly true for near coastal stations and depths greater than 150 m. Despite these, and the internal effects of vertical displacements, figure 28 gives a reasonably compatible set of plots of the depth of a dichothermal-like layer versus station position. The shoreward shallowing of the layer is associated with a similar decrease in the depth of the top of the pycnocline since, as expected for a surface influenced feature, the depth of penetration of the winter overtuning and cooling is clearly limited by the stability of the water column. Again, station 5

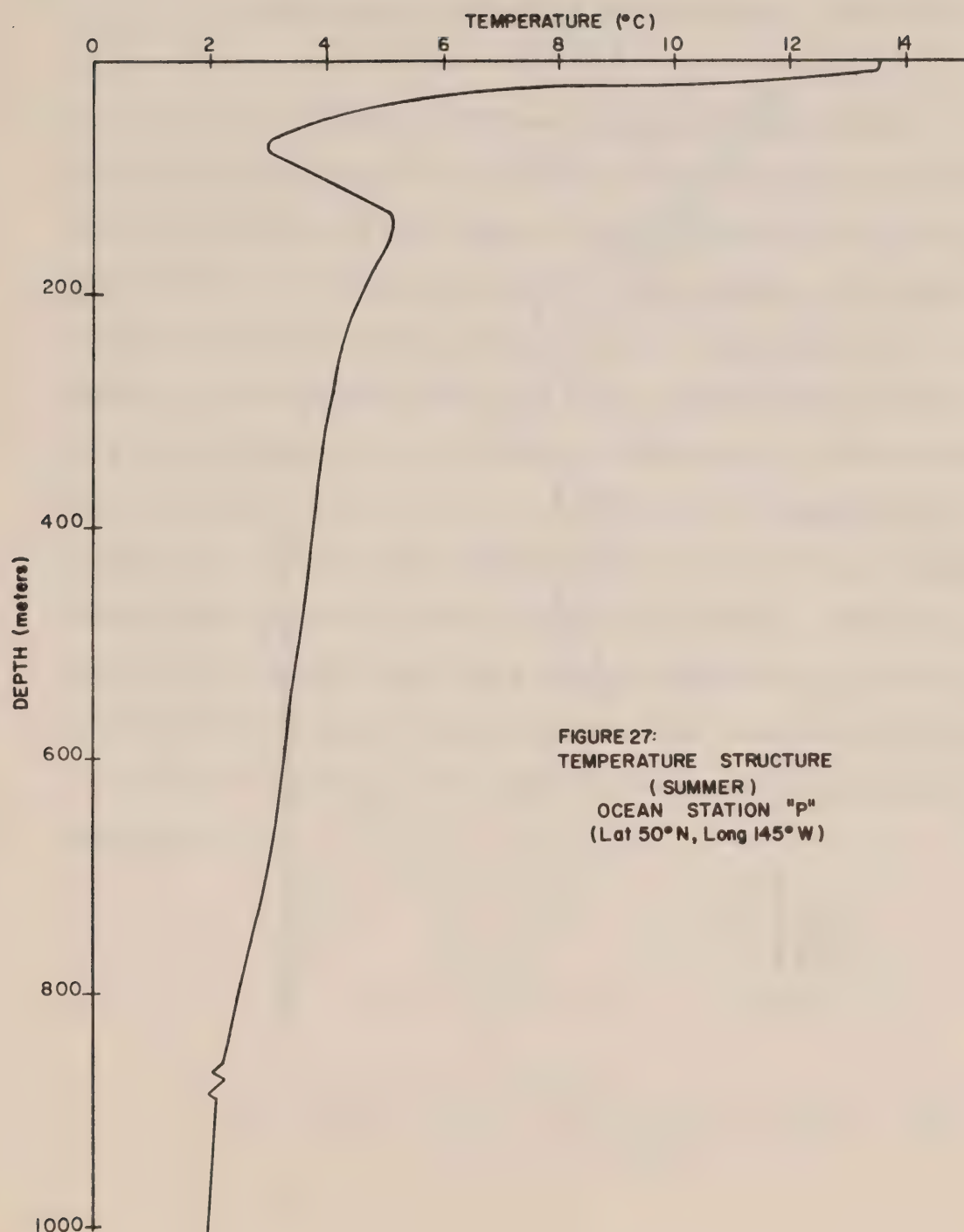


FIGURE 27:
TEMPERATURE STRUCTURE
(SUMMER)
OCEAN STATION "P"
(Lat 50°N, Long 145°W)

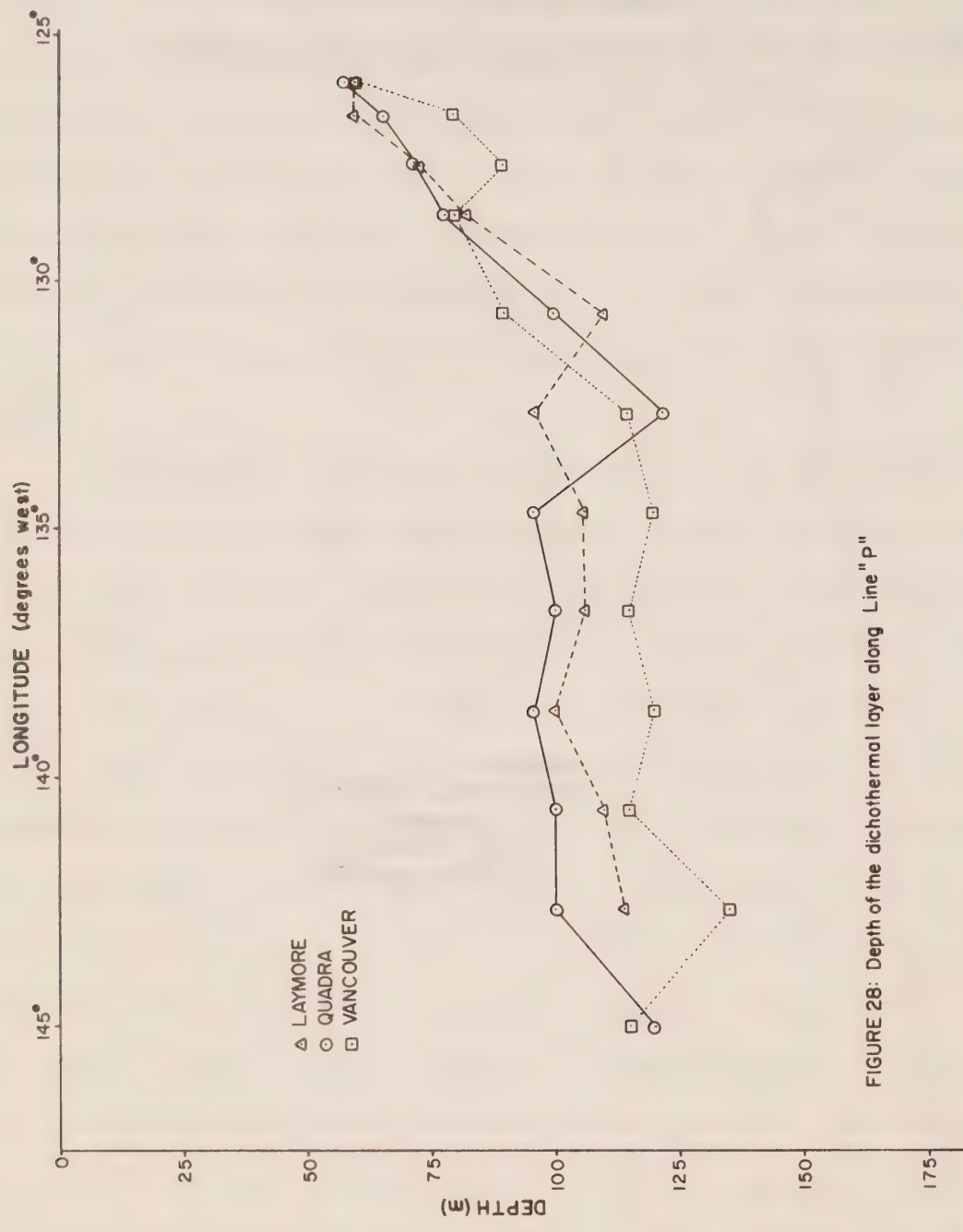


FIGURE 28: Depth of the dichothermal layer along Line "P"

appears to mark the transition from the coastal to the oceanic domain. In the latter region, the maximum depth of late winter cooling is seen to be around 100-125 m in agreement with Uda.

The temperature gradient of the dichothermal layer defined by

$$\partial T / \partial z \sim \Delta T / \Delta z ,$$

where ΔT is the temperature difference and Δz is the thickness, is given in figure 29 for the three sets of observations. Irrespective of the large amount of variation at each position due to stretching and compressing of the isotherms by internal wave motion, there appears to be a definite maximizing of the gradient near stations 3 and 4. Categorically, it is not possible to state whether this is a result of water mass mixing as described in §2.6. or whether it is the result of particularly vigorous mixing that occurred in the winter of 1971-72. Possibly it is a combination of both, although the fact that this region compared to others has relatively large temperature gradients to 1500 m, suggests the former. Therefore, the plots can be considered to identify the depth and temperature gradients of the dichothermal layer except in the vicinity of the coastal stations where the feature is masked by the horizontal confluence of the coastal and interior water masses.

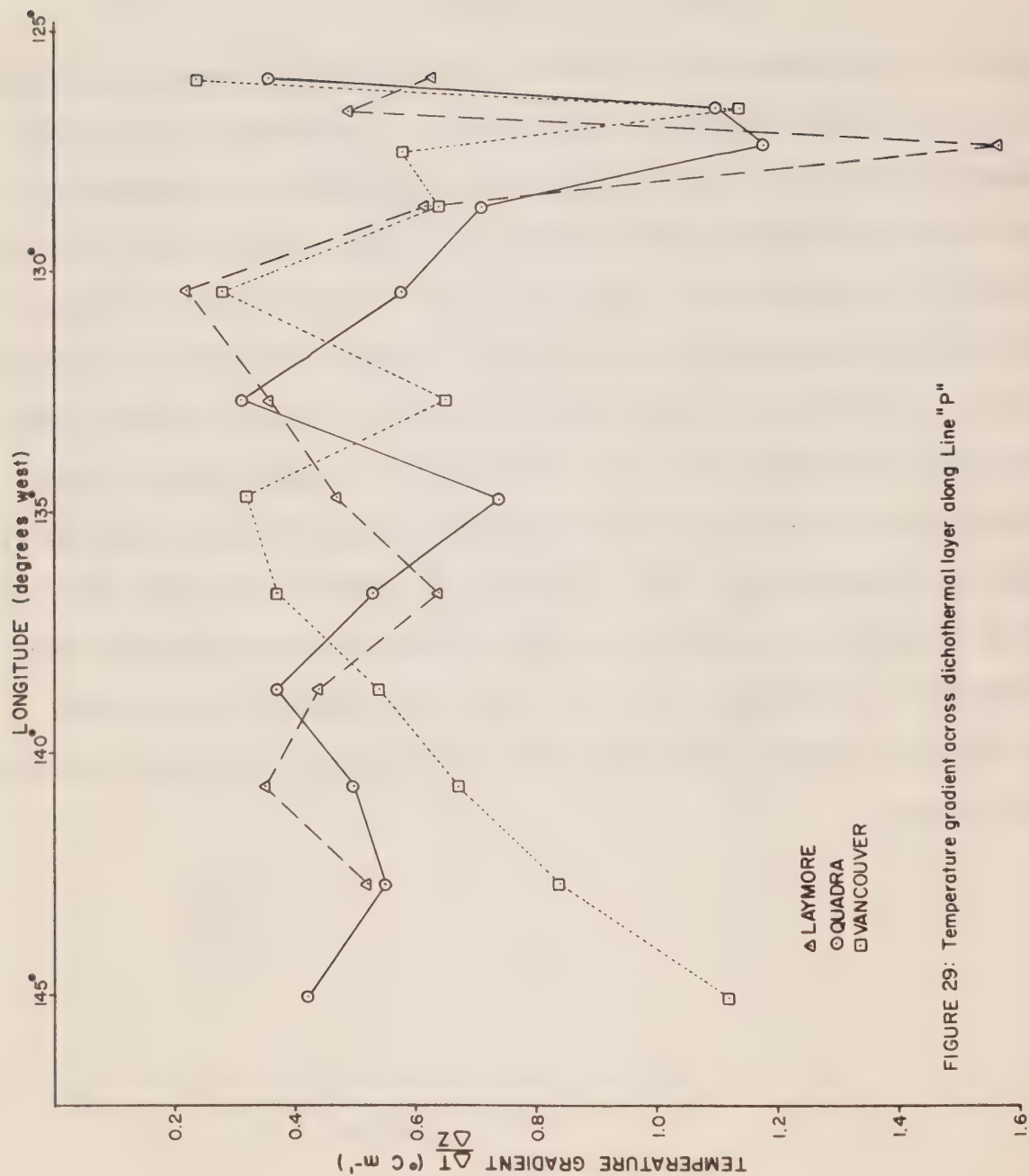


FIGURE 29: Temperature gradient across dichothermal layer along Line "P"

3.6. Geostrophic Mass Transport Across Line P

The concept of the geostrophic transport between two stations being proportional to their difference in the potential energy anomaly is based on steady-state calculations. Nonetheless, it is possible to obtain some idea of the flow variability with time if the adjustment period of the density structure is short compared to that between observations.

As indicated previously by the potential energy plots of figures 10a-g, the water motion in the vicinity of Line P would not be expected to have a constant component perpendicular to the Line. This is supported by figure 30 which gives the spatial variation of the potential energy relative to 1200 m for each of the three transects (in each case, the component of integrated transport at right angles to the Line is such that the large values are to the right facing in the direction of the flow). Subtracting the value at station 12 from that at station 4 for each cruise further indicates a variation in the mean total northward transport from 5.76 sv (sverdrups) during the period of the LAYMORE crossing, which decreases to 4.77 sv during that of the VANCOUVER, to 6.57 sv during the QUADRA cruise. The greatest amount of temporal variation in any one locality is between 128° and 135°W longitude where the eastward moving waters are being most influenced by the coastal regime. In the latter, between-station transport is maximum and directed parallel to the coast. Finally, taking 5.5 sv as the mean mass transport between stations 4 and 12 gives an average surface current speed v of

$$v \sim 0.43 \text{ cm/s}$$

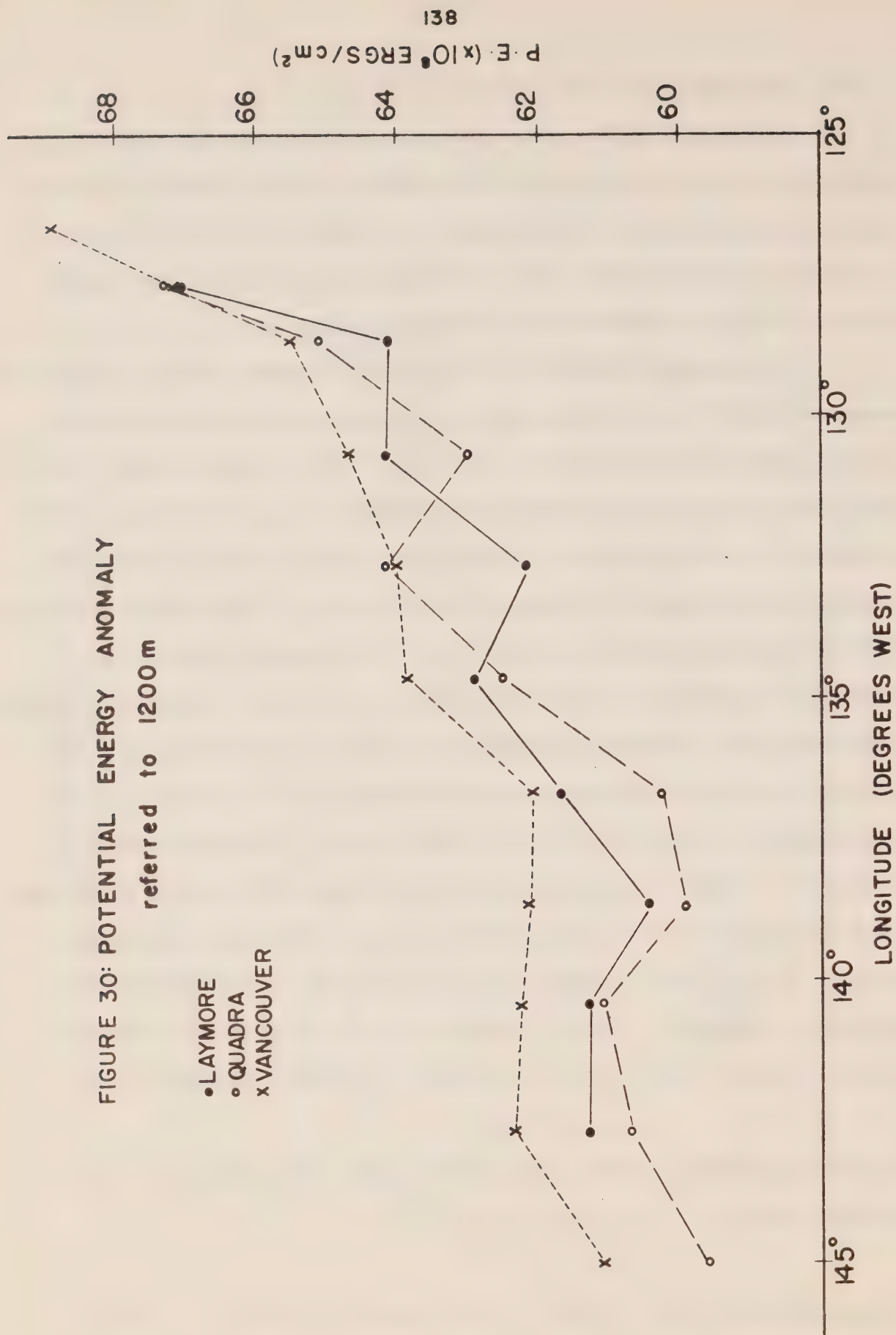
or about 0.4 km/day at right angles to the Line. This compares to a mean northward speed of

$$v \sim 2.63 \text{ cm/s}$$

between stations 4 and 5 alone, or a surface drift of about 2.3 km/day.

FIGURE 30: POTENTIAL ENERGY ANOMALY
referred to 1200 m

- LAYMORE
- QUADRA
- x VANCOUVER



3.7. Comparison of Temperature Variance Along Line P

The temperature variances versus longitude along Line P for the three separate cruises are plotted in figures 31a-g. The first two give the block averages for the ranges 0-300 m and 300-1500 m while the remaining plots give the variances in five two-hundred meter ranges from 300-1300 m. The last range 1300-1500 m is omitted since it is very similar to the 1100-1300 m range.

Averaged over the top 300 m, there is again the tendency for the near coastal values to be larger than the more oceanic regions. There is also a general increase in the coastal variances with time since chronologically the order of ship sampling east of station 6 was LAYMORE (out), VANCOUVER, QUADRA and LAYMORE (in). This increase, moreover, corresponds almost exactly with the deepening of the mixed layer with time in the coastal areas (figure 24). The indication then, is that the apparent increase in the amount of temperature microstructure in the 0-300 m block is actually a manifestation of the increased large scale vertical temperature gradients rather than the result of a change in the horizontal mixing of water masses. Such is not the case for the 300-1500 m block. The significantly large temperature variances east of Line P station 5(128°40'W) together with the consistently smaller values to the west are a good indication of the persistence of the mixing process off B.C. The changes between cruises in the coastal region are then the result of spatial shifting of the regions of confluence and perhaps of the degree of mixing.

Within each of the five two-hundred metre intervals, the spatial distribution of the variances closely emulates that of the average over these layers with maximum values during a particular cruise occurring in level 4 or level 5. The one exception is for the 500-700 m level(5) for

the QUADRA cruise which indicates relatively low coastal values and a marked maximal value at station 8 (134°40'W). The latter is perhaps a manifestation of the discrete spatial sampling in which the region of maximum horizontal mixing was missed.

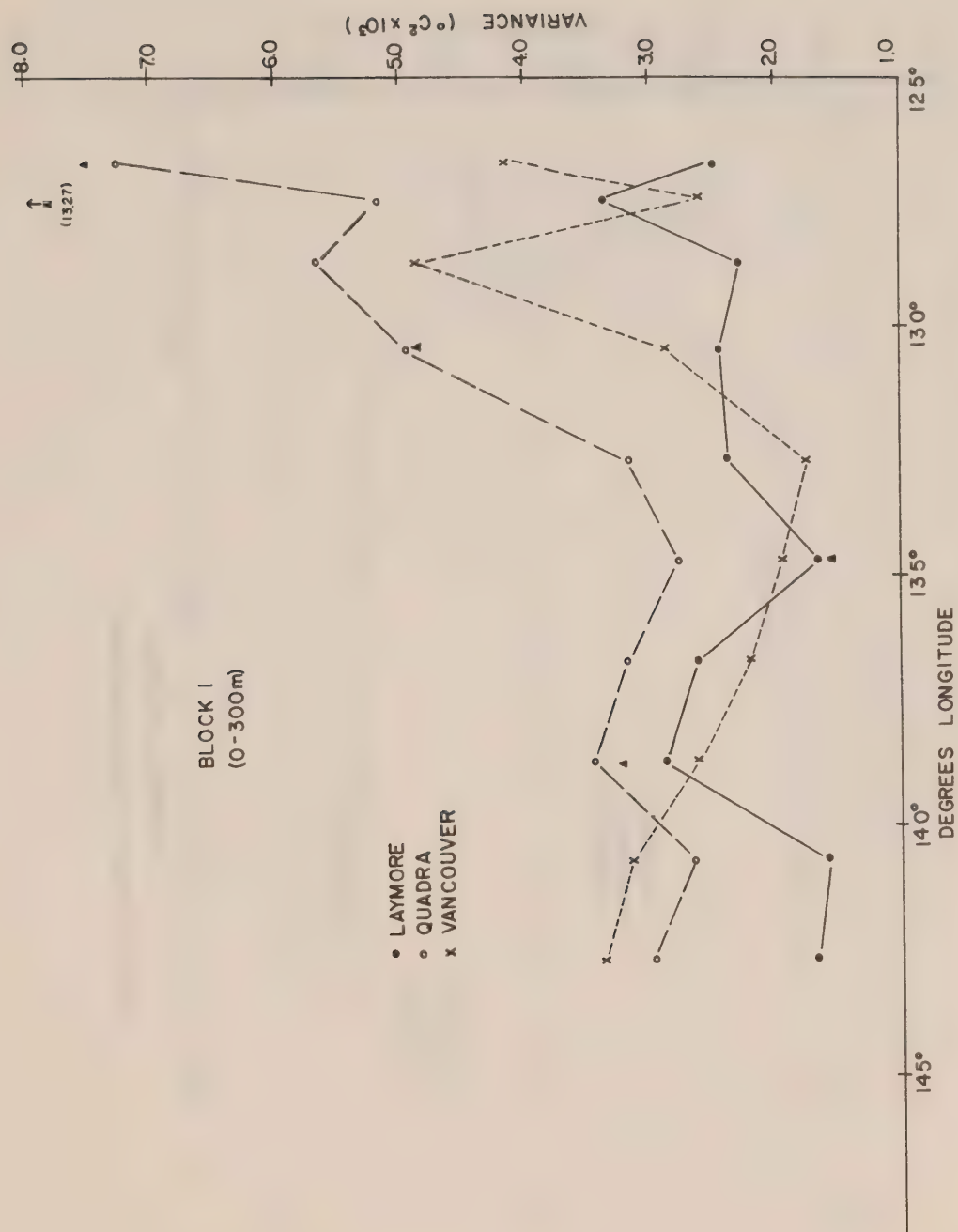


FIGURE 31a: Temperature variance along Line P for the depth interval 0-300 meters

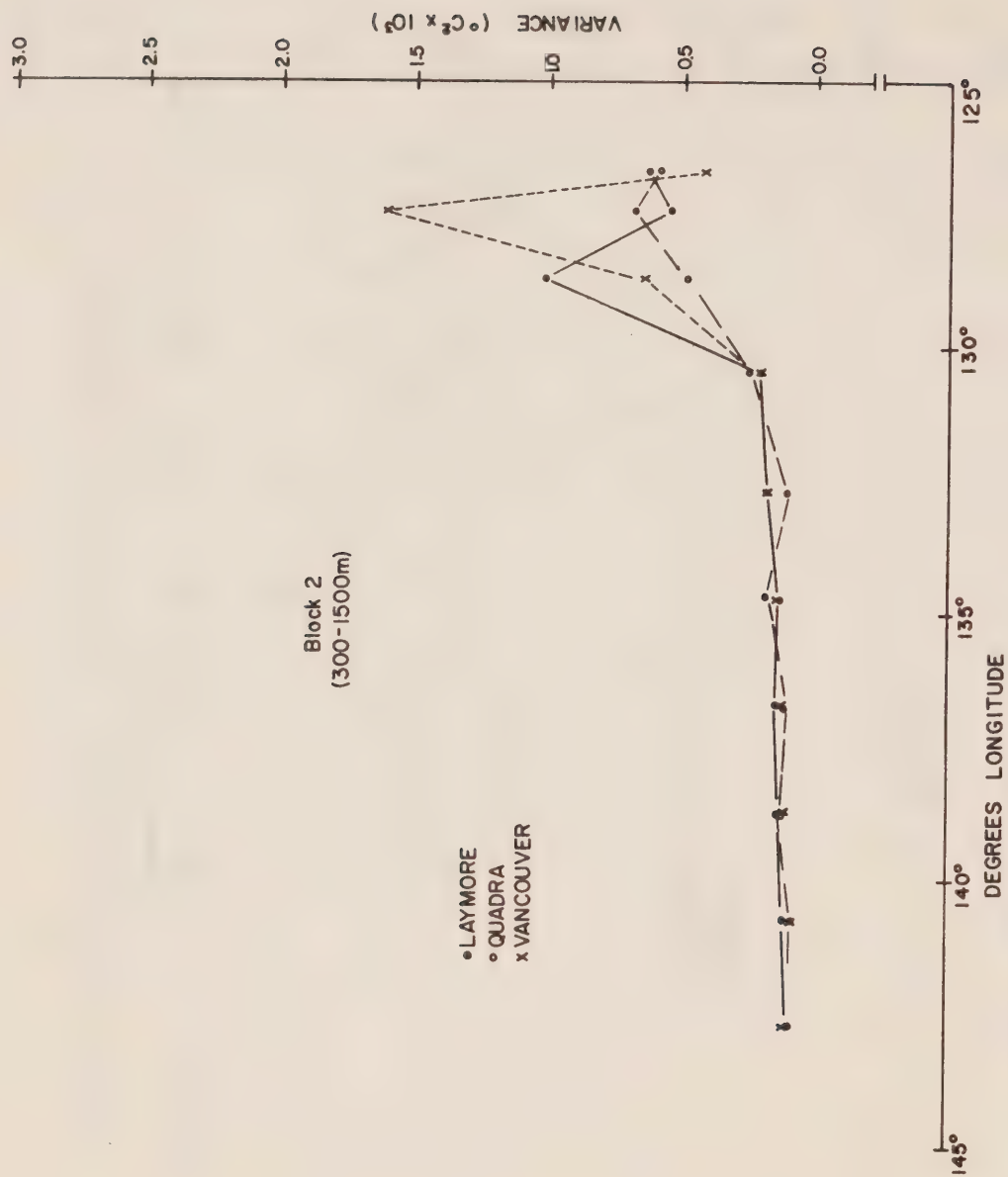


FIGURE 31b: Temperature variance along Line "P"

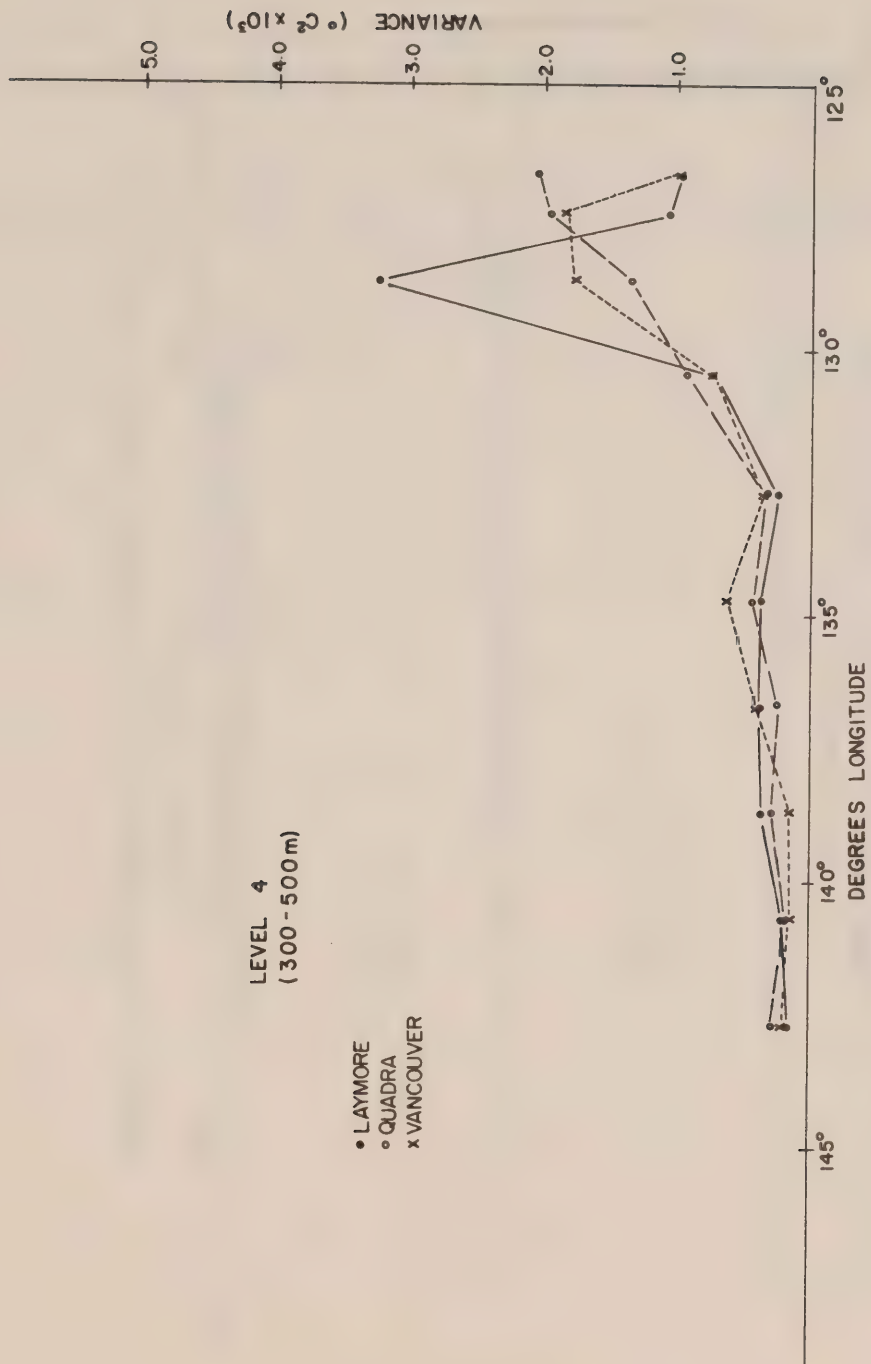


FIGURE 31c: Temperature variance along Line P

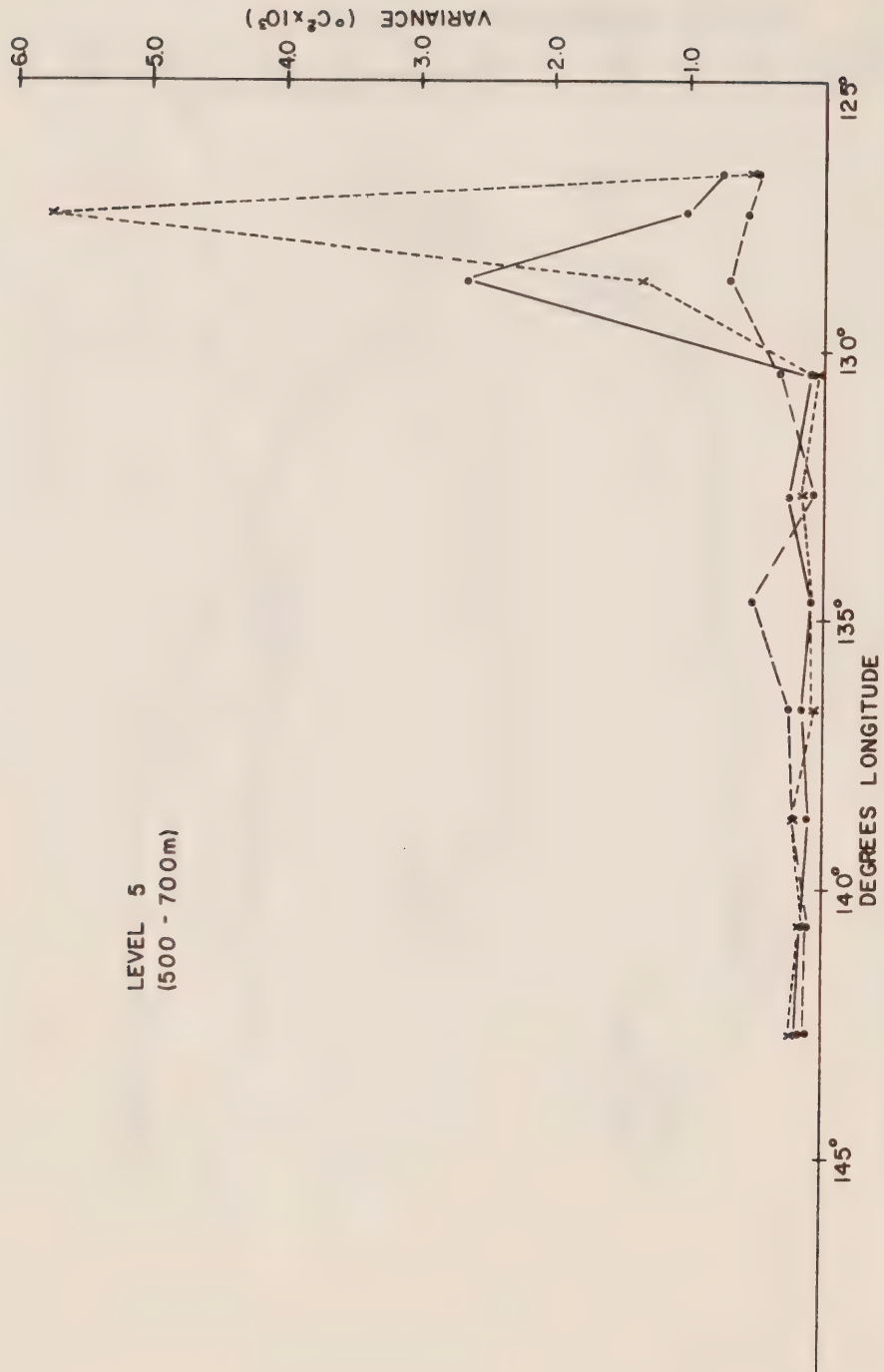
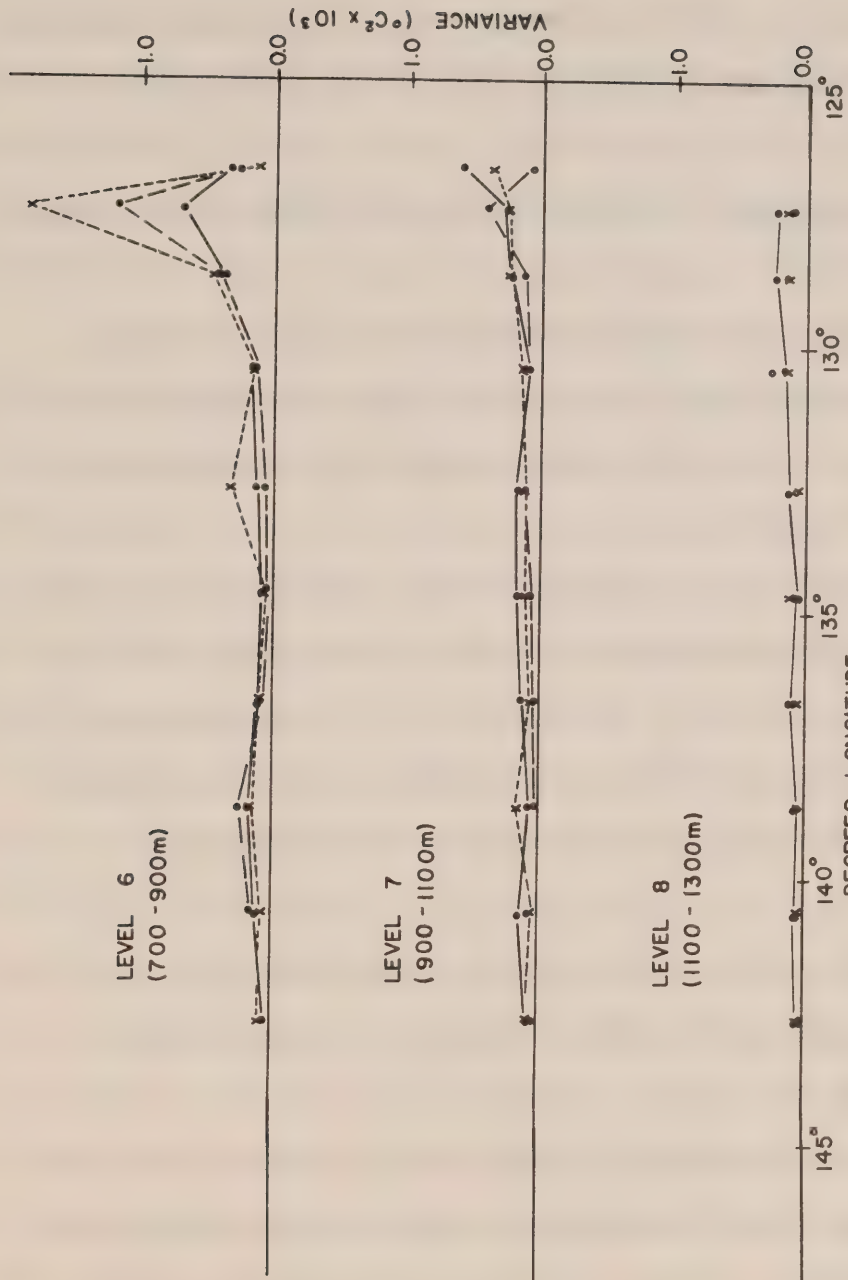


FIGURE 31 d: Temperature variance along Line P, • LAYMORE; ° QUADRA; x VANCOUVER



FIGURES 31e-g: Temperature variances along Line "P". • LAYMORE; ° QUADRA; x VANCOUVER

4. SUMMARY

This study described some results from the data collected by three ships in the vicinity of Line P during May 1972. Although the oceanographic region and time covered were rather limited, a number of findings have been obtained which have a much more extensive applicability in the subarctic Pacific.

Section 2 considered the data from the CFAV LAYMORE cruise alone, with the following results:

1) Horizontal sections of temperature and salinity and hence density (σ_t) showed a marked zonal distribution of the isopleths in the interior oceanic region which became more orientated with the shore as the coastal domain was approached.

2) The tendency for the contours of equal property to align themselves with the coast was apparent at all depths in which there was a spatially discernible difference in the magnitude of a given property.

3) The transition from the coastal domain to the oceanic domain along Line P appeared to occur in the vicinity of Line P station 5 ($48^{\circ}51'N$, $128^{\circ}40'W$).

4) In addition to the re-orientation of the contours as the coast was approached, there was a sharp increase in the spatial gradient and the time variability at most depths.

5) According to the potential energy anomaly sections, the mean northward mass transport in the coastal domain was much more intense than in the more oceanic regions. Moreover, the commonly observed splitting of the eastward flowing West Wind Drift in the latter region into northward and southward tending flow seemed to be taking place to south of Line P. In particular, evidence of the splitting in the limited area covered by the

LAYMORE survey was confined to the region south of latitude 48°N and west of longitude 134°W .

6) Comparison of the STD temperature survey and the XBT survey indicated a significant difference in detail as well as in actual value at a given location. In part, this was a result of the twice as many XBT as STD observations. Mostly, however, the difference was due to the much greater inaccuracy of the XBT's compared to the STD and the tendency of the XBT's to malfunction but still give believable traces.

7) Comparison of the surface temperatures obtained from the STD, XBT and bucket samples showed that, in most cases, the XBT values were closer to the bucket temperatures than were the STD values. This was associated with the fact that, in the surface layer in May, there is usually a decrease in temperature with depth. The STD, which must be lowered to about one meter to avoid surfacing of its sensors, then usually recorded a lower temperature than the other two.

The exceptions, which occurred frequently during the LAYMORE cruise, appeared to be associated with times of reduced insolation (cloud cover; rain) and winds of 10 knots or greater, thereby implying an increase of temperature with depth in the surface layer at these times.

8) The very small difference ($\leq 0.05^{\circ}/\text{oo}$) between the STD salinity and the bucket sample salinity indicated then near absence of any salinity gradients with depth at the ocean surface. Moreover, this implies that, in general, very little evaporation or precipitation was taking place at this time, although the fact the bucket values were consistently larger than those of the STD may have been indicative of a slightly evaporative situation.

9) Time variations in the depths of the $33.0^{\circ}/\text{oo}$ and $33.5^{\circ}/\text{oo}$ isohalines surfaces have indicated that the accumulated vertical displacements of surfaces of constant property over periods of hours were tidal/inertial in nature. The Lunisolar tide K1 (~ 1 cycle/day) and the Lunar tide M2 (~ 2 cycles/day) were the major constituents, with some magnitude, at other frequencies due to aliasing as a result of the brevity of the record (~ 10 days). Maximum vertical displacements associated with the combined tides and inertial motion were approximately 25 m.

10) In the upper 150 meters of water in the subarctic Pacific, the horizontal distribution of the variance associated with the temperature structure in the STD traces was closely related to the spatial variation in the intensity of the large scale temperature gradients (a manifestation of the low pass filtering technique). During the LAYMORE survey, for example, the spatial distribution of the temperature variance for the depth interval 0-50 meters appeared to be a measure of the spatial variation in magnitude of the thermocline at the bottom of the surface mixed layer. For the 50-150 meters depth interval, it appeared to be a measure of the spatial variation of the temperature gradients associated with diathermal layer (relative temperature minimum layer).

In both ranges, greatest magnitude and temporal change occurred near or within the region of transition from the oceanic to the coastal domain. Minimum values and minimum time variation occurred in the oceanic domain. In the case of the 0-50 m layer these findings were indicative of the greater amount of wind-mixing that occurred in the coastal region compared to the oceanic region over the period of the LAYMORE cruise.

11) Below 150 meters, the temperature variance calculated from the vertical STD traces gave a more accurate measure of the amount of 'micro-structure' than for shallower depths. That is, the magnitude of the temperature fluctuations about the mean at the former depths was determined by small-scale internal processes rather than by the large scale surface derived processes and the spurious values resulting from the filtering.

In particular, the horizontal distribution of the variance in the region studied, delineated the area of confluence between the warm northward moving water off the BC-Washington coast and the colder eastward moving water of the West Wind Drift. As shown, this mixing region was situated about 200-300 km offshore. Between 150-700 m, it extended more or less northeast across the area near 48° - 49° N and 130° W while between 700-1300 m it has shifted more towards the coast except for a tongue-like penetration to the west near 48° N. Despite the much reduced magnitude, the variance at 1300-1500 m continued to define the region of confluence but with a pattern similar to the former range (150-700 m) rather than latter range. A second geographic area of relative maximum temperature structure also appeared south of the Queen Charlottes at most depth levels. Seaward of these regions of confluence, the variance decreased rapidly to significantly smaller values. Minimum variances occurred invariably in the vicinity of stations 12, 13 and 14 ($\sim 143^{\circ}$ W longitude).

The much greater temporal variability in the variances in the coastal region than in the oceanic region was indicative of the shifting of the 'strip' of confluence and/or the intensity of intrusion of one water type into another off the coast. In the oceanic domain, the temporal changes in the variance are mostly associated with much smaller scale processes such as the breaking of short internal waves and cannot, therefore, begin to produce

temperature fluctuations of the same order as those due to the mixing of the two different water masses.

12) Considered in the vertical, the variances associated with the temperature structure below 150 m indicated a maximum at level 4 (300-500 m) for the geographic area east of Line P station 6 ($49^{\circ}02'N$, $130^{\circ}40'W$). West of station 6, the level of maximum variance varied between level 3 (150-300 m), level 4 (300-500 m) and level 5 (500-700 m). In the latter area, of course, maximum variances were much less than those in the more coastal areas except for the deepest levels where values became small everywhere.

The consistent maximum at level 4 for those areas east of station 6 is indicative of a greater temperature contrast between the water masses at this level or of the greater degree of mixing, or both. The spatial variability in the depth of maximum variance for the areas west of station 6 is indicative of the much smaller and more locally determined temperature structure found there.

Section 3 considered the data from the two weatherships surveys along Line P in May of 1972 together with that from the LAYMORE (outbound), with the following results:

1) A comparison of surface STD salinities for the three separate samplings of Line P showed that differences above instrument error occurred in the coastal domain only. The changes that did occur in the latter region were most likely associated with the effects of river runoff and/or variations in the local current patterns.

2) A comparison of surface STD temperatures indicated a general warming of the water with time along Line P. This was particularly true of the period following the LAYMORE observations during which winds were generally lighter and insolation greater than previously.

3) The temporal variation of the depth of the mixed layer at a given location during May was directly associated with corresponding variations in the magnitude of the surface wind-stress. Moreover, the response time of this depth to the wind appeared to be less than one day. Vertical velocities associated with a divergent (or convergent) Ekman layer, if present, did not seem to be of any importance in altering the depth of the mixed layer. Therefore variations in the intensity of turbulent mechanical mixing of the winds and not vorticity effects were responsible for changing the layer thickness.

In addition to the temporal variations, there was a distinctive shallowing of the mixed layer depth near the coast. This is related to the general upward displacement of all property surfaces in this region which, through increased water stability at shallower depths than in the interior regions, limits the depth of penetration of the mechanical wind mixing.

4) Qualitatively, the overall increase in depth of the $33.0^{\circ}/\text{oo}$ and $33.5^{\circ}/\text{oo}$ isohalines between the LAYMORE and weathership cruises along Line P appeared to have been related to a general anticyclogenesis in the wind activity over the region as a whole, rather than to the local wind magnitude. This would suggest that these isohalines, which lie well within the permanent halocline, have had their equilibrium level deepened through a decrease in the upward vertical velocity induced by the divergent surface Ekman layer usually associated with this part of the subarctic Pacific. Station-to-station fluctuations produced by internal waves (tides) were, of course, present but could not under most circumstances be responsible for the general shift of the mean levels.

Between the weathership samplings of Line P, the situation was less well defined although, in general, the depth for the two isohaline

surfaces appeared to have been slightly greater during the VANCOUVER cruise than during the QUADRA cruise.

5) The existence of a dichothermal layer along Line P indicated that fairly intense surface cooling had taken place in the winter of 1971-72. The shoreward decrease in the depth of this layer was again associated with the upward displacement of all property surfaces near the coast since the depth of penetration of winter cooling and wind mixing would have been limited by the stable water of the halocline.

Maximum temperature 'gradients' associated with the dichothermal layer occurred at Line P stations 3 and 4, which may be due to a greater intensity of winter cooling there or to the fact that these stations were situated within the region of confluence between two water masses of different temperature.

6) Comparison of the potential energy anomalies referred to 1200 m along Line P for the three surveys, showed a variation of 5 to $6\frac{1}{2}$ sverdrups in the total across-the-line mass transport. Maximum variability with time between the cruises occurred between 128° - 135° W longitude in the region where there existed the greatest tendency of the West Wind Drift to be forced to flow parallel to the coast.

7) Consistent with the results of the LAYMORE survey alone, weathership observations along Line P verified that the maximum variability in the STD temperature profiles existed in the vicinity of stations 4 and 5. Seaward of these stations there was a rapid decrease in the variance at all levels. As before, this implies the existence of mixing between a northward flowing coastal current and the eastward moving West Wind Drift off the coast. The significant variation with time of the coastal variances is a clear indication of the shifting position of confluence.

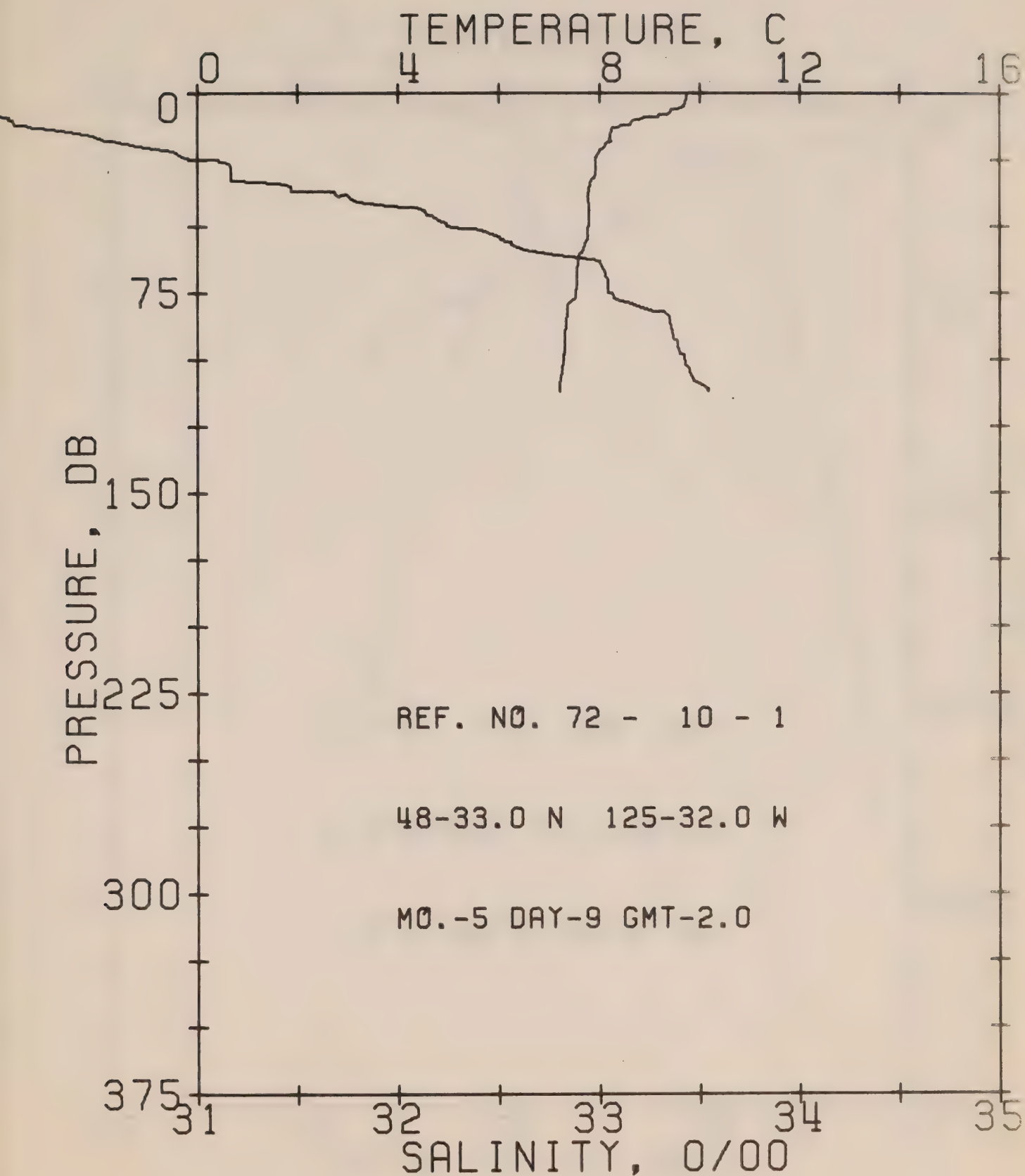
8) The combined results of all three ship surveys further confirms the location of Line P station 5 as marking the transition from the coastal to the oceanic domain along the Line.

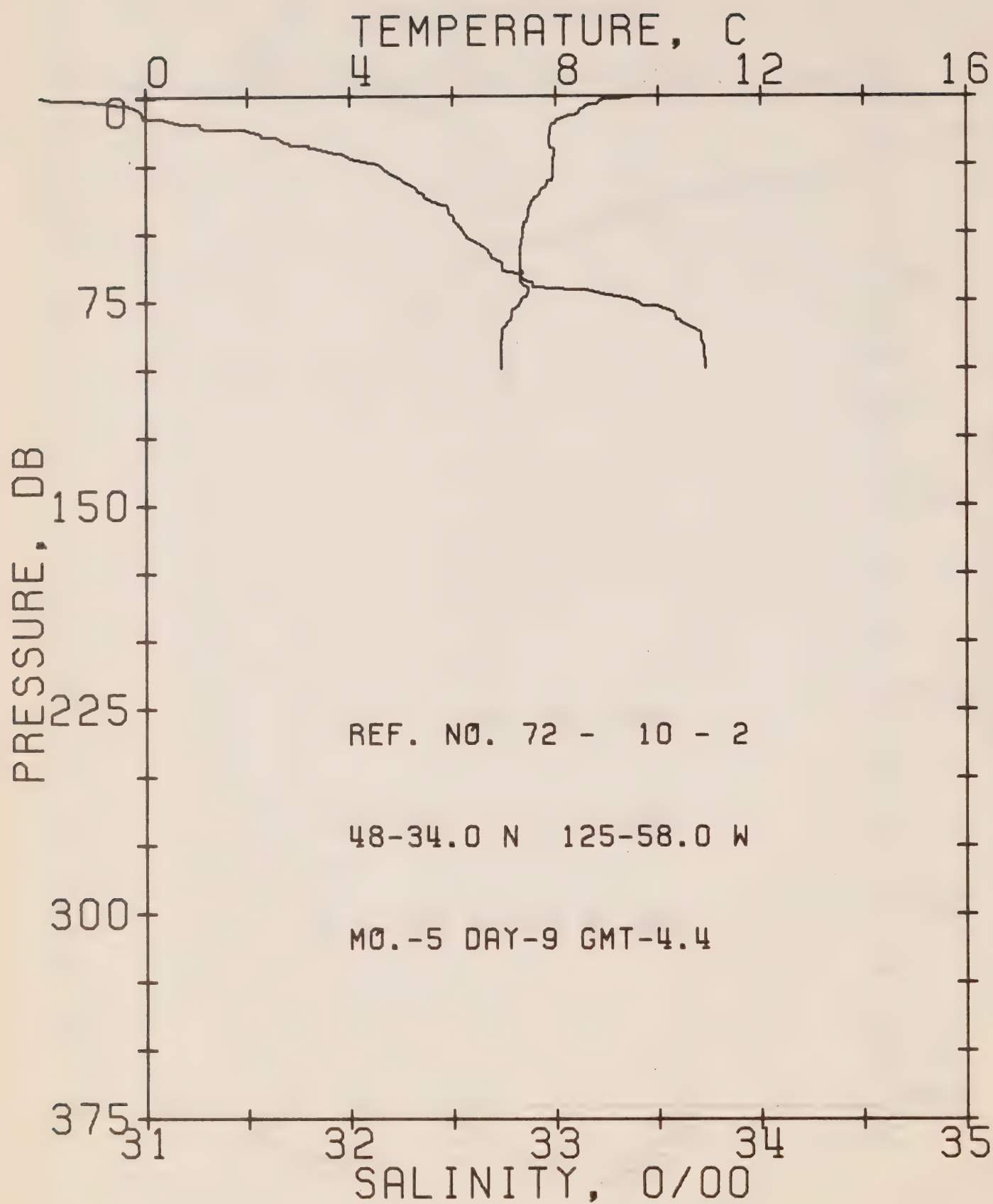
REFERENCES

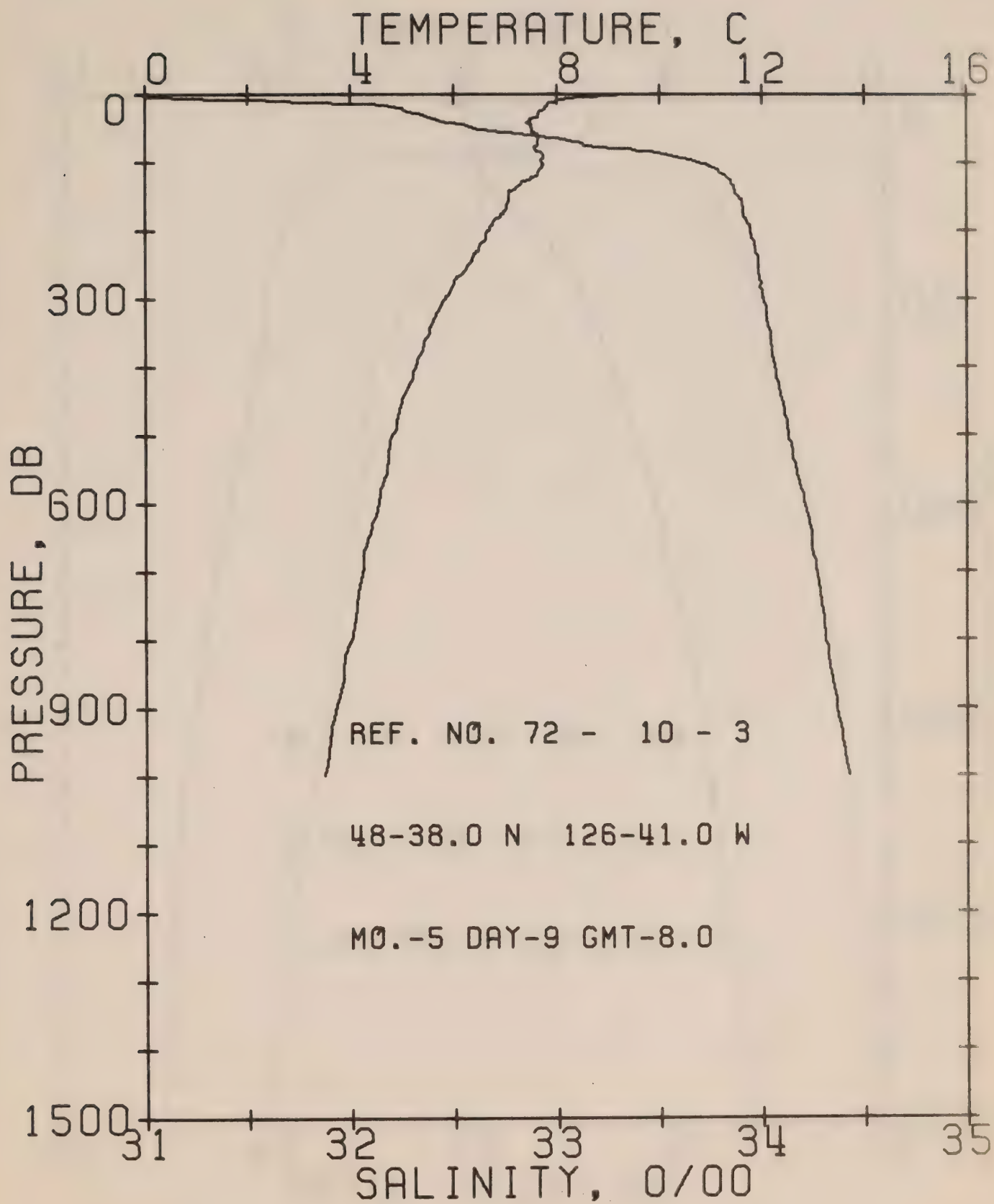
- Bellegay, R., D. Healey and W. Hansen, 1972: Oceanographic Observations at Ocean Station P (50°N, 145°W) August 6, 1971 - January 16, 1972. Environment Canada, Marine Sciences Directorate Manuscript Report Vol. 54.
- Denman, K.L., 1972: The response of the upper ocean to meteorological forcing. Ph.D. Thesis, University of British Columbia, 117 pp.
- Dodimead, A.J., F. Favorite and T. Hirano, 1963: Salmon of the North Pacific Ocean. Part II. Review of Oceanography of the Subarctic Pacific Region. Int. North Pacific Fish. Commission, Bulletin No. 13, 195 pp.
- Healey, D., P. Vandergugten and W. Hansen, 1972: Oceanographic Observations at Ocean Station P (50°N, 145°W) January 7 - May 18, 1972. Environment Canada, Marine Sciences Directorate Manuscript Report Vol. 53, 210 pp.
- Schureman, P., 1958: Manual of harmonic analysis and prediction of tides. United States Printing Office, Washington, D.C., 317 pp.
- Thomson, R.E., 1971: Theoretical studies of the circulation of the Subarctic Pacific Region and the generation of Kelvin type waves by atmospheric disturbances. Ph.D. Thesis, University of British Columbia, 244 pp.
- Uda, M., 1963: Oceanography of the Subarctic Pacific Ocean. J. Fish. Res. Bd. Canada 20 (1), 119-179.

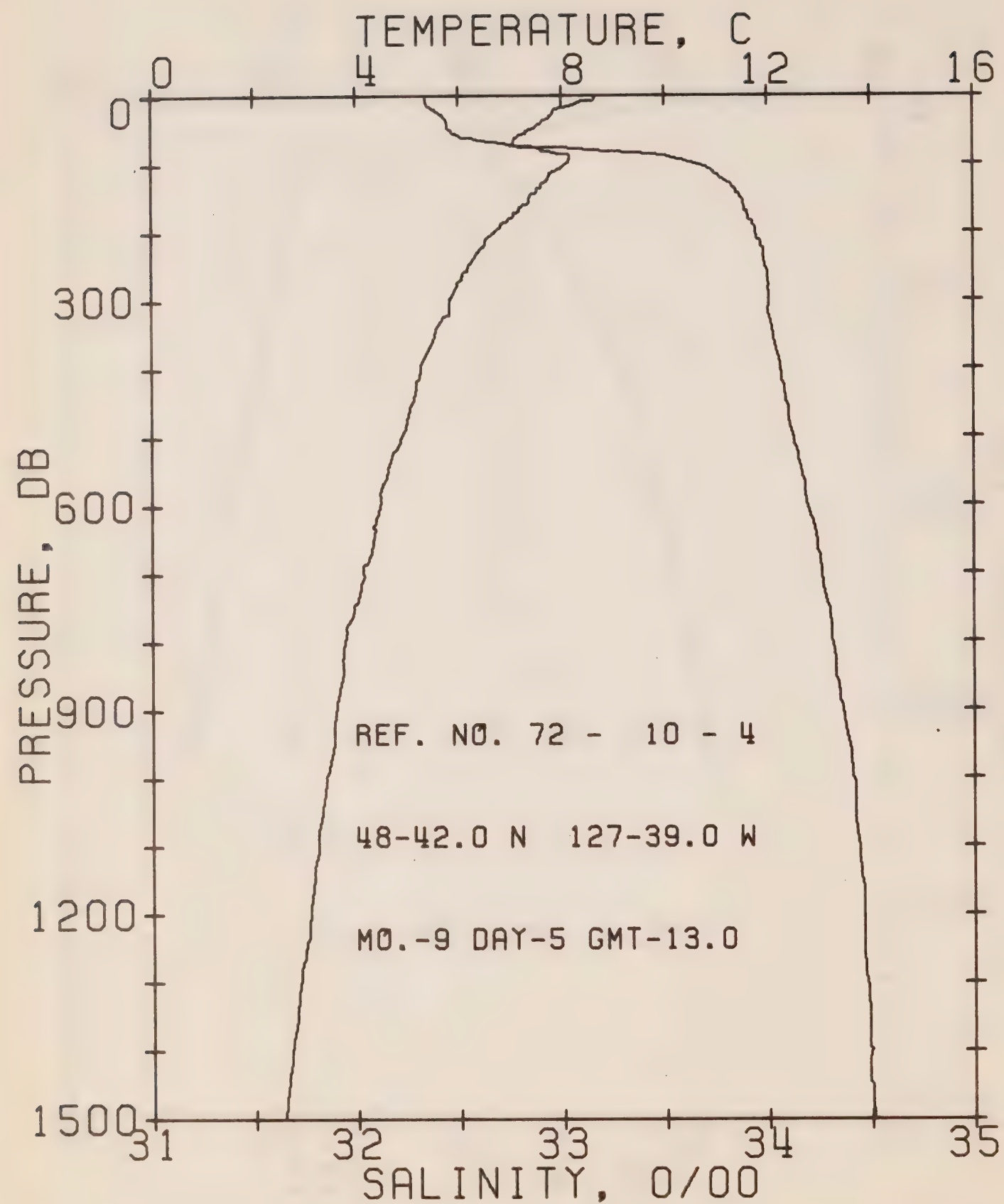
APPENDIX

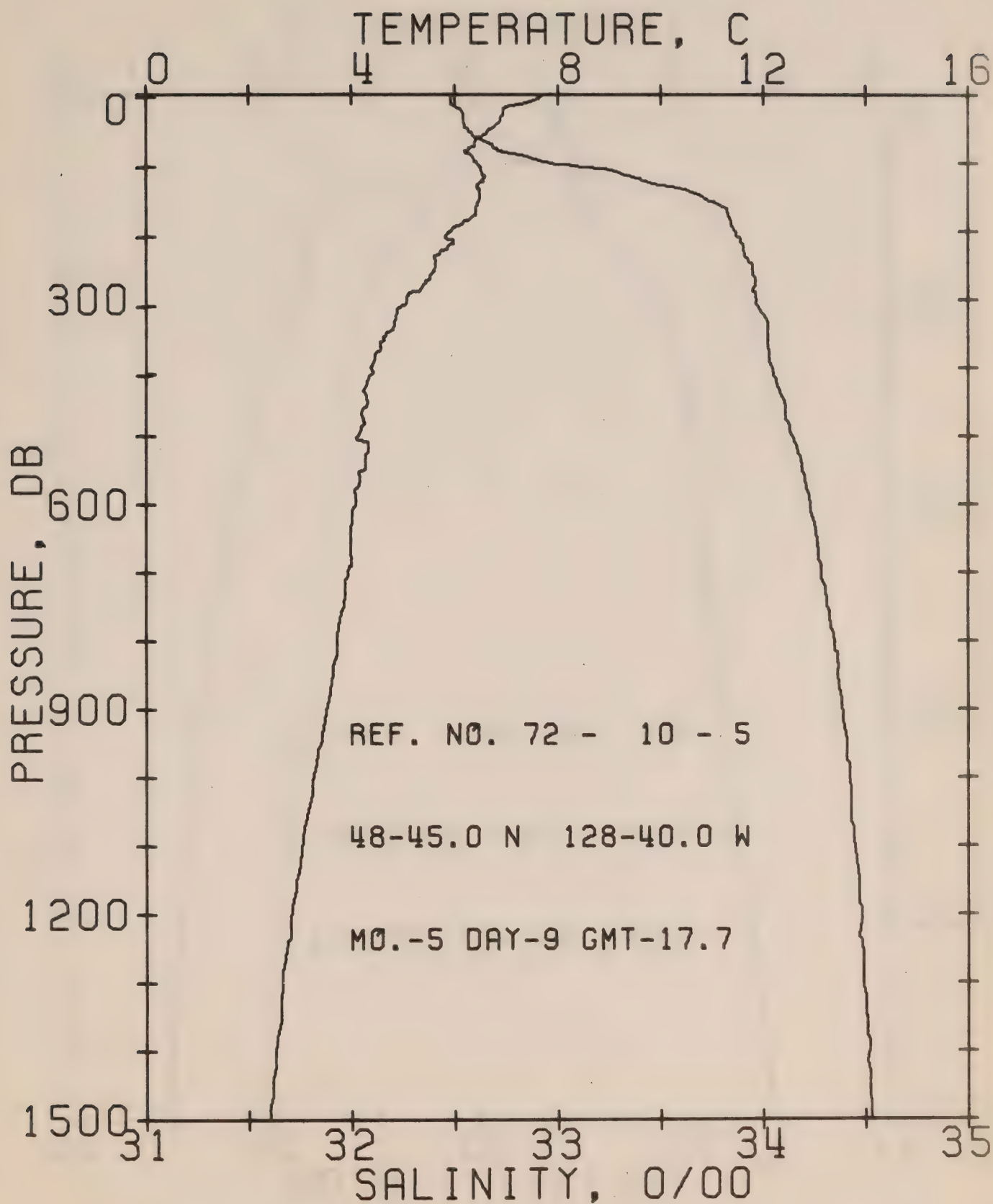
STD profiles for the CFAV LAYMORE cruise 72-10 (8-18 May, 1972).

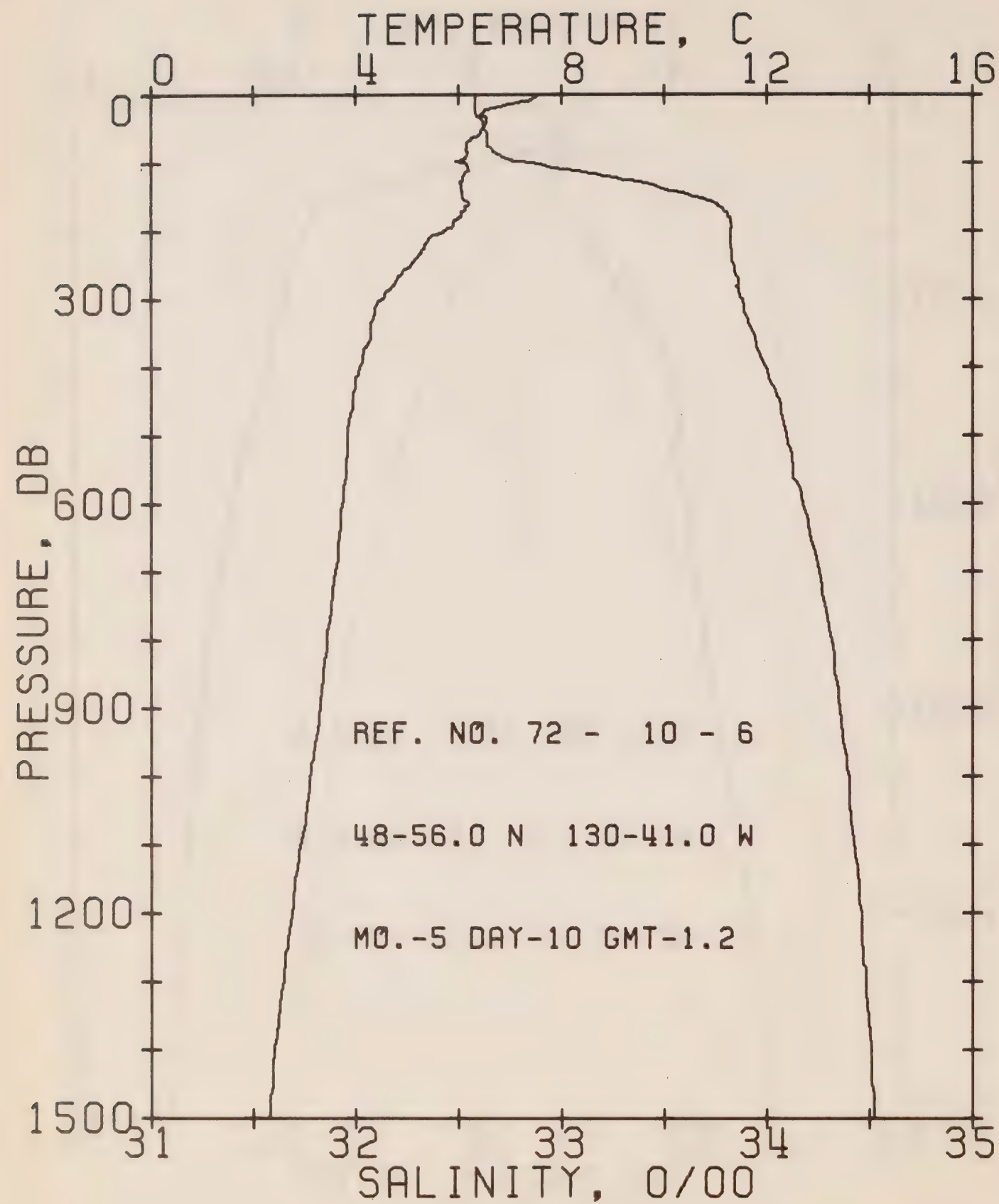


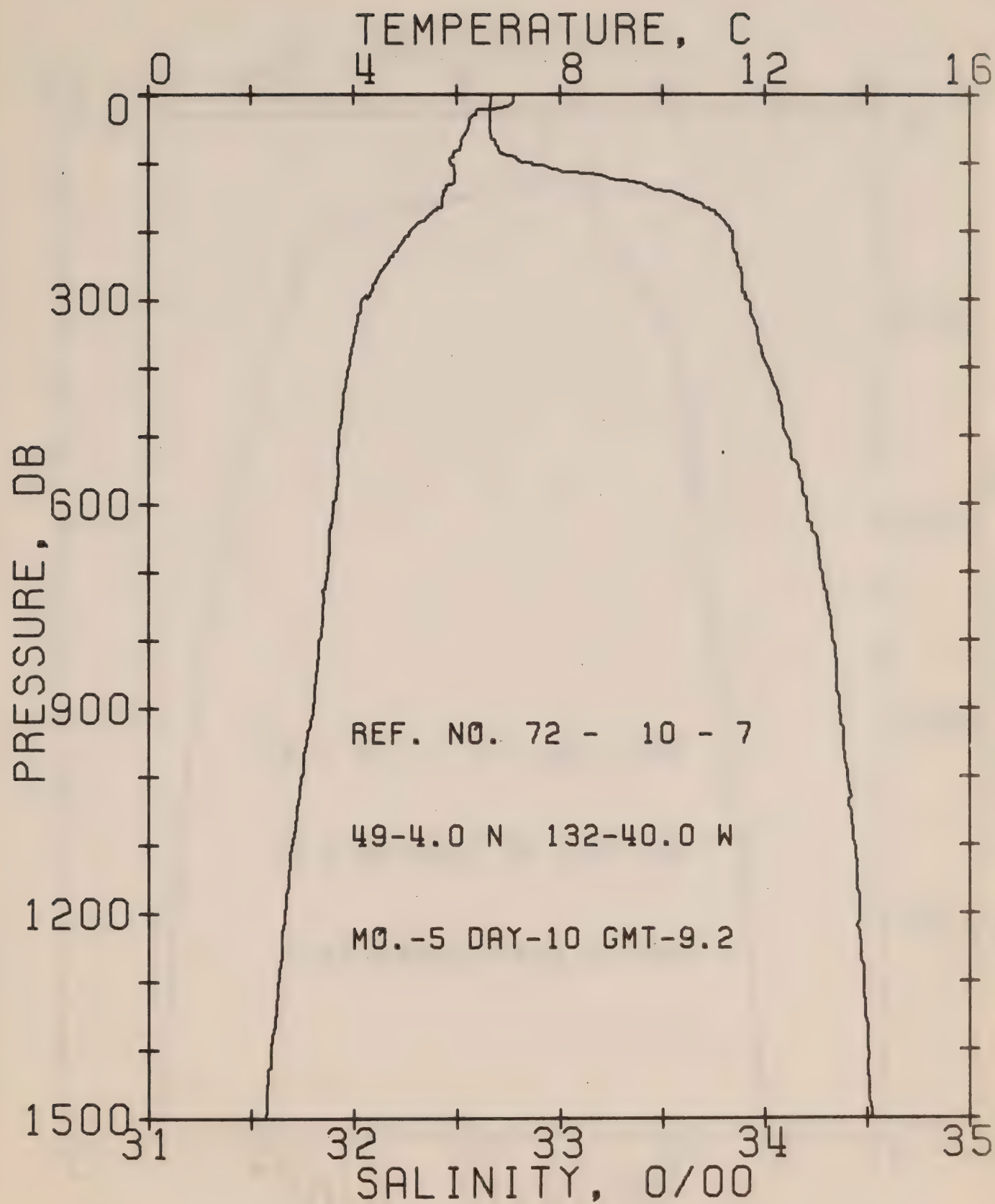


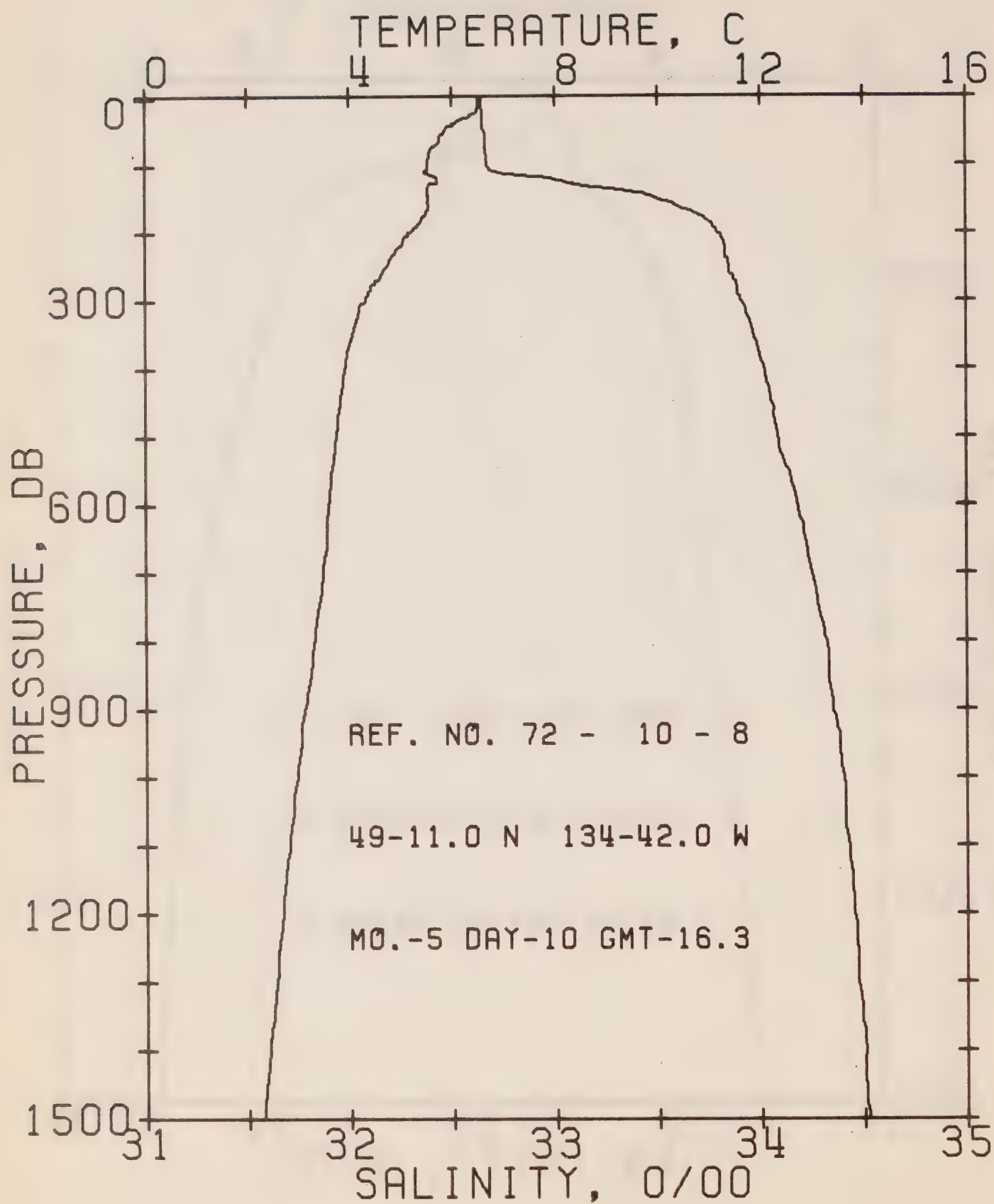


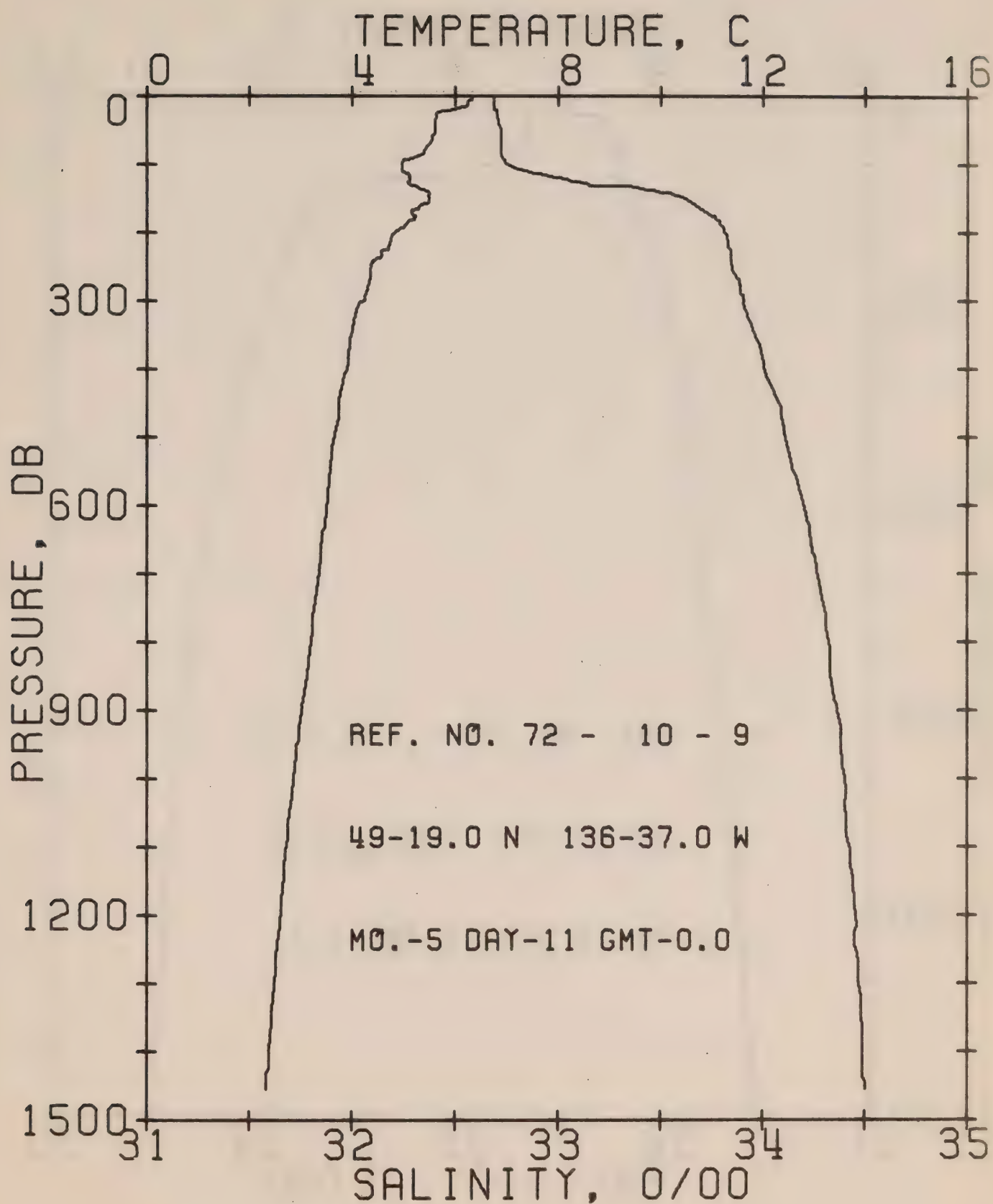


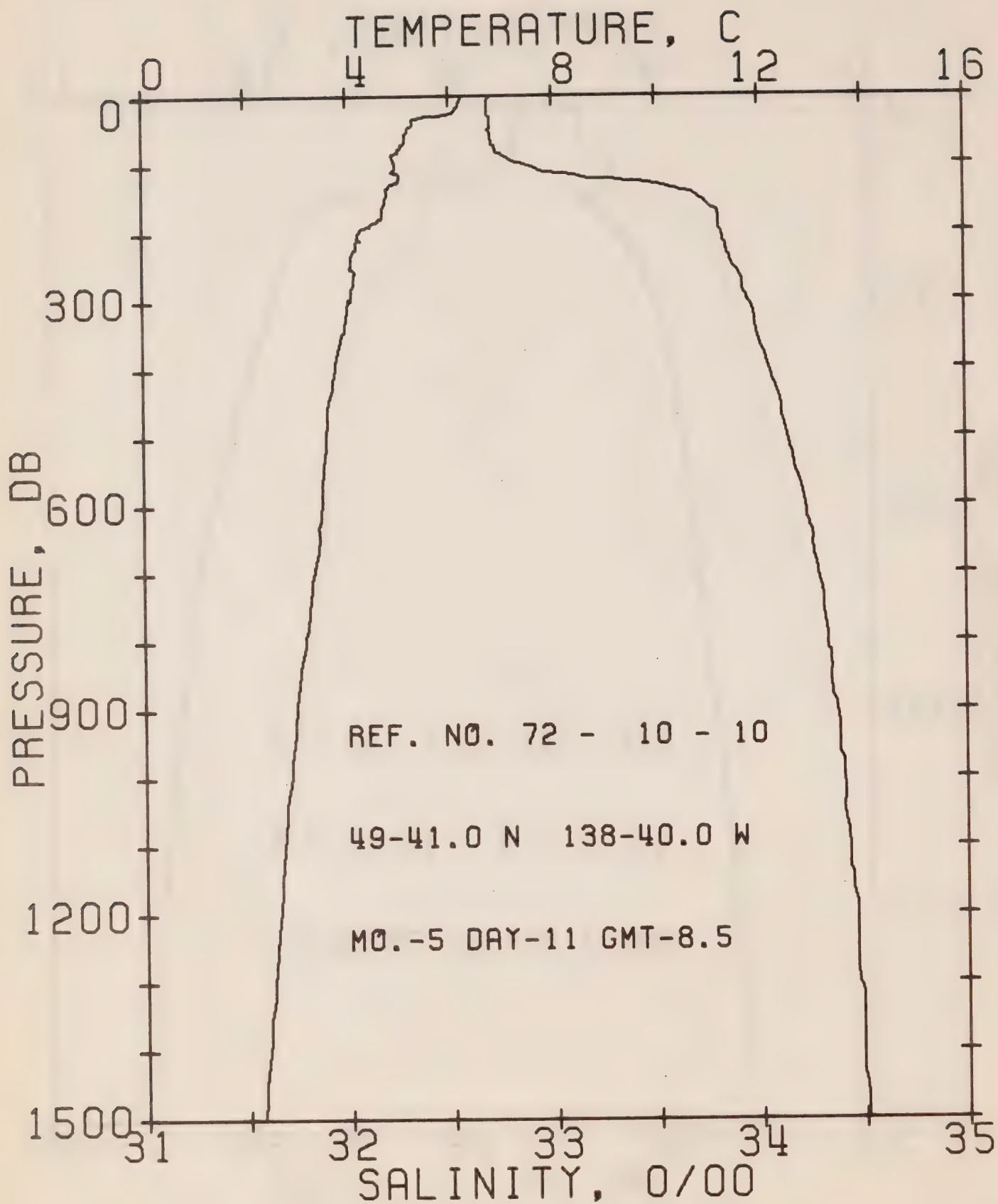


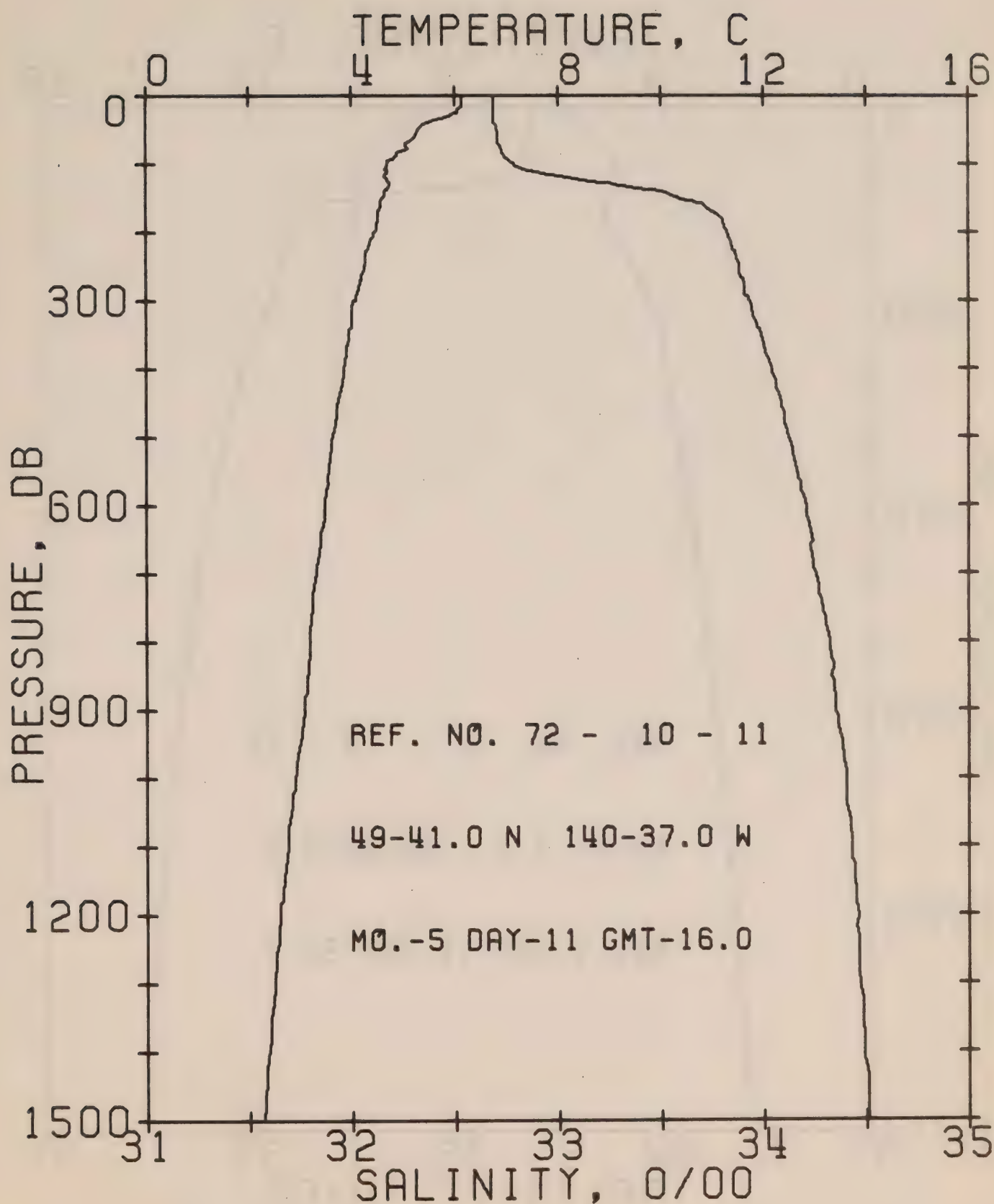


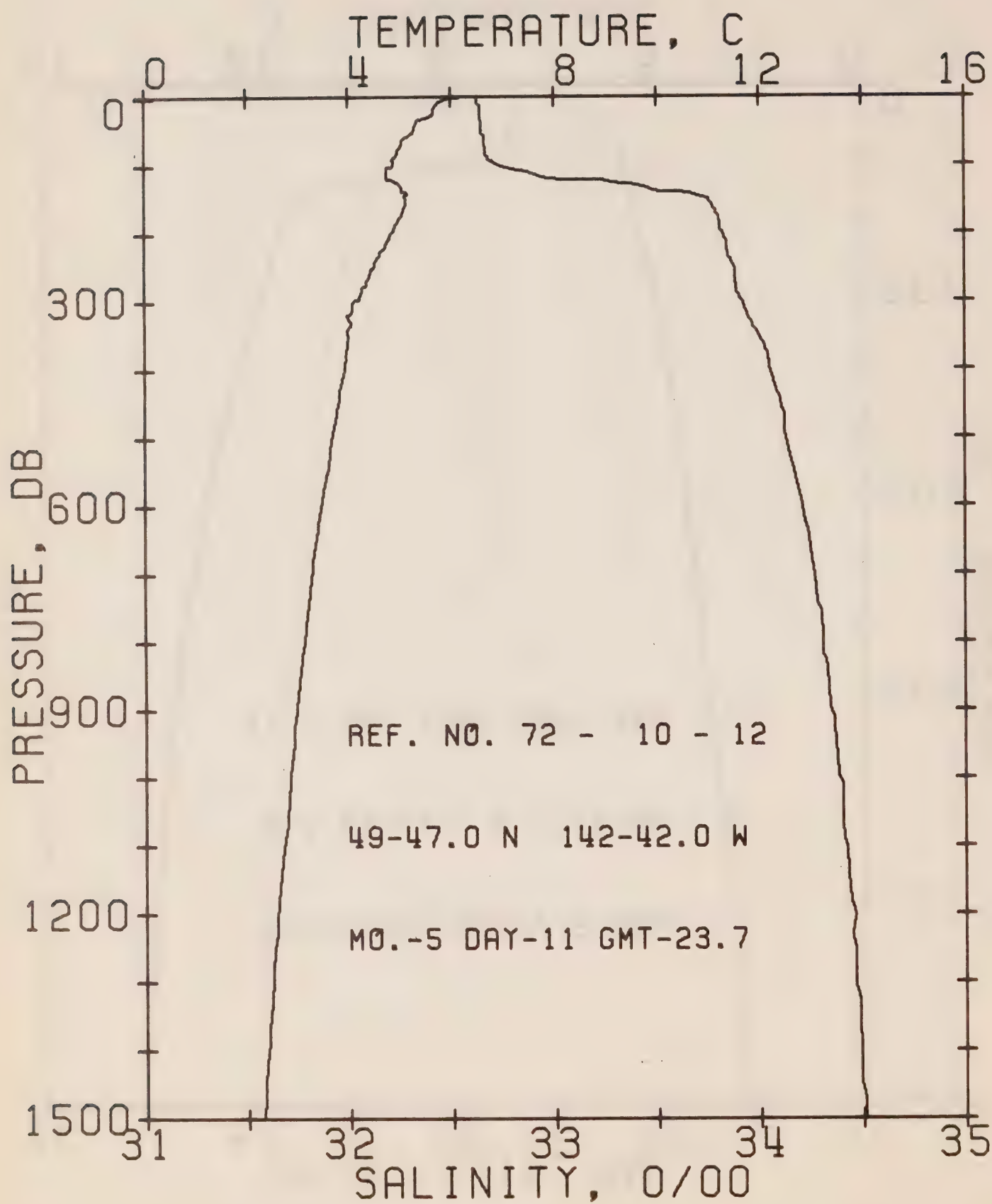


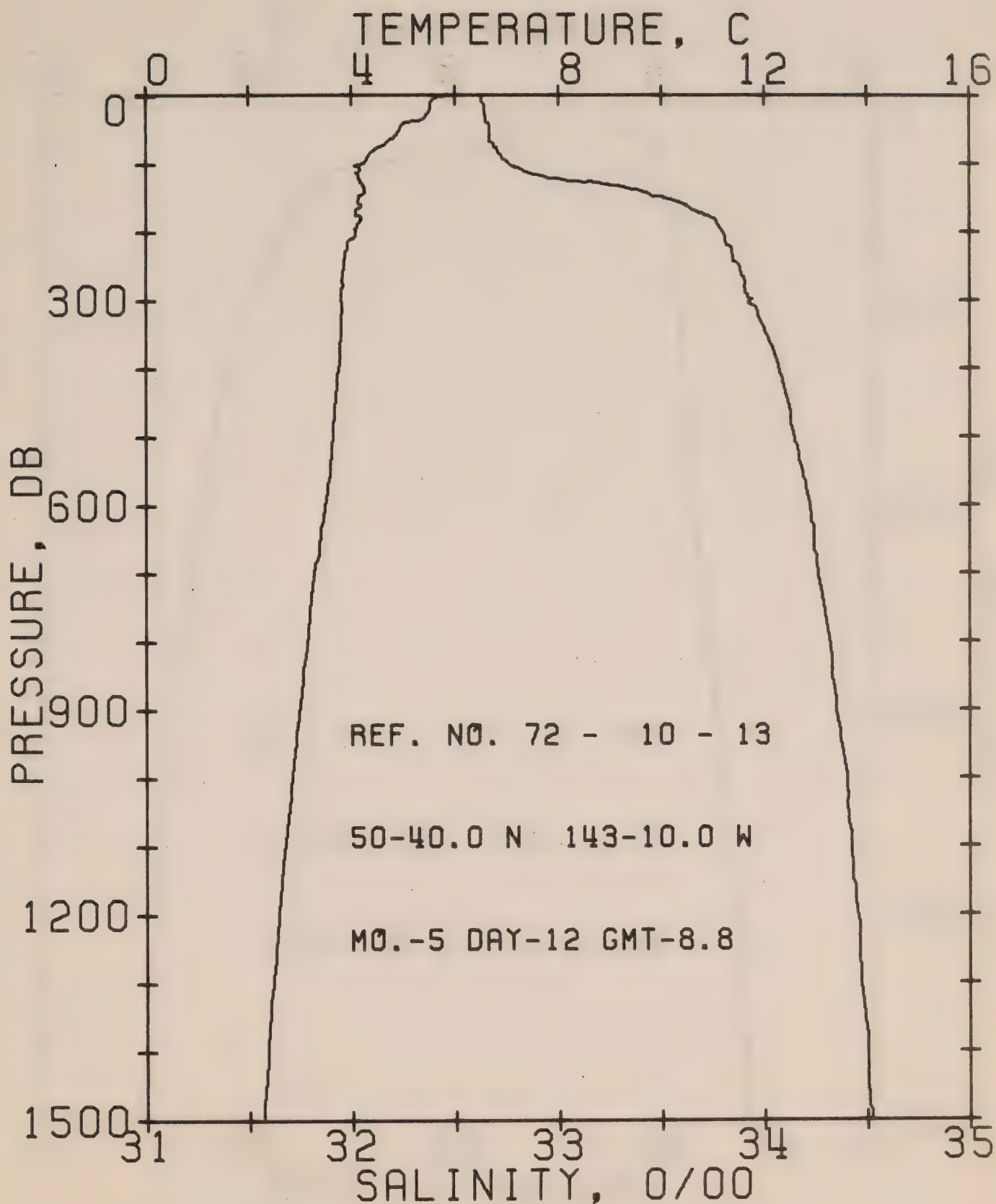


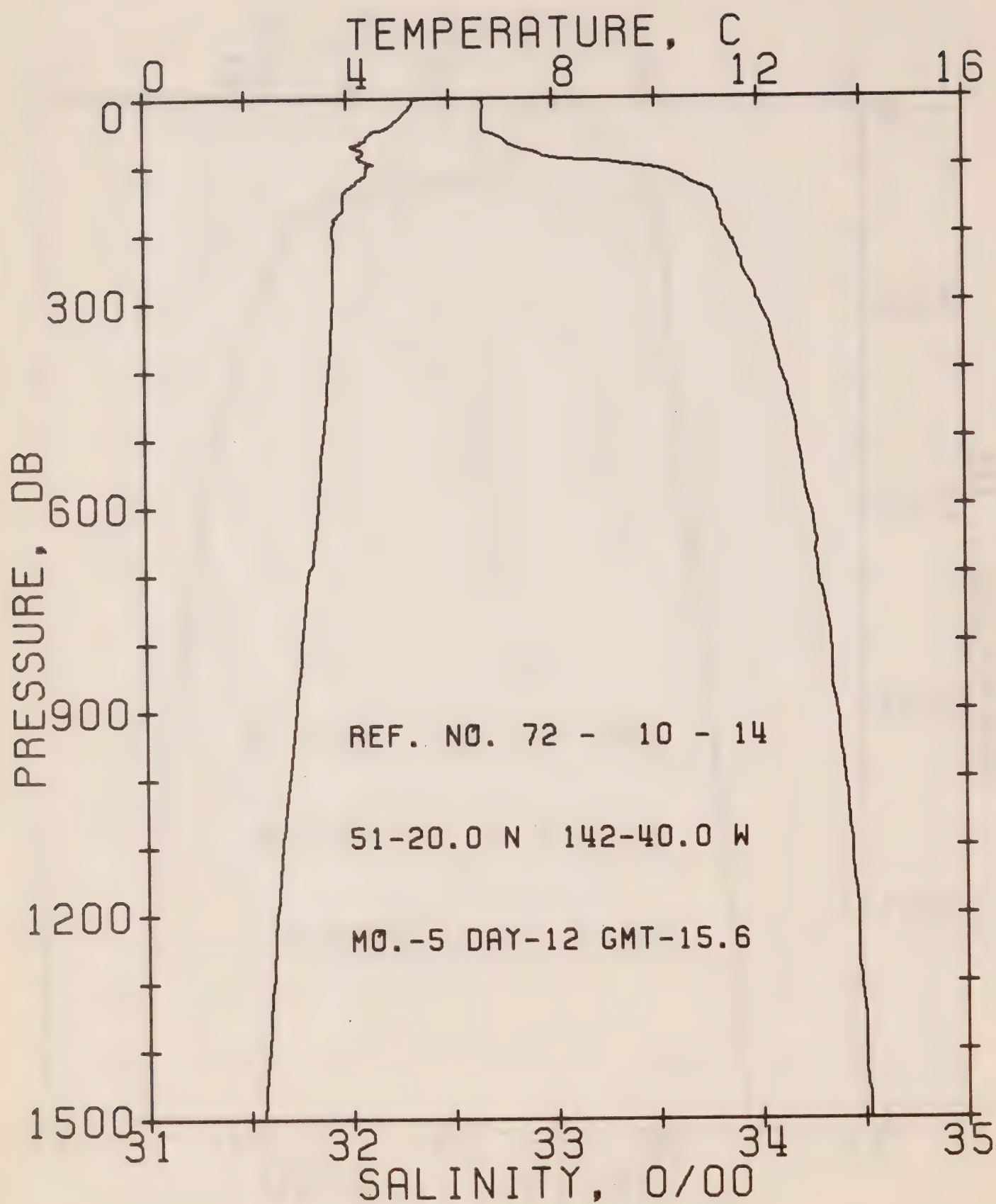


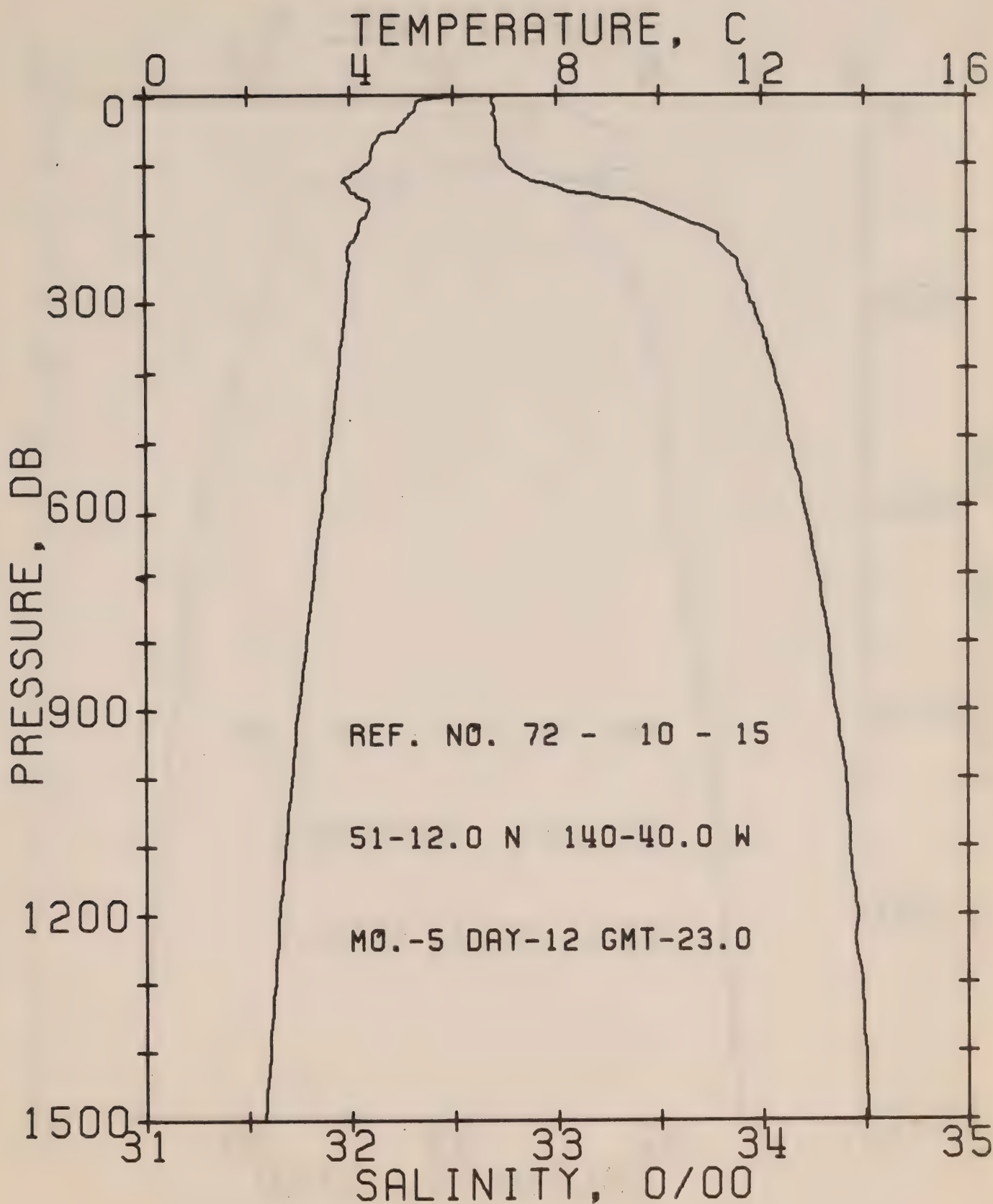


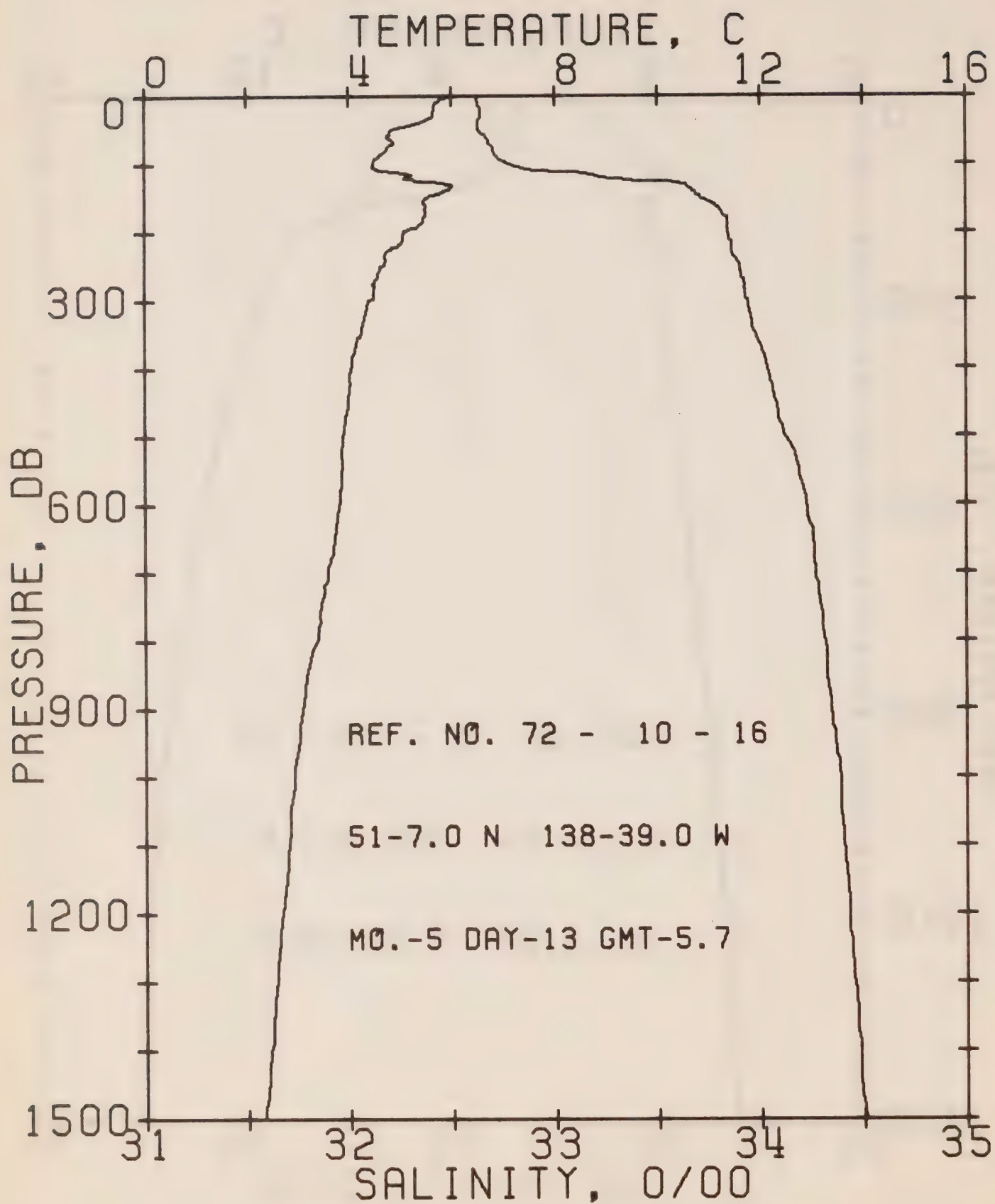


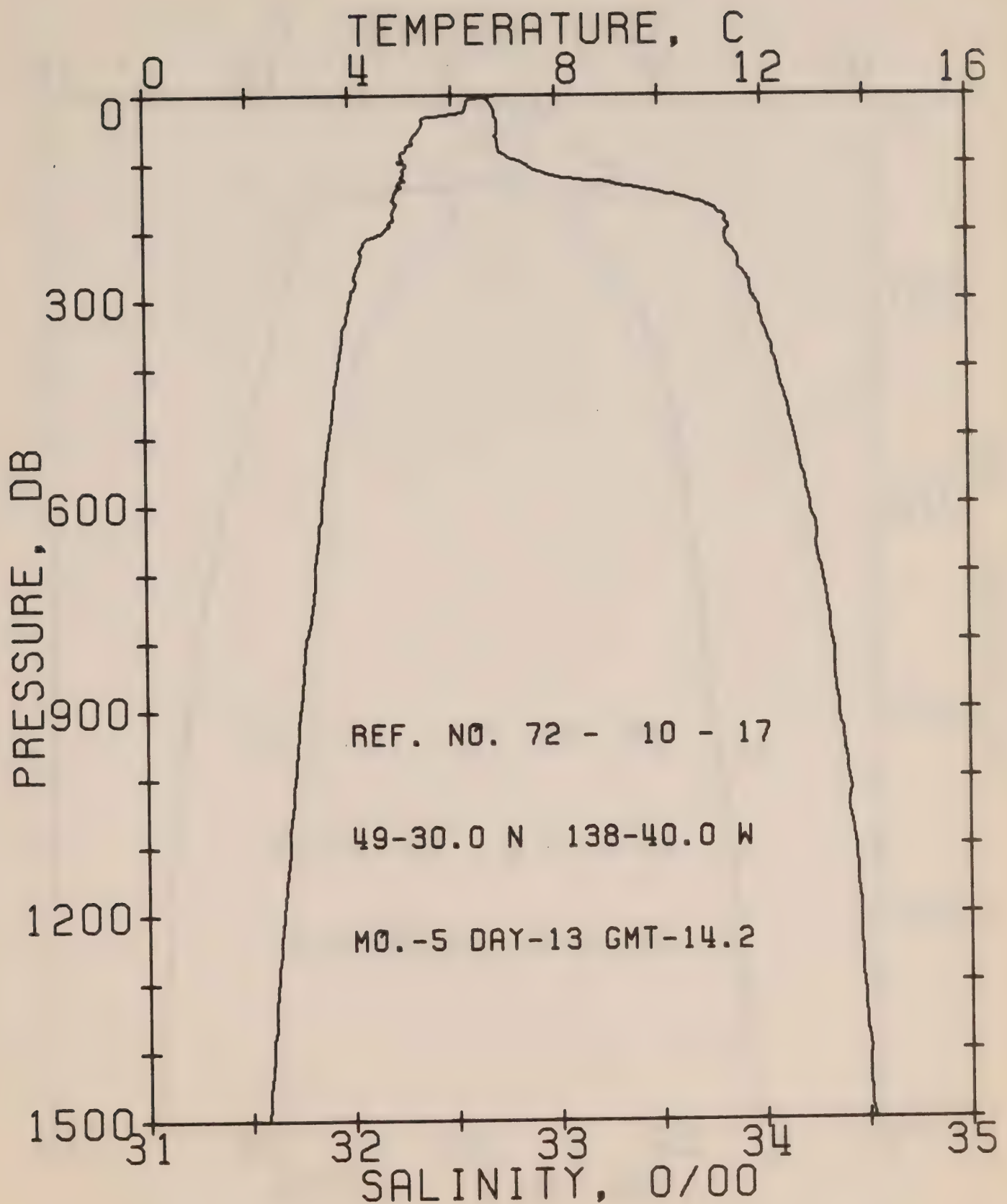


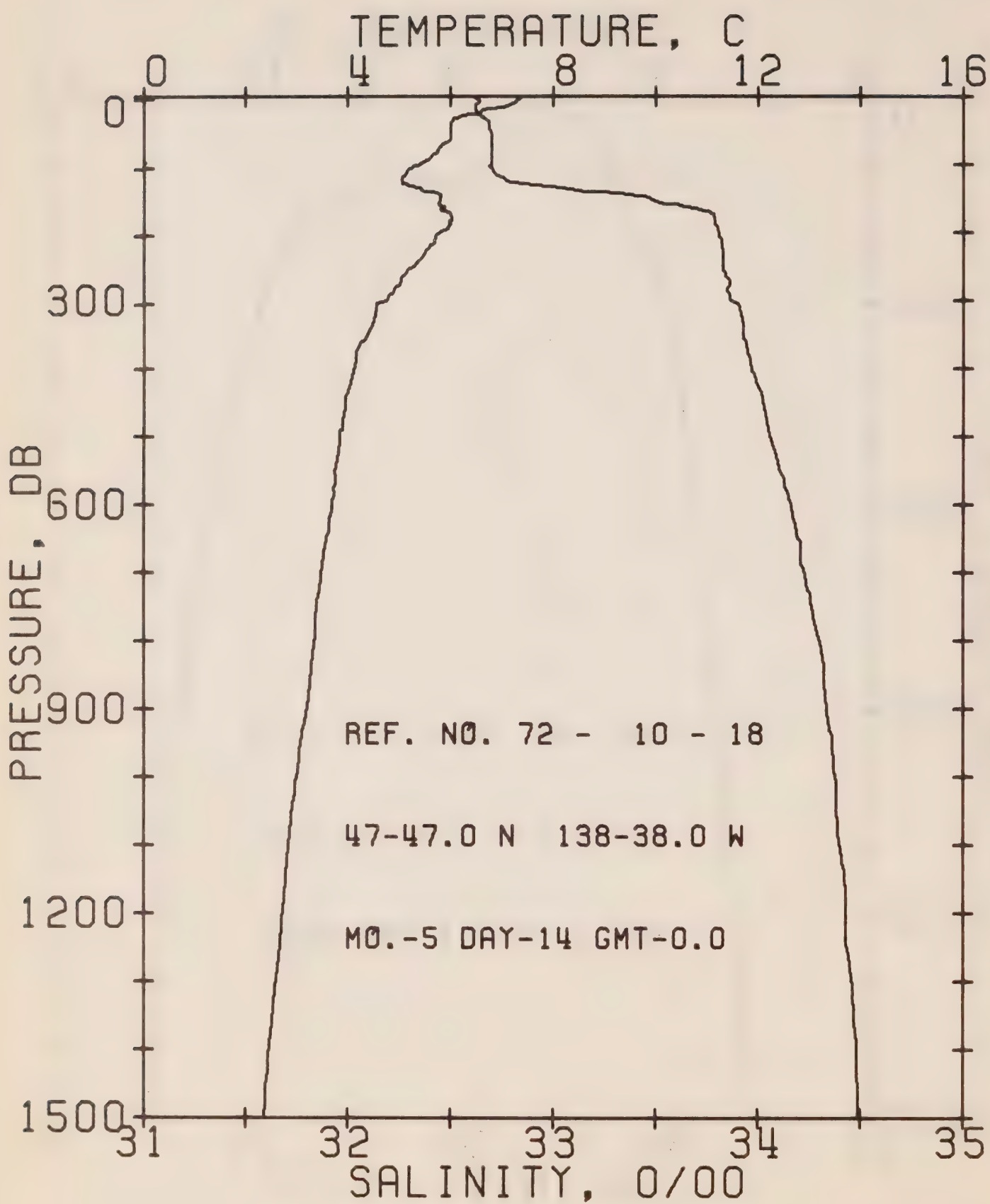


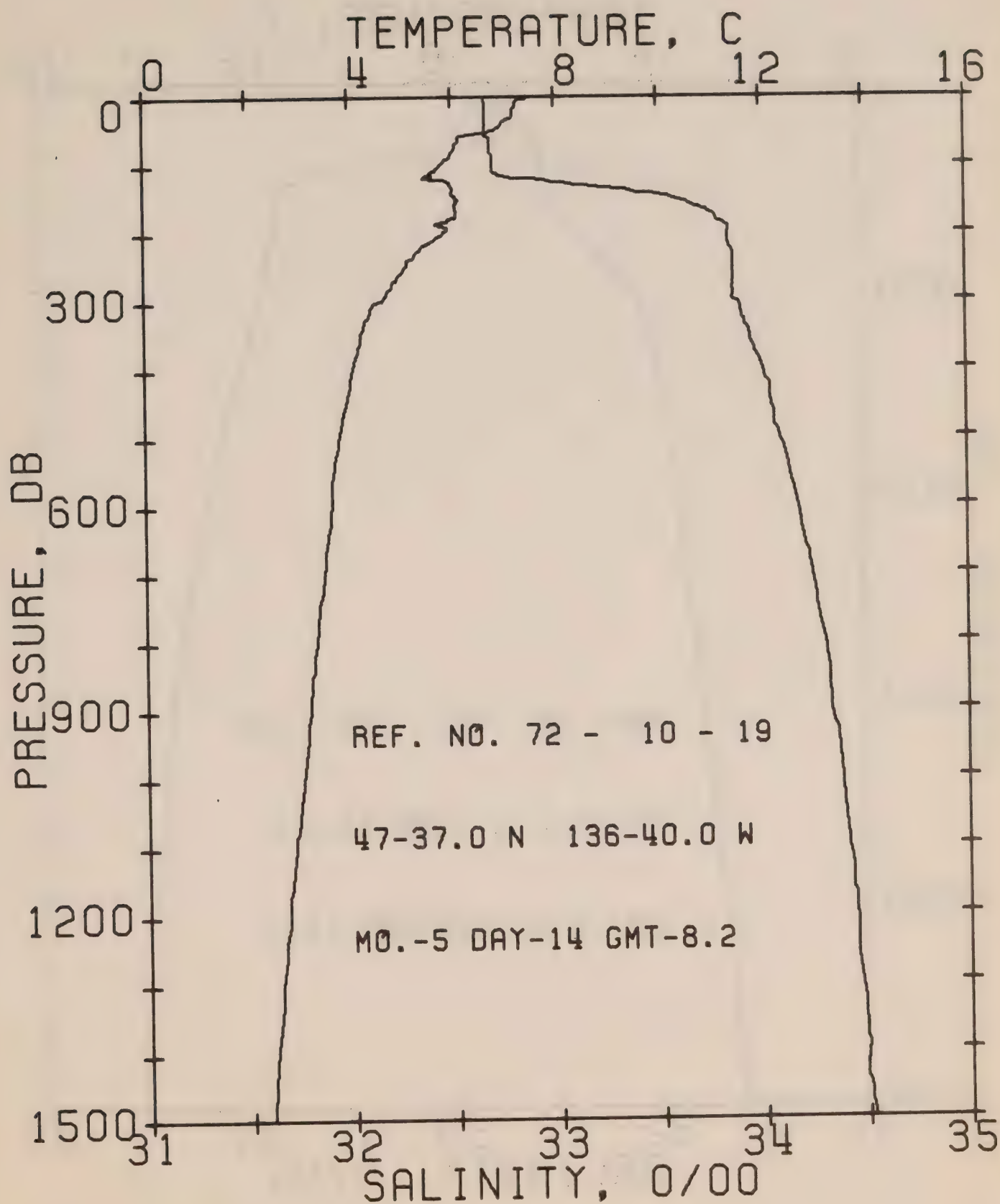


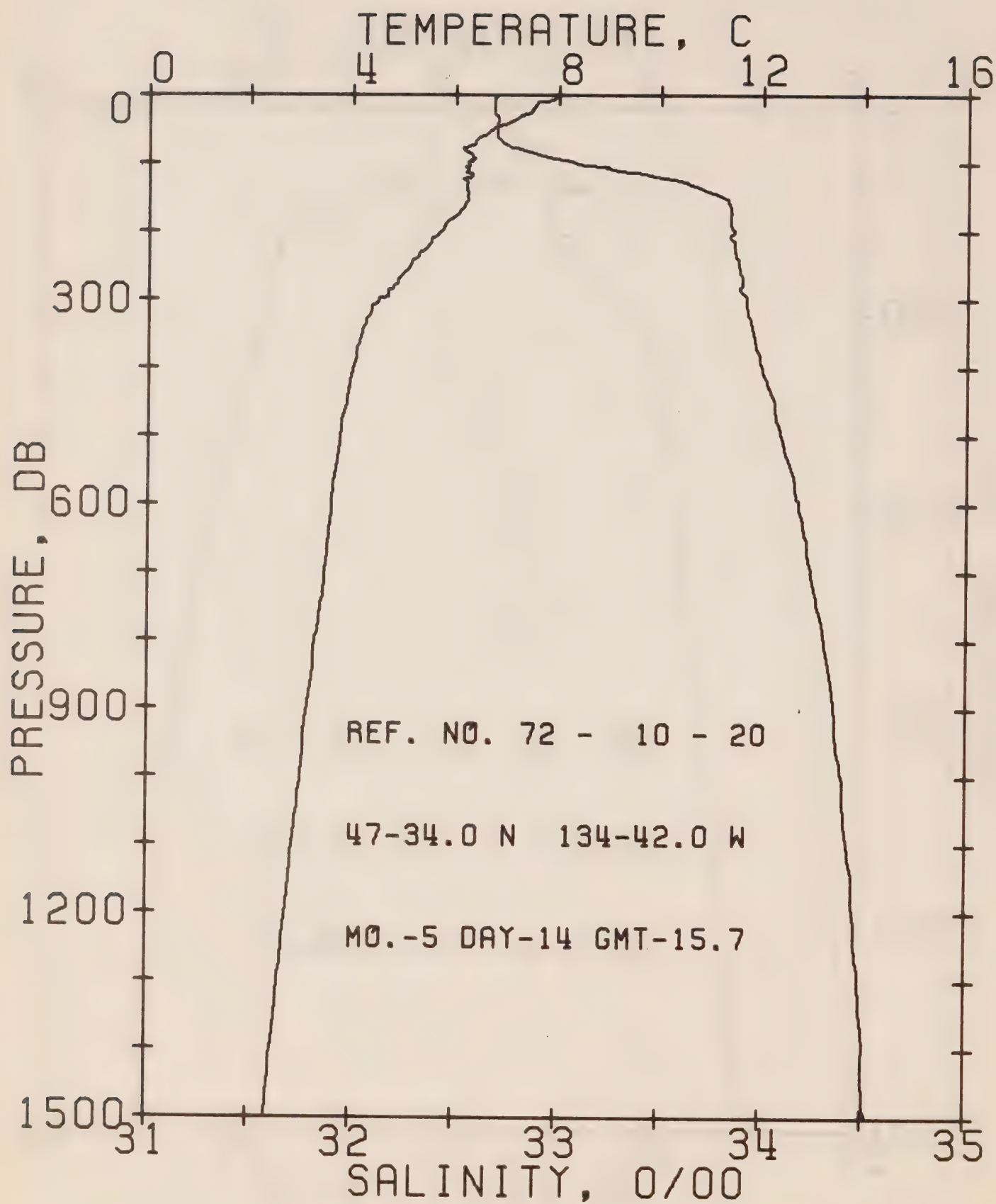


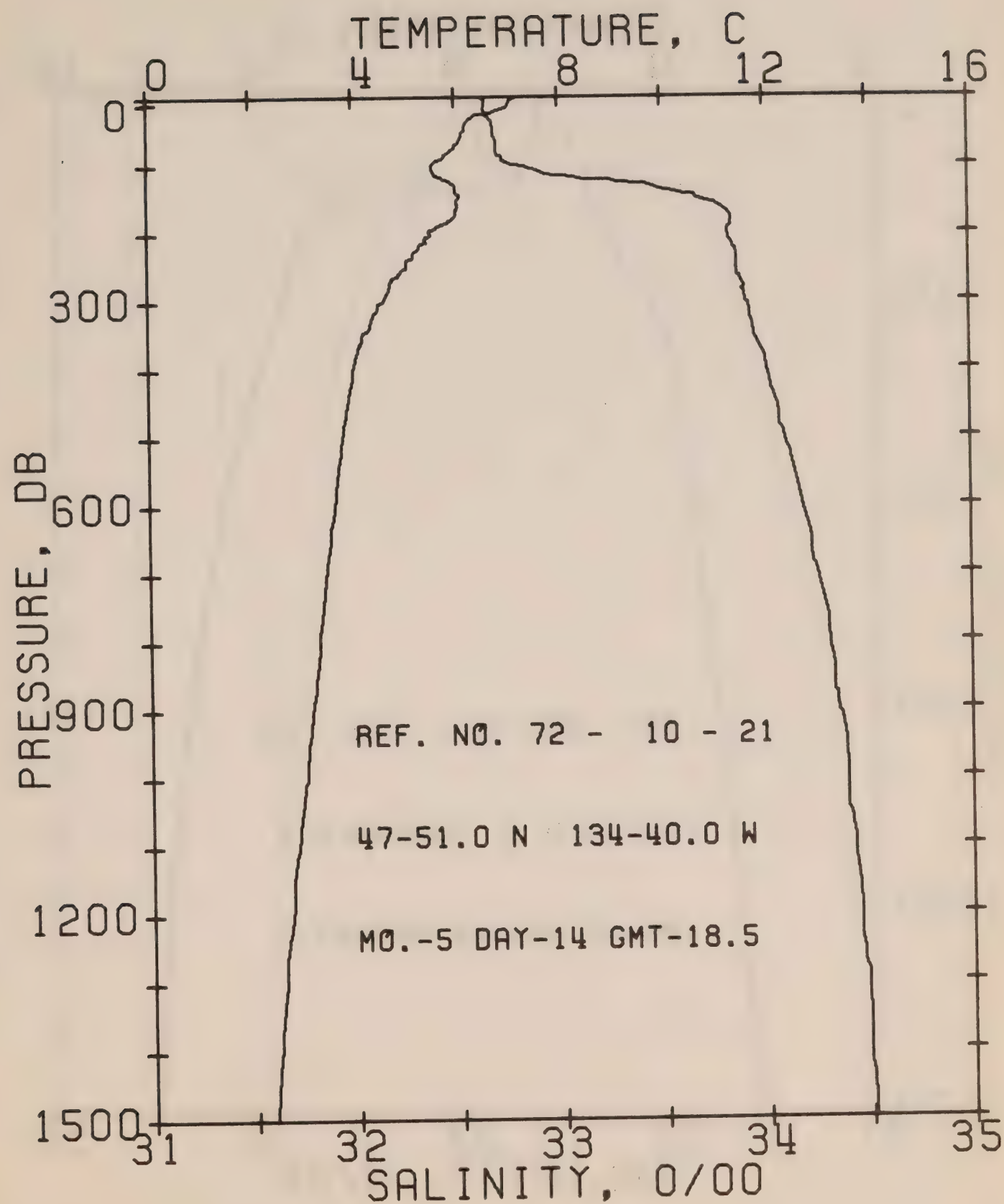


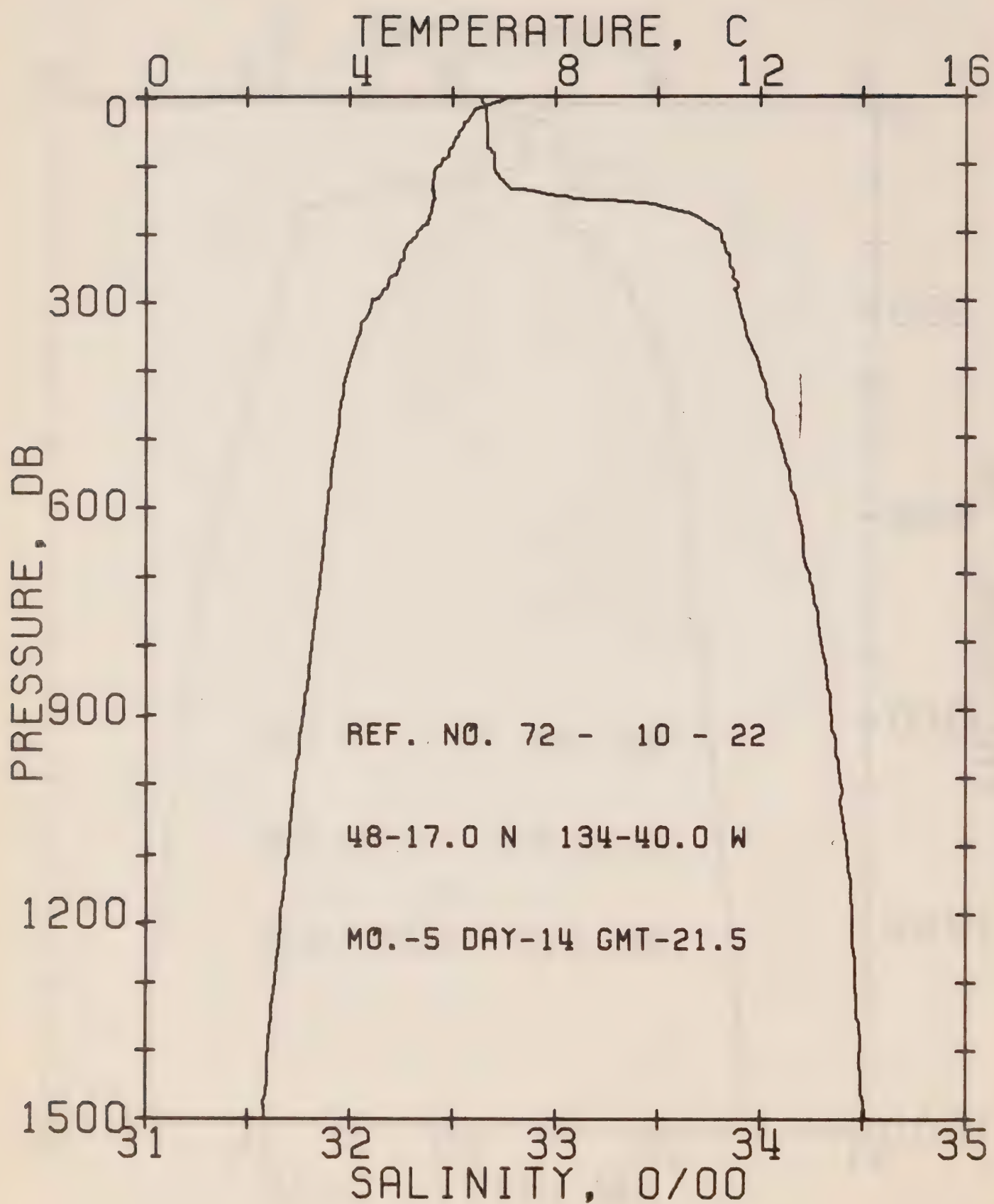


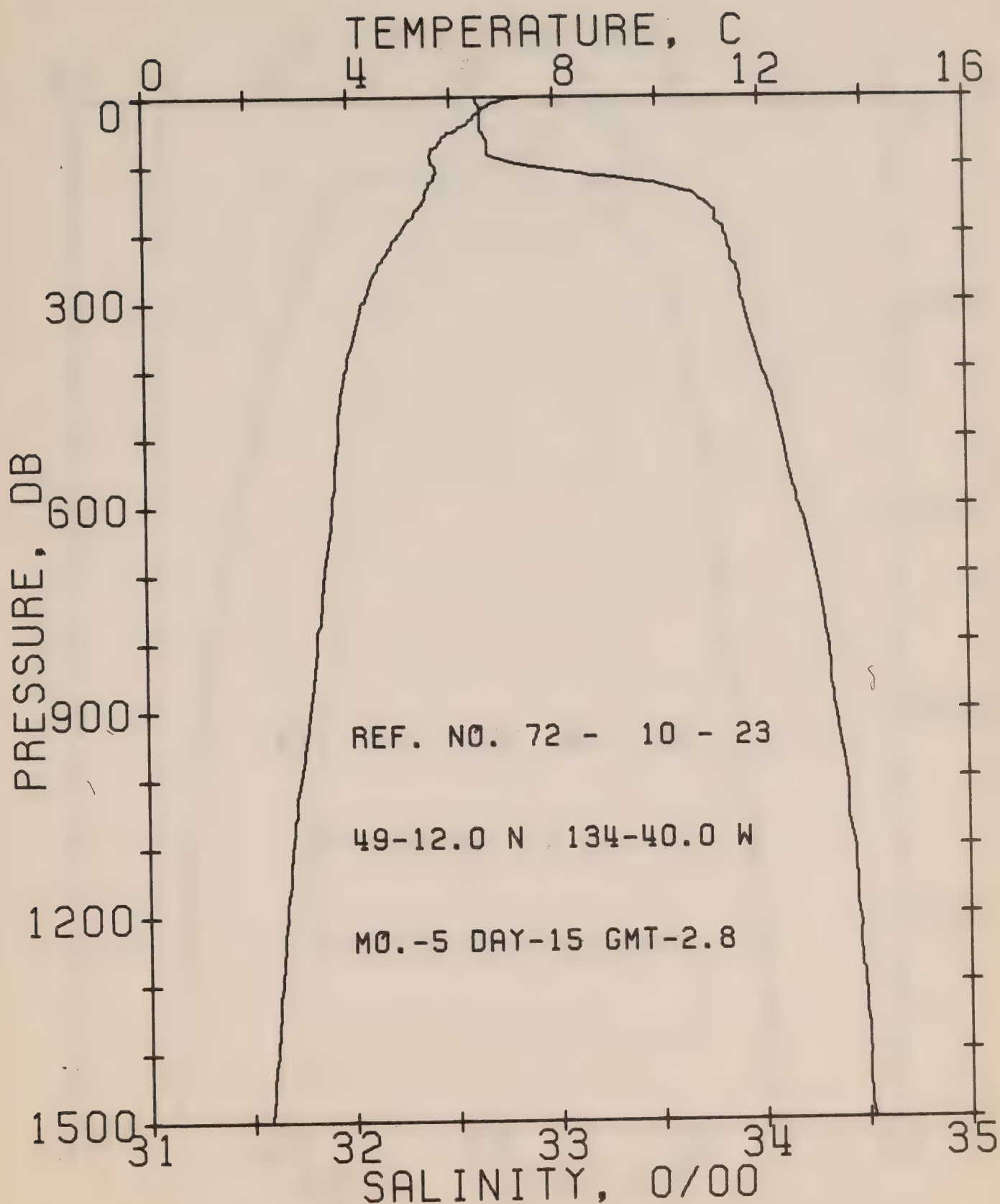


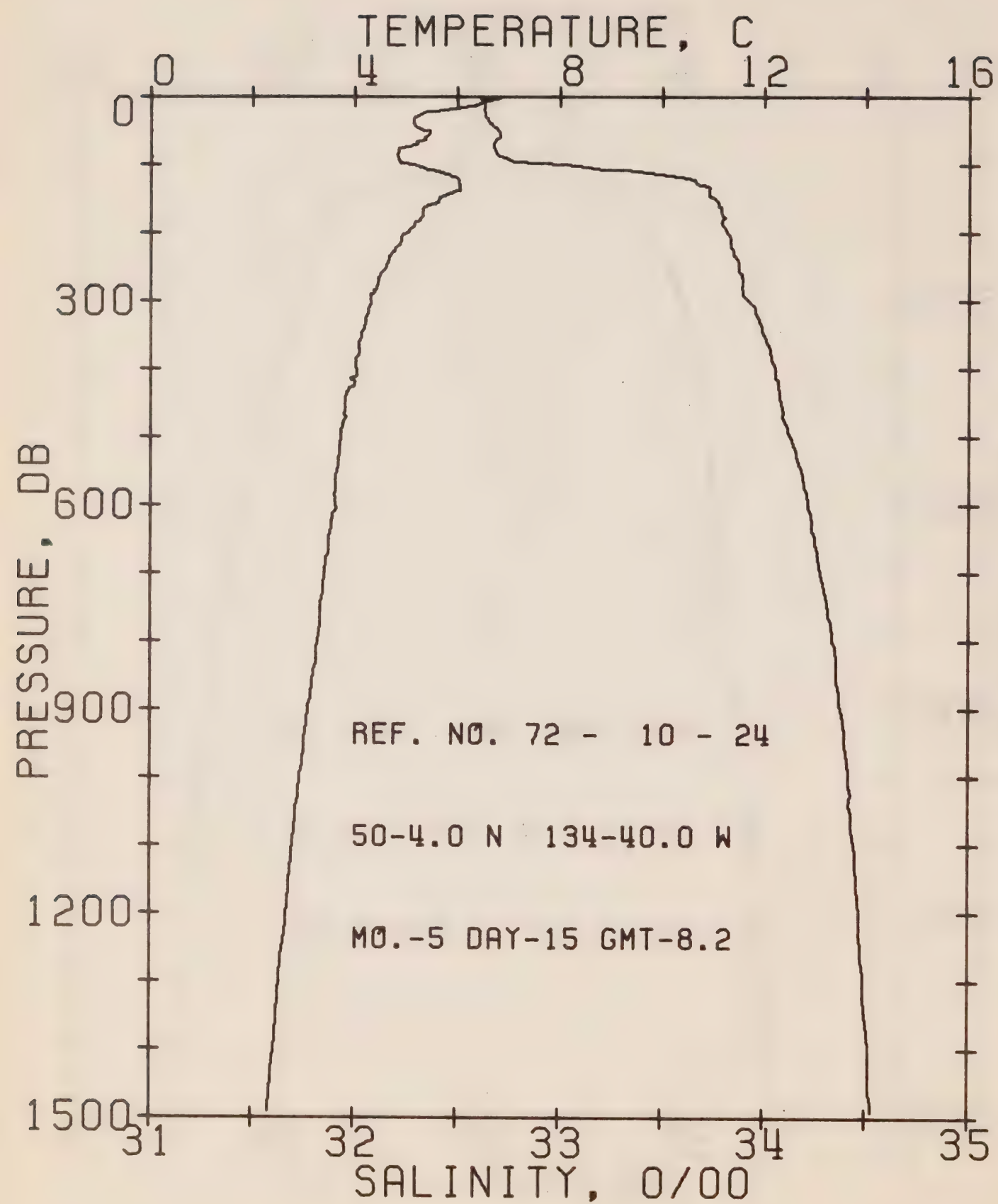


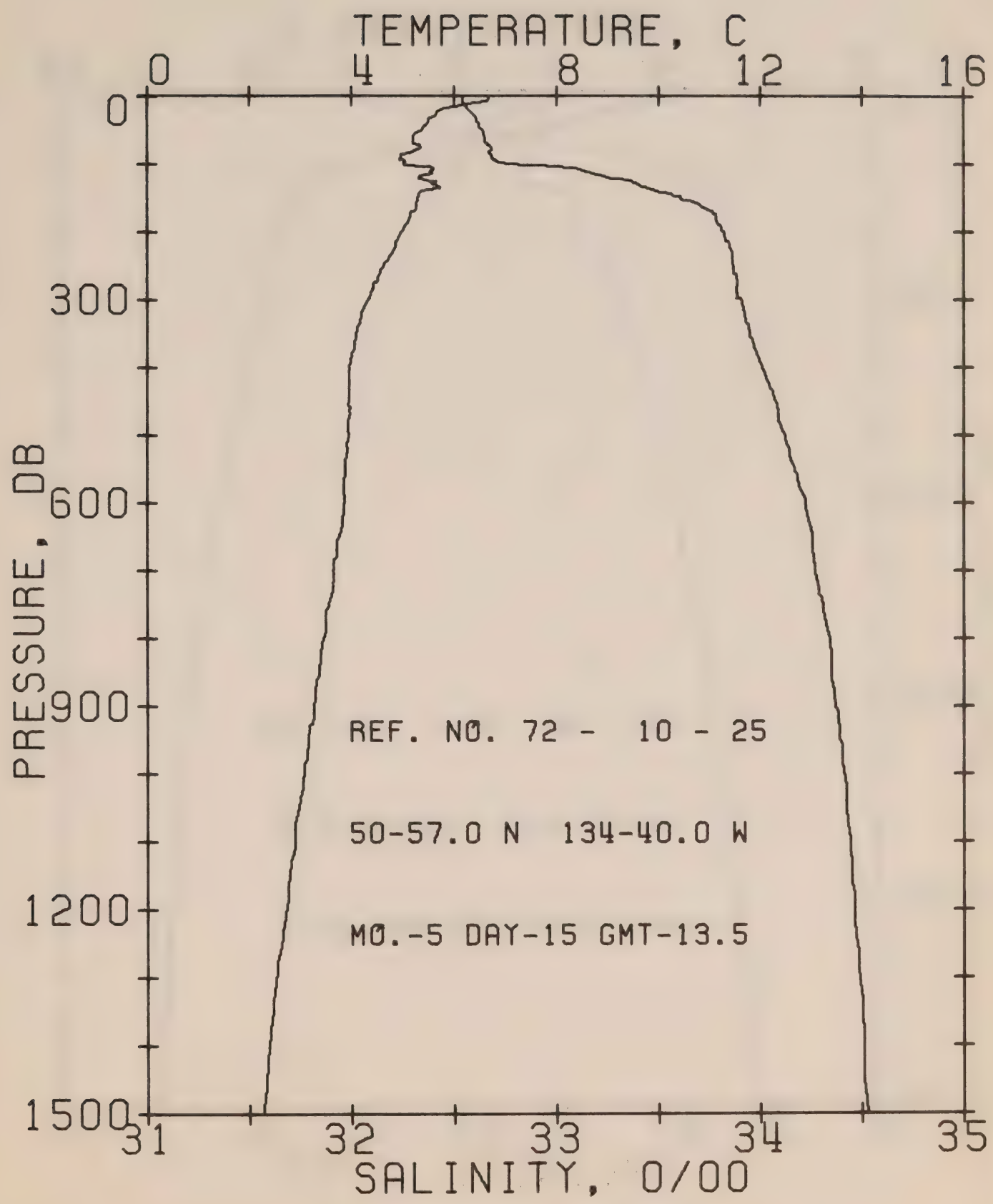


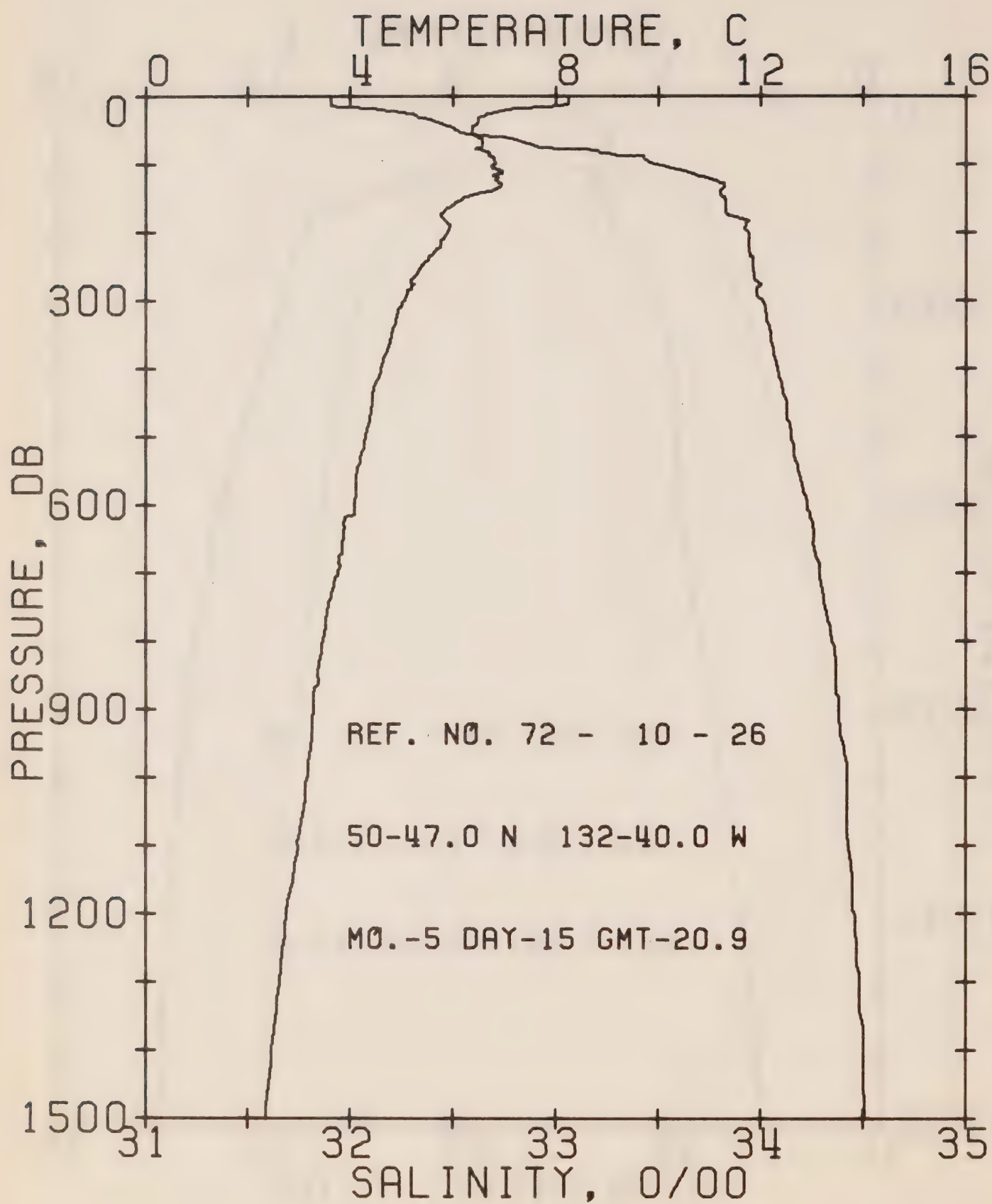


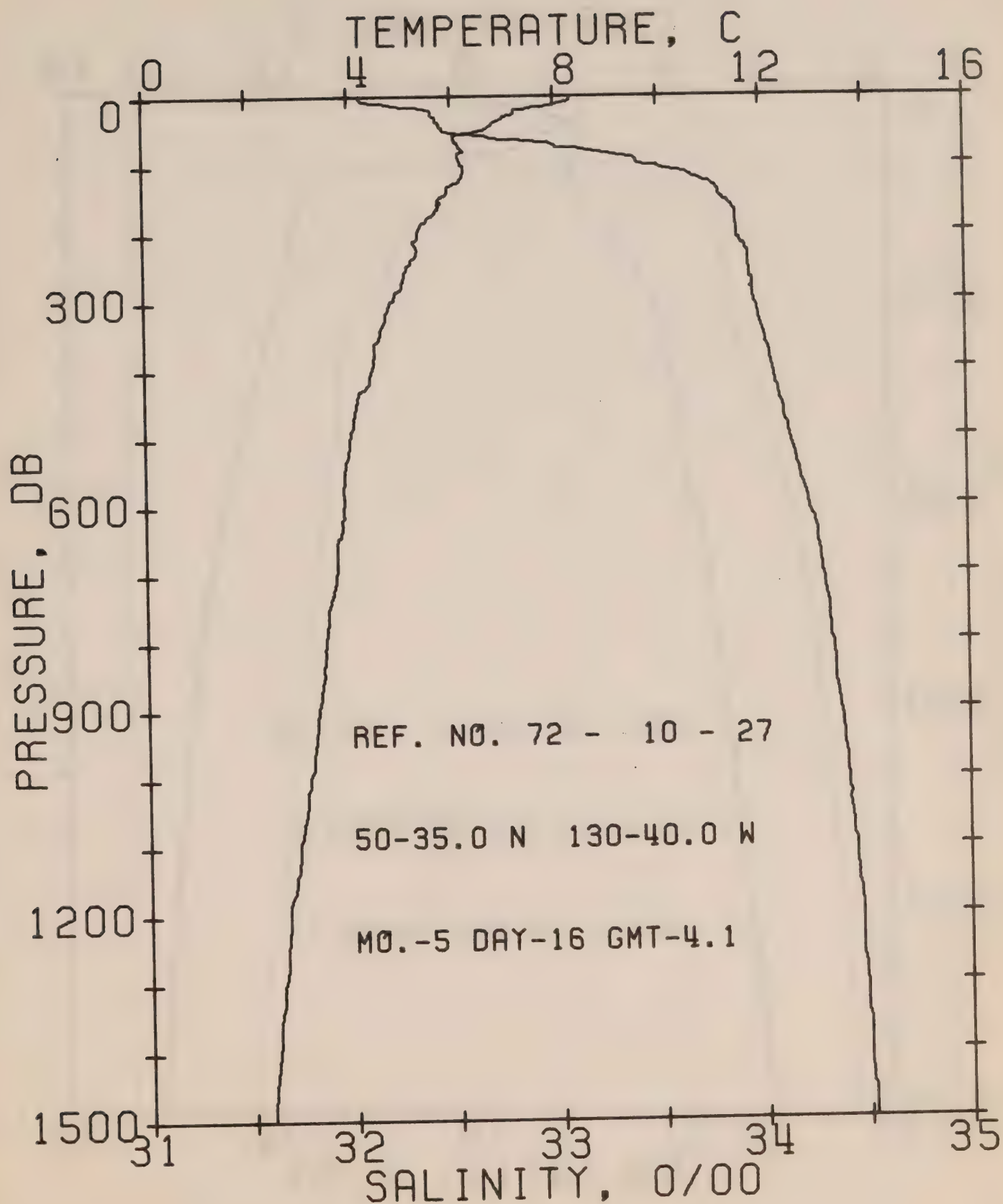


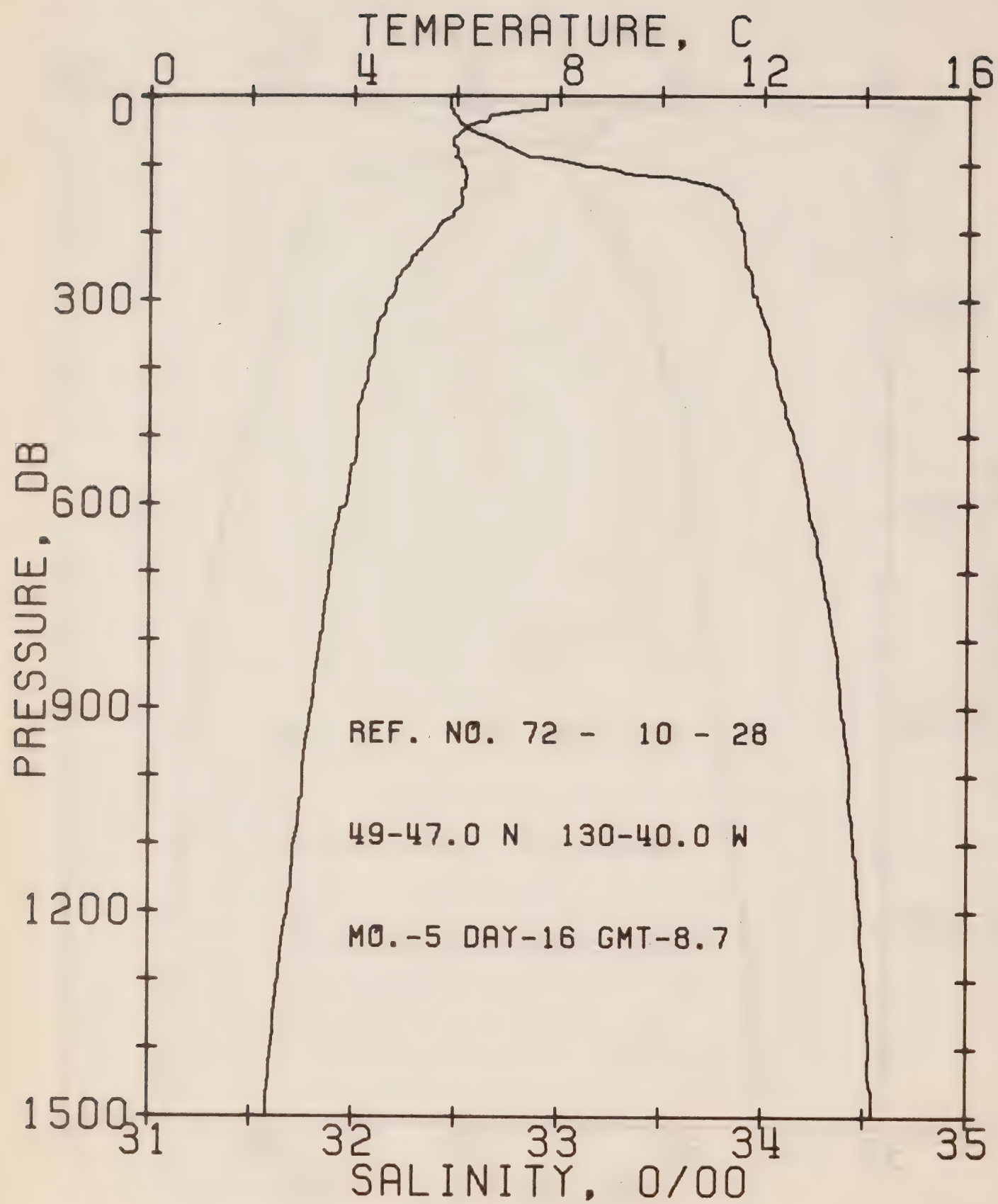


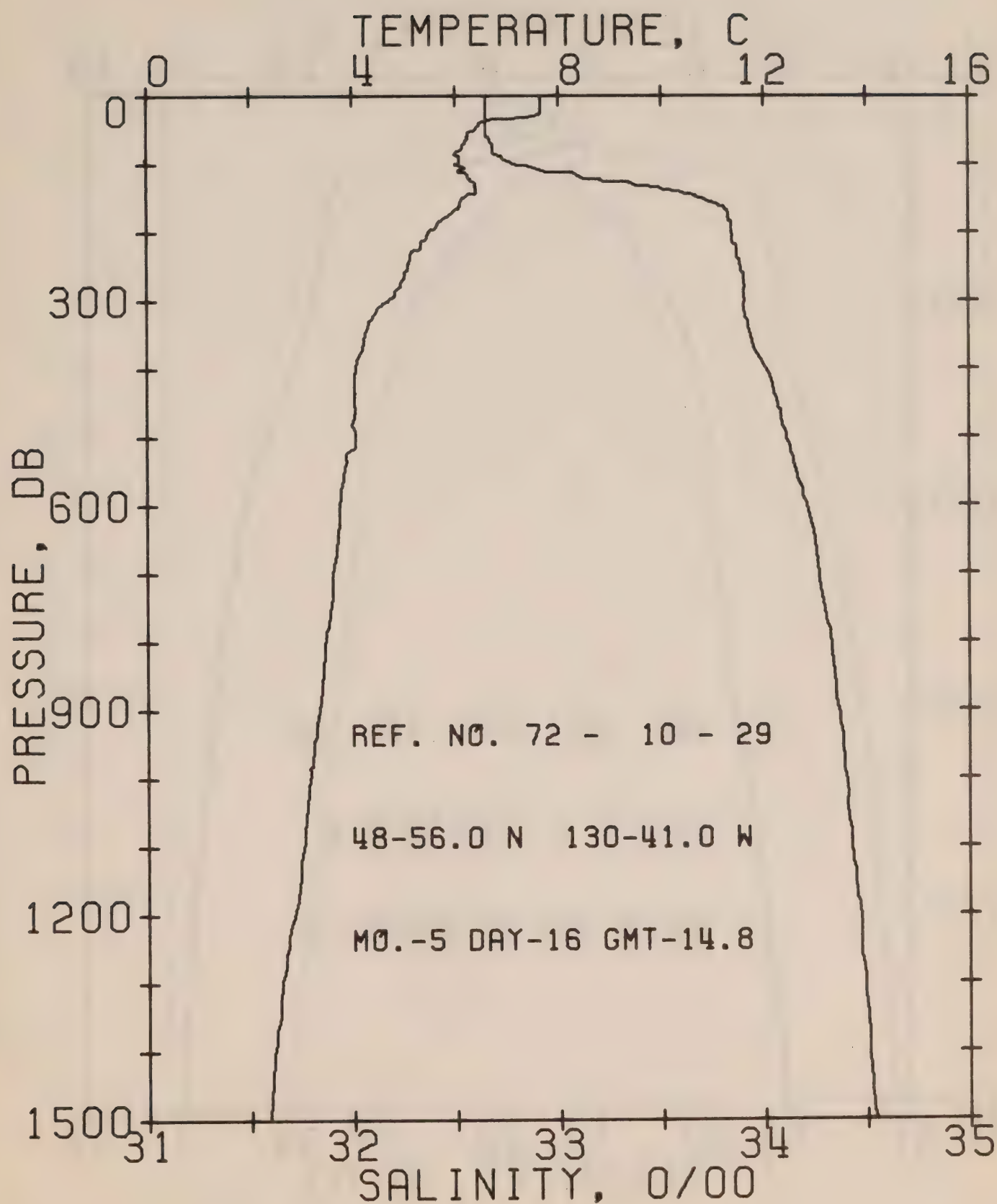


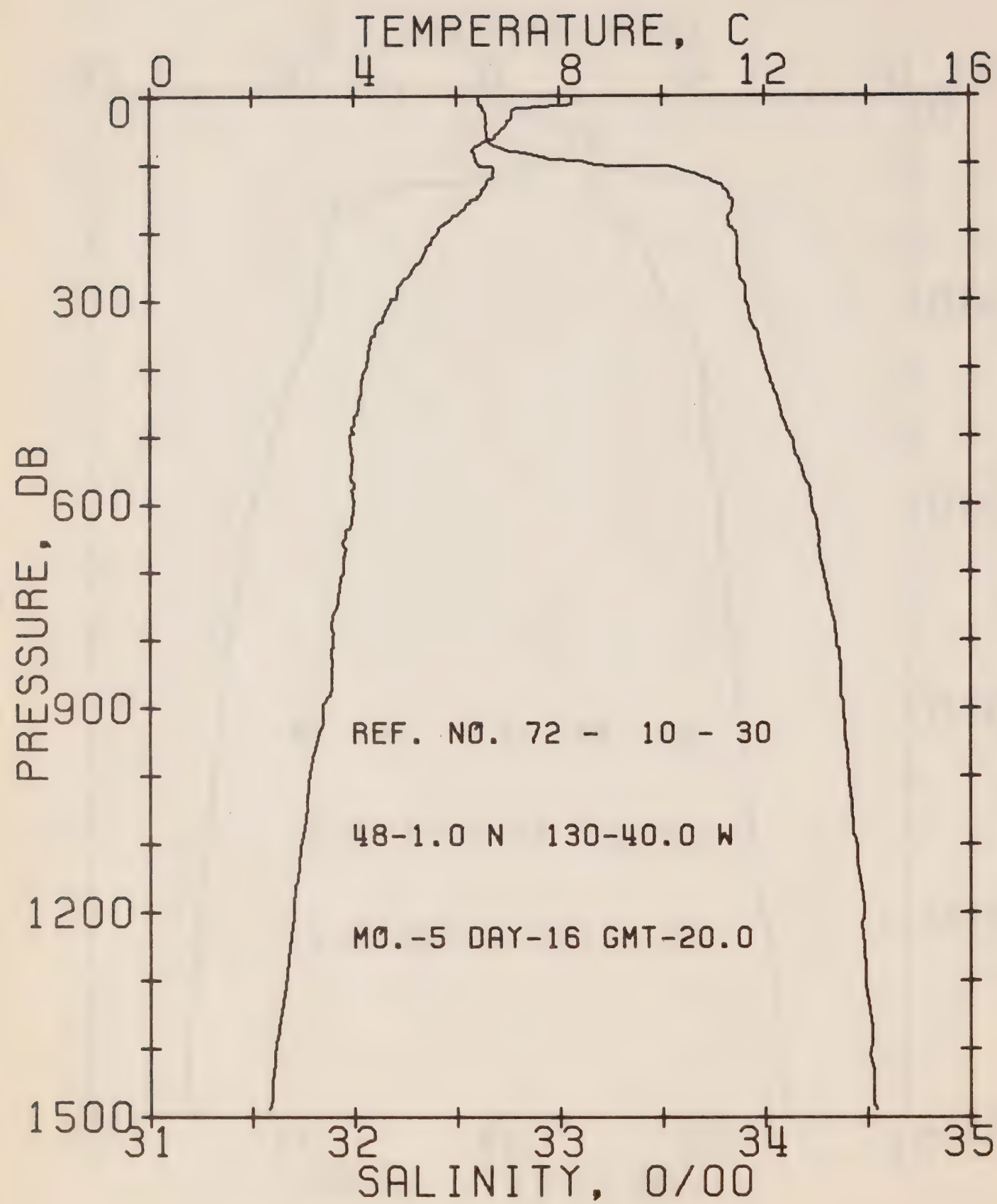


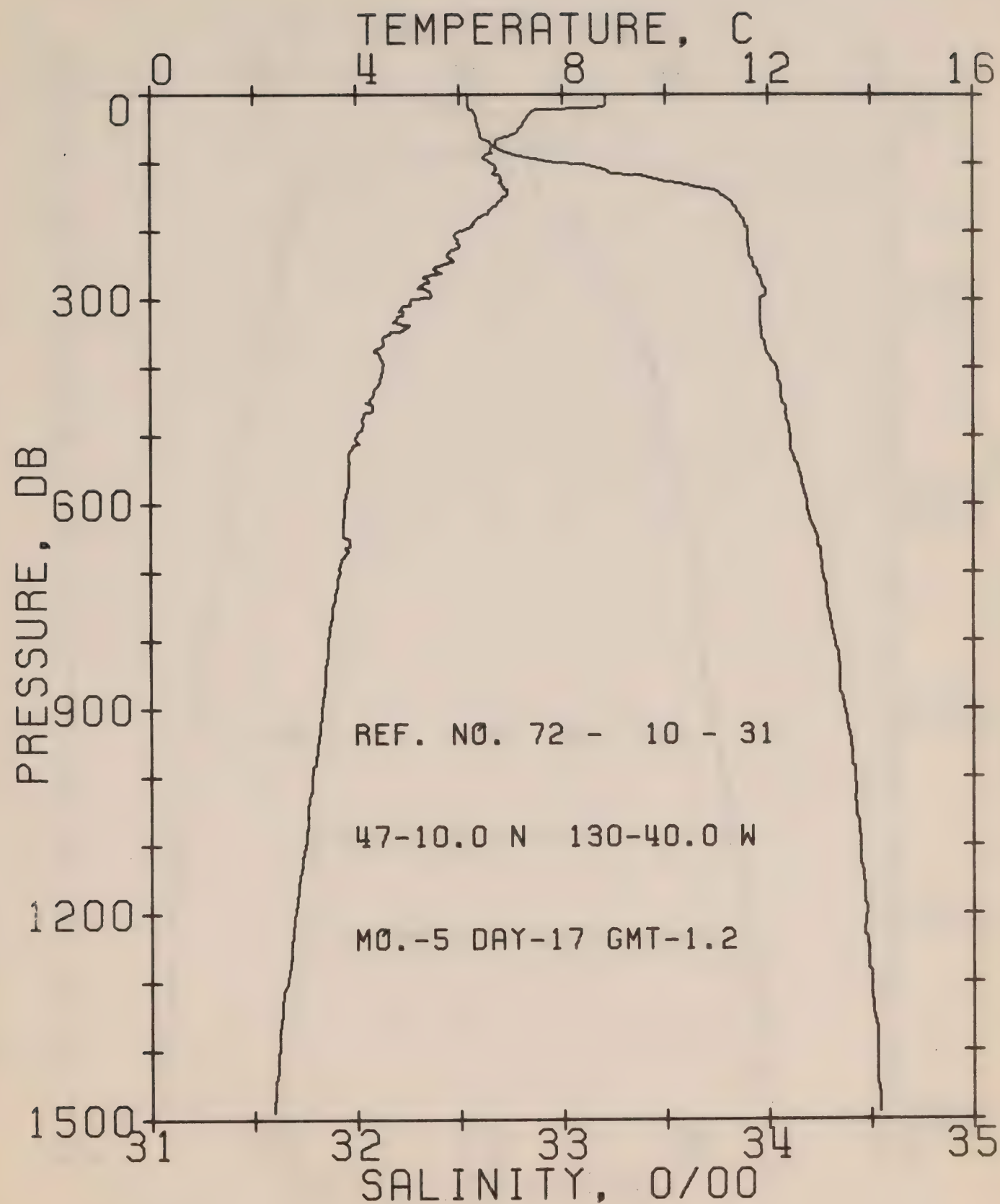


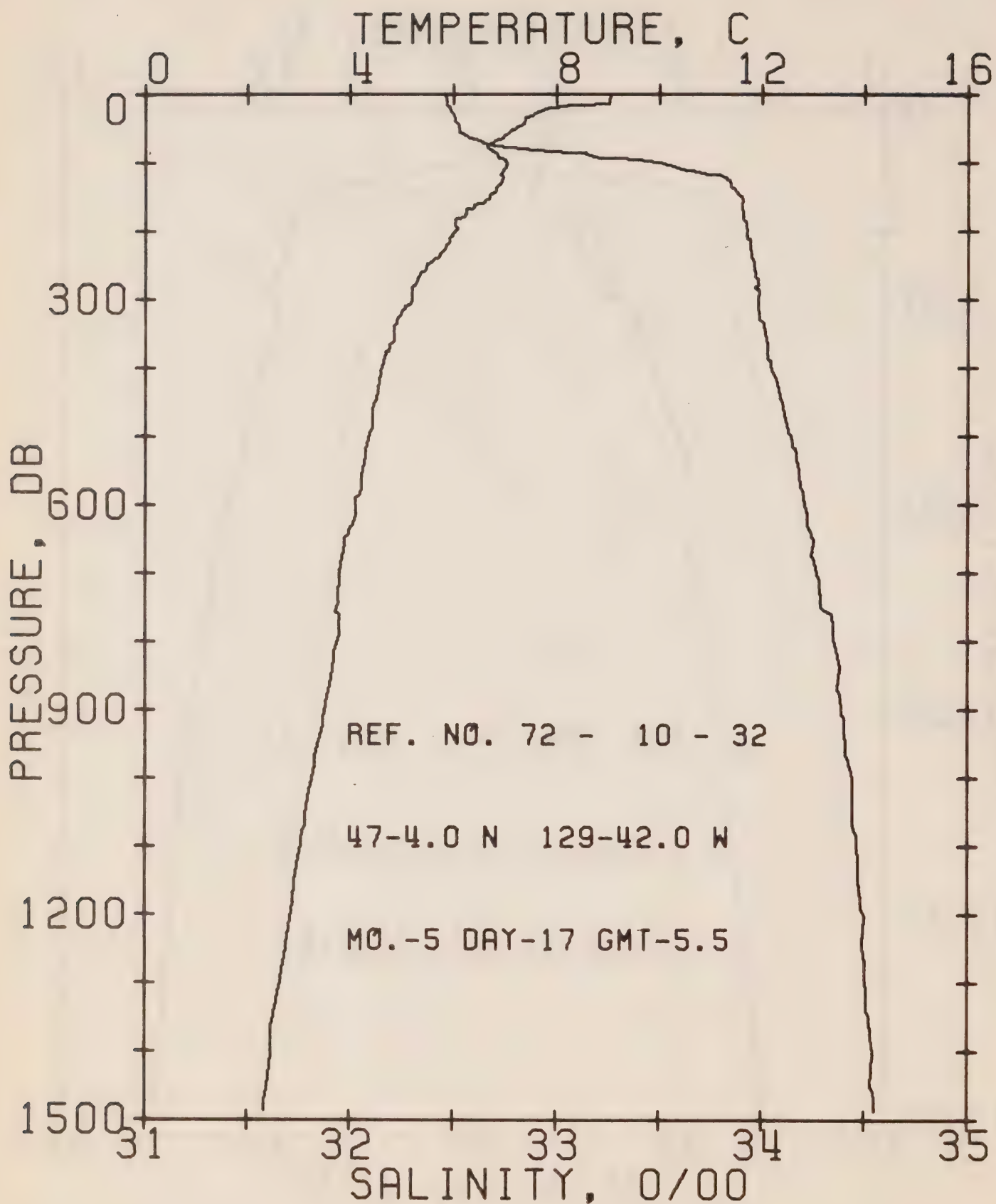


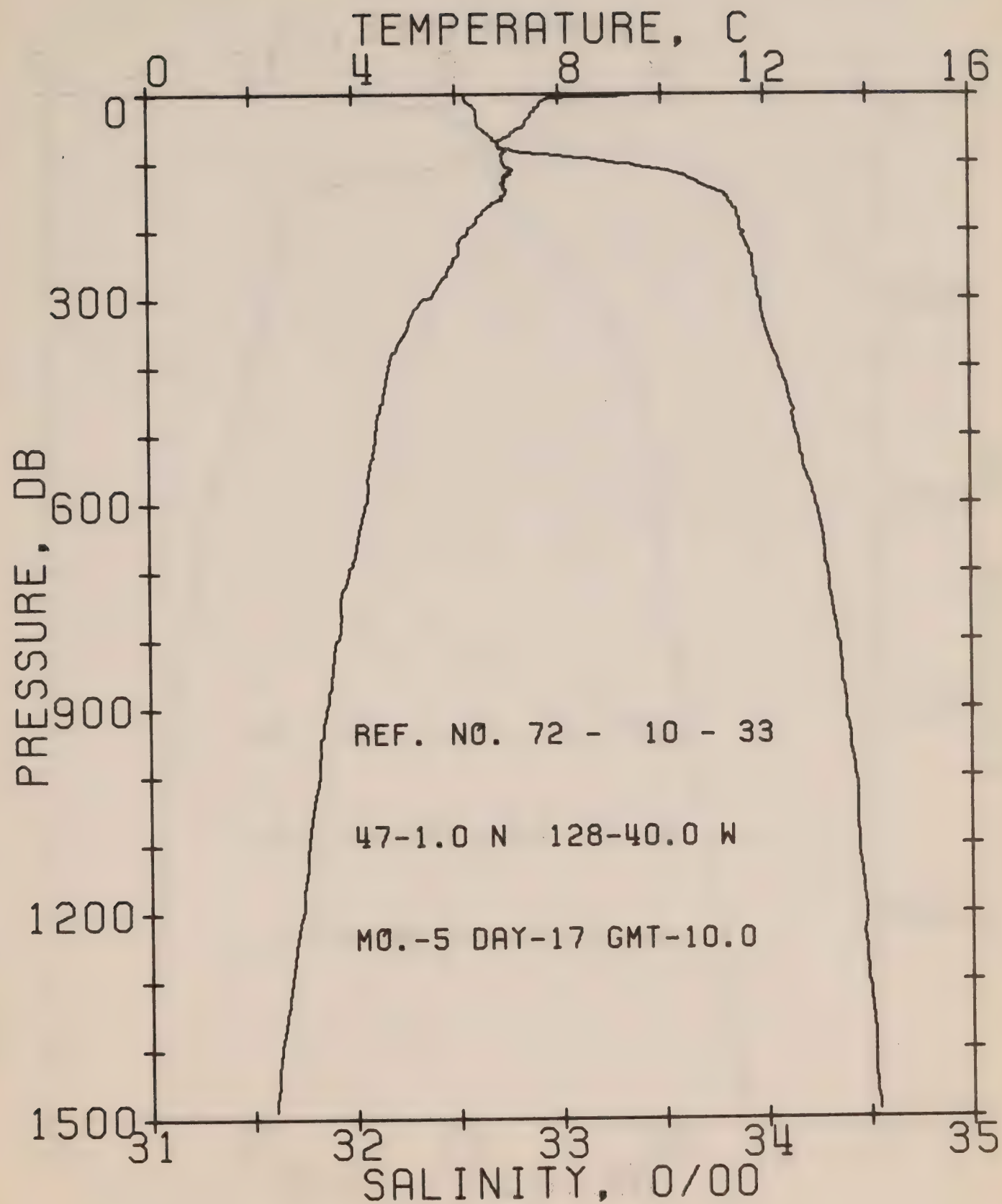


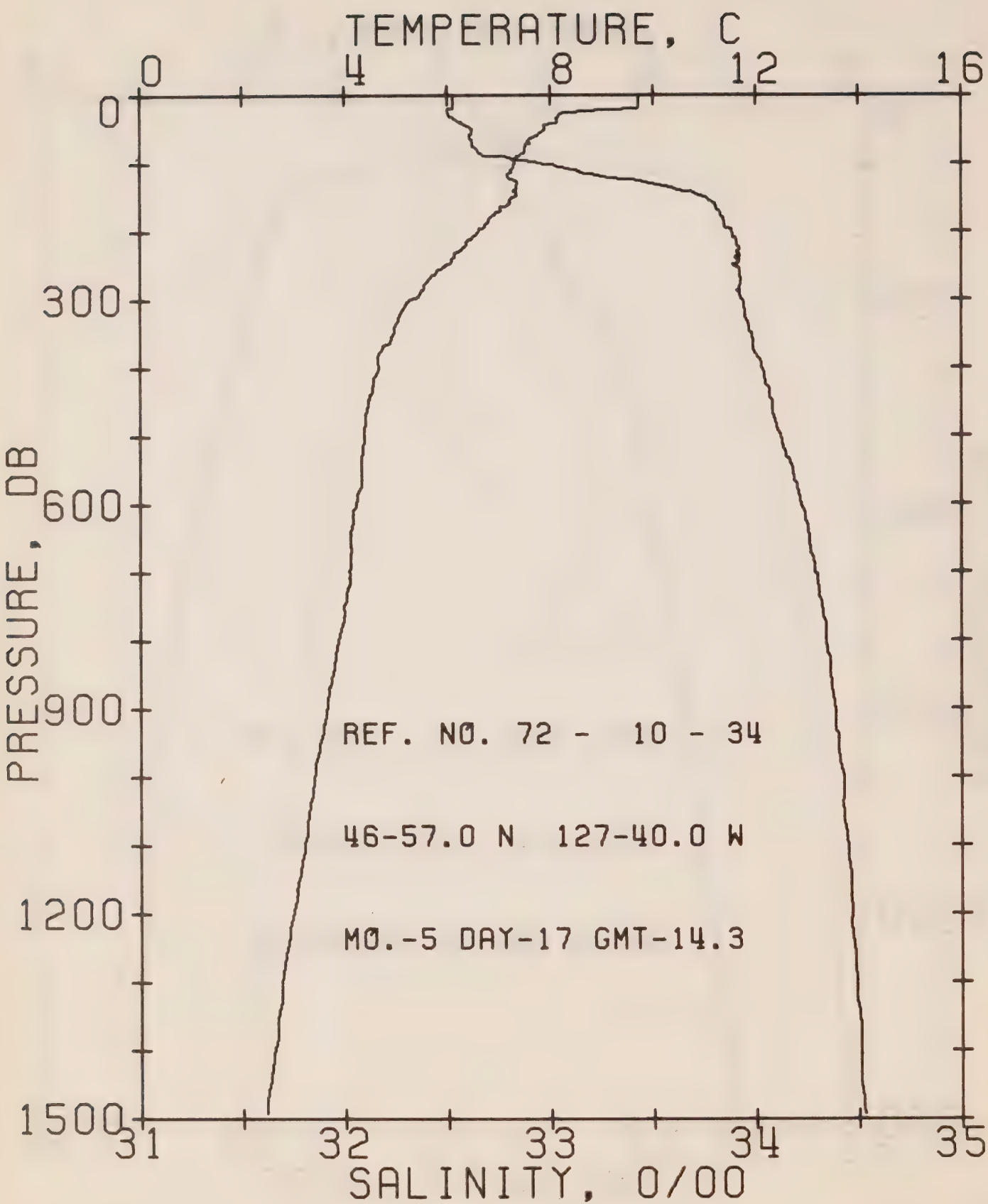


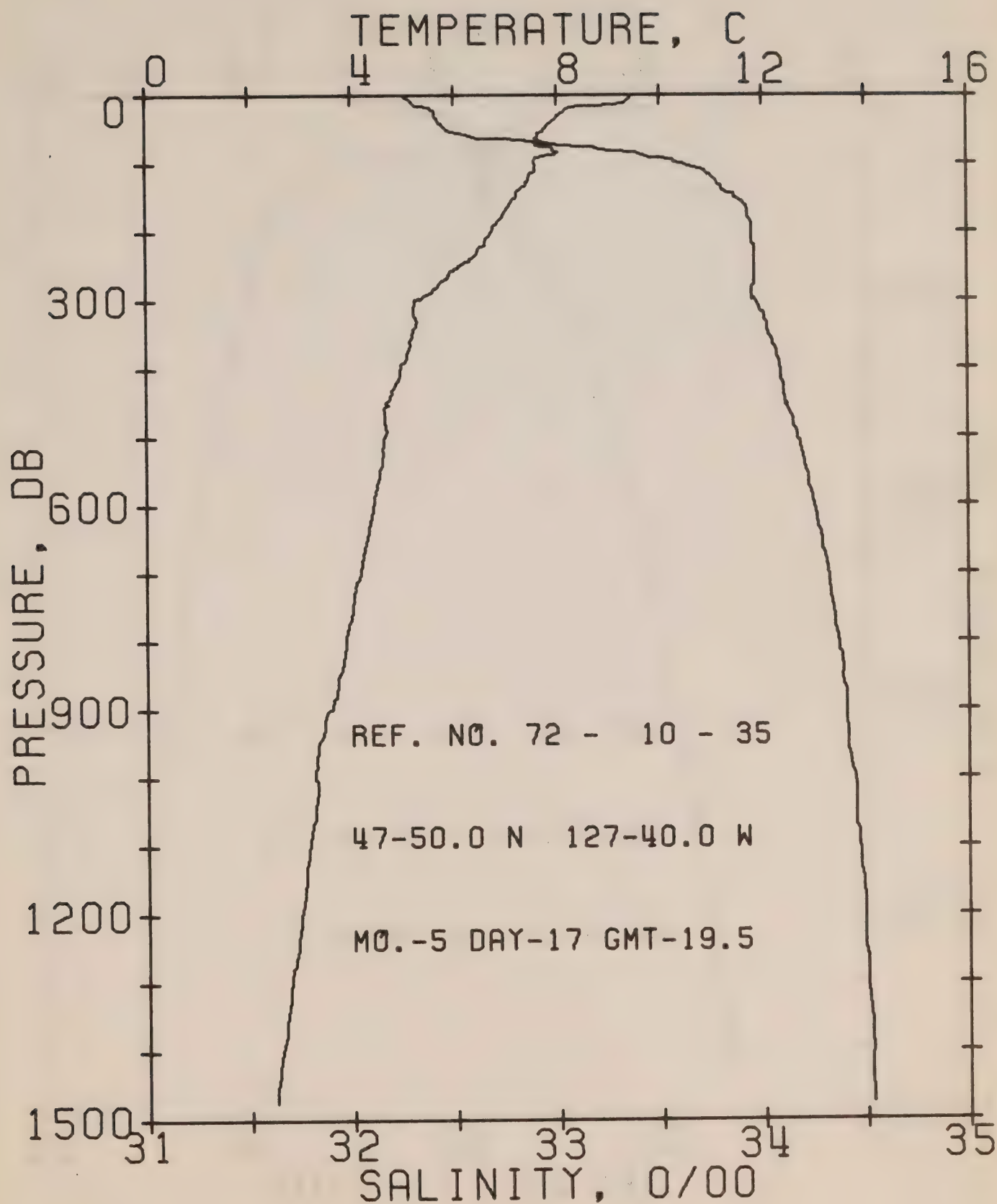


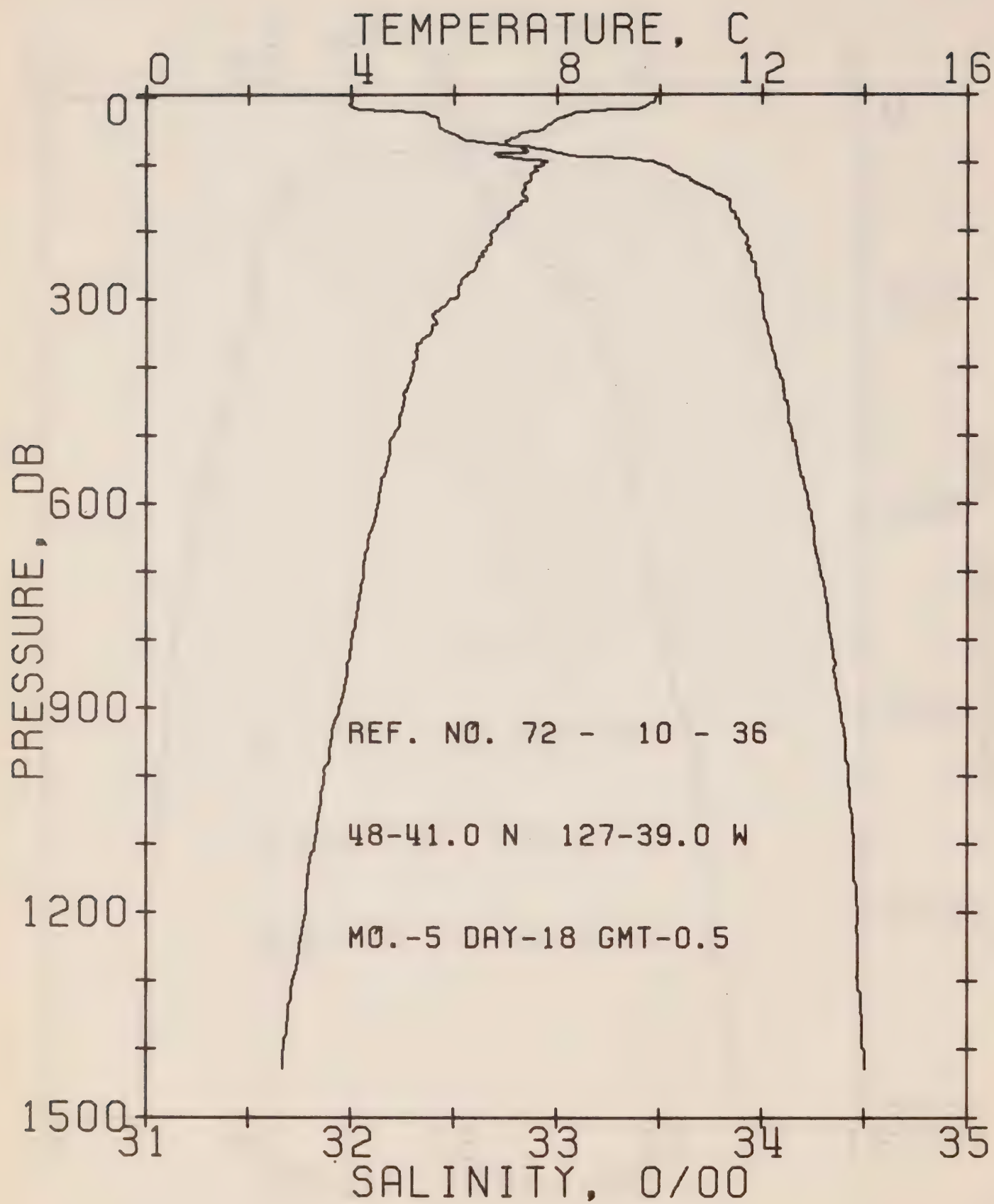


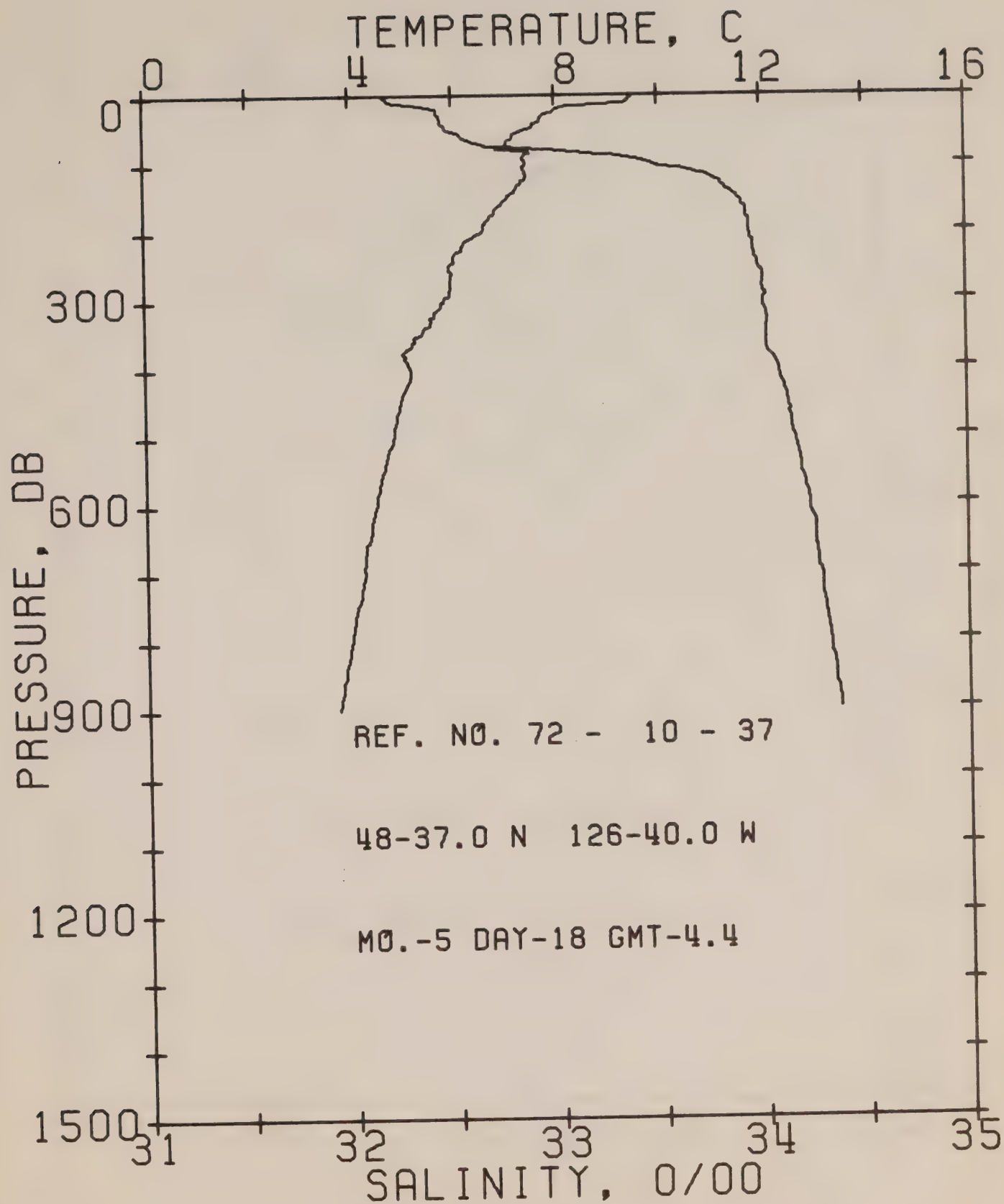


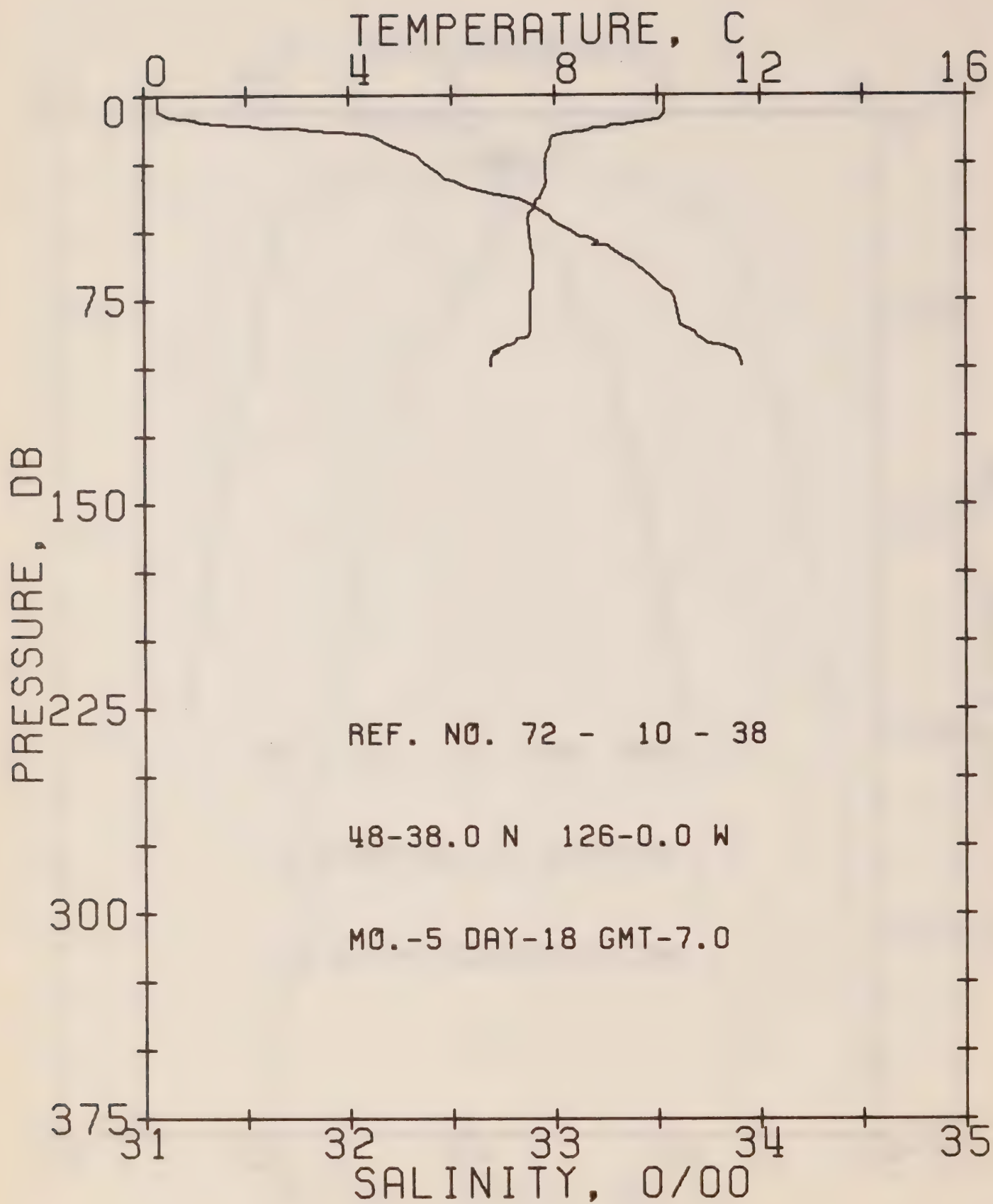








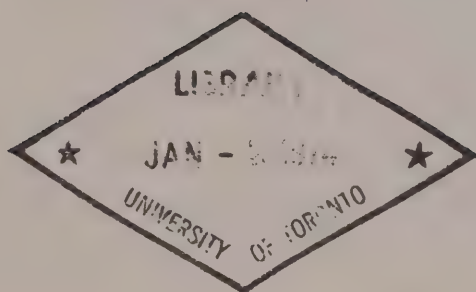




CAI EP 321
- 73R07

SUMMARY OF HYDROGRAPHIC AND OCEANOGRAPHIC INFORMATION ON SOME BRITISH COLUMBIA ESTUARIES

E.W. Marles, B.M. Lusk, and W.J. Rapatz



ENVIRONMENT CANADA
Fisheries and Marine Service
Marine Sciences Directorate
Pacific Region
1230 Government St.
Victoria, B.C.

MARINE SCIENCES DIRECTORATE, PACIFIC REGION

PACIFIC MARINE SCIENCE REPORT NO. 73-7

SUMMARY OF HYDROGRAPHIC AND OCEANOGRAPHIC INFORMATION

ON SOME

BRITISH COLUMBIA ESTUARIES

by

E.W. Marles, B.M. Lusk and W.J. Rapatz

Victoria, B. C.

Marine Sciences Directorate, Pacific Region

Environment Canada

July, 1973.

TABLE OF CONTENTS

	<u>PAGE</u>
INTRODUCTION.....	1
ACKNOWLEDGEMENTS	2
HYDROGRAPHIC CHART NO. 3599	3
HYDROGRAPHIC FIELD SHEET	4
CHART OF ESTUARY LOCATION	6
FRASER RIVER ESTUARY	8
INDIAN RIVER ESTUARY	12
SQUAMISH RIVER ESTUARY	15
COWICHAN RIVER ESTUARY	18
CHEMAINUS RIVER ESTUARY	20
NANAIMO RIVER ESTUARY	23
PUNTLEDGE-COURTENAY RIVER ESTUARY	26
CAMPBELL RIVER ESTUARY	29
SALMON RIVER ESTUARY	31
HOMATHKO RIVER ESTUARY	33
QUATSE RIVER ESTUARY	37
WANNOCK RIVER ESTUARY	39
BELLA COOLA RIVER ESTUARY	42
KITIMAT RIVER ESTUARY	45
SKEENA RIVER ESTUARY	48
GOLD RIVER ESTUARY	51
SOMASS RIVER ESTUARY	54

INTRODUCTION

This summary of hydrographic and oceanographic information on some British Columbia estuaries was initiated for the Pacific Region Board Working Group on Estuaries. It is concerned with those places on the Pacific Coast of Canada where industrial development and population growth are closely associated with river estuaries. The data sources include publications of the Fisheries Research Board of Canada, the Marine Sciences Directorate, Fisheries Service, and the University of British Columbia Institute of Oceanography. A great deal of the information was discovered upon personal enquiry to scientists and technicians in various government departments. Internal publications of these departments are often not catalogued in a fashion that makes them available to those people in other areas who could make use of them. A great quantity of data also remains on file, unpublished and thus not easily accessible. With changes in personnel and passage of time, data on file becomes less available and often later workers have an insufficient basis for evaluation of the information.

Owing to the difficulty of searching many diverse sources and the impossibility of communicating with every person working on estuaries in the many concerned agencies, the present collection of information cannot be considered complete. Further contributions and comments from those more intimately involved in some particular estuary are solicited and will serve to bring the study closer to being a complete survey.

The catalogue covers the estuaries of the rivers listed on page 5, in the order shown. Their location is shown on the first chart. For each estuary there is a chart with the area of concern outlined and the following information:

Hydrography

- Date of the most recent survey.
- Scale of field sheets (F.S.) available.
- Chart numbers and scales.
- Remarks on surveys where appropriate.
- An assessment of the adequacy of the survey coverage.

For those not familiar with hydrographic field sheets, a sample sheet, with the derived chart, is included at the end of this introduction.

Tidal

The location of the nearest tide gauge, the period over which tide heights have been analysed, and the date of analysis.

Oceanography

A narrative discussion of the information available.

Bibliography

An alphabetical listing by author of the known oceanographic publications on the estuary region.

The hydrographic section of the report was prepared by B.M. Lusk, the tidal information was collected by W.J. Rapatz, and the oceanographic bibliography was compiled by E.W. Marles.

Acknowledgements

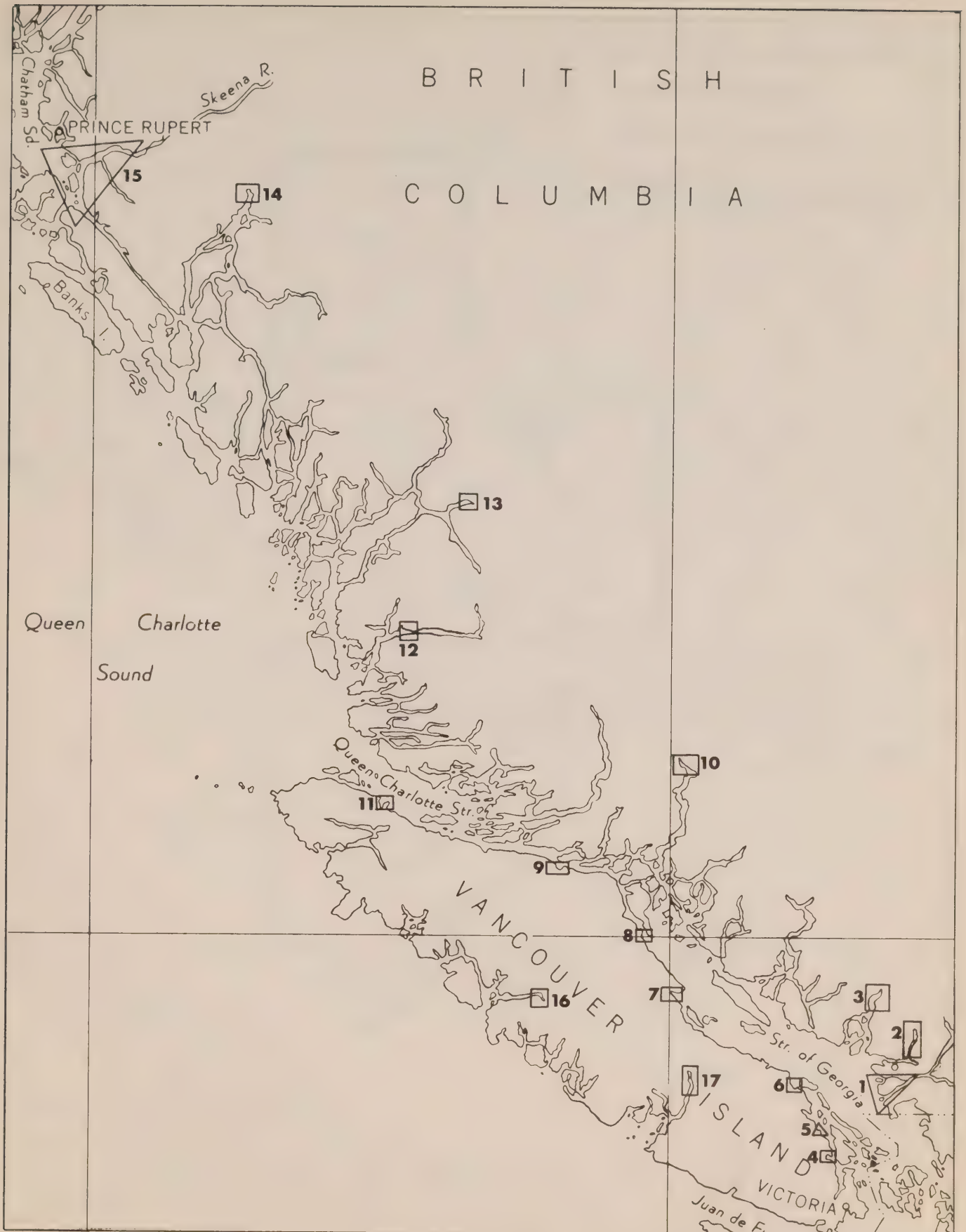
Appreciation is due to Dr. J.F. Garrett and Dr. W.N. English for helpful comments and criticism of the manuscript.

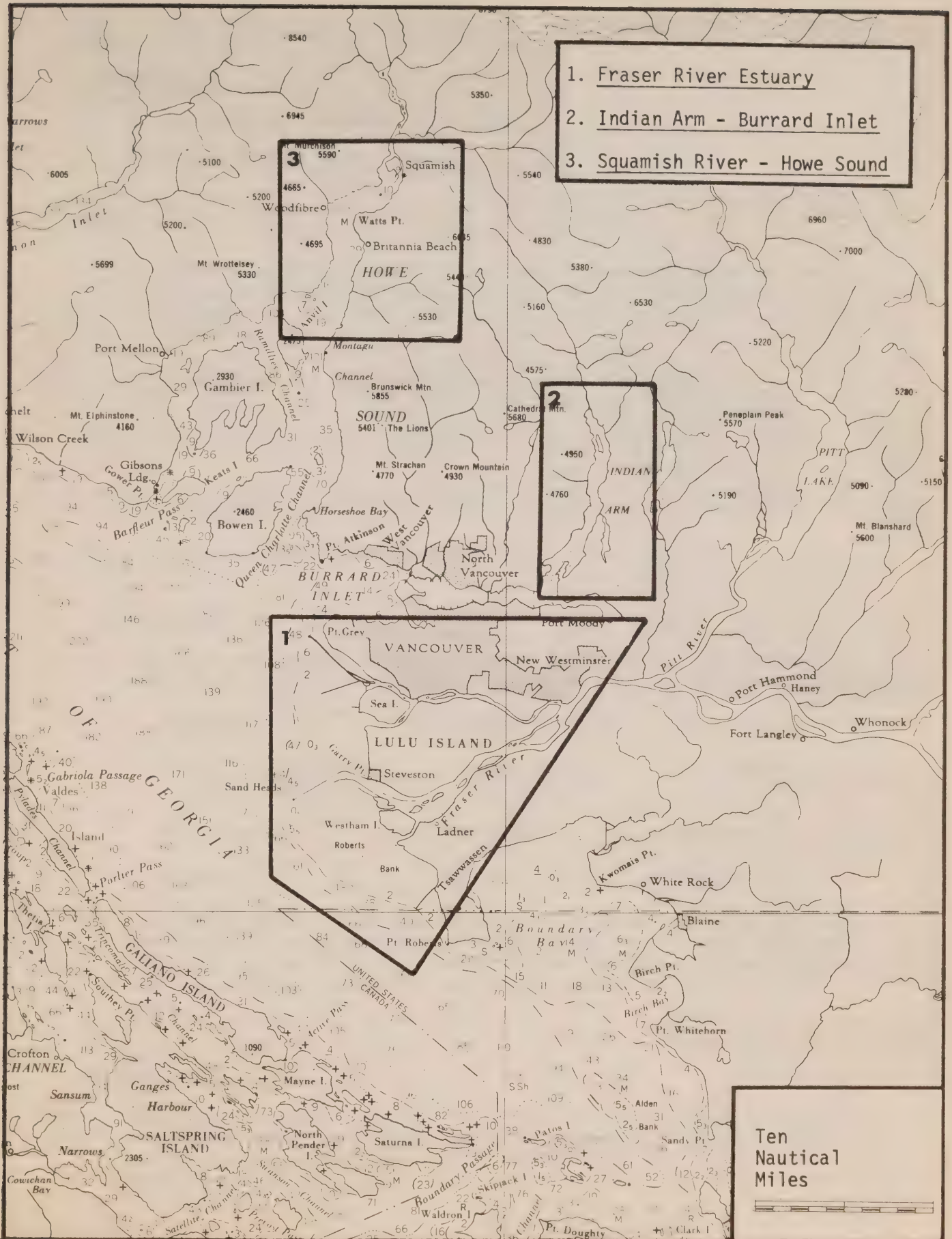


HYDROGRAPHIC FIELD SHEET

ESTUARY LOCATION ON THE BRITISH COLUMBIA COAST

1. Fraser River
2. Indian River - Indian Arm
3. Squamish River - Howe Sound
4. Cowichan River - Cowichan Bay
5. Chemainus River
6. Nanaimo River
7. Puntledge - Courtenay River - Comox Harbour
8. Campbell River
9. Salmon River - Kelsey Bay
10. Homathko River - Bute Inlet
11. Quatse River - Port Hardy
12. Wannonck River - Rivers Inlet
13. Bella Coola River - North Bentinck Arm
14. Kitimat River
15. Skeena River
16. Gold River - Muchalat Inlet
17. Somass River - Alberni Inlet





FRASER

Hydrography

1. Surveyed most recently in 1967/68.
2. Scale of F.S. 2273-L)
2274-L) 1:30,000 Strait of Georgia

F.S. 2272-L 1:15,000 Burrard Inlet
3. The Fraser River itself is continually being surveyed for depths by the Department of Public Works. The last hydrographic survey recorded on the river itself was in 1929, sheets 2209-L and 2210-L. Scale 1:12,650.
4. Chart scale of the river - Charts 3488 - 1:25,000
3489 - 1:18,000
5. Chart scale of Str. of Georgia 3450 - 1:80,000
1:50,000

Sounding Coverage

A modern survey with good coverage of tidal estuary.

Tidal Information

For a one year period in 1958-59 water level gauges were operated to Tidal Survey standards for a 12 month period at the following locations:

Steveston	Woodward Landing	Burr Landing
Fraser Street Bridge (North Arm)	New Westminster	Port Mann
Pitt River	Pitt Lake	Hammond
Wannock	Mission	Sardis

A numerical model of the Fraser estuary has been developed, in which the Strait of Georgia tides and river runoff can be input and water levels at any point in the estuary can be forecast. Several temporary tide gauges were operated in the Fraser estuary to calibrate this model.

Oceanography

The Fraser River Estuary, because of its size, proximity to populated centres and importance to the salmon fisheries of British Columbia, is one of the few intensively studied estuaries on the Pacific coast. The whole Strait of Georgia is often considered to be the Fraser Estuary due

to the magnitude of this great river's influence. Oceanography in the region immediately seaward of the delta front has been studied by the University of British Columbia, Fisheries Research Board of Canada, and the Marine Sciences Branch of the Department of Environment over many years. A study of the salt water intrusion in the estuary was published by Tabata and LeBrasseur (1958). Further studies in the lower river have been undertaken in connection with the disposal of sewage from the City of Vancouver. Ages (personal communication) and Bawden et al (1972) have collected some information on circulation and water characteristics on the shallow banks of the delta.

Bibliography

- Ages, A.B. _____. Salinity and temperature in the Fraser delta region. In progress. Marine Sciences Directorate.
- _____. Numerical model in the Fraser delta area - predicting heights and velocities, including circulation on Roberts Bank. In progress. Marine Sciences Directorate.
- Anon. 1953. Sewerage and drainage of the Greater Vancouver area, British Columbia. Ms. rept. to the chairman and members, Vancouver and Districts Joint Sewerage and Drainage Board.
- Baines, W.D. 1952. Water surface elevations and tidal discharges in the Fraser River Estuary, January 23 and 24, 1952. Rept. no. MH-32, Nat. Res. Council Can., Div. of Mechanical Eng., Ottawa.
- Bawden, C.A., W.A. Heath, and A.B. Norton. 1972. A preliminary baseline study of Roberts and Sturgeon Banks. Westwater Res. Centre. Inst. Oceanogr., Univ. British Columbia Ms. Rept., no. 27.
- Bawden, C.A., et al . . . Also identified as: 1973. Tech. Rept., no. 1. Westwater Res. Centre. Univ. British Columbia: 54 pp.
- Benedict, A.H., K.J. Hall, and F.A. Koch. 1973. A preliminary water quality survey of the lower Fraser River system. Tech. Rept., no. 2. Westwater Res. Centre. Univ. British Columbia: 50 pp.
- British Columbia Research Council. 1951. Study of tidal effects in the north arm of the Fraser River, April 23-24, 1951. Ms. Univ. British Columbia.
1972. Fraser River in the vicinity of Lulu Island. Water Quality Sampling Progress Repts. for Greater Vancouver Sewerage and Drainage District.
1972. Water movement studies in the south arm of the Fraser River. Project 1462. Available - Prov. British Columbia, Poll. Contr. Br., file F 26A.

- Fjarlie, R.L.I. 1950. The oceanographic phase of the Vancouver sewage problem. Pacific Oceanographic Group Ms., Nanaimo, B.C.
- Foundation of Canada Engineering Corp. Ltd. and Christiani and Nielsen of Canada Ltd. 1957. Deas Island Tunnel, report on hydrological studies in the main arm of the Fraser River. Unpub. manuscript.
- Giovando, L.F., and S. Tabata. 1970. Measurements of surface flow in the Strait of Georgia by means of free-floating current followers. Fish. Res. Bd. Can. Tech. Rept., no. 163.
- Hutchinson, A.H. 1928. A bio-hydrographical investigation of the sea adjacent to the Fraser River mouth. Trans. Roy. Soc. Can., ser. 3, 22: 293-310.
- Murray, J.W., J.L. Luternauer, C.H. Pharo, and T.M. McGee. 1972. Preliminary study of the sediment budget of the Fraser River delta-front. Ms. Rept., Dept. Geological Sciences, Univ. British Columbia.
- Neu, H.J.A. 1966. Proposals for improving flood and navigation conditions in the lower Fraser River. Unpub. manuscript.
- Pacific Oceanographic Group. 1951. Data Record. Fraser River Estuary project, 1950. Fish. Res. Bd. Can. Ms., Nanaimo Biol. Sta.
1953. Physical and chemical data record, Strait of Georgia, 1930, 1931, 1932. Fish. Res. Bd. Can. Ms., Nanaimo Biol. Sta.
1954. Physical and chemical data record, Strait of Georgia, 1949-1953, with appendix 1, current measurements, March 1953. Fish. Res. Bd. Can. Ms., Nanaimo Biol. Sta.
1956. Data Record. Fraser River Estuary, Steveston Cannery Basin, August 3, 1954-October 6, 1955. Fish. Res. Bd. Can. Ms., Nanaimo Biol. Sta.
- Parkinson, W. 1955. Prototype studies of the lower Fraser River, British Columbia Fraser River model. Ms. Rept., no. 220, Dept. Civil Engineering, Univ. British Columbia, and Nat. Res. Council Can.
- Pretious, E.S. 1969. The sediment load of the lower Fraser River, British Columbia. Ms. Rept., Dept. Civil Engineering, Univ. British Columbia.
- Tabata, S., and R.J. LeBrasseur. 1958. Sea water intrusion into the Fraser River and its relation to incidence of shipworms in Steveston Cannery Basin. J. Fish. Res. Bd. Can., 15(1): 91-113.

- Tabata, S., L.F. Giovando, and D. Devlin. 1971. Current velocities in the vicinity of the Greater Vancouver Sewerage and Drainage Districts Iona Island Outfall, 1968. Fish. Res. Bd. Can. Tech. Rept., no. 263.
- Tabata, S. 1972. The movement of Fraser River influenced surface water in the Strait of Georgia as deduced from a series of aerial photographs. Pacific Marine Science Rept. 72-6, Environment Canada, Marine Sciences Directorate, Victoria, B.C.
- Tiffin, D.L., J.W. Murray, I.R. Mayers, and R.E. Garrison. 1971. Structure and origin of foreslope hills, Fraser River Delta, British Columbia. Bull. Can. Petrol. Geol., 19(3): 589-600.
- Tully, J.P., and A.J. Dodimead. 1957. Properties of the water in the Strait of Georgia, British Columbia and influencing factors. J. Fish. Res. Bd. Can., 14(3): 241-319.
- Waldichuk, M. 1957. Physical oceanography of the Strait of Georgia, British Columbia. J. Fish. Res. Bd. Can., 14(3): 321-486.
1958. Drift bottle observations in the Strait of Georgia. J. Fish. Res. Bd. Can., 15(5): 1065-1102.
- Waldichuk, M., J.R. Markert, and J.H. Meikle. 1968. Fraser River Estuary, Burrard Inlet, Howe Sound and Malaspina Strait, physical and chemical oceanographic data, 1957-1966. 2 vols. Fish. Res. Bd. Can. Ms. Rept., no. 939.

INDIAN (BURRARD)

Hydrography

1. Surveyed most recently in 1954.
2. Scale of F.S. 2255-S - 1:24,320.
3. Chart number and scale 3435 - 1:24,300.

Sounding Coverage

Very poor bathymetric definition of estuary at this scale.

Tidal Information

<u>Nearest Gauge</u>	<u>Period of Analysis</u>	<u>Year of Analysis</u>
Deep Cove	1 month	1964
Lake Buntzen	1 month	1912

Oceanography

Gilmartin (1962) describes the data record in Indian Arm as "the most complete set of oceanographic data available on a British Columbia fjord". He has "established in some detail the characteristic annual cycle of fjord oceanographic properties". The Indian River influences the estuarine circulation within this inlet as a significant fresh water source. A detailed study of the estuary near the Indian River mouth has not yet been published but the understanding of the whole inlet as an estuarine body of water is much better than average.

Bibliography

- Anon. 1953. British Columbia Inlet Cruises, 1953. Data report no. 3. Inst. Oceanogr., Univ. British Columbia.
1956. Indian Arm, 1956. Data report no. 10. Inst. Oceanogr., Univ. British Columbia.
1957. Indian Arm cruises, 1957. Data report no. 12. Inst. Oceanogr., Univ. British Columbia.
1958. Indian Arm cruises, 1958. Data report no. 14. Inst. Oceanogr., Univ. British Columbia.
1959. Indian Arm cruises, 1959. Data report no. 16. Inst. Oceanogr., Univ. British Columbia.

- Anon. 1960. Indian Arm cruises, 1960. Data report no. 18. Inst. Oceanogr., Univ. British Columbia.
1961. British Columbia inlet cruises, 1961. Data report no. 19. Inst. Oceanogr., Univ. British Columbia.
1962. British Columbia inlet cruises, 1962. Data report no. 21. Inst. Oceanogr., Univ. British Columbia.
1963. British Columbia inlet cruises, 1963. Data report no. 23. Inst. Oceanogr., Univ. British Columbia.
1968. British Columbia inlet cruises, 1968. Data report no. 28. Inst. Oceanogr., Univ. British Columbia.
1969. British Columbia inlets and Pacific cruises, 1969. Data report no. 30. Inst. Oceanogr., Univ. British Columbia.
1970. British Columbia inlets and Pacific cruises, 1970. Data report no. 32. Inst. Oceanogr., Univ. British Columbia.
- Campbell, N.J. 1954. A study of lateral circulation in an inlet. Thesis, Univ. British Columbia.
- Carter, N.M. 1934. Physiography and oceanography of some British Columbia fiords. Proc. Fifth Pacific Science Congress 1933, vol. 4: 721-733.
- Fisheries Research Board of Canada. 1931. Oceanographic data for Burrard Inlet and Indian Arm, 1931. Nanaimo Biol. Sta. Ms.
- Gilmartin, M. 1962. Annual cyclic changes in the physical oceanography of a British Columbia fjord. J. Fish. Res. Bd. Can., 19(5): 921-974.
- Goyette, D.E. _____. Extensive surveys in Burrard Inlet - T/S and DO. Data on file. Environmental Protection Service.
- LaCroix, G.W. 1950. Report on current investigation, Burrard Inlet, for Greater Vancouver Sewerage and Drainage District. Prov. B.C., Poll. Contr. Branch, file no. G-39.
- Lasalle Hydraulic Laboratory Ltd. 1970a. Hydraulic model study of current patterns and velocities in the area of Coal Harbour. Rept. no. NV, 748: 13 p. (unpub.)
- 1970b. Hydraulic model study of the rate of water exchange in the area of Coal Harbour. Report no. NV, 749: 36 p. (unpub.)
- 1970c. Hydraulic model study of the Brockton Point Sewage Outfall flow effect on water quality in the area of Coal Harbour. Rept. no. NV, 750: 30 p. (unpub.)

- Pickard, G.L. 1961. Oceanographic features of inlets in the British Columbia mainland coast. J. Fish. Res. Bd. Can., 18(6): 907-999.
- Stockner, J.G. _____. Indian Arm T/S, DO, Zoopl. and P. Prod. Data on file. Environment Canada, Pacific Environment Institute.
- Swan Wooster CBA. 1970. Burrard Inlet crossing report K4019/1. T.W. Beak Consultants Ltd., Vancouver, B.C.
1970. Report on hydrological studies, stage 2, field observations. Nat. Harbours Bd., Burrard Inlet Crossing Rept., no. 9, vol. 1-6.
- Tabata, S. 1970. A brief oceanographic description of the waters of Burrard Inlet and Indian Arm. Report prepared as background material for the Environmental Impact Study Associated with the Third Burrard Inlet Crossing. Department of Environment, Marine Sciences Directorate.
- Waldichuk, M. 1965. Water exchange in Port Moody, British Columbia, and its effect on waste disposal. J. Fish. Res. Bd. Can., 22(3): 801-822.
- Waldichuk, M., J.R. Markert, and J.H. Meikle. 1968. Fraser River Estuary, Burrard Inlet, Howe Sound and Malaspina Strait, physical and chemical oceanographic data, 1957-1966. 2 vols. Fish. Res. Bd. Can. Ms. Rept., no. 939.

SQUAMISH

Hydrography

1. Surveyed most recently in 1939 small scale.
1930 large scale.
2. Scale of F.S. 2213-S - 1:12,160.
3. Chart number and scale 3586 - 1:37,500.
4. WM. J. STEWART will be carrying out a hydrographic survey of Squamish at a scale of 1:8,000 in May 1973.

Sounding Coverage

Bathymetry in estuary poorly defined at this scale.

Tidal Information

<u>Nearest Gauge</u>	<u>Period of Analysis</u>	<u>Year of Analysis</u>
Squamish	1 year	1961

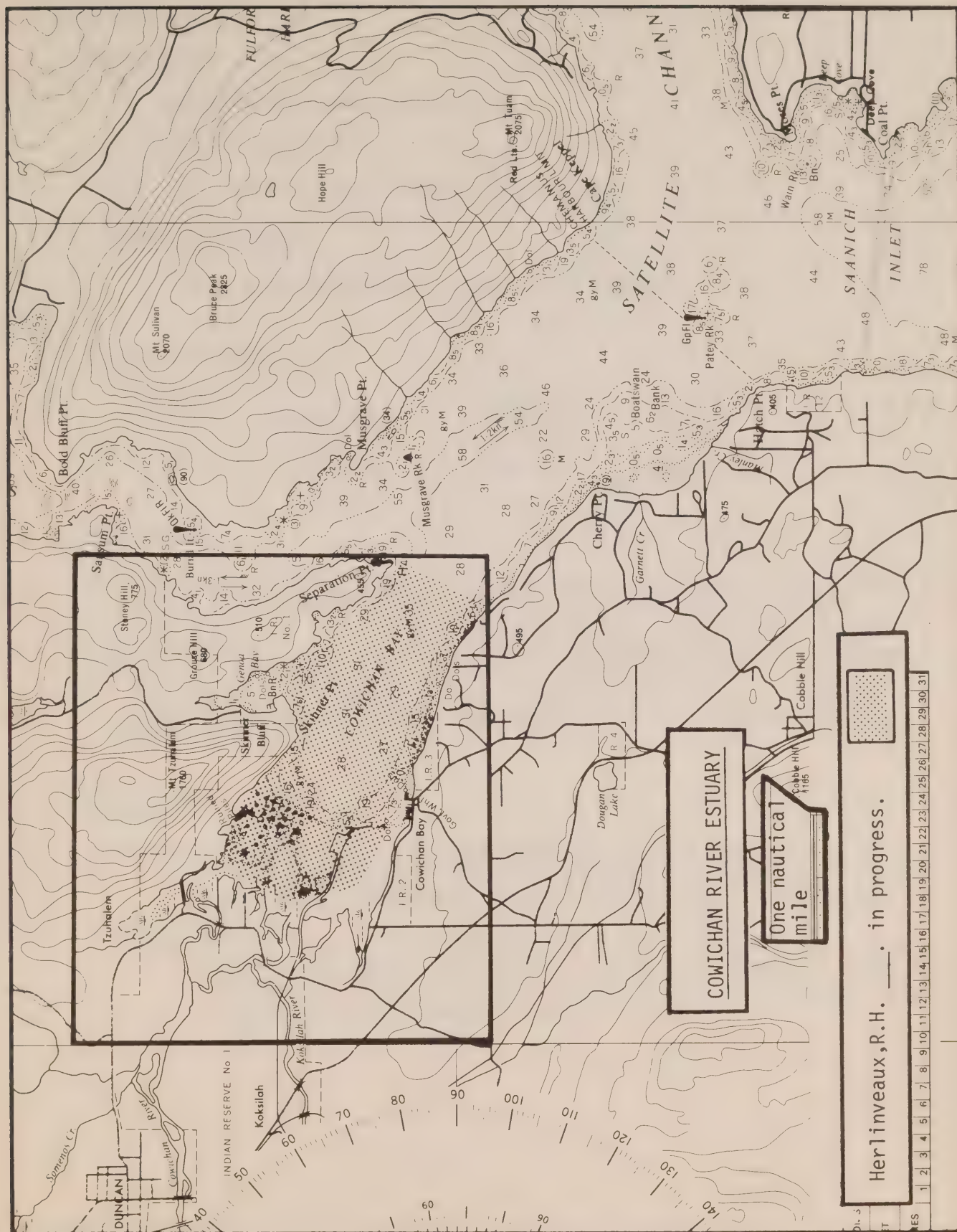
Oceanography

The recent study of the Squamish Estuary in relation to harbour developments, (Dept. of Environment, 1972) provides the first "study in depth" of all facets of estuarine ecology and oceanography on the British Columbia coast. Squamish therefore joins the select group of regions on the Pacific coast with a data base of some substance due to their importance in the industrial economy of the Province of British Columbia.

Bibliography

- Anon. 1957. British Columbia inlet cruises, 1957. Data report no. 11. Inst. Oceanogr., Univ. British Columbia.
1961. British Columbia inlet cruises, 1961. Data report no. 19. Inst. Oceanogr., Univ. British Columbia.
1964. British Columbia and Alaska inlet cruises, 1964. Data report no. 24. Inst. Oceanogr., Univ. British Columbia.
1965. British Columbia and Alaska inlet cruises, 1965. Data report no. 25. Inst. Oceanogr., Univ. British Columbia.
1967. British Columbia inlet cruises, 1967. Data report no. 27. Inst. Oceanogr., Univ. British Columbia.

- Anon. 1968. British Columbia inlet cruises, 1968. Data report no. 28. Inst. Oceanogr., Univ. British Columbia.
1969. British Columbia inlet cruises, 1969. Data report no. 30. Inst. Oceanogr., Univ. British Columbia.
1970. British Columbia inlets and Pacific cruises, 1970. Data report no. 32. Inst. Oceanogr., Univ. British Columbia.
- Carter, N.M. 1934. Physiography and oceanography of some British Columbia fiords. Proc. Fifth Pacific Science Congress 1933, 4: 721-733.
- Department of Environment, Canada. 1972. Effects of existing and proposed industrial development on the aquatic ecosystem of the Squamish Estuary prepared for Federal-Provincial task force on the Squamish Estuary harbour development, Vancouver, B.C.
- Parker, R.R., and B.A. Kask. 1972. First - fourth progress reports on studies of the ecology of the outer Squamish Estuary, 1972. Fish. Res. Bd. Can. Ms. Rept., nos. 1192, 1193, 1194, 1195.
- Pickard, G.L. 1961. Oceanographic features of inlets in the British Columbia mainland coast. J. Fish. Res. Bd. Can., 18(6): 907-999.
- Stockner, J.G. _____. T/S, DO, Zoopl., P. Prod. Data on file. Pacific Environment Institute.
- Tabata, S. 1972. Oceanographic features of Howe Sound, Contribution to Dept. of Environment paper on Squamish Estuary Development.
- Waldichuk, M., J.R. Markert, and J.H. Meikle. 1968. Fraser River Estuary, Burrard Inlet, Howe Sound, and Malaspina Strait, physical and chemical oceanographic data, 1957-1966. Fish. Res. Bd. Can. Ms. Rept., no. 939. 2 vols.
- Waldichuk, M. _____. Howe Sound 26 July-8 Aug., 1971. Data on file. Pacific Environment Institute, W. Vancouver, B.C.



COWICHAN

Hydrography

1. Surveyed most recently in 1960.
2. Scale of F.S. 1177-L - 1:12,160.
3. Chart number and scale 3470 - 1: 18,000.

Sounding Coverage

Fairly good bathymetric definition of estuary.

Tidal Information

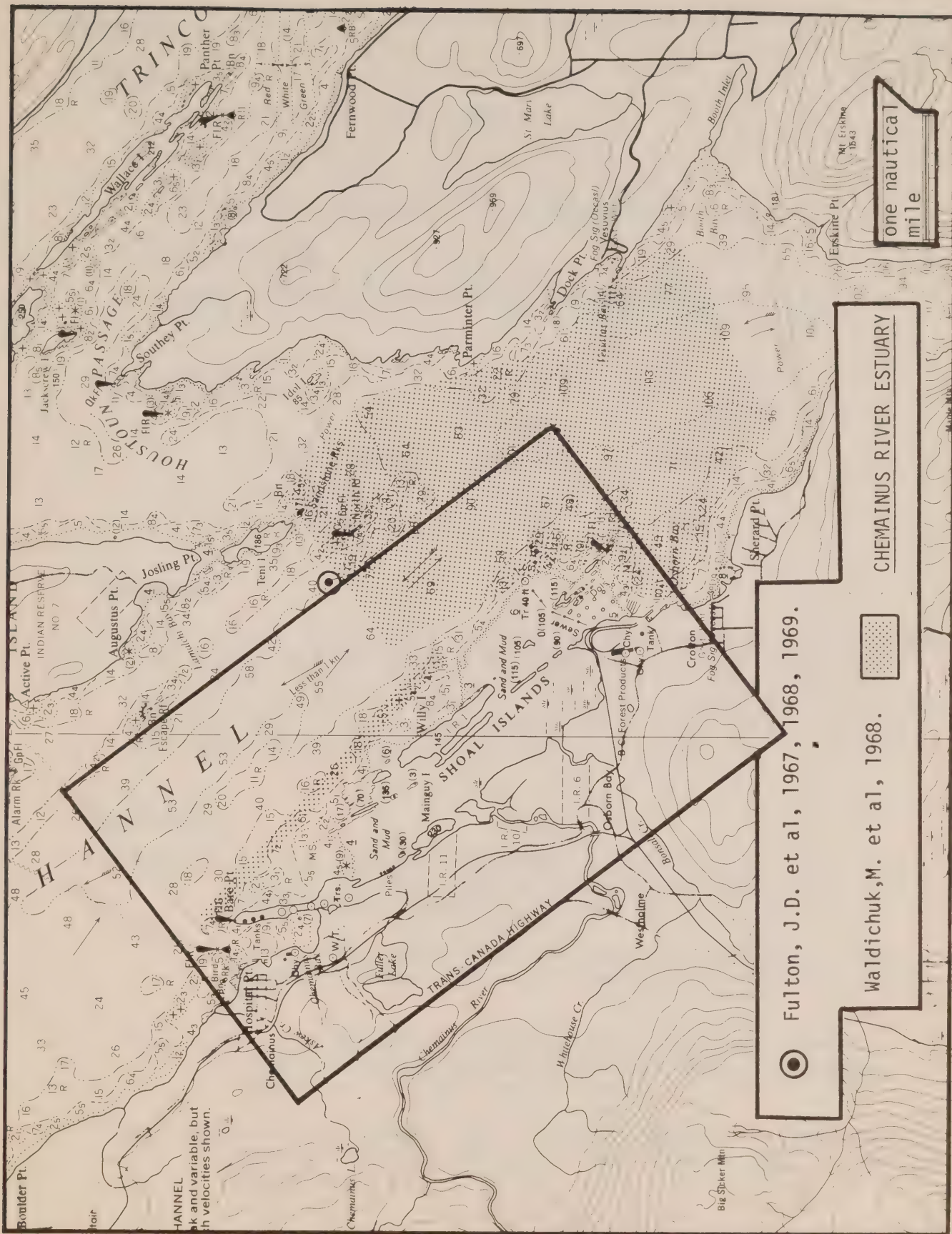
<u>Nearest Gauge</u>	<u>Period of Analysis</u>	<u>Year of Analysis</u>
Cowichan Bay	1 month	1959

Oceanography

Although no studies of the Cowichan Estuary have been published, some surface drift information and temperature/salinity data have been collected within Cowichan Bay and river mouth. (Herlinveaux, personal communication). Surface drift data and temperature/salinity relations were also investigated in conjunction with the chinook and coho project of the Nanaimo Biological Station in the Cowichan Estuary. Sparrow (personal communication) has a manuscript report in progress on these data in his files.

Bibliography

- Herlinveaux, R.H. _____. Oceanographic features of Cowichan Bay - surface movements and temperature/salinity distributions. In progress. Environment Canada, Marine Sciences Directorate.
- Sparrow, R.A.H.* _____. Cowichan Bay and estuary, May-July 1967, April 6-June 14, 1966. T/S profiles and surface currents - with H. Godfrey. Data on file. Nanaimo Biol. Sta.* now with Fish and Wildlife, Province of British Columbia.



CHEMAINUS

Hydrography

1. Surveyed most recently in 1962.
2. Scale of F.S. 1197-S - 1:9,120.
3. Chart number and scale - 3471 - 1:12,000

Sounding Coverage

Fairly recent survey but not too much definition of estuary bathymetry.

Tidal Information

<u>Nearest Gauge</u>	<u>Period of Analysis</u>	<u>Year of Analysis</u>
Chemainus	1 month	1961
Crofton	1 year	1961

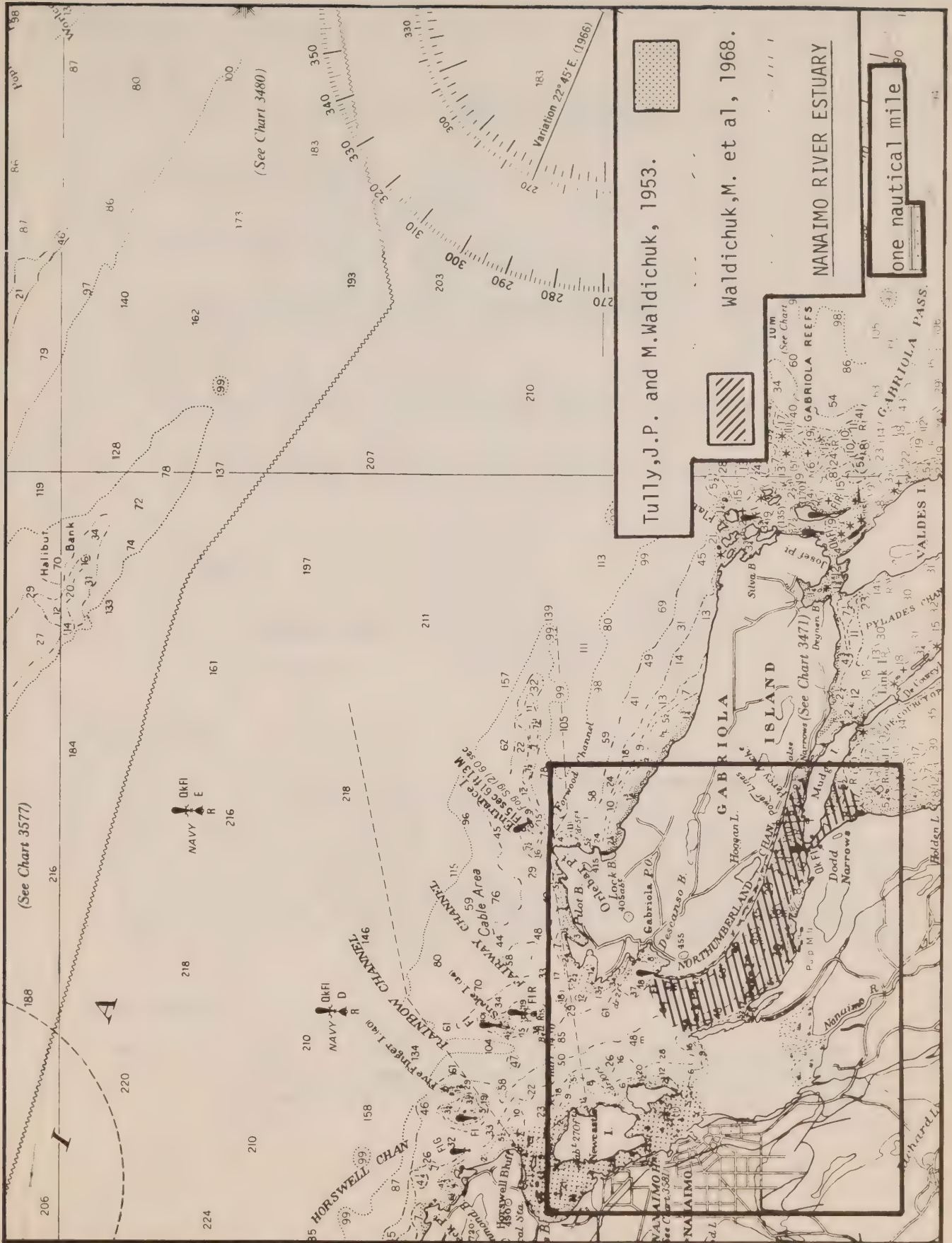
Oceanography

There is again, no published data dealing specifically with the Chemainus River Estuary, but Waldichuk et al (1968) have obtained oceanographic data in Stuart Channel and along the Chemainus River delta front in studying the effects of a pulp mill at Crofton. Fulton et al (1967, 1968, 1969) have collected some information at a repetitive station in mid-channel off the river mouth.

Bibliography

- Fulton, J.D., O.D. Kennedy, K. Stephens, and J. Skelding. 1967. Data record. Physical, chemical and biological data, Strait of Georgia, 1966. Fish. Res. Bd. Can. Ms. Rept., no. 915.
1968. Data record. Physical, chemical and biological data, Strait of Georgia, 1967. Fish. Res. Bd. Can. Ms. Rept., no. 968.
- Fulton, J.D., O.D. Kennedy, J. Skelding, and K. Stephens. 1969. Physical, chemical and biological data, Strait of Georgia, 1968. Fish. Res. Bd. Can. Ms. Rept., no. 1049.
- Pacific Oceanographic Group. 1954. Physical and chemical data record, Strait of Georgia, 1949-1953. Fish. Res. Bd. Can. Ms. Rept., Nanaimo Biol. Sta.

- Waldichuk, M. 1955. Effluent disposal from the proposed pulp mill at Crofton, B.C. Fish. Res. Bd. Can. Prog. Rept. Pacific Coast Sta., no. 102: 6-9.
1958. Summer oceanography in Osborn Bay, B.C. Fish. Res. Bd. Can. Prog. Rept. Pacific Coast Sta., no. 110: 6-12.
1964. Dispersion of Kraft mill effluent from a submarine diffuser in Stuart Channel, British Columbia. J. Fish. Res. Bd. Can., 21(5): 1289-1316.
- Waldichuk, M., J.H. Meikle, and J.R. Markert. 1968. Physical and chemical oceanographic data from the east coast of Vancouver Island, 1954-1966. Fish. Res. Bd. Can. Ms. Rept., no. 989.
- Waldichuk, M. _____. Data on file. Stuart Channel 4-17 Aug., 1969 - 26 July-8 Aug., 1971. Pacific Environment Institute, W. Vancouver, B.C.



Tully, J.P. and M. Waldichuk, 1953.

Waldichuk, M. et al, 1968.

NANAIMO RIVER ESTUARY

one nautical mile

NANAIMO

Hydrography

1. Surveyed most recently in 1965/67 - Estuary
1937 - Harbour
2. Scale of F.S. 1193-L - 1:12,000
1138-L - 1:6,080
3. Chart number and scale 3581 - 1:6,100
3456 - 1:18,000
4. New survey of harbour area scheduled for 1974.

Sounding Coverage

F.S. 1193-L shows low water in the estuary, however no sounding was taken during the years 1965/67.

F.S. 1138-L shows soundings north of this low water line. Soundings acquired years ago.

Tidal Information

<u>Nearest Gauge</u>	<u>Period of Analysis</u>	<u>Year of Analysis</u>
Nanaimo	1 month	1926

Oceanography

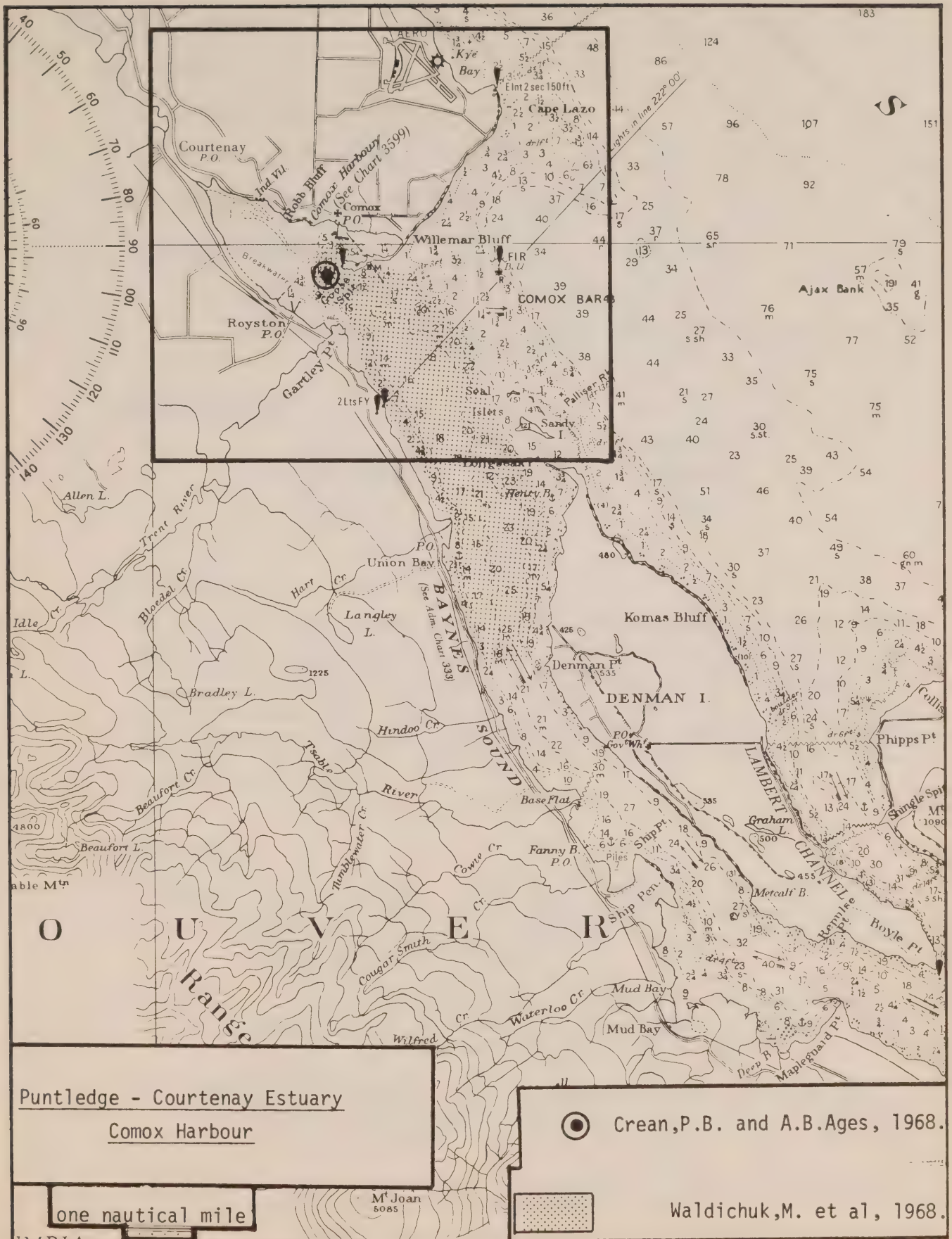
Tully and Waldichuk (1953) produced some surface current information below the delta front of the Nanaimo River Estuary. Waldichuk et al (1968) obtained some data in Northumberland Channel adjacent to the pulp mill established there. The majority of this data is in a restricted channel to the south of the Nanaimo River and not directly related to the estuary. Some temperature/salinity data is on file at the Nanaimo Biological Station. K. Stephens (personal communication). The total volume of data in the Nanaimo Estuary seems to be very small.

Bibliography

Henry, R.F., and T.S. Murty. 1971. Three dimensional circulation in a stratified bay under variable wind-stress. Third Liege Colloquium on Ocean Hydrodynamics, Univ. of Liege, 3-8 May, 1971.

Stephens, K. _____. T/S, DO. Data on file. Nanaimo Biol. Sta.

- Tully, J.P., and M. Waldichuk. 1953. The oceanographic phase of the Nanaimo sewage problem. Pacific Oceanogr. Group Ms., Nanaimo Biol. Sta.
- Waldichuk, M. _____. Departure Bay study, 1968. Ms. report in progress. Pacific Environment Inst., West Vancouver, British Columbia.
- Waldichuk, M., and J.P. Tully. 1953. Pollution study in Nanaimo Harbour. Fish. Res. Bd. Can. Prog. Rept. Pacific Coast Sta., no. 97: 14-17.
- Waldichuk, M., J.H. Meikle, and J.R. Markert. 1968. Physical and chemical oceanographic data from the east coast of Vancouver Island, 1954-1966. Vol. 2. Fish. Res. Bd. Can. Ms. Rept., no. 989.



PUNTLEDGE - COURTENAY

Hydrography

1. Surveyed most recently in 1969.
2. Scale of F.S. 1201-L - 1:10,000
3. Chart number and scale 3599 - 1:10,000.

Sounding Coverage

Bathymetry in estuary good and at a large scale.

This F.S. and Chart used as an example of estuary sounding coverage.

Tidal Information

<u>Nearest Gauge</u>	<u>Period of Analysis</u>	<u>Year of Analysis</u>
Comox	1 year	1968

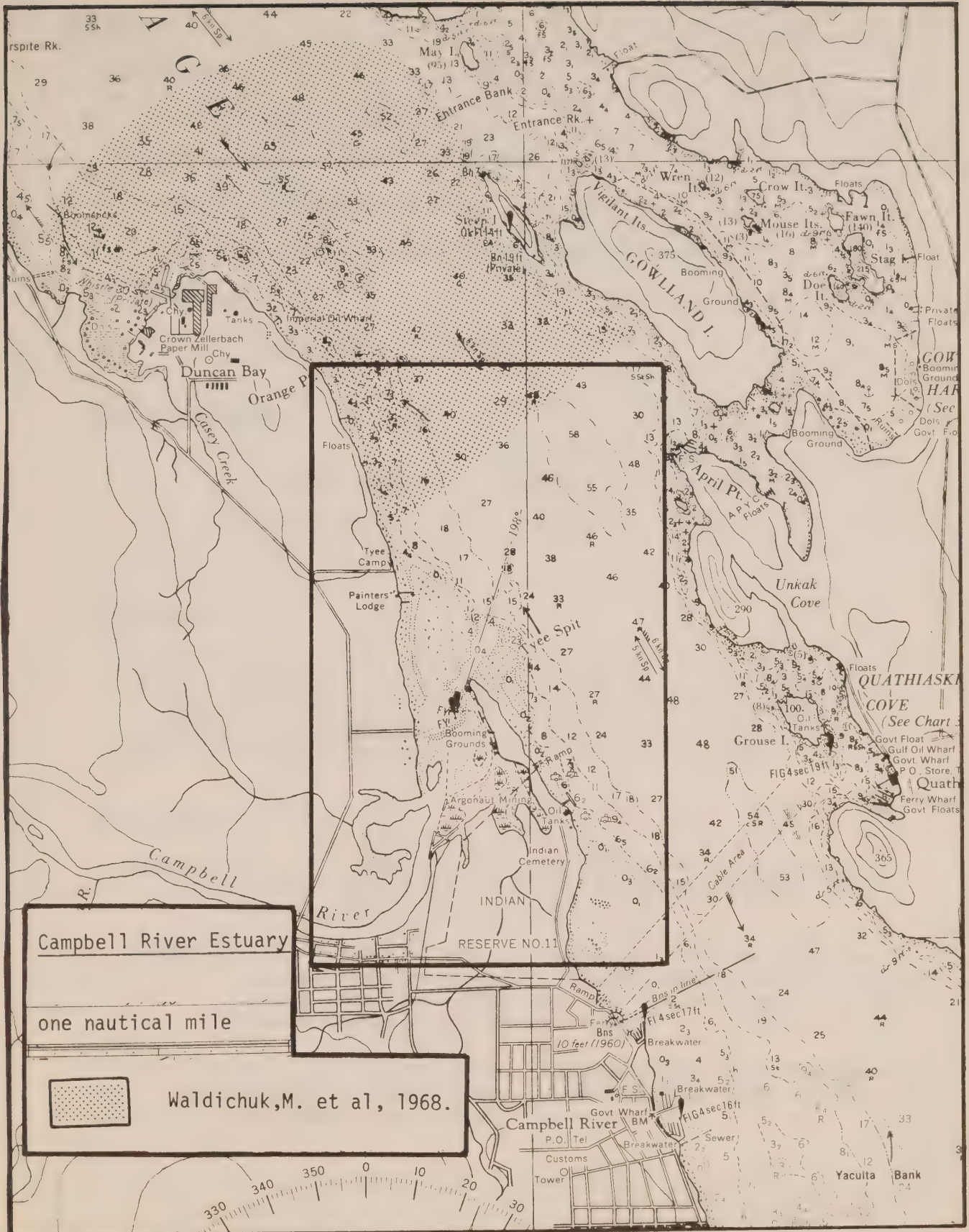
Oceanography

Oceanographic data by Waldichuk et al (1968) and Crean and Ages (1968) was collected within Comox Harbour. The Pollution Control Branch of the Province of British Columbia is operating an investigation of oceanographic conditions for water quality evaluation. (Webster, personal communication). There has been some work in the Puntledge River in connection with dam construction which might bear upon the estuarine situation. The oceanographic information does not extend upstream beyond the delta front.

Bibliography

- Crean, P.B., and A.B. Ages. 1968. Oceanographic records from twelve cruises in the Strait of Georgia and Juan de Fuca Strait. Dept. Energy, Mines and Resources Ms. Rept., Marine Sciences Branch, Victoria. 5 vols.
- Waldichuk, M. 1962. Oceanographic characteristics of Comox Harbour and approaches in relation to sea disposal of sewage. Fish. Res. Bd. Can., Nanaimo Biol. Sta.: 49 p. Mimeo.
- Waldichuk, M., J.H. Meikle, and J.R. Markert. 1968. Physical and chemical oceanographic data from the east coast of Vancouver Island, 1954-1966. Fish. Res. Bd. Can., Ms. Rept., no. 989.
- Webster, I. _____. T/S, DO for water quality. Prov. British Columbia Poll. Contr. Br. Data on file.

Waldichuk, M. _____. Baynes Sound - Comox Harbour, data on file -
4-17 Aug., 1969 and 26 July-8 Aug., 1971. Pacific Environment
Institute, W. Vancouver, B.C.



CAMPBELL

Hydrography

1. Surveyed most recently in 1950.
2. Scale of F.S. 1164-L - 1:18,240.
3. Chart number and scale 3556 - 1:18,247.
4. Patch on Chart 3556 recently surveyed by revisory surveys 1972.

Sounding Coverage

Fairly poor estuary definition at this scale.

Tidal Information

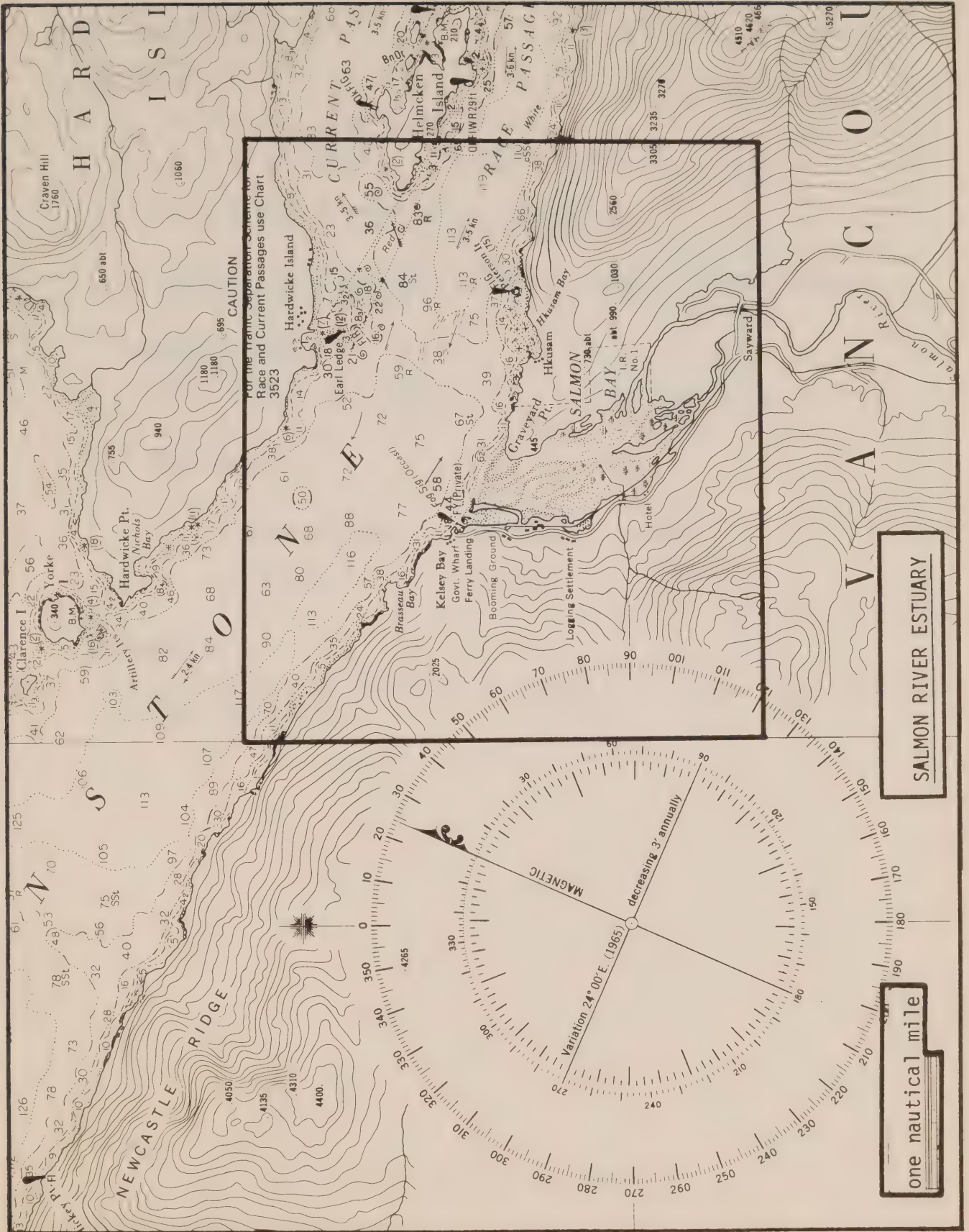
<u>Nearest Gauge</u>	<u>Period of Analysis</u>	<u>Year of Analysis</u>
Campbell River (permanent gauge)	1 year	1967

Oceanography

No information directly related to the Campbell River Estuary has come to light. Huggett (personal communication) has, on file, the results of some drift pole current studies in Discovery Passage. Waldichuk et al (1968) has provided some data for the area north of Campbell River from studies in Duncan Bay adjacent to the Elk Falls pulp mill.

Bibliography

- Huggett, W.S. _____. Drift pole current measurements in Discovery Passage, 1966. Data on file. Environment Canada, Marine Sciences Directorate, Victoria.
- Waldichuk, M., J.H. Meikle, and J.R. Markert. 1968. Physical and chemical oceanographic data from the east coast of Vancouver Island, 1954-1966. Fish. Res. Bd. Can. Ms. Rept., no. 989. (Several stations off the river mouth.)
- Waldichuk, M. _____. Alberni Inlet, Muchalat Inlet - Quatsino Sound and Discovery Passage Survey, 19 Aug.-1 Sept., 1968. Pacific Environment Institute, W. Vancouver, B.C.



SALMON (KELSEY BAY)

Hydrography

1. Surveyed most recently in 1938.
2. Scale of F.S. 2215-L - 1:24,320.
3. Chart scale and number 3567 - 1:37,500
3523 - 1:25,000
4. Numerous revisory surveys and patches from engineering drawings since original surveys.

Sounding Coverage

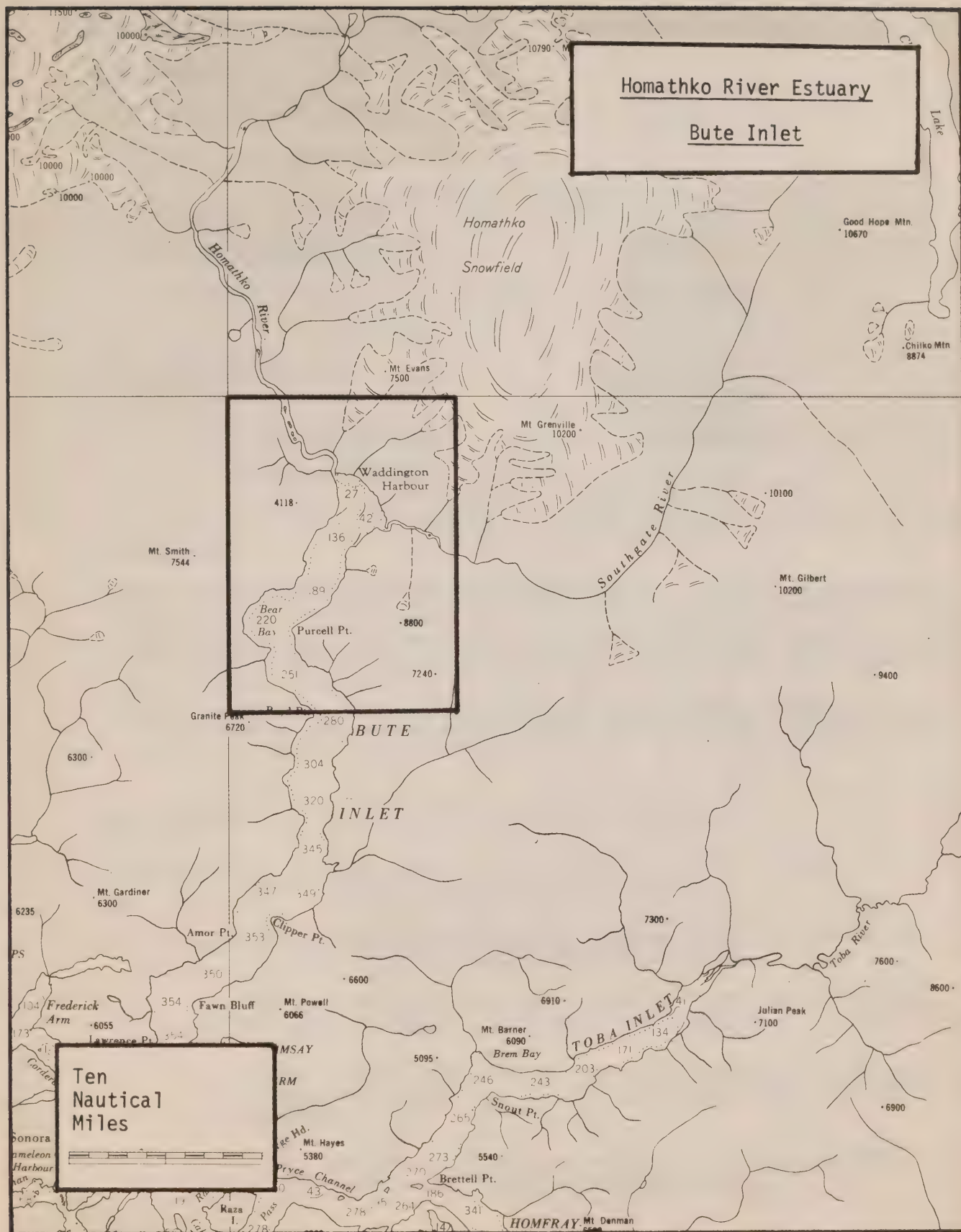
Survey at this scale does not show much of the estuary bathymetry.

Tidal Information

<u>Nearest Gauge</u>	<u>Period of Analysis</u>	<u>Year of Analysis</u>
Kelsey Bay	1 month	1916

Oceanography

No oceanographic information in the region of the Salmon River Estuary has been discovered.



HOMATHKO (BUTE)

Hydrography

1. Surveyed most recently in 1957.
2. Scale of F.S. 2252-L - 1:36,480.
3. Chart scale and number 3524 - 1:75,000.

Sounding Coverage

Bathymetry not too well defined at the charted scale.

Tidal Information

<u>Nearest Gauge</u>	<u>Period of Analysis</u>	<u>Year of Analysis</u>
Waddington Harbour	1 month	1909

Oceanography

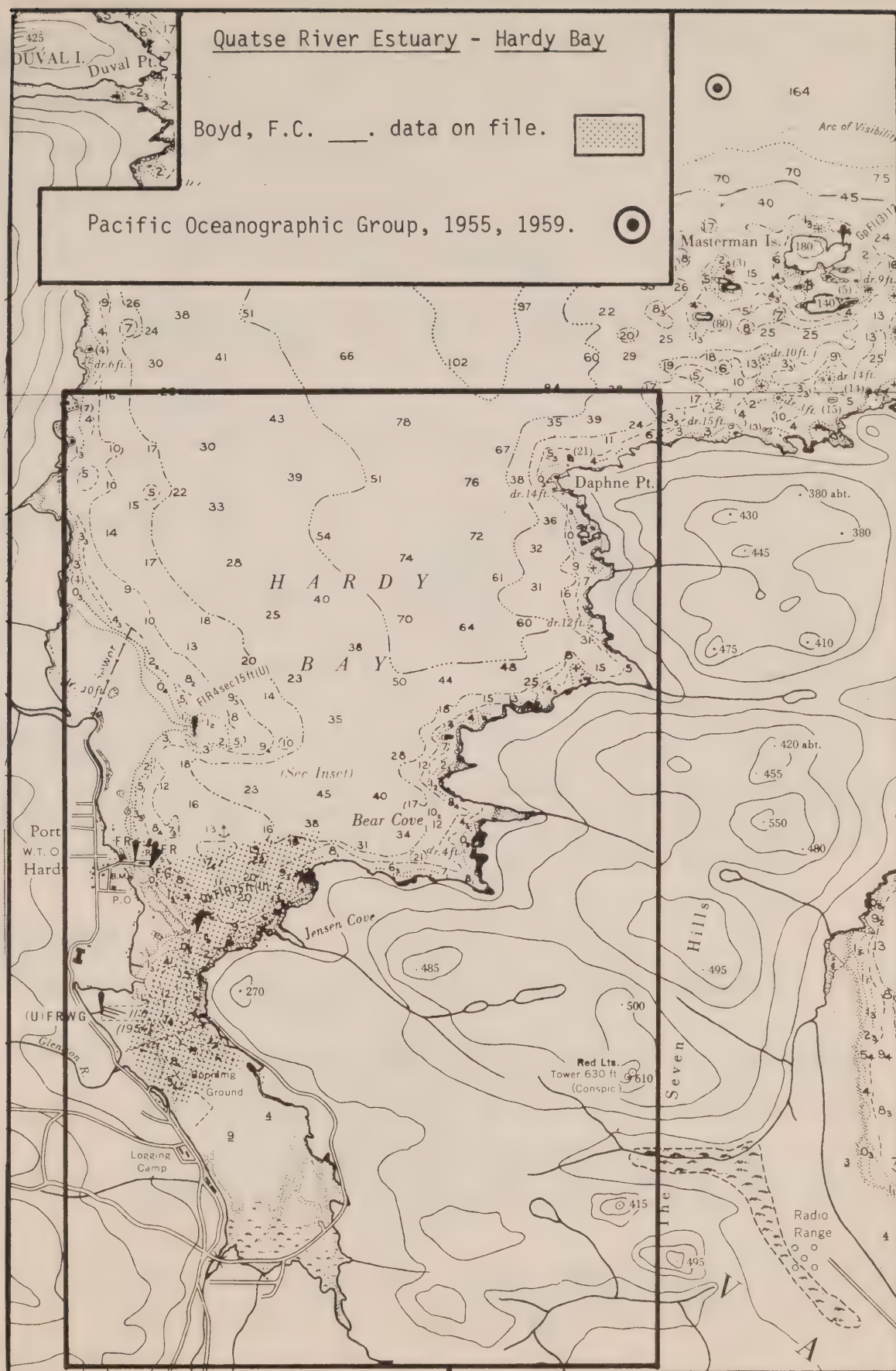
Many oceanographic stations have been occupied in Bute Inlet by personnel from the Institute of Oceanography, University of British Columbia. The repetitively sampled station (no. 8) at the head of Bute Inlet in Waddington Harbour is the closest station in this series to the Homathko River mouth. This sampling programme was continued from 1951 to the present, providing a good time series of observations. Tabata and Pickard (1957) have published a study of the oceanography of Bute Inlet considering the whole inlet to be the estuary of the Homathko River.

Bibliography

- Anon. 1951. British Columbia inlet study, 1951. Data report, no. 1. Inst. Oceanogr., Univ. British Columbia.
1952. British Columbia inlet cruise, 1952. Data report no. 2. Inst. Oceanogr., Univ. British Columbia.
1953. British Columbia inlet cruises, 1953. Data report no. 3. Inst. Oceanogr., Univ. British Columbia.
1953. C.G.M.V. Cancolim II survey of the British Columbia coast. Data report no. 4. Inst. Oceanogr., Univ. British Columbia.
1954. British Columbia inlet cruise, 1954. Data report no. 6. Inst. Oceanogr., Univ. British Columbia.

- Anon. 1955. British Columbia inlet cruise, 1955. Data report no. 7. Inst. Oceanogr., Univ. British Columbia.
1956. British Columbia inlet cruise, 1956. Data report no. 8. Inst. Oceanogr., Univ. British Columbia.
1957. British Columbia inlet cruise, 1957. Data report no. 11. Inst. Oceanogr., Univ. British Columbia.
1958. British Columbia inlet cruise, 1958. Data report no. 13. Inst. Oceanogr., Univ. British Columbia.
1959. British Columbia inlet cruise, 1959. Data report no. 15. Inst. Oceanogr., Univ. British Columbia.
1960. British Columbia inlet cruise, 1960. Data report no. 17. Inst. Oceanogr., Univ. British Columbia.
1961. British Columbia inlet cruise, 1961. Data report no. 19. Inst. Oceanogr., Univ. British Columbia.
1962. British Columbia inlet cruise, 1962. Data report no. 21. Inst. Oceanogr., Univ. British Columbia.
1964. British Columbia and Alaska inlet cruises, 1964. Data report no. 24. Inst. Oceanogr., Univ. British Columbia.
1965. British Columbia and Alaska inlet cruises, 1965. Data report no. 25. Inst. Oceanogr., Univ. British Columbia.
1966. British Columbia and Alaska inlets and Pacific cruises, 1966. Data report no. 26. Inst. Oceanogr., Univ. British Columbia.
1967. British Columbia inlet cruises, 1967. Data report no. 27. Inst. Oceanogr., Univ. British Columbia.
1968. British Columbia inlet cruises, 1968. Data report no. 28. Inst. Oceanogr., Univ. British Columbia.
1969. British Columbia inlets and Pacific cruises, 1969. Data report no. 30. Inst. Oceanogr., Univ. British Columbia.
1970. British Columbia inlets and Pacific cruises, 1970. Data report no. 32. Inst. Oceanogr., Univ. British Columbia.
- Kirsch, M. 1956. Ionic ratios of some of the major components in river-diluted sea water in Bute and Knight Inlets, British Columbia. J. Fish. Res. Bd. Can., 13(3): 273-289.
- Pickard, G.L., and L.F. Giovando. 1960. Some observations of turbidity in British Columbia inlets. Limnol. Oceanogr., 5(2): 62-70.

- Stockner, J.G. _____. T/S, DO, Zoopl., P. Prod., Bute Inlet. Data on file. Pacific Environment Institute.
- Tabata, S., and G.L. Pickard, 1957. The physical oceanography of Bute Inlet, British Columbia. J. Fish. Res. Bd. Can., 14(4): 487-520.
- Trites, R.W. 1955. A study of the oceanographic structure in British Columbia inlets and some of the determining factors. Thesis, Univ. British Columbia.



QUATSE (PORT HARDY)

Hydrography

1. Surveyed most recently in 1942.
2. Scale of F.S. 1152-L - 1:12,160.
3. Chart number and scale - 3572 - 1:37,500
Insert - 1:12,200
4. Numerous corrections to chart from revisions and public works plans since original survey.

Sounding Coverage

Bathymetry not well defined in estuary.

Tidal Information

<u>Nearest Gauge</u>	<u>Period of Analysis</u>	<u>Year of Analysis</u>
Port Hardy (permanent gauge)	1 year	1970

Oceanography

The 1971 float and dye studies (Boyd, personal communication) in the Quatse River Estuary appear to be the only work available inside Hardy Bay. The study was initiated as a result of the proposal by Dist. of Port Hardy to establish a sewer outfall at the head of Hardy Bay.

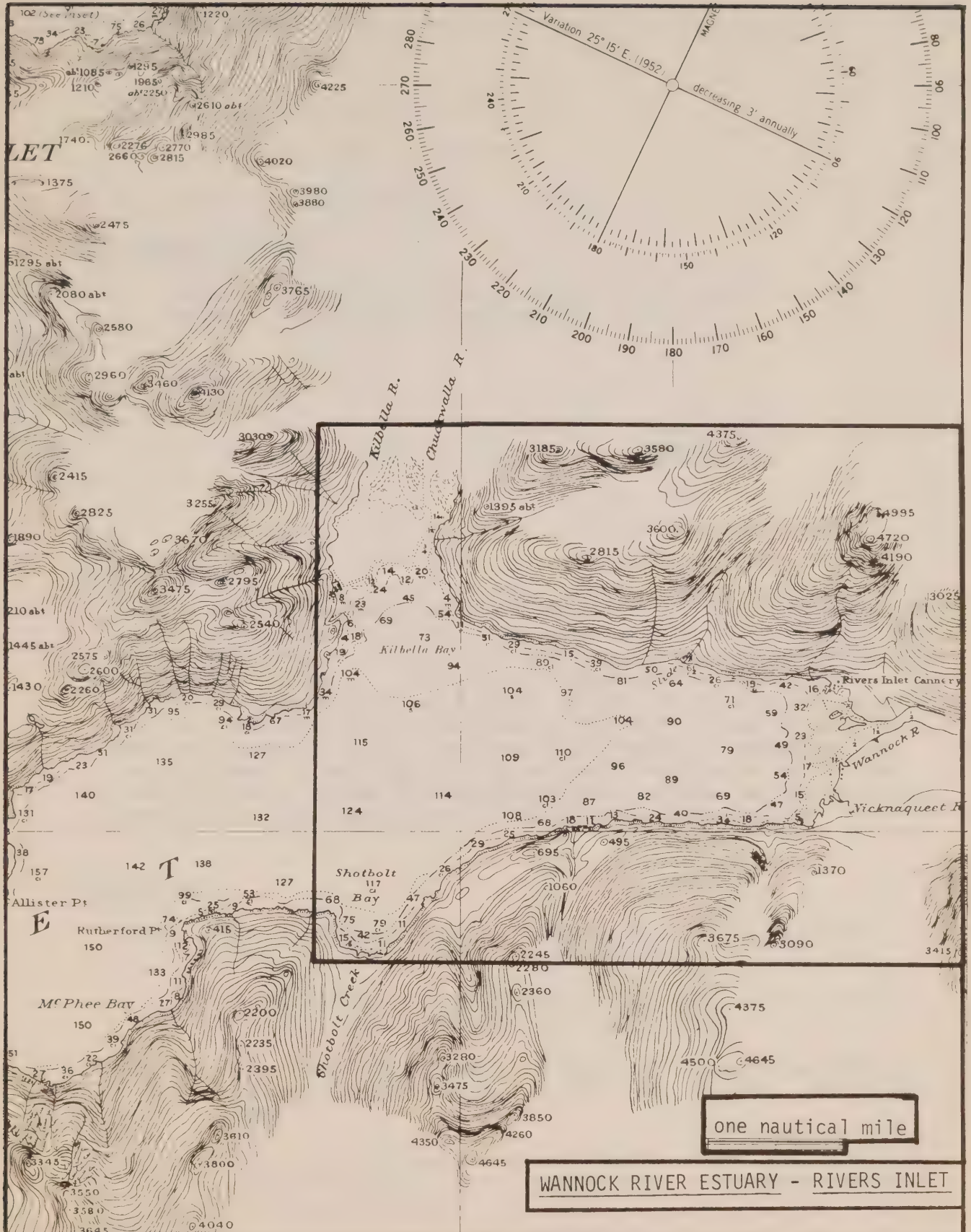
Bibliography

Boyd, F.C. _____. Float studies in Hardy Bay, 1971. Data on file.
Fisheries Service.

Pacific Oceanographic Group. 1955. Physical and chemical data record, Hecate Project, 1954. Queen Charlotte Sound, Hecate Strait, Dixon Entrance. Fish. Res. Bd. Can. Ms., Nanaimo Biol. Sta.

1959. Physical and chemical data record, Coastal Seaways Project, March 31-April 22, 1959. Fish. Res. Bd. Can. Ms. Rept. OL, no. 47. (1 station, mouth of Hardy Bay.)

1959. Oceanographic data record, Coastal Seaways Project, June 8-July 1, 1959. Fish. Res. Bd. Can. Ms, Rept. OL, no. 52. (1 station, mouth of Hardy Bay.)



WANNOCK (RIVERS INLET)

Hydrography

1. Surveyed most recently in 1936.
2. Scale of F.S. 4422-L - 1:36,480.
3. Chart scale and number 3778 - 1:73,600.

Sounding Coverage

Bathymetry in estuary not well defined at this scale. Rather ancient. Few revisions since original survey.

Tidal Information

<u>Nearest Gauge</u>	<u>Period of Analysis</u>	<u>Year of Analysis</u>
Wadhams	1 year	1910

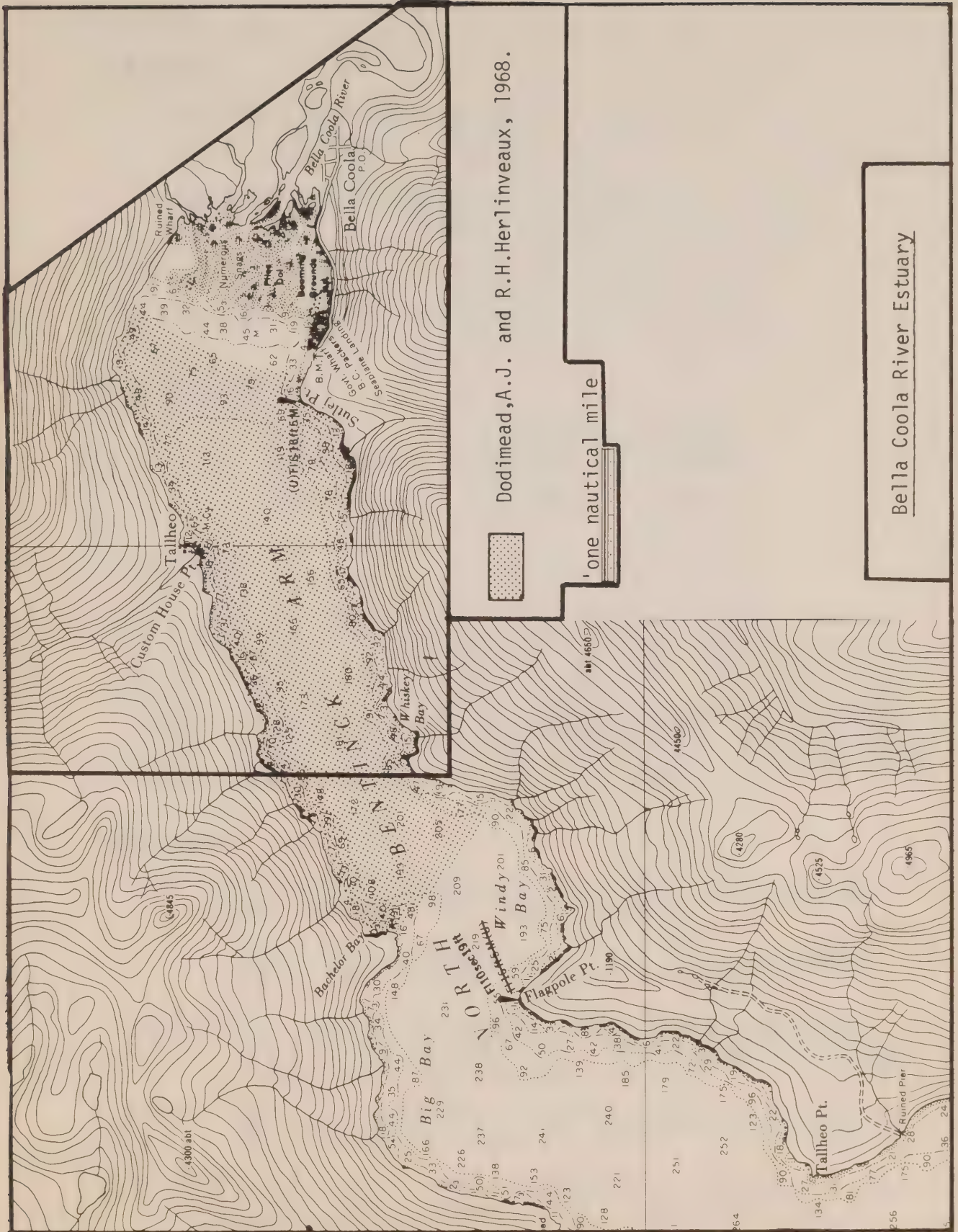
Oceanography

Data in Rivers Inlet adjacent to the Wannock River seems extremely sparse considering this river's importance as a salmon producing source. Fisheries studies in the river and above in Owikeno Lake have been continuing for many years. Echo soundings have been collected almost daily from 1968-1972 and returns interfering with fish counting have been attributed to density structure in the water column (Wood, F.E.A., personal communication). Some temperature/salinity information was obtained when the echo sounding interference was studied but may have been discarded. Aerial photography of plume patterns in the inlet were undertaken to investigate gillnet location and effectiveness.

Bibliography

- Anon. 1951. British Columbia inlet study, 1951. Data report no. 1. Inst. Oceanogr., Univ. British Columbia.
1956. British Columbia inlet cruise, 1956. Data report no. 8. Inst. Oceanogr., Univ. British Columbia.
- Pickard, G.L. 1961. Oceanographic features of inlets in the British Columbia mainland coast. J. Fish. Res. Bd. Can., 18(6): 907-999.
- Wood, F.E.A. _____. Density structure interpreted from echo soundings 1968-1972 approx. daily. Data on file. Fisheries Service, Environment Canada.

Schutes, D. _____. Current patterns from aerial photos of river plume.
Data on file. Fisheries Service, Environment Canada.



BELLA COOLA

Hydrography

1. Surveyed most recently in 1956.
2. Scale of F.S. 4495-S - 1:18,240.
3. Chart number and scale 3730 - 1:75,000
Wharf - 1:2,500

Sounding Coverage

Bathymetry good at a good scale.

Tidal Information

<u>Nearest Gauge</u>	<u>Period of Analysis</u>	<u>Year of Analysis</u>
Bella Coola	1 year	1966

Oceanography

Oceanographic information in the Bella Coola Estuary does not extend above the delta front. Dodimead and Herlinveaux (1968) discuss the region immediately below the river but the bulk of their data is further down the channel, in North Bentinck Arm and in other reaches of this inlet. Goyette (personal communication) reports data on file including temperature/salinity and dissolved oxygen from one survey. The data available cannot adequately portray the variability of oceanographic parameters in the Bella Coola River mouth.

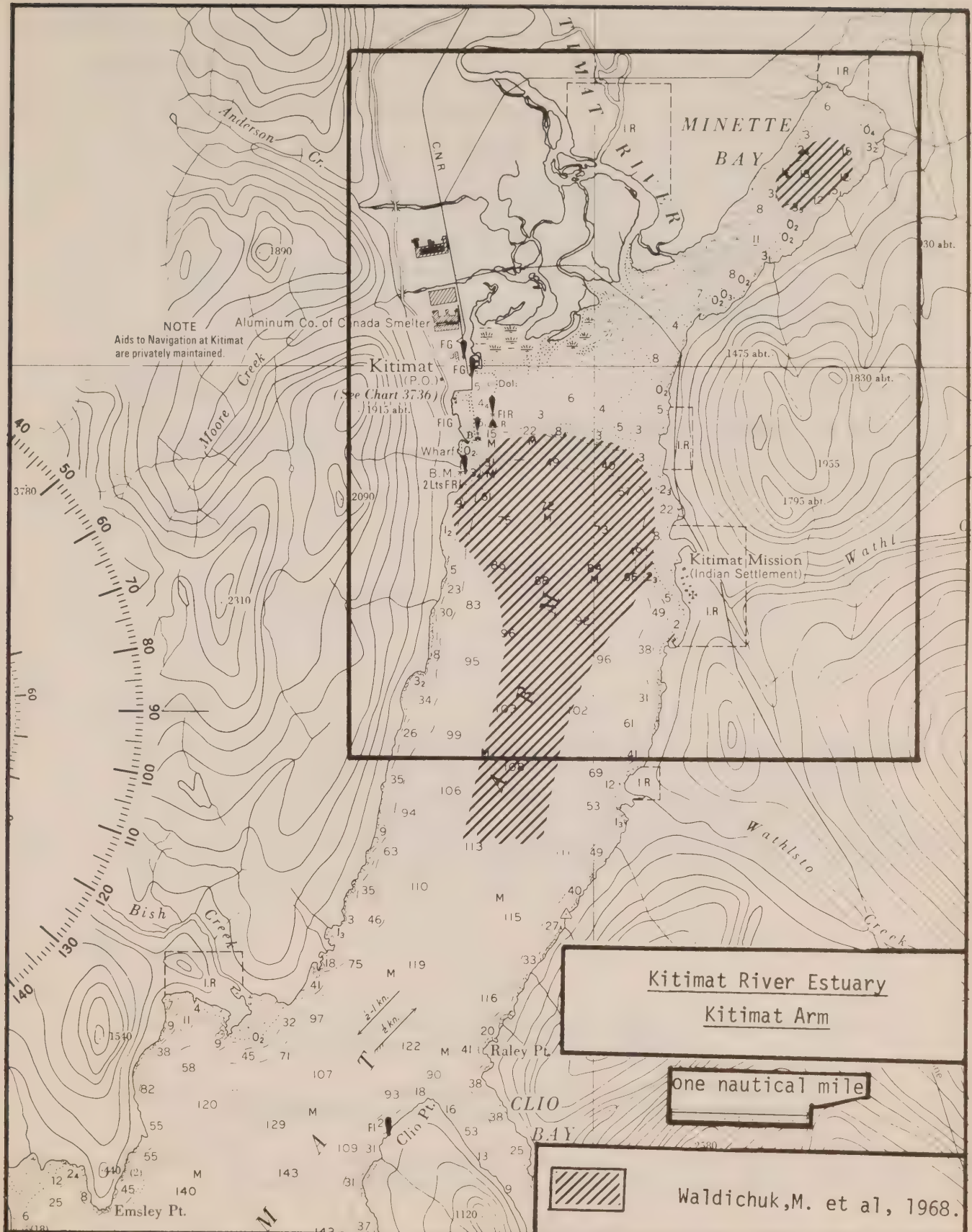
Bibliography

- Anon. 1951. British Columbia inlet study, 1951. Data report no. 1. Inst. Oceanogr., Univ. British Columbia.
1956. British Columbia inlet cruise, 1956. Data report no. 8. Inst. Oceanogr., Univ. British Columbia.
- Dodimead, A.J., and R.H. Herlinveaux. 1968. Some oceanographic features of the waters of the central British Columbia coast. Fish. Res. Bd. Can. Tech. Rept., no. 70.
- Goyette, D.E. _____. One survey T/S and DO. Data on file. Environmental Protection Service.
- Herlinveaux, R.H. 1968. Drift card releases and recoveries in Burke Channel, British Columbia, 1967. Fish. Res. Bd. Can. Ms. Rept., no. 970.

Herlinveaux, R.H. _____. Some oceanographic features of a British Columbia inlet, Burke Channel, 1966-1967. In progress. Environment Canada, Marine Sciences Directorate.

_____. Surface water movements in a central British Columbia inlet. In progress. Environment Canada, Marine Sciences Directorate.

Pickard, G.L. 1961. Oceanographic features of inlets in the British Columbia mainland coast. J. Fish. Res. Bd. Can., 18(6): 907-999.



KITIMAT

Hydrography

1. Surveyed most recently in 1952.
2. Scale of F.S. 3323-S - 1:12,160.
3. Chart scale and number 3736 - 1:12,165.
4. Corrections to Chart 3736, as far as can be determined have all come from various plans and dredge surveys.
5. No revisions or further hydrography has been gathered since original survey.

Sounding Coverage

Bathymetry in estuary is good though construction additions to mills etc. have altered original western quarter.

Tidal Information

<u>Nearest Gauge</u>	<u>Period of Analysis</u>	<u>Year of Analysis</u>
Kitimat	1 year	1953

Oceanography

Like many others, the Kitimat River Estuary remains largely unstudied. Waldichuk et al (1968) have collected four series of oceanographic survey data in connection with the pulp mill established at the head of Kitimat Arm. The Environmental Protection Service has undertaken two surveys of temperature/salinity and dissolved oxygen, also connected with the pulp mill. The University of British Columbia has only one data record with information in this inlet.

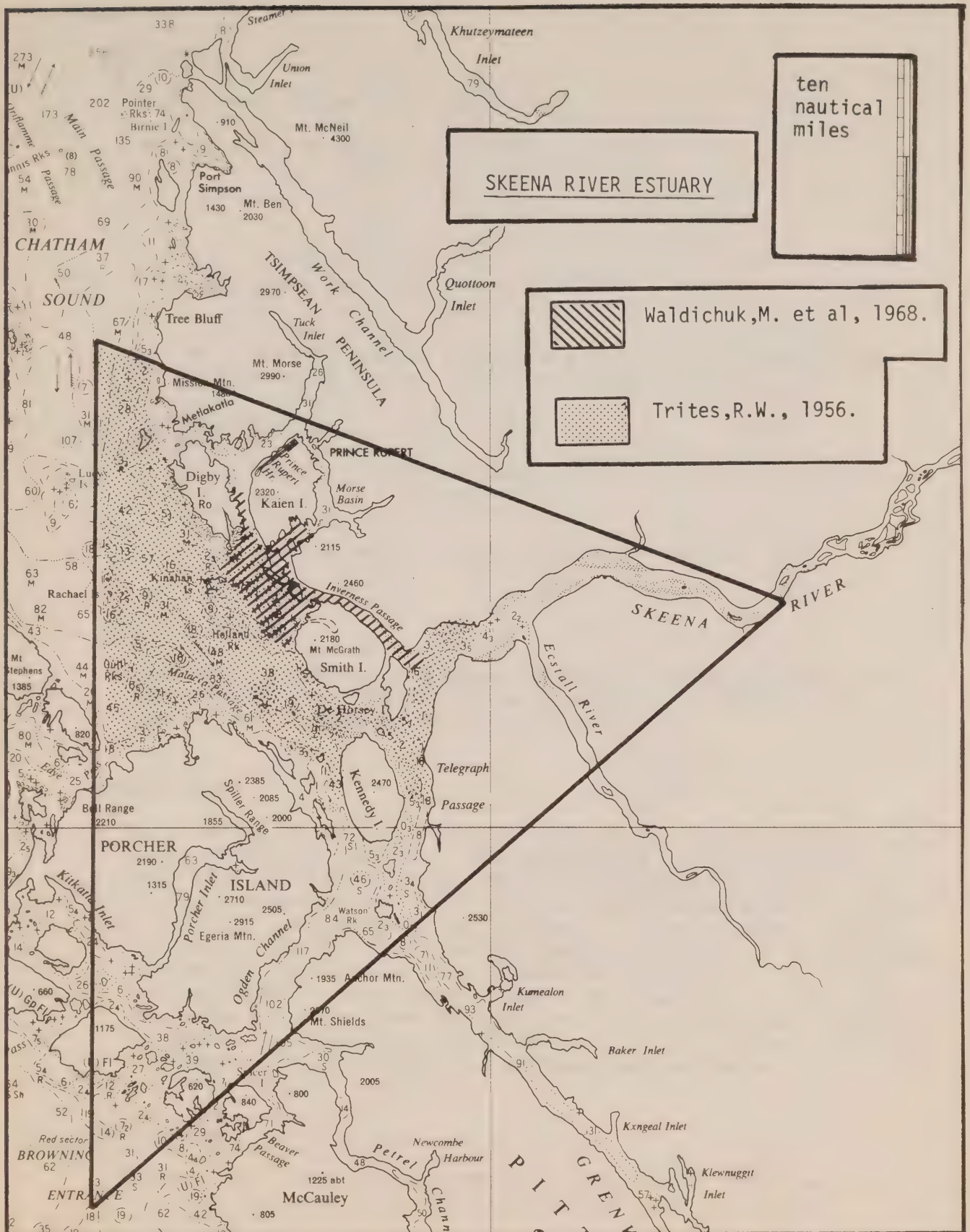
Bibliography

- Anon. 1951. British Columbia inlet study, 1951. Data report no. 1. Inst. Oceanogr., Univ. British Columbia.
- Goyette, D.E. _____. Two surveys of T/S and DO in Kitimat Arm. Environmental Protection Service. Data on file.
- Pickard, G.L. 1961. Oceanographic features of inlets in the British Columbia mainland coast. J. Fish. Res. Bd. Can., 18(6): 907-999.

Waldichuk, M., J.R. Markert, and J.H. Meikle. 1968. Physical and chemical oceanographic data from the west coast of Vancouver Island and the northern British Columbia coast, 1957-1967. Fish. Res. Bd. Can. Ms. Rept., no. 990.

Waldichuk, M. _____. Fisher Channel - Cousins Inlet, Douglas Channel - Kitimat Arm and Prince Rupert area oceanographic surveys, 15-28 Sept., 1969. Pacific Environment Institute, W. Vancouver, B.C.

_____. Ocean Falls, Kitimat and Prince Rupert, 17-30 July, 1972. Pacific Environment Institute, W. Vancouver, B.C.



SKEENA

Hydrography

1. Surveyed most recently in 1949.
2. Scale of F.S. 3318-L - 1:18,240) 1949
3317-L - 1:18,240)

3301-L - 1:24,320) 1914
3302-L - 1:24,320)
3. Chart number and scale 3756 - 1:23,100
3713 - 1:31,700
4. WM. J. STEWART will be conducting a hydrographic survey in the Kennedy Island area at a scale of 1:30,000 in 1973.

Sounding Coverage

3318-L and 3317-L - Good definition of river and estuary but now 24 years old.

3301-L)
3302-L) Good definition of river but now 59 years old.

Tidal Information

Tide gauge stations were operated for several months in 1949 at Khyex Point and Kwinitsa. Gauge stations were previously operated at Claxton, Port Essington, and in the Ecstall River.

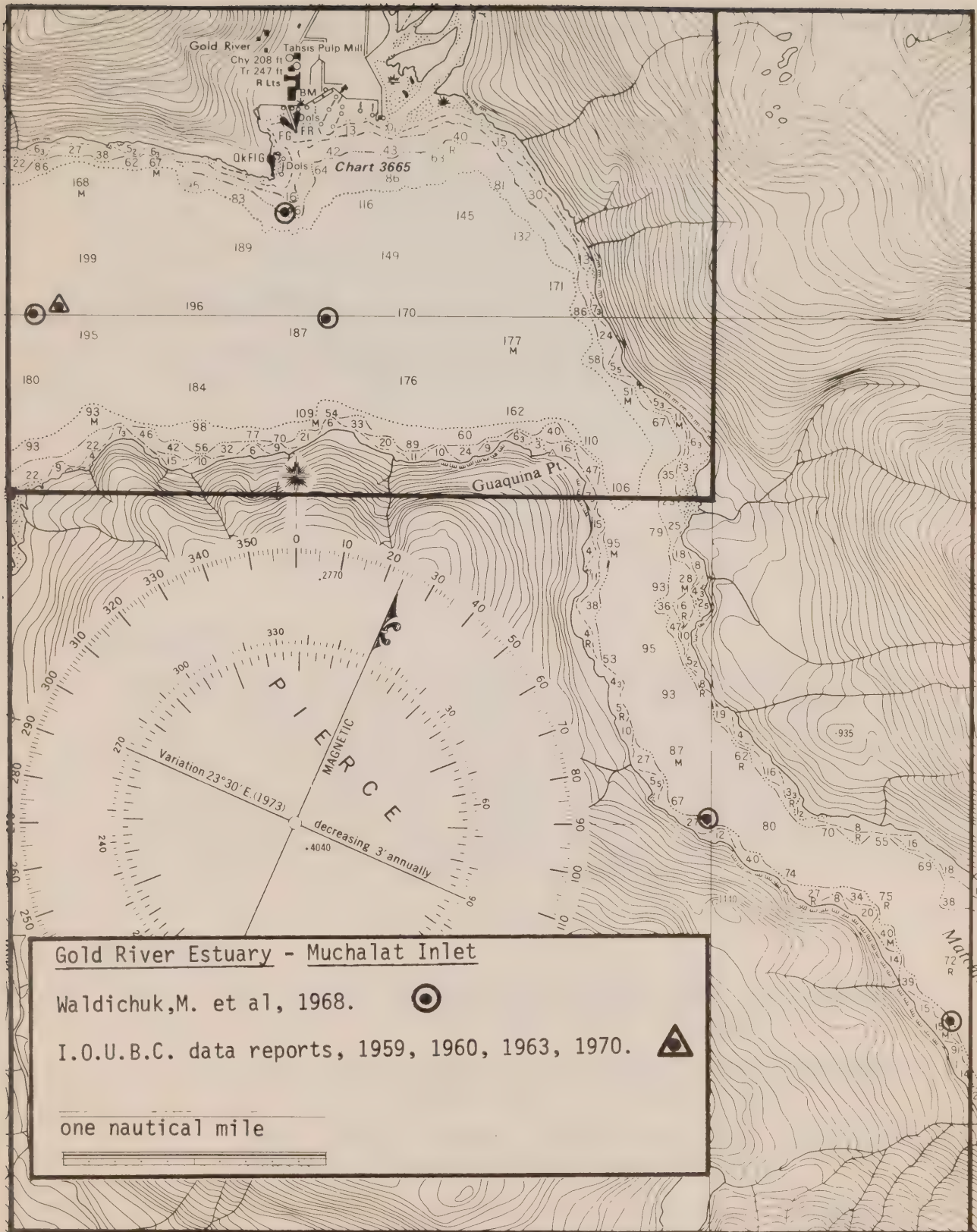
Oceanography

There is little oceanographic information in the shallow inshore region of the Skeena River Estuary. The influence of Skeena River water extends some distance offshore. The work of Cameron (1948) and Trites (1956) is concerned with fresh water entering Chatham Sound. Waldichuk et al (1968) studied the Wainwright Basin - Porpoise Harbour area in relation to pulp mill pollution and took several stations in the Skeena River mouth. The bulk of this information refers to the restricted passages north of the estuary. Higgins and Schouwenburg (1973), in a continuing programme, have obtained some temperature/salinity data in the estuary in conjunction with Fisheries studies. The Hecate project is a source of considerable data offshore from the Skeena River.

Bibliography

Cameron, W.M. 1948. Fresh water in Chatham Sound. Fish. Res. Bd. Can. Prog. Rept. Pacific Coast Sta., no. 76: 71-75.

- Herlinveaux, R.H. _____. Time series T/S data on file by W.M. Cameron. 1948. Environment Canada, Marine Sciences Directorate.
- Higgins, R.J., and W.J. Schouwenburg. 1973. Biological assessment of fish utilization of the Skeena River Estuary with specific reference to port development in Prince Rupert. Fish. and Marine Service Tech. Rept., 1973-1.
- Mackay, B.S. 1954. Tidal current observations in Hecate Strait. J. Fish. Res. Bd. Can., 11(1): 48-56.
- Pacific Oceanographic Group. 1955a. Physical and chemical data record, Hecate Project, 1954. Nanaimo Biol. Sta. Ms.
- 1955b. Data record. Current measurements, Hecate Project, 1954. Nanaimo Biol. Sta. Ms.
- 1955c. Physical and chemical data record, Hecate Project, with appendix 1, current observations, 1955. Nanaimo Biol. Sta. Ms.
1956. Physical and chemical data record, Dixon Entrance, Hecate Strait and Queen Charlotte Sound, 1934, 1937, 1938, 1951. Nanaimo Biol. Sta. Ms.
- Trites, R.W. 1956. The oceanography of Chatham Sound, British Columbia. J. Fish. Res. Bd. Can., 13(3): 385-434.
- Waldichuk, M., J.R. Markert, and J.H. Meikle. 1968. Physical and chemical oceanographic data from the west coast of Vancouver Island and the northern British Columbia coast. Fish. Res. Bd. Can. Ms. Rept., no. 990.
- Waldichuk, M. _____. Unpublished data record. Oceanographic studies in Prince Rupert area, July-August, 1967. Pacific Environment Institute, W. Vancouver, B.C.
- _____. Fisher Channel - Cousins Inlet, Douglas Channel - Kitimat Arm and Prince Rupert area surveys, 15-28 September, 1969. PEI, W. Vancouver, B.C.
- _____. Ocean Falls, Kitimat and Prince Rupert, 17-30 July, 1972. PEI, West Vancouver, B.C.



GOLD (VANCOUVER ISLAND)

Hydrography

1. Surveyed most recently in 1967. .
2. Scale of F.S. 1240-S - 1:10,000
1200-L - 1:1,200 Wharf plans
3. Chart number and scale 3665 - 1:12,000.

Sounding Coverage

No estuary bathymetry on F.S. 1200-L.
Very little bathymetry of estuary on 1240-S.

Tidal Information

<u>Nearest Gauge</u>	<u>Period of Analysis</u>	<u>Year of Analysis</u>
Gold River	1 month	1967

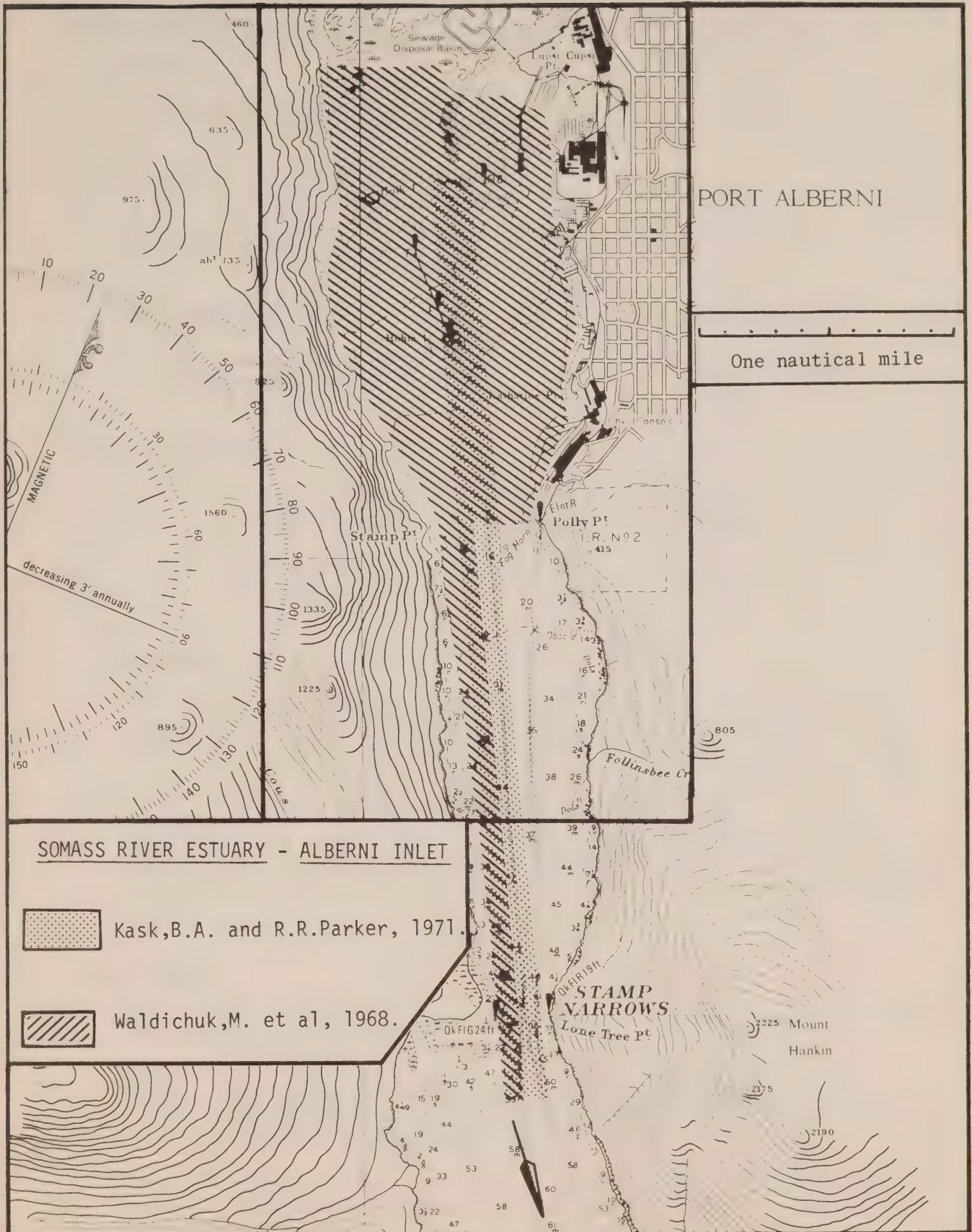
Oceanography

Although there is no published data dealing specifically with the estuary of the Gold River, the sampling locations of Waldichuk et al (1968) and those of the Institute of Oceanography, University of British Columbia, are located in the main channel of Muchalat Inlet as shown on the accompanying chart. Oceanographic information in this area was collected to evaluate conditions for effluent disposal from a pulp mill established at Gold River. Several series of temperature/salinity data have been collected by Environmental Protection Service personnel and are on file. Goyette (personal communication).

Bibliography

- Anon. 1959. British Columbia inlet cruise, 1959. Data report no. 15. Inst. Oceanogr., Univ. British Columbia.
1960. British Columbia inlet cruise, 1960. Data report no. 17. Inst. Oceanogr., Univ. British Columbia.
1963. British Columbia inlet cruise, 1963. Data report no. 23. Inst. Oceanogr., Univ. British Columbia.
1970. British Columbia inlets and Pacific cruises, 1970. Data report no. 32. Inst. Oceanogr., Univ. British Columbia.

- Goyette, D.E. _____. Several surveys T/S and DO. Environmental Protection Service. Data on file.
- Pickard, G.L. 1963. Oceanographic characteristics of inlets of Vancouver Island, British Columbia. J. Fish. Res. Bd. Can., 20(5): 1109-1144.
- Tully, J.P. 1937. Oceanography of Nootka Sound. J. Biol. Bd. Can., 3(1): 43-69.
- Waldichuk, M., J.R. Markert, and J.H. Meikle. 1968. Physical and chemical oceanographic data from the west coast of Vancouver Island and the northern British Columbia coast, 1957-1956. Vol. 1. Fish Res. Bd. Can. Ms. Rept., no. 990.
- Waldichuk, M. _____. Alberni Inlet - Muchalat Inlet - Quatsino Sound and Discovery Passage Survey, 19 Aug.-1 Sept., 1968. Pacific Environment Institute, W. Vancouver, B. C.



SOMASS (ALBERNI)

Hydrography

1. Surveyed most recently in 1959 - 1172-L.
after Tsunami 1964 - 1225-S.
2. Scale of F.S. 1172-L - 1:12,160
1225-S - 1:6,080
3. Chart number and scale 3609 - 1:38,800
Insert - 1:9,000

Sounding Coverage

Good bathymetric definition of estuary. Numerous revisions to area since original surveys.

Tidal Information

<u>Nearest Gauge</u>	<u>Period of Analysis</u>	<u>Year of Analysis</u>
Port Alberni (permanent gauge)	1 year	1971

Oceanography

The Somass River Estuary is one of the more heavily studied areas of the British Columbia coast because of a pulp mill established in Port Alberni discharging effluent at the mouth of the Somass River. There is extensive oceanographic information in the area directly below the delta front of the river. A baseline inventory of physical and biological conditions of the delta region has been prepared. (Howard Paish and Assoc. Ltd., 1972.) The data records in the bibliography include cross seasonal and annual coverage for long terms and therefore could provide one of the best data bases available in a British Columbia estuary.

Bibliography

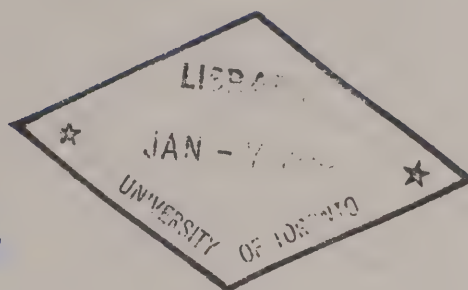
- Anon. 1959. British Columbia inlet cruise, 1959. Data report no. 15. Inst. Oceanogr., Univ. British Columbia.
- Farmer, D.M. 1972. The influence of wind on the surface waters of Alberni Inlet. Pacific Marine Science Report 72-16, Marine Sciences Directorate, Victoria.
- Howard Paish and Assoc. Ltd. 1972. Physical and biological baseline inventory of the Somass River delta. Rept. for MacMillan & Bloedel Ltd.

- Kask, B.A., and R.R. Parker. 1971. Data report. Estuarine pollution, Alberni Inlet, British Columbia. Fish. Res. Bd. Can. Ms. Rept., no. 1161. 6 vols.
- Pacific Oceanographic Group. 1957. Physical and chemical data record, Alberni Inlet and Harbour, 1939 and 1941. Ms. Rept., Nanaimo Biol. Sta.
- Parker, R.R., and J. Sibert. 1971. Effects of pulp mill effluent on dissolved oxygen supply in Alberni Inlet, British Columbia. Fish. Res. Bd. Can. Tech. Rept., no. 316.
1973. Effects of pulpmill effluent on dissolved oxygen in a stratified estuary - I. Empirical observations. Water Res., 7(4): 503-514.
1973. Effects of pulpmill effluent on dissolved oxygen in a stratified estuary - II. Numerical model. Water Res., 7(4): 515-523.
- Pickard, G.L. 1963. Oceanographic characteristics of inlets of Vancouver Island, British Columbia. J. Fish. Res. Bd. Can., 20(5): 1109-1144.
- Sibert, J., and R.R. Parker. 1971. A numerical model to demonstrate the effect of pulp mill effluent on oxygen levels in a stratified inlet. Fish. Res. Bd. Can. Tech. Rept., no. 307.
- Tully, J.P. 1949. Oceanography and prediction of pulp mill pollution in Alberni Inlet. Fish. Res. Bd. Can. Bull., no. 83.
1958. On structure, entrainment and transport in estuarine embayments. J. Marine Res., 17: 523-535.
1960. Waste disposal in the marine environment. Pergamon Press.
- Waldichuk, M. 1956. Pulp mill pollution in Alberni Harbour, British Columbia. Sewage and industrial wastes, 28(2): 199-205.
1958. Some oceanographic characteristics of a polluted inlet in British Columbia. J. Marine Res., 17: 536-551.
- _____. Unpublished data record. Alberni Inlet - Muchalat Inlet - Quatsino Sound and Discovery Passage - 19 Aug. - 1 Sept., 1968. Pacific Environment Institute, West Vancouver, British Columbia.
- Waldichuk, M., J.H. Meikle, and W.F. Hyslop. 1968. Alberni Inlet and Harbour physical and chemical oceanographic data, 1954-1967. Fish. Res. Bd. Can. Ms. Rept., no. 937.
- Waldichuk, M., J.R. Markert, and J.H. Meikle. 1969. Seasonal physical and chemical data for Alberni Harbour and Somass River, 1958-1969. Fish. Res. Bd. Can. Ms. Rept., no. 1028.

Werner, A.E., and W.F. Hyslop. 1967. Distributions of Kraft mill effluent in a British Columbia harbour. J. Fish. Res. Bd. Can., 24(10): 2137-2153.

AN EVALUATION OF THE TRISPONDER 202A WITH MODEL 210 TRANSPONDERS

by



**M.V. Woods, N.M. Anderson, F.A. Coldham,
R.D. Popejoy**

Canadian Hydrographic Service

ENVIRONMENT CANADA
Fisheries and Marine Service
Marine Sciences Directorate
Pacific Region
1230 Government St.
Victoria, B.C.



MARINE SCIENCES DIRECTORATE, PACIFIC REGION

PACIFIC MARINE SCIENCE REPORT NO. 73-8

AN EVALUATION OF THE TRISPONDER 202A
WITH MODEL 210 TRANSPONDERS

by

M.V. Woods

N.M. Anderson, F.A. Coldham, R.D. Popejoy

CANADIAN HYDROGRAPHIC SERVICE

Victoria, B.C.
Marine Sciences Directorate, Pacific Region
Department of the Environment
October 1973

CONTENTS

	<u>PAGE</u>
INTRODUCTION.	1
EQUIPMENT	1
INSTALLATION AND OPERATION.	3
METHOD OF TESTS	3
TOTAL SYSTEM ACCURACY	5
RADAR INTERFERENCE.	6
HELICOPTER OPERATION WITH TRISPONDER.	7
CONCLUSIONS	7
REFERENCES.	8
ILLUSTRATIONS	
APPENDICES	

INTRODUCTION

In 1971 the Canadian Hydrographic Service development group, under A.R. Mortimer, tested the Trisponder Model 202A pulsed radar positioning system. Some changes have been made to the system since then, the most significant being new transponders and antennae.

In September 1973 Computing Devices of Canada Limited lent the system with new Model 210 transponders to the Hydrographic development group for range/accuracy evaluation. During the few days the system was available signal stability tests were conducted on a survey launch over a distance of 30 kilometres (km), and precision and stability tests were conducted over seven land baselines previously established by tellurometer traverse and triangulation (Anderson et al, 1973).

Following these tests, the system was evaluated by the B.C. Forest Service for positioning a helicopter used for aerial photography. Mr. Woods assisted in the airborne operations and further observed the system's operational characteristics.

THE EQUIPMENT

A. The Distance Measuring Unit (DMU)

This unit is basically the same as that tested by A.R. Mortimer (1972). The DMU contains the range measuring circuitry and operating controls. Two digital displays present the measured distances in metres (m). Its power consumption is 40 watts and it requires a 22-32 volt d.c. power supply.

The system measures the distance to each remote transponder by using an X-band frequency and averaging 10 or 100 (depending upon front panel control setting) sequential measurements. An average of 10 readings resolves the distance to the nearest 10 m and 100 to the nearest metre. Remote identification is achieved by utilizing separate coded pulse repetition frequencies (PRF) for each transmitter. The averaged measurement is displayed on the DMU digital display at one second intervals.

The DMU has 4 separate calibration screws for 4 transponders, any 2 of which may be selected for use at any one time.

The model tested was equipped with a "time sharing option" that enables up to 4 master units to operate simultaneously with the same 2 transponders. It also features a manual update control, in which the last range measurement is held until the operator manually initiates a new reading. This feature may be particularly useful during shoal examinations.

Red fault lamps warn of signal loss or interruption during the measurement sequence which may be caused by a loss of line of sight, loss of transponder power, etc.

B. The Master Transmitter/Receiver (Master Transponder)

The master transmitter interrogates the remote transponders and receives the transponder's reply. It utilizes a 6 decibel (db) omnidirectional antenna which is coupled to it by a simple quick release connector. The antenna's vertical beam width is 30° .

The transmitter's magnetron is tunable from 9300 to 9475 megahertz (MHz), and its power output is 1000 watts at +60 dbm (power output in db above 1 milliwatt). Power consumption is 17 watts. The receiver sensitivity is -74 dbm (sensitivity in db below 1 milliwatt). The unit requires a 22-32 volts d.c. power supply, which is supplied by the DMU.

C. The Transponders

The transceivers of the remote transponders are identical to the master transceiver. However, instead of an omnidirectional antenna, they use a 16 db vertical slotted array directional antenna with a horizontal beam width of 87° and a vertical of 5° .

The transponders operate from 22-32 volts d.c., which is normally supplied by two 12 volt batteries, and the power consumption is 17 watts. Forty minutes after interrogation ceases, the transponders switch to a standby mode in which the power consumption is reduced to 8 watts, thus

extending the period in which the remote stations can be left unattended.

All transponders can be mounted on standard tripods, European tripods, or a one inch threaded pipe. The manufacturer's specifications are listed in Appendix I. Plate 1 illustrates the equipment.

INSTALLATION AND OPERATION

The portability of the DMU allows it to be installed in any convenient place aboard a launch, although it is not adaptable to a standard 19 inch rack. Fifty feet of cable is supplied to connect the master transceiver to the DMU; since the antenna and master transceiver are one unit, this allows the antenna to be attached to a mast or other suitable location. During the launch tests the master unit was mounted on a Wild tripod lashed to the mast step. The remote transponders, also mounted on tripods, were located at known shore stations.

Before operation, the system must be calibrated over a known distance; preferably this distance should be one approximating the central distances used during the survey.

Since the DMU provides binary coded decimal (BCD) output, peripheral equipment may be used aboard the sounding vessel, such as a remote read-out, track plotter, left/right indicator, etc.

METHOD OF TESTS

A. Calibration

At the calibration distance of 2102.4 m, transponder A was reading 1 m high and B was 1 m low. Rather than adjusting the read-out on the DMU, the appropriate correction was made to the raw data.

B. Stability Aboard a Survey Launch

In order to determine the stability of any one distance reading, the same tests were conducted as had been used for the Mini-Ranger tests in 1973

and the Trisponder tests in 1971. The method is to put both transponders at the same shore station, approximately six feet apart on a line 90° to the launch so the distance from the launch to each transponder is essentially the same. The launch is then steered along an arc of constant distance at the centre of the beam pattern and both range readings are recorded simultaneously. The readings are then plotted on a graph and a curve of best fit is drawn to eliminate erratic movements of the launch. The dispersion of the readings about this line, plotted on a straight line graph, show the measure of instability, (see Figure 1).

In our tests launch breakdown and lack of time allowed for just a single run at 30 km. The root mean square (r.m.s.) of the dispersion of readings about the actual launch course is ± 1.7 m. Stability at shorter ranges should be the same or better unless the system is affected by outside interference.

Stability of the Trisponder may be affected by "ducting", similar to other pulsed radar positioning systems (Anderson et al, 1973). While steaming straight away from the transponders the readings began fluctuating at 15,500 m and continued until approximately 16,000 m. Stability broke down even to the point where the radiofrequency (RF) link to the transponders was broken and the "remote off" fault lights flickered on and off. It was at about this same distance at the same location, that the Mini-Ranger experienced stability breakdown during the tests in the spring of 1973. Such occurrences are random in nature and may or may not happen in various geographic locations.

C. Stability of the System Over Precise Land Baselines

Land tests were conducted with the master unit set up on the Mount Douglas Geodetic station and the transponders were taken by car to seven previously measured points from 2 to 21.5 km. These are shown in Figure 2. At each station the transponder antennae were pointed directly at the master (0° , or the centre of the beam pattern) and 10 readings were recorded. The transponders were then turned to 20° , 40° , 60° , 80° , 90° , 100° , 120° , 140° , 160° , and 180° from the centre of the beam pattern enabling the accuracy to be examined at the edge of the beam pattern.

Unfortunately, some data for transponder B had to be deleted due to pointing errors caused by fog.

The dispersion (or standard deviation) of the 10 readings taken at each angular increment may also be regarded as the measure of stability. The most instability was found at a distance of 15.4 km with the other ranges showing stability equal to or better than this range. Therefore, by combining the values at 15.4 km and 21.5 km a value for the entire test range is found. The root mean square (r.m.s.) value at 15.4 km, centre of the beam pattern, is ± 1.8 m and at 90° it is ± 2.7 m. At 21.5 km the r.m.s. for stability at 0° is ± 1.2 m and at 90° it is ± 2.1 m. By combining these four figures a total r.m.s. value for the stability of the system from 2 to 21.5 km and covering 90° of the beam pattern is ± 2.1 m.

In order to determine instability caused by roll or pitch of a moving launch, the master antenna was tilted towards and away from the remote station (which was pointed directly at the master) in increments of 10° . Signal instability occurred at 30° from the vertical which should not cause any problems under normal sounding circumstances.

D. Precision

The precision of any one position line within the beam pattern of the transponders can be determined from the mean differences of the range readings from the known baselines. These differences from each known distance are tabulated in Appendix II. The total r.m.s. value about the median of the mean differences, from 2 to 21.5 km is ± 6.5 m, between 0° and 90° . Figures 3 and 4 show a graphical representation of the mean differences for the system calibrated at 2 km. Figure 5 shows the precision contour for the average of all readings. As with other radar positioning systems, these contours can be changed by altering the distance at which the transponders are calibrated.

TOTAL SYSTEM ACCURACY

In the previous Trisponder evaluation stability and precision were combined with a third factor, repeatability, to give total system accuracy. Since we

had the Model 210 for only a few days a series of calibration checks could not be made to determine frequency drift. However, if we assume that frequent calibrations made over a long period of time would maintain steady repeatability, we can use ± 1 m. This assumption is based on the original findings of A.R. Mortimer (1972) and the fact that the DMU is essentially the same unit.

Therefore total system accuracy from the land tests is:

$$\begin{aligned}\text{Total} &= \sqrt{E_1^2 + E_2^2 + E_3^2} \\ &= \sqrt{\pm 2.1^2 + \pm 6.5^2 + \pm 1^2} \\ &= \pm 6.9 \text{ m (throughout } 90^\circ \text{ of the beam pattern)}\end{aligned}$$

E_1 = stability error, E_2 = precision error, and E_3 = repeatability error.

Figure 6 shows the overall accuracy contours for the system calibrated at 2 km.

RADAR INTERFERENCE

During the launch tests (conducted in close proximity to several vessels operating radar), no radar interference was experienced; a noticeable difference from 1971. This is due, apparently, to changes made in the gating techniques used in signal reception.

Each transponder receives a series of coded pulses at a particular pulse repetition frequency (PRF), each PRF being different for each transponder. Signals are sent back to the master at the same PRF as received, thus distinguishing one transponder from the other. Each transponder has an electronic "gate" which is only open to accept its particular PRF for 2 1/2 microseconds out of a 1 millisecond interval (or about .02% of the time), thus eliminating outside interference such as radar (von der Heide, 1973).

HELICOPTER OPERATION WITH TRISPONDER

Following our tests the Trisponder was lent to the B.C. Forest Service. Their application of the system was to position a helicopter during low level aerial photography of various stands of timber. This exercise took place in the Cowichan Valley near Duncan, B.C. The transponders were placed so that line of sight would be maintained in the working area. To check the system's stability a set of readings from one transponder was recorded while the helicopter was flown along an arc of 10,500 m. Normally a curve of best fit could be applied to this graph but it was so smooth that little or no dispersion due to instability can be detected. This graph is shown in Figure 7.

Overall, the precision and stability of Trisponder aboard a helicopter should be as good as on a launch provided the aircraft stays within the vertical and horizontal beam patterns of the antennae.

CONCLUSIONS

The full range and reliability of the Trisponder with new "Model 210" transponders has not been evaluated since the system was available for only a few days; however, the new transponders seem to have solved the main problems encountered with the earlier system evaluated by Mortimer (1972).

Accuracies deal with one position line only and accuracy breakdown due to geometrical configuration will have to be accounted for when using the system in a range/range mode. Accuracies of ± 6 m should be attainable up to a range of 30 km as long as the system is calibrated within the working area; for example, to survey between 15 and 30 km the system should be calibrated between 20 and 25 km. For a range of 12 km the transponders could be set up with the centre of the beam pattern perpendicular to the shore and an accuracy of ± 5 m could be maintained for a distance of 7.5 km along the shore, for a calibration within 2-12 km.

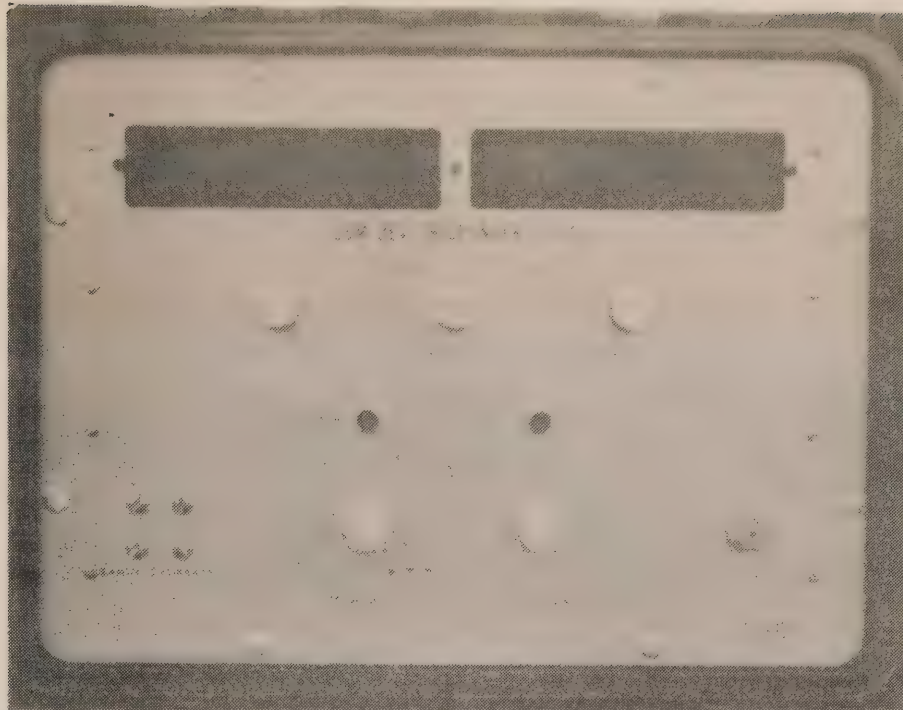
REFERENCES

- Anderson, N.M., F.A. Coldham, R.D. Popejoy, and M.V. Woods. 1973. An evaluation of the Mini-Ranger positioning system. *Pacific Marine Science Report 73-11, Marine Sciences Directorate, Victoria, B.C.*: 12 pp.
- Mortimer, A.R. 1972. An evaluation of the Trisponder positioning system. *Pacific Marine Science Report 71-9, Marine Sciences Branch, Victoria, B.C.*: 16 pp.
- von der Heide, Jack C. 1973. Trisponder positioning, the basis for a variety of systems. Unpublished manuscript. *Del Norte Technology Inc., Euless, Texas.*

ILLUSTRATIONS

	<u>PLATE</u>
DISTANCE MEASURING UNIT AND MASTER TRANSMITTER/RECEIVER . . .	1
REMOTE TRANSPONDER.	2
	<u>FIGURE</u>
TRISPONDER STABILITY GRAPH.	1
LAND BASELINES USED FOR TESTS	2
LAND BASED PRECISION TESTS.	3
PRECISION OF AVERAGED READINGS.	4, 5
TOTAL SYSTEM ACCURACY	6
HELICOPTER STABILITY.	7

Distance Measuring Unit (DMU)



Master Transmitter/Receiver



Remote Transponder



Figure 1

Stability At 30 Km.

Dispersion About The Launch Track

Transponder A - □ Transponder B - ■



Root Mean Square of Dispersion = ± 1.7 metres

Figure 2

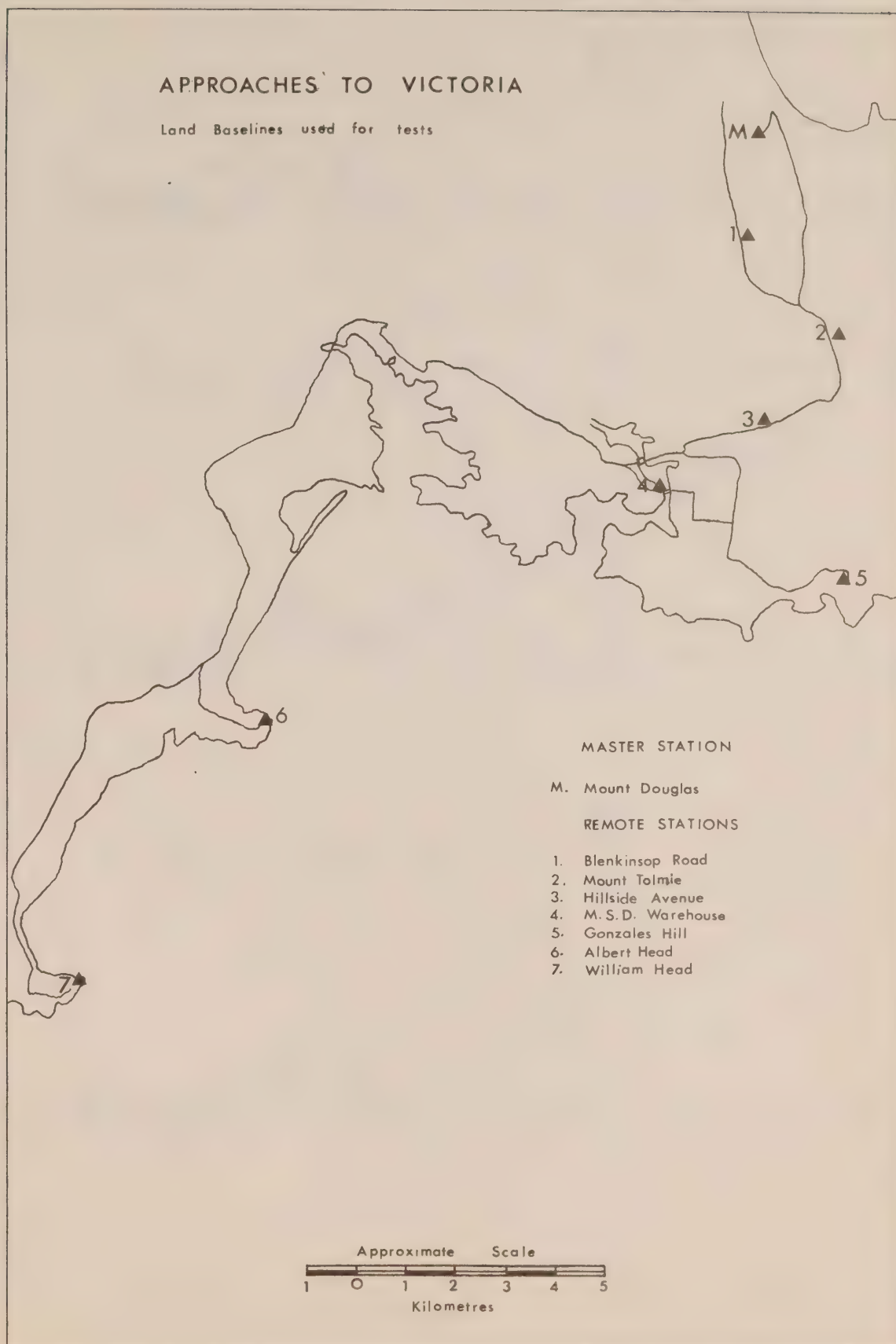


Figure 3

Land Based Precision Tests

TRANSPONDER A

TRANSPONDER B

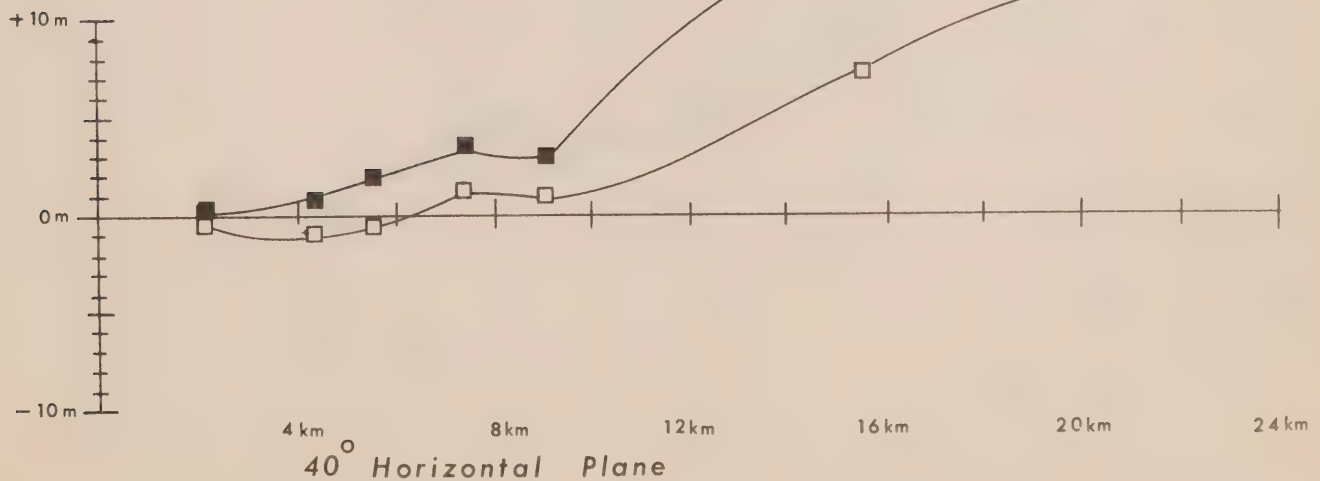
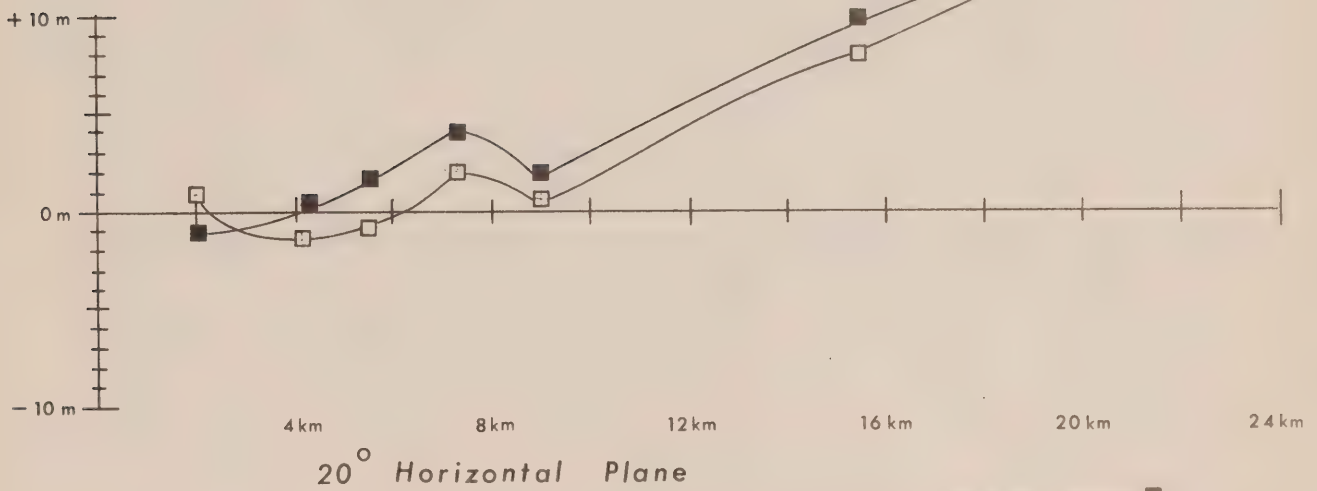
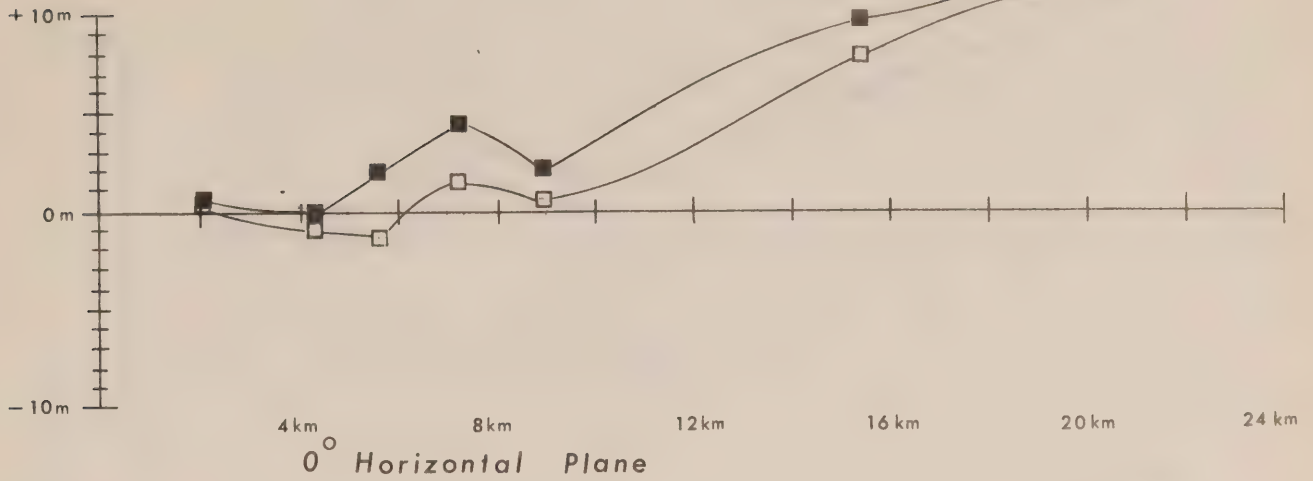


Figure 4

Land Based Precision Tests

TRANSPONDER A — □

TRANSPONDER B — ■

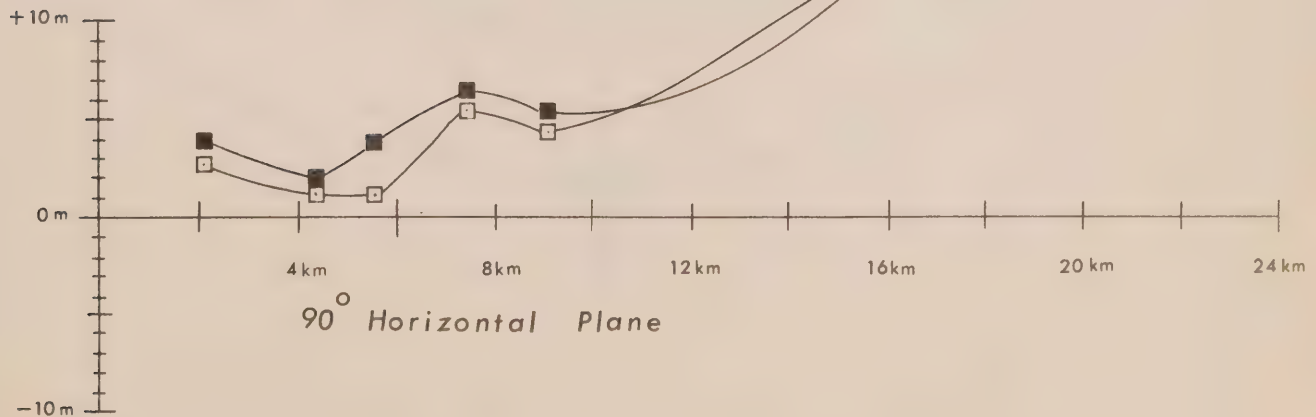
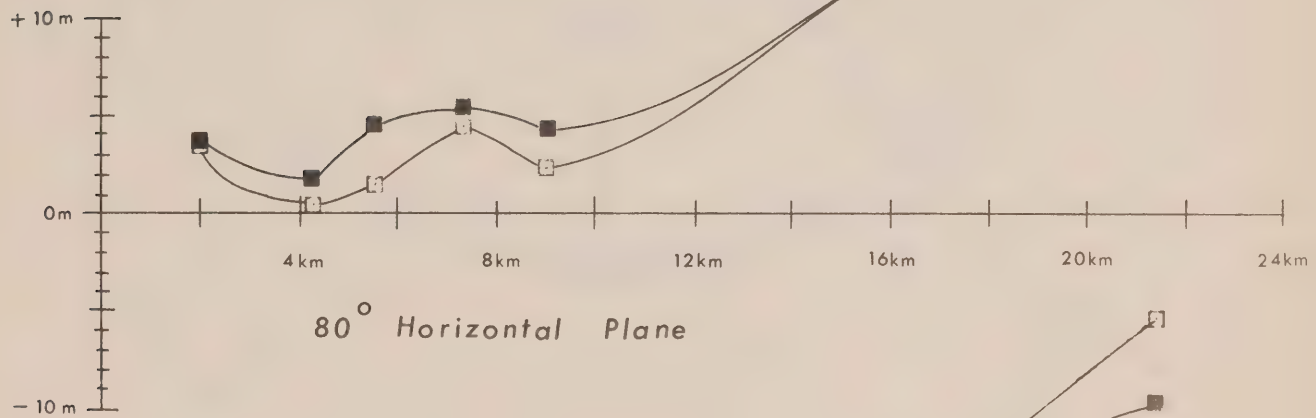
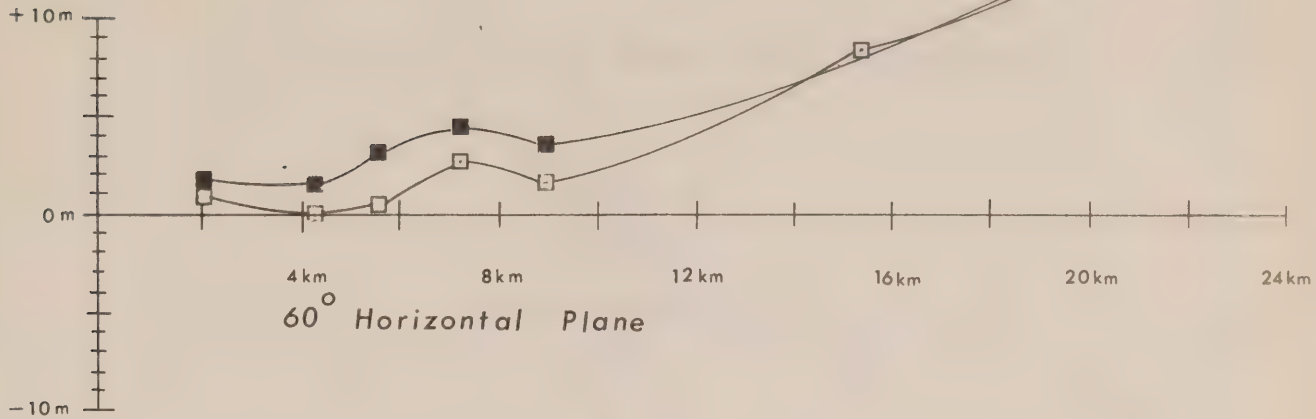


Figure 5

Precision of Averaged Readings

Contours in
Metres

Calibration distance = 2 km

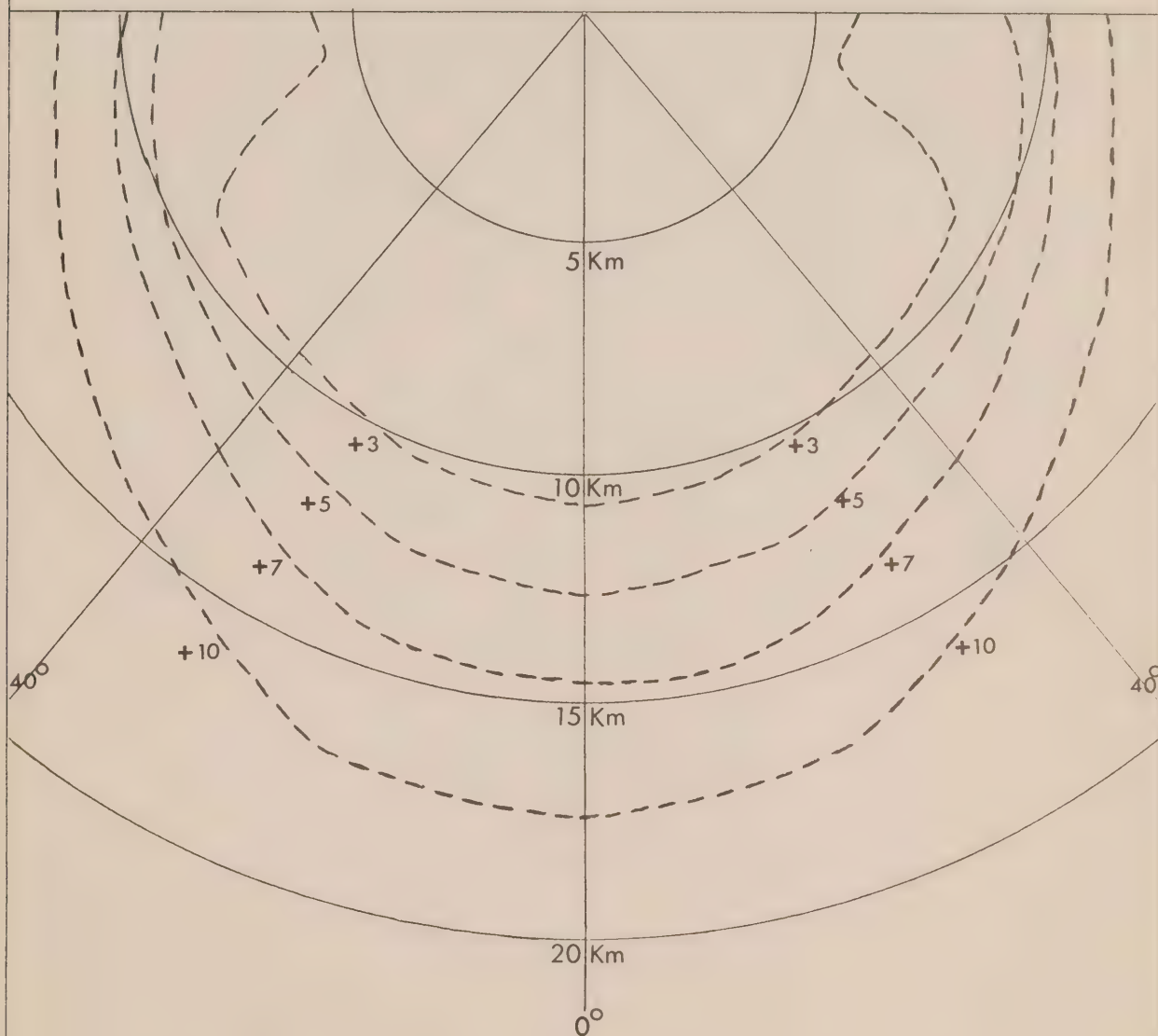
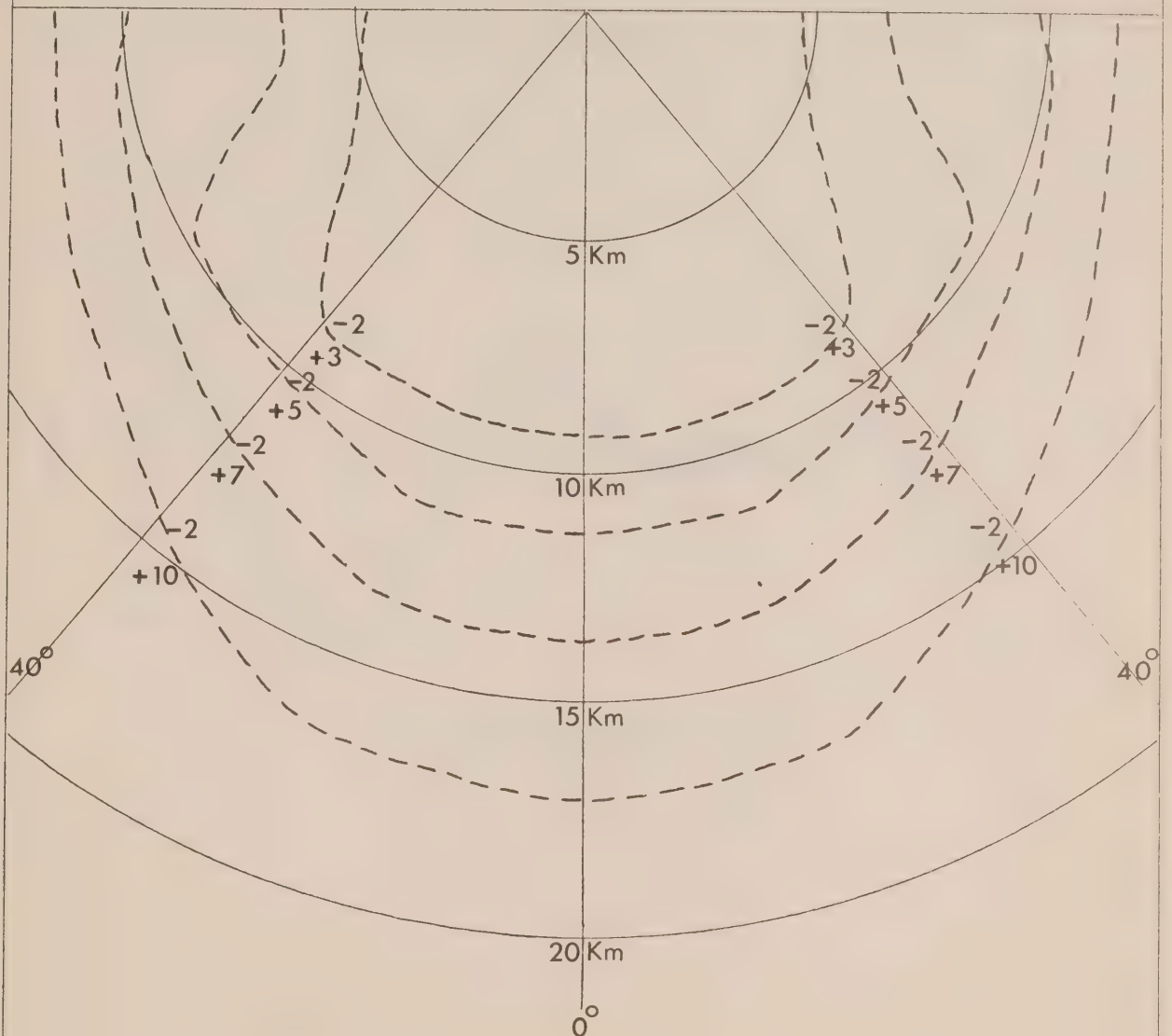


Figure 6

Total System Accuracy

Contours in Metres

Calibration distance = 2 km



The lower boundary is -2m due to the positive curve of the precision graphs

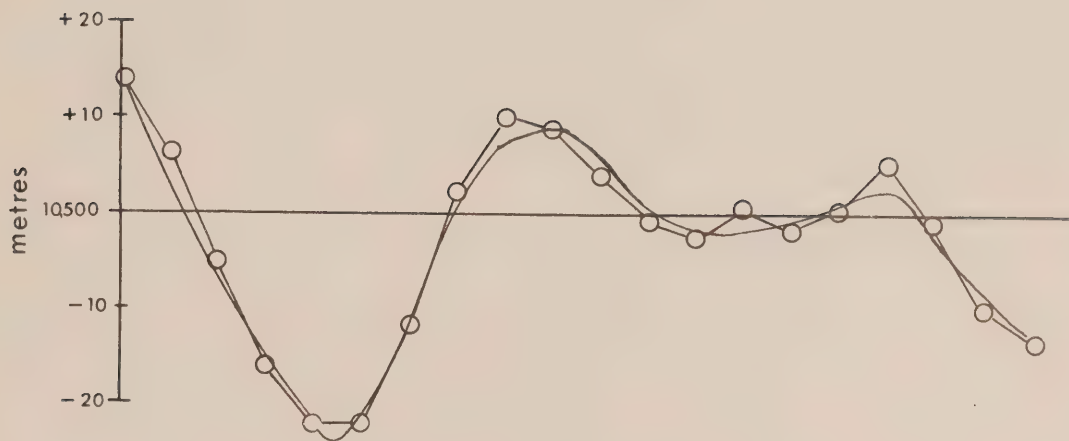
Figure 7

Helicopter Stability

Transponder B

Raw Data — ○

Curve of Best Fit — ~



Indicated Stability = ± 1 Metre

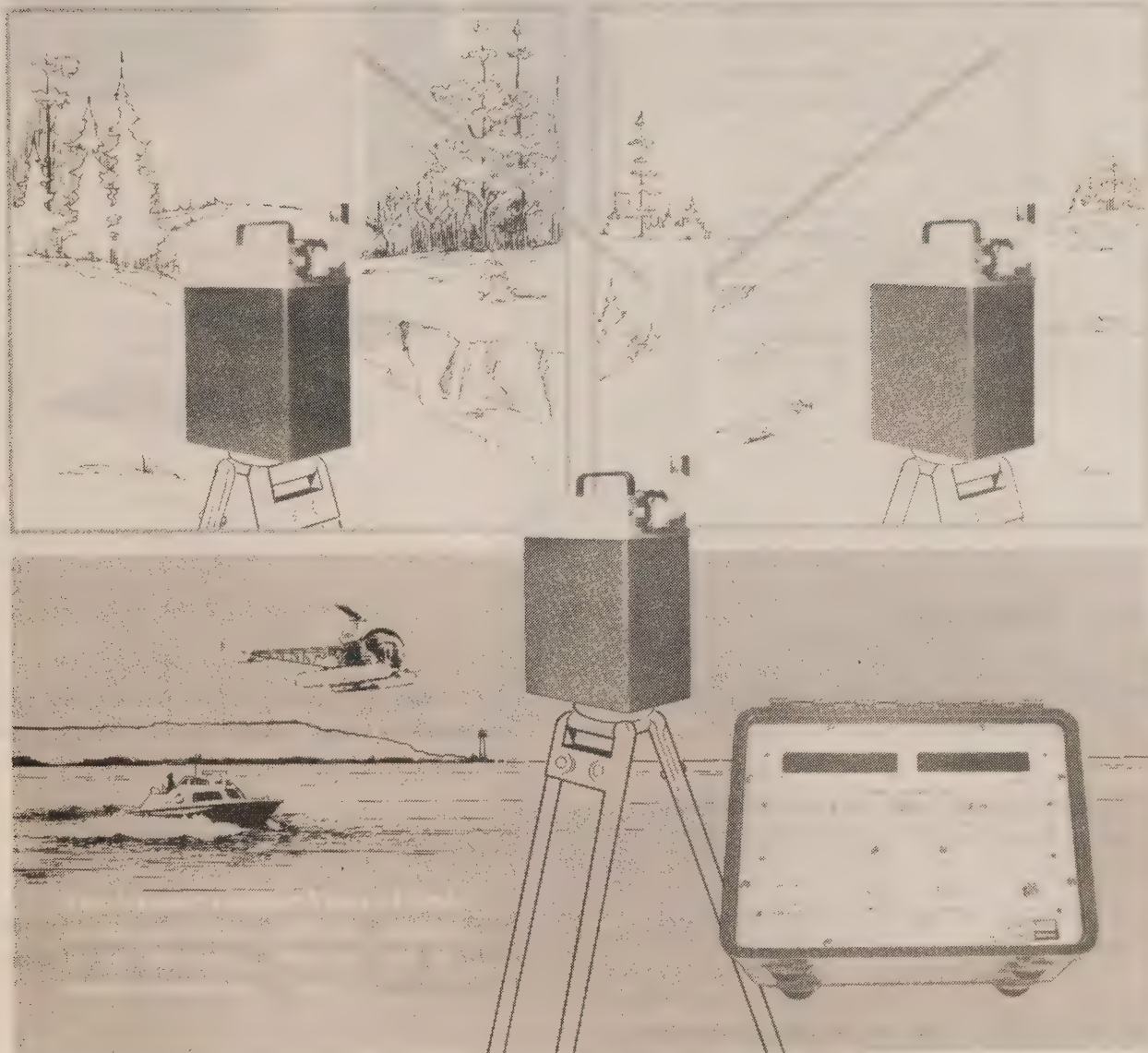
APPENDICES

APPENDIX I
MANUFACTURER'S SPECIFICATIONS

Specification Sheet

ComDev Trisponder

MODEL 202A



COMPUTING DEVICES OF CANADA LIMITED

A SUBSIDIARY OF CONTROL DATA CORPORATION

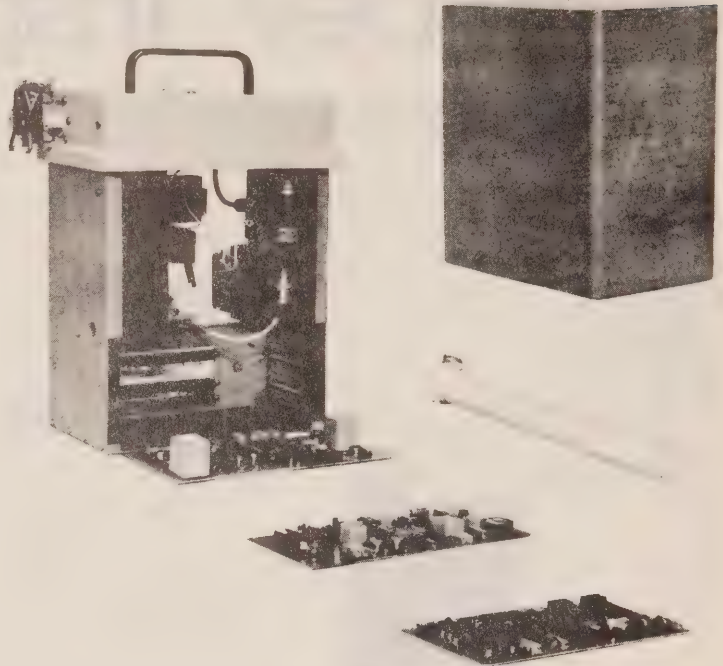
ComDev

IN-1011

HEAD OFFICE: 100 RIVERVIEW AVENUE, SCARBOROUGH, ONTARIO M1V 1B1 CANADA REGIONAL OFFICES: 100 RIVERVIEW AVENUE, SCARBOROUGH, ONTARIO M1V 1B1 CANADA

Trisponder Model 202A-MS02-M2

The ComDev Trisponder Model 202A is an automatic distance measuring system which provides a mobile vehicle with a highly accurate position relative to two fixed locations, up to a range of 15 miles line-of-sight (up to 50 miles line-of-sight with the long range system). Using radar principles and digital techniques for measuring the elapsed times of rf signals between the mobile master and two remote slave stations, the Trisponder System accurately determines and simultaneously displays the resultant two ranges. The mobile's position can then be trilaterated manually or by automated methods depending on which of the optional peripherals are interfaced with the basic Trisponder System.



System Features

Minimum size and weight — ideal for small marine craft and airborne applications

Solid state electronics built to withstand tropical to Canadian arctic environmental conditions

Built-in capability for selecting any two of four slave transponders

Low voltage monitor provides automatic shutdown before battery failure *

Standard BCD logic outputs

Master and remote units interchangeable — minimum spares required *

In $\times 1$ mode the average of 10 (optionally 100) independent range measurements are displayed and updated at one-second intervals

Simple range calibration adjustment

Automatic call-up — remote station activated by interrogation signal; reverts to standby when interrogation terminated *

**Mobile antenna — omni/ 30° slotted waveguide
Remote antenna — $87/5^\circ$ vertical slotted array**

*** Available with long range transponders**

Unit Specifications

TRISPONDER MODEL 319X the short range system

RF Power	Peak transmitter power 400 watts minimum
Frequency	X-band 9,200 to 9,500 MHz
Environmental	Operating temperature range -35°F to 165°F
Power Supply	22 to 32V dc 30 watts duty
Size	$4\frac{1}{2} \times 6 \times 7$ inches
Weight	10 pounds (including antenna)
Housing	Rugged, weatherproof drawn aluminum case

TRISPONDER MODEL 319Y the long range system

Transmitter
Pulse Power
Receiver
Tuning Range
Antenna Connector
Environmental
Power Supply
Power Consumption
Automatic Call-up
— Operate
— Standby
Automatic Power Control
Size (less antenna)
Weight

Range	Line-of-sight up to 15 miles (short range system) Up to 50 miles (long range system)
Accuracy	± 3 metres
Resolution	10 metres in $\times 10$ Mode (Coarse) 1 metre in $\times 1$ Mode (Fine)
Display	Two 5-digit ranges displayed simultaneously in metres
Calibration	Simple adjustment of preset controls
Outputs	BCD output 1-2-4-8 code +5V logic level
Power Supply	22 to 32V dc 40 watts
Size	$16 \times 12 \times 8\frac{1}{2}$ inches
Weight	25 pounds (less batteries)
Housing	Rugged, weatherproof aluminum transit case

Options

100-SUM OPTION

Stable readout obtained by summing and averaging 100 distance measurements from each remote station. Display is updated at one-second intervals.

TIME-SHARING ADAPTOR

Allows two or more mobile stations to operate with the same pair of remote stations.

AUTOPLOT SYSTEM

Provides conversion of range data to map coordinates in Transverse Mercator, Lambert, or other grid system for track plotting directly on an X.Y. Recorder.

ANTENNAS - REMOTE

45°/45° horn for airborne operations.
87°/5° vertical slotted array for marine operations.

AUTOMATIC POSITION RECORDING SYSTEM APRS-301

Provides printed record of Trisponder range data at selected intervals of one second to one hour. Optional printouts of time and BCD data, e.g., depth, temperature, etc., can be included.

RF LINK SIMULATOR

The operation of transponders can be simulated for testing the Distance Measuring Unit. RF outputs representing a variety of ranges can be individually selected.

PORTABLE RF DETECTOR

Received signals are converted to an audio output to confirm that mobile/remote stations are radiating.

LEFT/RIGHT TRACK INDICATOR

Enables a mobile station to steer a course parallel to any preselected line of position.

REMOTE DISPLAY UNIT

Provides a remote display of range data from the Trisponder DMU.

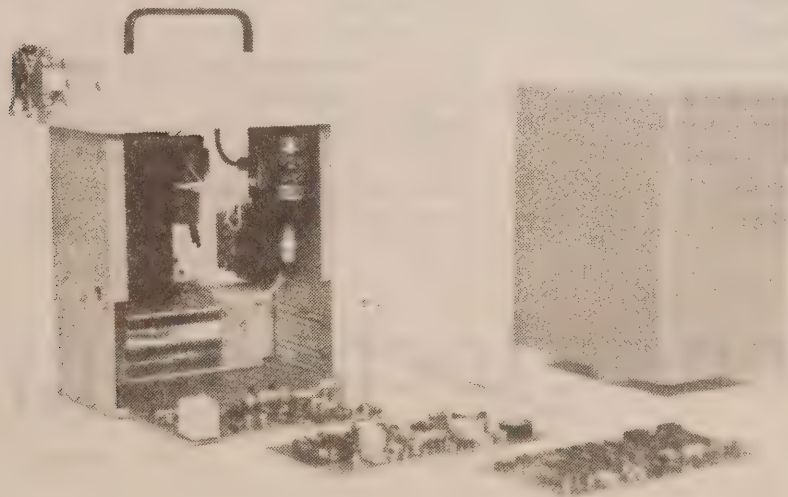
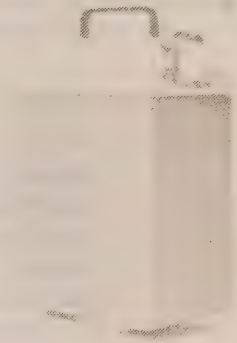


del norte

model 210 microwave transponder

the only transponder designed specifically for positioning systems

- **efficient:** requires only 17 watts operating, 8 watts in stand-by, with automatic transfer between stand-by and operate modes.
- **accurate:** advanced video processor and receiver provide ± 3 meter accuracy to 80 Km.
- **powerful:** a 1 Kw transmitter and -74dbm receiver provide a 50-mile range with an omnidirectional antenna.
- **reliable:** designed for continuous operation; internally protected against low voltage, reversed polarity, and adjacent high-powered radar.
- **portable:** engineered and packaged for rugged marine, land, and air craft environments—yet easily hand carried.



- **accessible:** all components are easily removed.

Developed for the **Del Norte Model 210**, Del Norte's Model 210 is the only transponder designed specifically for positioning systems and thus offers significant advantages over general purpose units.

Ranges in excess of 50 miles are obtained with standard 202A vertical slotted array antennas; rotating antennas are not required. An advanced receiver and video processor result in nearly constant pulse delays at signal levels as low as -74dbm . Thus, an accuracy of ± 3 meters is maintained to maximum range. Performance is further enhanced by a digital range gate which rejects interfering signals.

A highly efficient power converter and extensive use of C-MOS circuitry result in an operating power input of only 17 watts. Power used by remote stations during stand-by periods is reduced to 8 watts by the Automatic Call-up feature. Call-up from stand-by to operate is initiated by a coded interrogation from the master station; transfer to stand-by is automatic 40 minutes after normal interrogation ceases. Based on an 8-hour operating day, a Model 210 remote station will operate 12 days on two 12-volt 70 amp-hour storage batteries.

In designing the Model 210, components with reliable performance records were selected. Circuit parameters were so set that operation is well within established ratings. For example, the transmitter employs a hi-rel magnetron operating at $\frac{1}{4}$ its normal rating. This design approach has resulted in a transponder which provides dependable performance in continuous duty service.

Access to the interior of the transponder is accomplished by removing four self-sealing screws and slipping off the waterproof cover. A majority of the electronics are on plug-in PC boards and, as potted modules are not used, components may be checked and easily replaced. Since the master station is identical to the remote, only one spare is required for complete back-up. An optional test fixture allows system gain checks plus transmitter and receiver retuning to be accomplished easily in the field.

The Model 210 is compatible without change in any **Del Norte Model 210** system; engineering assistance is available for other applications.

Range	300 feet to 50 miles (100m to 80 Km)
Transmitter	Magnetron, tunable, 9300-9475 MHz
Pulse Power	1000 watts (+60dbm)
Pulse Width	0.5 \pm 0.1 microseconds
Receiver	-74dbm , solid state, tunable, 9300-9500 MHz
Intermediate Frequency	60 \pm 5 MHz with 12 MHz bandwidth
Power Input	22-32 vdc, 8w stand-by, 17w operate
Automatic Call-up	1 min. by coded interrogation from master
Stand-by	40 min. after last interrogation
Size, less antenna	14" h x 6" w x 10.5" d (35.6 x 15.3 x 26.7 cm)
Weight	15# (6.8 Kg)
Mounting	U. S. and European Tripod plus 1" NPT
Antenna Connector	UG40/U wave guide flange, quick disconnect
Wave Guide	WG-16, WR-90, RG-52
Power Connector	PT00E-14-12P, mating connector PT06W-14-12S
Temperature	-30°C to $+70^{\circ}\text{C}$ (-22°F to $+158^{\circ}\text{F}$)
Altitude	.760 to 1mm Hg (with vent)
Packaging	Marine environment

del norte technology, inc.

P.O. BOX 696

EULESS, TEXAS 76039

(817) 267-3541

APPENDIX II
TABULATION OF LAND BASED TESTS

TRANSPONDER A MEAN DIFFERENCE = MEAN STANDARD DEVIATION = S.D.

(Average of 10 Trisponder readings minus tellurometer distance)

RANGE	0 DEGS.	20 DEGS.	40 DEGS.	60 DEGS.	80 DEGS.	90 DEGS.
	MEAN	S.D.	MEAN	S.D.	MEAN	S.D.
2 KM	0.2	1.1	0.1	1.0	0.7	0.6
4 KM	-1.3	1.8	-1.6	1.0	1.2	1.1
6 KM	-1.4	1.7	-0.7	0.9	2.0	1.6
7 KM	1.7	1.2	2.1	1.3	1.3	1.2
9 KM	0.6	0.7	0.7	0.6	0.6	0.7
15 KM	7.8	2.3	8.0	1.2	2.1	1.4
21 KM	11.9	0.7	13.9	1.2	14.6	1.5

RANGE	100 DEGS.	120 DEGS.	140 DEGS.	160 DEGS.	180 DEGS.		
	MEAN	S.D.	MEAN	S.D.	MEAN	S.D.	
2 KM	3.5	0.5	4.2	0.4	6.9	0.7	0.0
4 KM	1.2	1.2	1.4	0.8	2.3	0.8	0.0
6 KM	2.6	0.7	1.9	1.9	5.8	0.4	1.0
7 KM	5.9	1.4	6.7	0.7	8.8	0.8	2.0
9 KM	4.1	0.6	3.7	1.4	5.1	0.7	1.0
15 KM	14.6	2.3	17.4	1.6	23.5	3.4	1.0
21 KM	21.8	1.4	24.6	2.8	37.5	7.8	0.0

TRANSPONDER B MEAN DIFFERENCE = MEAN STANDARD DEVIATION = S.D.
 (Average of 10 Trisponder readings minus tellurometer distance)

RANGE	0 DEGS.	20 DEGS.	40 DEGS.	60 DEGS.	80 DEGS.	90 DEGS.
	MEAN	S.D.	MEAN	S.D.	MEAN	S.D.
2 KM	-0.2	0.6	-0.1	0.7	1.1	1.3
4 KM	0.0	0.9	0.4	1.0	1.4	0.9
6 KM	2.2	1.0	1.9	0.9	3.1	1.3
7 KM	4.7	0.7	3.8	1.3	4.6	0.7
9 KM	2.0	1.8	2.0	1.3	3.5	1.4
15 KM	9.7	1.8	9.4	2.1	14.7	1.3
21 KM	12.6	1.6	14.1	0.7	18.5	1.3

RANGE	100 DEGS.	120 DEGS.	140 DEGS.	160 DEGS.	180 DEGS.	
	MEAN	S.D.	MEAN	S.D.	MEAN	S.D.
2 KM	5.6	0.7	11.7	1.6	13.2	1.0
4 KM	2.1	1.5	1.8	1.3	5.1	1.5
6 KM	5.2	1.0	6.2	1.4	-25.5	22.1
7 KM	6.1	1.2	7.7	0.5	13.5	1.7
9 KM	4.3	1.4	5.2	1.1	8.3	1.8
15 KM	23.0	2.1	36.5	4.4	*****	*****
21 KM	20.3	1.5	21.6	2.5	*****	*****

